Functional analysis of the interactions of the spindle assembly checkpoint proteins BubR1 and Bub1 at the kinetochore

Inaugural-Dissertation
zur
Erlangung des Doktorgrades
Dr. rer. nat.

der Fakultät für Biologie
an der
Universität Duisburg-Essen

vorgelegt von
Katharina Overlack
aus Duisburg

durchgeführt am
Max Planck Institut für molekulare Physiologie
Abteilung für mechanistische Zellbiologie

Oktober 2016

Die der vorliegenden Arbeit zugrunde liegenden Experimente wurden am Max Planck Institut für molekulare Physiologie in der Abteilung für mechanistische Zellbiologie durchgeführt.

1. Gutachter: Prof. Dr. Andrea Musacchio
2. Gutachter: Prof. Dr. Stefan Westermann
3. Gutachter: Prof. Dr. Silke Hauf

Vorsitzender des Prüfungsausschusses: Prof. Dr. Hemmo Meyer

Tag der mündlichen Prüfung: 25. Januar 2017

In the context of this doctoral work, the following articles were published:

- Katharina Overlack*, Ivana Primorac*, Mathijs Vleugel, Veronica Krenn, Stefano Maffini, Ingrid Hoffmann, Geert J P L Kops, Andrea Musacchio. 2015. "A molecular basis for the differential roles of Bub1 and BubR1 in the spindle assembly checkpoint." *eLife* 4:e05269

* equal contribution

- Katharina Overlack, Ivana Primorac, Tanja Bange, Florian Weissmann, Alex C. Faesen, Stefano Maffini, Franziska Müller, Jan-Michael Peters, Andrea Musacchio. 2016. "The loop of BubR1 determines BubR1 SAC function." *manuscript in preparation*

- Katharina Overlack, Veronica Krenn, Andrea Musacchio. 2014. "When Mad met Bub." *EMBO reports* 15: 326-328

- Veronica Krenn, Katharina Overlack, Ivana Primorac, Suzan van Gerwen, Andrea Musacchio. 2014. "KI motifs of human Knl1 enhance assembly of comprehensive spindle checkpoint complexes around MELT repeats." *Current Biology* 24: 29-39

Content

List of figures

List of tables

List of abbreviations

APC/C	anaphase promoting complex/cyclosome
ATP	adenosine triphosphate
B	BamH1
B1	Bub1
B3BD	Bub3-binding domain
bp	base pair
BR1	BubR1
BSA	bove serum albumin
Bub	budding uninhibited by benzimidazoles
CCAN	constitutive centromere associated network
Cdk	cyclin-dependent kinase
CENP	centromeric protein
CFP	cyan fluorescent protein
CPC	chromosomal passenger complex
CREST	calcinosis, Raynaud's syndrome, esophageal dysmotiliy, sclerodactyly, telangiectasia
CTE	C-terminal extension
DAPI	4,6-diamidin-2-phenylindoldihydrochlorid
DMEM	Dulbecco's modified eagle medium
DMSO	Dimethyl sulfoxide
DNA	desoxyribonucleic acid
DTT	Dithiothreitol
f	forward
FBS	fetal bove serum
fl	full-length
FRAP	fluorescence recovery after photobleaching
GFP	green fluorescent protein
H	helix
H_2O	aqua bidest
IF	immunofluorescence
IP	immunoprecipitation

KARD	kinetochore associated regulatory domain
kb	kilobase
KI	lysine-isoleucine
KMN	Knl1-complex/Mis12-complex/Ndc80-complex
L	short loop
LL	long loop
Mad	mitotic arrest deficient
MBP	maltose binding protein
MCC	mitotic checkpoint complex
MELT	methionine-glutamic acid-leucine-threonine
Mps	monopolar spindle
MS	mass spectrometry
MW	molecular weight
P	phospho
PBS	phosphate buffered saline
PCR	polymerase chain reaction
PMSF	Phenylmethylsulfonyl fluoride
PP1	protein phosphatase 1
PP2A	protein phosphatase 2A
r	reverse
RNA	ribonucleic acid
RZZ	Rod/Zwilch/Zw10
S	Sal1
SAC	spindle assembly checkpoint
SDS-PAGE	sodium dodecyl sulfate polyacrylamide gel electrophoresis
SEC	size exclusion chromatography
SILAC	stable isotope labeling by amino acids in cell culture
TCEP	Tris-(2-carboxyethyl)-phosphine
TPR	tetratrico peptide repeat
Ub	Ubiquitin
wt	wild type
Xh	Xho1

1 Introduction

The ability to reproduce is essential for the regeneration of life and the continuation of every species. All organisms are derived from a single cell through the process of cell division, required for the continuation of the germ line and the production of somatic cells to build and maintain individuals. In a multicellular organism, most cells differentiate and enter a quiescent state. In contrast, continous or uncontrolled cell reproduction is a hallmark of cancer cells. Regardless of obvious organismal differences, the basic machinery cells use to reproduce is remarkably similar amongst eukaryotes with its most fundamental task to pass on the genetic material to the offspring. In 1882, Walther Flemming orginally coined the term mitosis, which is used today to summarize the processes leading to the segregation of chomosomes into two equal daughter cells (Mitchison & Salmon, 2001).

1.1 The Cell Cycle and Mitosis

The eukaryotic cell cycle is defined as the highly regulated set of events that leads to the duplication of a eukaryotic cell (Alberts et al, 2008). It is characterized by the temporal uncoupling of genome replication, happening during the synthesis (S)-phase, and the segregation of the duplicated chromosomes into individual daughter cells, occuring during the mitotic (M)-phase. These phases are separated by gap phases (G1 and G2), providing additional time for cell growth and regulation of the progression to the next cell cycle stage (Alberts et al, 2008). The time between two M-phases, which consists of G1-, S- and G2-phase, is also called interphase (Figure 1-1).

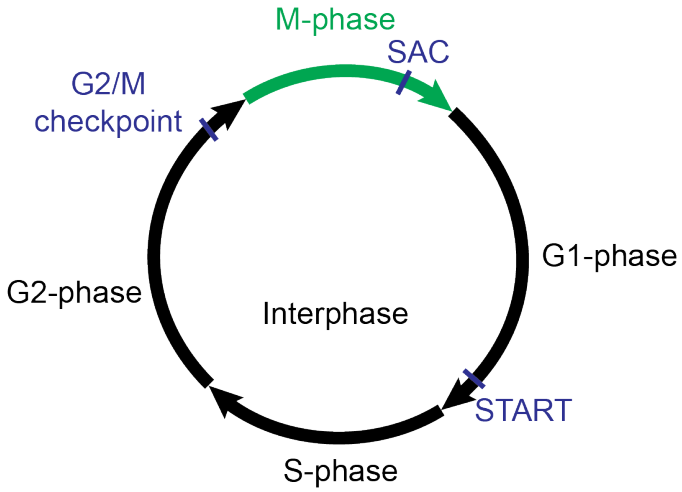

Figure 1-1 The eukaryotic cell cycle

The four phases of the eukaryotic cell cycle as well as the three main checkpoints (in blue) that operate during the cell cycle are schematically shown. Details are described in the text. SAC, spindle assembly checkpoint.

To maintain the fidelity of cell reproduction, which has to occur with very high accuracy, the cell cycle control system has evolved to make sure that cell cycle events occur at the correct time and in the correct order (Murray & Kirschner, 1989). The central players of the cell cycle control system are called "cyclin-dependent kinases (Cdks)", which belong to the serine-threonine kinase family. Cdk activities oscillate throughout the cell cycle, correlated with cyclical changes in phosphorylation of protein substrates, which in turn effect the initiation of distinct cell cycle events. Cdks are activated by binding to proteins called "Cyclins". Cyclin levels oscillate throughout the cell cycle. Different Cyclin types are made at distinct times during the cell cycle resulting in the formation of specific Cyclin/Cdk complexes at definite times, triggering different cell cycle events (Coudreuse & Nurse, 2010; Loog & Morgan, 2005; Morgan, 1997). The Cdk1/Cyclin B complex is, for example, the crucial regulator of M-phase.

The cell cycle control system monitors cell cycle progression at three major checkpoints (Figure 1-1). Checkpoints are defined as transition points in the cell cycle at which progression to the next phase can be blocked by negative feedback signals, if the phase has not been completed correctly (Morgan, 2007). The first checkpoint in late G1-phase is called "start". Here, cells commit to genome duplication and entry into the cell cycle (Hartwell, 1974). The G2/M checkpoint is the

second checkpoint, where early mitotic events are triggered, only if DNA replication has been successful. The third checkpoint operates in mitosis and is called the spindle assembly checkpoint (SAC). The SAC allows for sister-chromatid separation only after proper attachment of all chromosomes to the mitotic spindle is achieved (Musacchio & Salmon, 2007).

Mitosis is the process during which the previously duplicated chromosomes are distributed into two daughter cells. This process is highly complex and needs to be tightly coordinated and regulated, since maintenance of genome integrity is crucial for the viability of a cell. Defects occuring during chromosome segregation can therefore be deleterious to the cell, leading to abnormal chromosome numbers, so-called aneuploidy, and genetic instability often resulting in cell death or the development of a number of diseases, such as cancer (Lengauer et al, 1998). M-phase typically consists of two main events: nuclear division (mitosis) and cell division (cytokinesis). These can be divided into five successive phases [schematically depicted in Figure 1-2, (Alberts et al, 2008; Morgan, 2007)]. In prophase, chromosomes start to condense into a compact form through the help of a protein called condensin and microtubules start to nucleate from structures called centrosomes. At the beginning of prometaphase, the nuclear envelope breaks down (though not in all organisms), microtubules start to organize in a structure called the mitotic spindle and attach to large protein assemblies on the centromere of chromosomes (known as kinetochores). During metaphase, chromosomes are aligned at the metaphase plate in the centre of the spindle. Sister chromatids need to be attached to microtubules originating from opposite spindle poles, reaching a status called bi-orientation. Anaphase is initiated by the degradation of Cyclin B, resulting in inactivation of the mitotic driver kinase Cdk1, and cleavage of cohesin by the protease Separase resulting in loss of sister chromatid cohesion. Thus, sister chromatids can be segregated by the force produced by depolymerizing microtubules to opposite spindle poles. In telophase, a new nuclear envelope is assembled around each set of sister chromatids creating two identical daughter nuclei and chromosomes start to decondense, completing the process of mitosis. During cytokinesis, a contractile ring forms at the site of cell division, which eventually separates the two cells.

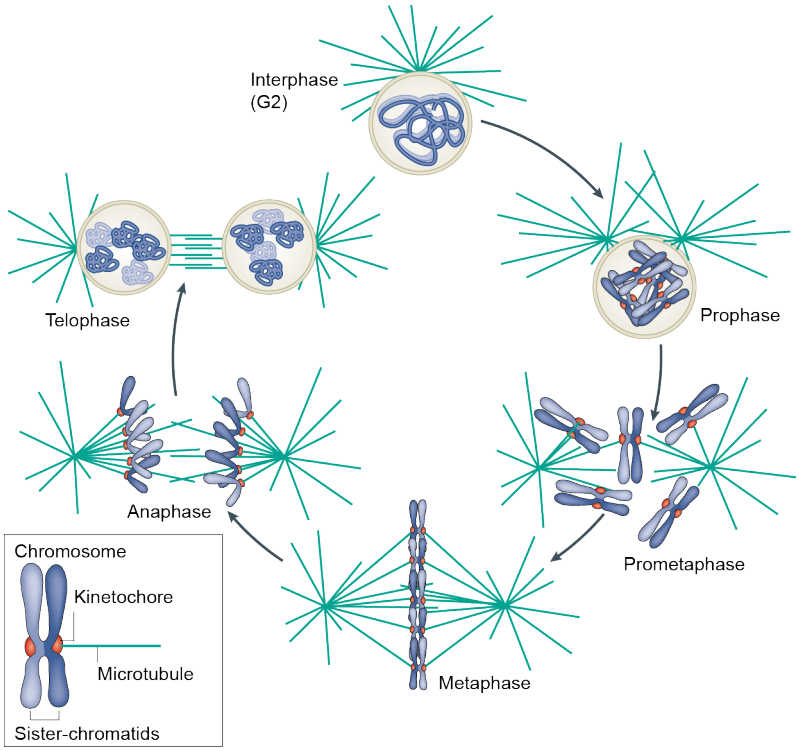

Figure 1-2 Schematic overview of mitotic cell division

Replicated chromatin is condensed during prophase. After nuclear envelope breakdown, microtubule-kinetochore interactions start being established during prometaphase. In metaphase, bi-orientation of chromosomes in the middle of the spindle is achieved. In anaphase, separated sister chromatids are pulled to opposite spindle poles. During telophase, two daughter nuclei form around the chromatin masses. M-phase is completed by cytokinesis (not shown here). Figure adapted from (Cheeseman & Desai, 2008).

1.2 Kinetochore function and organization

The initial observation that fibers of the spindle interact with a distinct "kinetic region" on chromosomes by Metzner in 1894 subsequently lead to the definition of this region as "kinetochores". Kinetochores represent the connection between chromatin and microtubules and are therefore required to allow chromosome movement.

1.2.1 Structural composition of kinetochores

Kinteochores are large protein assemblies built on centromeric chromatin. These macromolecular complexes consist of nearly 100 proteins, organized in a hierarchical order with the primary function to create load-bearing attachments of chromosomes to microtubules during cell division (Walczak & Heald, 2008; Wittmann et al, 2001). Kinetochores are thightly regulated and their overall function and architecture are conserved from yeast to mammals (Kitagawa & Hieter, 2001; Meraldi et al, 2006;

Weir et al, 2016). Initial studies based on genetics, RNA interference and biochemistry are increasingly complemented and validated by biochemical reconstitution, structural and functional studies shedding more and more light onto the organizational principles of kinetochores (Pesenti et al, 2016).

The kinetochores of *Saccharomyces (S.) cerevisiae* are regarded as the simplest kinetochores, because they bind to a single microtubule (Winey et al, 1995). The position of the budding yeast kinetochore is defined by a highly-conserved 125 bp DNA stretch, termed a point centromere (Meraldi et al, 2006; Pluta et al, 1995). This is considerably different from the arrangement in fission yeast and vertebrates, where centromeres extend from tens of thousands up to million bps of usually repetitive DNA sequence (regional centromeres) (Malik & Henikoff, 2009) and are attached to bundles of 3-20 microtubules (McEwen et al, 2001). In *Caenorhabditis (C.) elegans* the centromere even extends over the entire length of the chromosome (holocentric) (Maddox et al, 2004). In all of these species the centromere is not specified by the underlying DNA sequence as in budding yeast, but rather defined epigenetically by the presence of the histone H3 variant centromeric protein A (CENP-A) (Black et al, 2007; Earnshaw & Rothfield, 1985).

In electron micrographs, vertebrate kinetochores appear as being composed of three different layers, with an electron dense inner and outer kinetochore layer and an electron lucent middle layer (McEwen et al, 2007) (Figure 1-3).

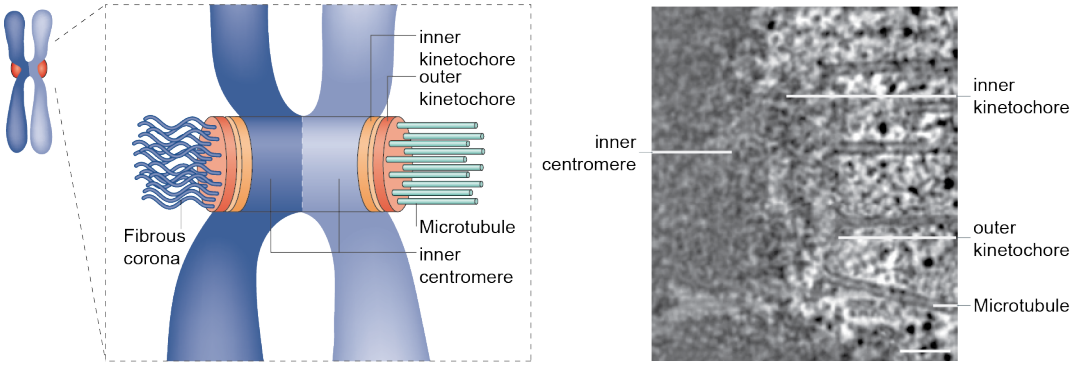

Figure 1-3 Structure of the vertebrate kinetochore

On the left a schematic view of a mitotic chromosome is shown. The left chromatid is unattached, the right chromatid is attached to microtubules. Four modules of kinetochores, the fibrous corona, the inner centromere and the inner and outer kinetochore are highlighted. On the right an electron micrograph of a human kinetochore is shown with the visible modules highlighted (the fibrous corona can only be identified on unattached kinetochores). It represents a single slice from a tomographic

volume of a high-pressure frozen mitotic cell. Scale bar: 100 nm. Figure adapted from (Cheeseman & Desai, 2008).

This trilaminar appearance can be correlated with the main functions of kinetochores, that can be grouped in four modules (Santaguida & Musacchio, 2009):

1. The inner centromere refers to the chromatin located between the sister kinetochores. It contains an error correction machinery, including the chromosomal passenger complex (CPC), that discriminates improper from proper attachments, de-stabilizing the former and stabilizing the latter in a tension-dependent manner (Liu et al, 2009; Wang et al, 2010) (described in more detail in section 1.3).
2. The inner kinetochore or constitutive centromere associated network (CCAN) consists of a 16-subunit protein network that persists throughout the cell cycle providing a connection to centromeric DNA and a sturdy platform for the assembly of outer kinetochore proteins (Foltz et al, 2006; Okada et al, 2006) (see section 1.2.2).
3. The outer kinetochore or Knl1-Mis12-Ndc80 (KMN) network bridges the inner kinetochore and the microtubules by providing the physical interaction sites for spindle microtubules (see section 1.2.3).
4. A fibrous corona is only visible at unattached kinetochores. It contains proteins of the spindle assembly checkpoint (SAC), the feedback control mechanism that monitors the state of kinetochore-microtubule attachments to synchronize the formation of correct attachments with cell cycle progression (the SAC will be discussed in detail in section 1.4).

1.2.2 The constitutive centromere associated network (CCAN)

The discovery in the 1980s that autoimmune sera from patients suffering from calcinosis, Raynaud's syndrome, esophageal dysmotility, Sclerodactyly and Telangiectasia (CREST) syndrome recognize the centromere region (Moroi et al, 1980) as well as the identification of the first human centromeric proteins [CENP-A,-B and -C, (Earnshaw & Rothfield, 1985)] allowed the direct investigation of centromeres. These CENPs (CENP for centromeric protein, followed by a letter) were later identified to form the inner kinetochore or the constitutive centromere associated network (CCAN), which constitutes the inner kinetochore layer of the structure shown in Figure 1-3 (Foltz et al, 2006; Okada et al, 2006). To date, at least

16 CCAN subunits have been identified, most of which localize constitutively to kinetochores in distinct sub-complexes throughout the cell cycle (Basilico et al, 2014; Cheeseman et al, 2008; McClelland et al, 2007; Weir et al, 2016) (Figure 1-4).

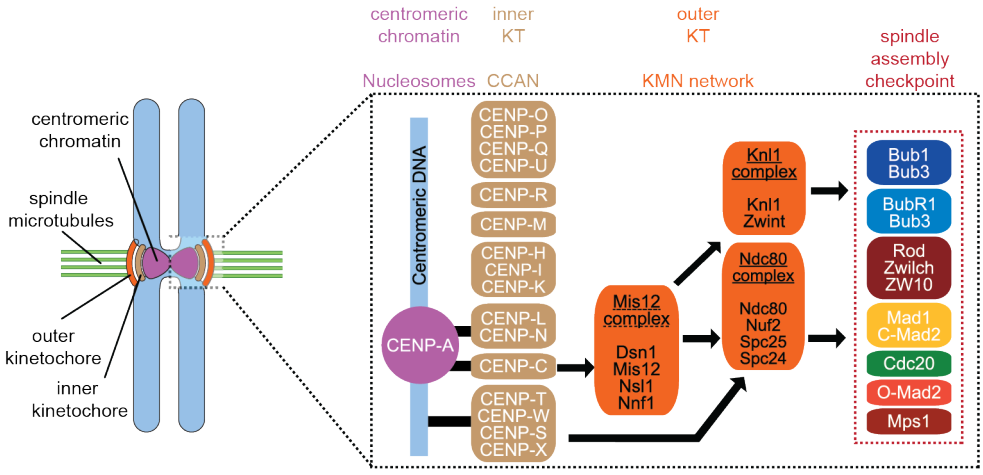

Figure 1-4 Modular organization of the vertebrate kinetochore

Schematic of the vertebrate kinetochore organization. Black lines indicate direct connections to centromeric DNA. Arrows indicate recruitment dependencies. Details are described in the text. Figure modified from (Basilico et al, 2014).

The primary function of the CCAN is to generate a high affinity interaction site for CENP-A which allows the establishment of the outer kinetochore, which in turn constitutes the microtubule binding interface (Weir et al, 2016).

CENP-A, a centromere specific variant of the histone H3 (Palmer et al, 1991), is the conserved hallmark that specifies the centromere and the position of the CCAN (Earnshaw & Migeon, 1985; Marshall et al, 2008). Recruitment of all inner and outer kinetochore proteins depends on CENP-A, underlining its key function as kinetochore building block (Collins et al, 2005). Two CCAN components interact directly with CENP-A-containing nucleosomes, CENP-N (Carroll et al, 2009) and CENP-C (Carroll et al, 2010; Saitoh et al, 1992). CENP-C is the largest CCAN subunit and predicted to be mostly disordered. It has been suggested to contain an intrinsic construction plan for kinetochore assembly (Klare et al, 2015). In its C-terminal region, CENP-C contains binding sites for CENP-A (Kato et al, 2013; Milks et al, 2009). Upstream of that it interacts with other CCAN sub-complexes, CENP-HIKM (which in turn is required to recruit the CENP-O/P/Q/U/R complex) and CENP-LN (Klare et al, 2015;

McKinley et al, 2015; Milks et al, 2009; Okada et al, 2006). Via its N-terminal region, CENP-C binds to the Mis12 complex of the outer kinetochore (Kwon et al, 2007; Przewloka et al, 2011; Screpanti et al, 2011). Thus, CENP-C acts as a bridge between centromeric chomatin and the outer kinetochore. Interestingly, in *D. melanogaster* and *C. elegans*, CENP-C is the only identified CCAN component, emphasizing the importance of its function (Meraldi et al, 2006; Richter et al, 2016).
The histone-fold-containing proteins CENP-T/W and CENP-S/X form a tight complex that is able to bind and supercoil DNA (Nishino et al, 2012). CENP-T/W was found to bind histone H3- (and not CENP-A) containing nucleosomes, interspersed within CENP-A chromatin, via its C-terminal histone-fold (Hori et al, 2008; Ribeiro et al, 2010). The N-terminal region of CENP-T was demonstrated to bind to the Ndc80 complex of the outer kinetochore (Gascoigne et al, 2011) showing that also CENP-T contributes to outer kinetochore assembly in addition to CENP-C (Figure 1-4). However, although initially proposed to provide an independent axis for the connection of centromeric chromatin to the outer kinetochore (Cheeseman, 2014; Gascoigne et al, 2011; Rago et al, 2015), it appears that also CENP-T recruitment depends on CENP-C (Basilico et al, 2014; Carroll et al, 2010; Suzuki et al, 2014). This leads to a model in which both CENP-C and CENP-T, that bind to distinct regions of centromeric chromatin, direct outer kinetochore assembly in an interdependent pathway (Pesenti et al, 2016).

1.2.3 The outer kinetochore Knl1-Mis12-Ndc80 (KMN) network

The ten subunit KMN network, assembling from the two-subunit Knl1-complex, the four-subunit Mis12-complex and the four-subunit Ndc80-complex, constitutes the core of the outer kinetochore (Cheeseman & Desai, 2008; Foley & Kapoor, 2013). It binds the CCAN scaffold via direct interactions between the Mis12-complex and CENP-C (Przewloka et al, 2011; Screpanti et al, 2011) and between the Ndc80-complex and CENP-T (Gascoigne et al, 2011), respectively and provides a direct physical interaction interface with microtubules (Janke et al, 2001; Wigge & Kilmartin, 2001). The KMN network has been shown to be highly conserved in different species (Cheeseman et al, 2006; Cheeseman et al, 2004; DeLuca et al, 2006; Obuse et al, 2004). In contrast to the CCAN, the KMN network is recruited upon entry into mitosis and dissociates again during late ana-/telophase (Cheeseman & Desai, 2008). The

main function of the KMN network is to establish a microtubule-binding interface to transduce the forces required for chromosome segregation from the microtubules of the mitotic spindle to the centromere. Moreover, it can monitor the status of attachment in a tension dependent manner and crucially contributes to the establishment of a SAC signal by providing a recruitment platform for almost all SAC components (Kiyomitsu et al, 2007; Martin-Lluesma et al, 2002; Musacchio & Salmon, 2007). An overview of the organization of the KMN network is presented in Figure 1-5. The three KMN subcomplexes have specialized functions, which will be briefly described for each complex.

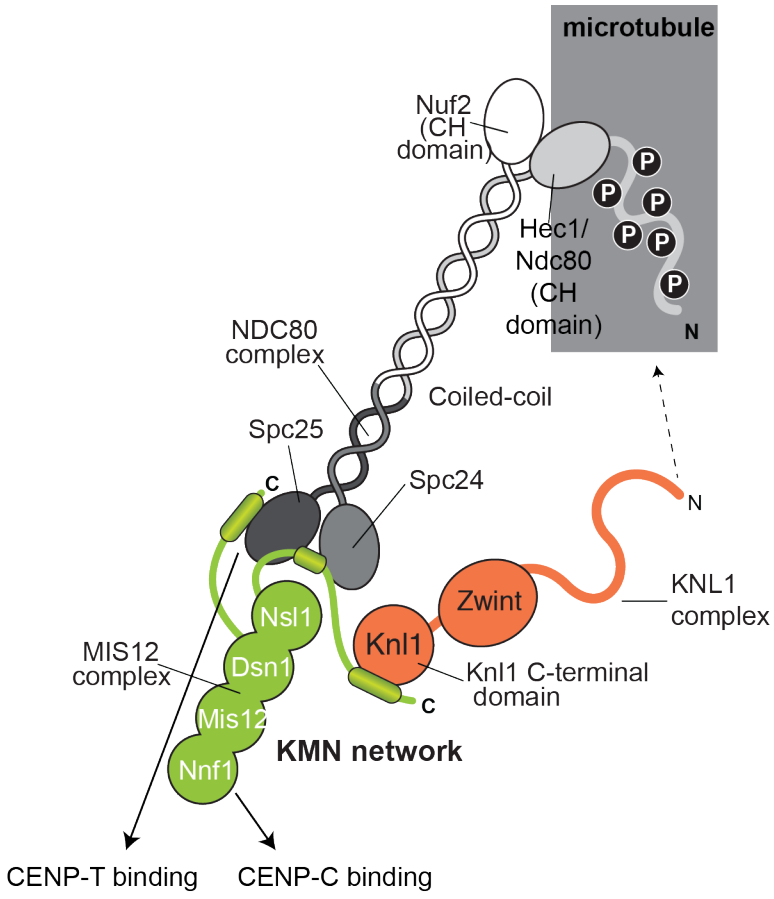

Figure 1-5 The KMN network

Schematic organization of the KMN network. The main interactions are discussed in the text. Connections to CCAN components are indicated by arrows. Figure adapted from (Pesenti et al, 2016).

The Knl1-complex contains the Knl1 (also known as Blinkin, AF15q14, Casc5, Spc105 and Spc107) and Zwint-1 subunits, with Knl1 being the largest core kinetochore protein in humans (2316 residues). Zwint-1 binds to the C-terminal

region of Knl1 (Cheeseman et al, 2008; Kiyomitsu et al, 2007). Furthermore, the C-terminal region of Knl1 binds to the Nsl1 subunit of the Mis12-complex, which accounts for Knl1 kinetochore localization (Kiyomitsu et al, 2011; Kiyomitsu et al, 2007; Petrovic et al, 2010). The N-terminal region of Knl1 has been implicated in microtubule binding, although mutants in *C. elegans* in this region do not show strong defects in establishing load-bearing attachments (Cheeseman et al, 2006; Espeut et al, 2012; Pagliuca et al, 2009; Welburn et al, 2010). Knl1 plays an important role in recruitment of SAC proteins, both directly via its N-terminal region (Kiyomitsu et al, 2007; Krenn et al, 2014; Krenn et al, 2012; London et al, 2012; Primorac et al, 2013; Shepperd et al, 2012; Yamagishi et al, 2012) and indirectly via Zwint-1, which has been suggested to recruit the Zw-10 protein (Starr et al, 2000). Zw-10 is a part of the Rod-Zwilch-Zw10 (RZZ) complex, which has been reported to be involved in SAC activation as well as in SAC silencing (discussed in more detail in 1.4.3). The N-terminal part of Knl1 also contains a motif for binding to the protein phosphatase 1 (PP1), the activity of which contributes to chromosome alignment and SAC silencing by counteracting Aurora B kinase (Kiyomitsu et al, 2007; Liu et al, 2010; Rosenberg et al, 2011).

The Mis12-complex contains the four subunits Mis12, Nnf1, Dsn1 and Nsl1 and forms an elongated structure with a long axis of approximately 22 nm (Goshima et al, 2003; Kline et al, 2006; Petrovic et al, 2014; Petrovic et al, 2010). The Mis12-complex directly binds to the N-terminal region of CENP-C via its Nnf1 subunit, required for its kinetochore localization (Gascoigne et al, 2011; Przewloka et al, 2011; Screpanti et al, 2011). Aurora B phosphorylation of Dsn1 has been shown to enhance the Mis12-complex:CENP-C interaction (Emanuele et al, 2008; Kim & Yu, 2015; Welburn et al, 2010). Mis12-complex mutants show defects in kinetochore assembly and chromosome segregation (Goshima et al, 2003; Kline et al, 2006). This is consistent with the role of the Mis12-complex as a central "hub" within the KMN network, since it does not only bind directly to the inner kinetochore, but also directly to the other two KMN components, the Knl1-complex (Petrovic et al, 2014; Petrovic et al, 2010) and the Ncd80-complex (Ciferri et al, 2008; Hornung et al, 2011; Malvezzi et al, 2013; Petrovic et al, 2010; Wei et al, 2006).

The Ndc80-complex consists of the Ndc80 (also known as Hec1), Nuf2, Spc24 and Spc25 subunits. It forms an approximately 55 nm long dumbbell-like structure with two globular heads at each end separated by a long coiled-coil region and represents an important organizational element of the KMN network (Bharadwaj et al, 2004; Ciferri et al, 2005; DeLuca et al, 2005; Hori et al, 2003; McCleland et al, 2003; Wei et al, 2005; Westermann et al, 2003). RNAi-mediated depletion of Ndc80-complex subunits causes a kinetochore-null-phenotype, underscoring the important role of the Ndc80-complex in forming stable kinetochore-microtubule attachments, in chromosome alignment and the localization of SAC proteins (DeLuca et al, 2002; McCleland et al, 2003; McCleland et al, 2004; Meraldi et al, 2004). The globular heads of the Spc24/Spc25 dimer are essential for kinetochore localization of the Ndc80-complex, since they directly interact with the Nsl1 and Dsn1 subunits of the Mis12-complex (Cheeseman et al, 2006; Ciferri et al, 2008; DeLuca et al, 2006; Malvezzi et al, 2013; Petrovic et al, 2010). The N-terminal region of CENP-T also interacts with the Spc24/Spc25 dimer, in a phosphorylation dependent manner (Schleiffer et al, 2012; Suzuki et al, 2011). This interaction is competitive with binding of Spc24/Spc25 to Mis12 (Malvezzi et al, 2013; Nishino et al, 2012). The globular heads of the Hec1/Nuf2 dimer at the opposite (N-terminal) end of the Ndc80-complex structure, which fold into a calponin-homology (CH) domain, bind to the plus end of microtubules to create load-bearing attachments (Cheeseman et al, 2006; Ciferri et al, 2008; DeLuca et al, 2006; Wei et al, 2007). Binding to microtubules is furthermore dynamically regulated through Aurora B-mediated phosphorylation of a positively charged N-terminal tail of Hec1, with phosphorylation weakening the binding to microtubules (Alushin et al, 2010; Ciferri et al, 2008; DeLuca et al, 2006; DeLuca et al, 2011; Zaytsev et al, 2015). High-resolution imaging suggested that the Ndc80-complex binds to microtubules in at least two ways. First, it binds via an electrostatic interaction of the positively charged Hec1-tail with negatively charged C-terminal tails of tubulin monomers (E-hooks). Secondly, it recognizes both α- and ß-tubulin at the intra- and inter-tubulin interfaces via the CH-domain of Hec1 (Alushin et al, 2010; Ciferri et al, 2008; Wei et al, 2007). This is thought to facilitate Ndc80 oligomerization on microtubules and to allow binding in a cooperative manner.

1.3 Regulation of kinetochore-microtubule attachments

Being able to discriminate between correct (amphitelic, bi-oriented) and incomplete (monotelic) or incorrect (syntelic, merotelic) kinetochore-microtubule attachments, destabilizing and correcting the latter and stabilizing the first, is crucial for correct chromosome segregation during cell division (Li & Nicklas, 1995; Nicklas & Koch, 1969) (Figure 1-6).

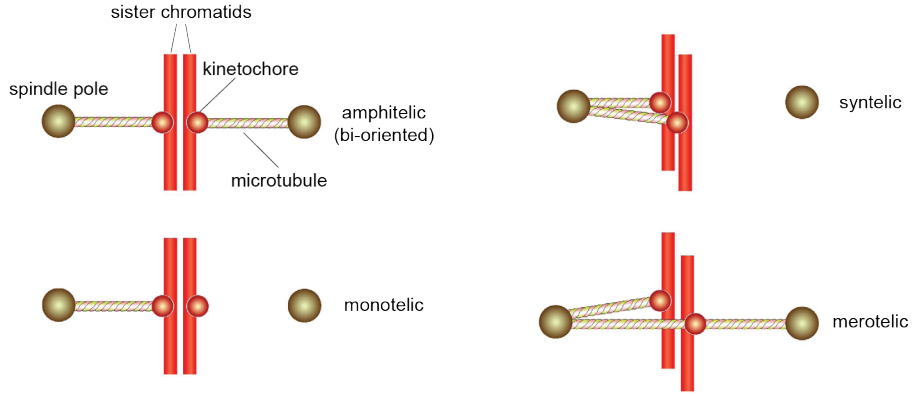

Figure 1-6 Kinetochore-microtubule attachment configurations

In the amphitelic (bi-oriented, correct) configuration sister kinetochores are attached to microtubules emanating from opposite spindle poles. Monotelic attachment is an intermediate condition occuring during prometaphase with only one kinetochore attached to spindle microtubules. In a syntelic attachment (incorrect), both sister kinetochores are attached to microtubules emanating from the same spindle pole. In a merotelic attachment (incorrect) a kinetochore is attached to both spindle poles. Adapted from (Santaguida & Musacchio, 2009).

This implies that microtubule binding of kinetochores on the one hand needs to be sufficiently dynamic so that erroneous attachments can be eliminated. On the other hand, once a correct attachment is stabilized, kinetochores have to remain attached to growing and shrinking microtubules, since chromosome movement in anaphase needs to be powered by microtubule depolymerization. The Dam1 complex in yeast and its potential functional homolog Ska complex in metazoans have been identified as additional microtubule binding complexes that likely contribute to a persistent high affinity kinetochore-microtubule interaction (Asbury et al, 2006; Hanisch et al, 2006; Miranda et al, 2005; Welburn et al, 2009; Westermann et al, 2005; Westermann et al, 2006). Both complexes have been proposed to work through regulation of microtubule binding of the Ndc80-complex, the main microtubule binding complex of

the outer kinteochore (see 1.2.3) (Gaitanos et al, 2009; Schmidt et al, 2012; Tien et al, 2010; Welburn et al, 2009).

Kinetochore-microtubule attachment dynamics are regulated through reversible phosphorylation events by several kinetochore localized kinases and phosphatases, belonging to the "error correction" pathway. Aurora B, a Ser/Thr kinase, and protein phosphatase 2A with a B56 regulatory subunit ($PP2A^{B56}$) are the main players in this pathway (Foley & Kapoor, 2013). Aurora B was originally identified in *S. cerevisiae* as being required for maintenance of ploidy and therefore named Ipl1 (increase in ploidy-1) (Chan & Botstein, 1993). As a part of the chromosomal passenger complex (CPC) together with Survivin, INCENP and Borealin (Carmena et al, 2012), Aurora B localizes to centromeres and plays a conserved role in destabilizing erroneous kinetochore-microtubule attachments (Lampson et al, 2004; Pinsky et al, 2006). For example, inhibition of Aurora B activity with a small-molecule inhibitor results in artificial stabilization of incorrect attachments, whereas re-activation of Aurora B after inhibitor washout allows for the correction of erroneous attachments (Ditchfield et al, 2003; Lampson et al, 2004). This role of Aurora B is at least in parts achieved through phosphorylation of several substrates at the kinetochore, for which it has been suggested that phosphorylation decreases microtubule binding affinity (Welburn et al, 2010). In particular, Aurora B phosphorylates the positively charged N-terminal tail of Hec1, as mentioned above, thereby decreasing the microtubule binding affinitiy *in vitro* and reducing microtubule-induced clustering of Ndc80-complexes (Alushin et al, 2010; Ciferri et al, 2008; DeLuca et al, 2006; DeLuca et al, 2011; Zaytsev et al, 2015). Additionally, Knl1, the Dsn1 subunit of the Mis12-complex and CENP-U are phosphorylated by Aurora B (Akiyoshi et al, 2013; Emanuele et al, 2008; Hua et al, 2011; Welburn et al, 2010; Yang et al, 2008). The effects of these phosphorylation events on kinetochore-microtubule attachments, however, are not fully understood. As the Dam1- and Ska complex are important for the stabilization of kinetochore-microtubule interactions and for retaining the Ndc80-complex at depolymerizing microtubules, Aurora B-mediated phosphorylation of these complexes has also been shown to negatively regulate their association with the Ndc80-complex to prevent precocious stabilization of incorrect attachments (Chan et al, 2012; Schmidt et al, 2012; Tien et al, 2010).

How Aurora B activity is maximized in the presence of incorrect attachments remains a matter of debate. Current models suggest that the spatial separation of Aurora B from its substrates upon the establishment of tension on bi-oriented kinetochores leads to differential levels of phosphorylation of Aurora B substrates. The intra-kinetochore distance (measured from CENP-A to the centromere proximal end of Hec1) has been shown to increase from ~65 nm without tension to ~102 nm in the presence of tension in drosophila S2 cells with similar changes observed in yeast and human (Joglekar et al, 2009; Maresca & Salmon, 2009; Wan et al, 2009). On erroneously attached or unattached kinetochores tension is low and centromere-localized Aurora B is located closer to its kinetochore substrates, leading to a higher level of phosphorylation. Upon bi-orientation, the increase in intra-kinetochore tension limits the access of Aurora B to its substrates, therefore preventing further phosphorylation and allowing phosphatases to reverse Aurora B phosphorylation events (Figure 1-7). This has been elegantly shown with an Aurora B FRET-sensor that reports constitutive, tension-independent phosphorylation positioned close to Aurora B and tension-sensitive phosphorylation of substrates positioned further away from Aurora B (Liu et al, 2009).

A very recent study proposed that the outer kinetochore swivels around the inner kinetochore leading to a distinct mechanical change in kinetochore structure (Smith et al, 2016). The loss of microtubule pulling forces increases swivel. Observed swivel changes are greater than changes in three dimensional intra-kinetochore distance. Thus, this study suggests that instead of changes in intra-kinetochore tension rather changes in swivel are responsible for the proximity change between Aurora B and its substrates. How exactly swivel influences Aurora B kinase activity remains to be investigated (Smith et al, 2016).

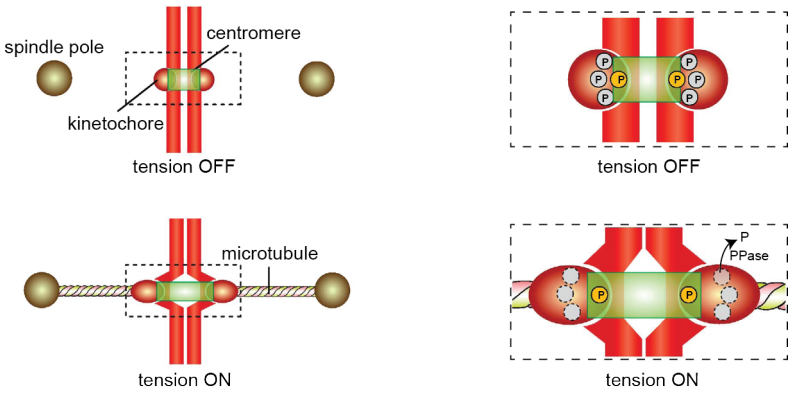

Figure 1-7 Phosphorylation status of kinetochores in response to tension

Left side: schematic of the geometry of the centromere-kinetochore interface in the absence (OFF) and presence (ON) of tension, respectively. Right side: enlargement of the boxed regions on the left showing the tension-induced change in the phosphorylation status of kinetochores. Without tension, kinetochores are closer to the centromere, where Aurora B is located, allowing phosphorylation (P) of centromere (yellow circle) and kinetochore substrates (grey circles). Upon the establishment of tension, kinetochores stretch and distance from centromeres increases, allowing for substrates that cannot be reached anylonger by Aurora B kinase activity to become dephosphorylated by a phosphatase (PPase), whereas phosphorylation of close centromeric substrates persists. Adapted from (Santaguida & Musacchio, 2009).

However, regarding the tension model it is unclear how stable attachments can be generated at the start of mitosis, since in prometaphase (or complete depolymerization of microtubules upon nocodazole treatment) tension is low and therefore accessibility of Aurora B to kinetochore substrates is expected to be highest. Importantly, Aurora B activity is counteracted by the phosphatases $PP2A^{B56}$ and PP1 (Foley et al, 2011; Liu et al, 2010). $PP2A^{B56}$, recruited to unattached kinetochores, is thought to dephosphorylate Aurora B substrates upon an increase in tension, when initial lateral attachments are established, thereby most likely facilitating the establishment of stable end-on attachments (Foley & Kapoor, 2013; Magidson et al, 2011). PP1, most likely targeted to attached kinetochores, additionally ensures that phosphorylation remains low on bi-oriented kinetochores (Liu et al, 2010). However, little is known about the substrate specificity and dynamic regulation of PP1 and PP2A phosphatases at kinetochores.

Several additional proteins contribute to the regulation of kinetochore-microtubule attachments, among them Polo-like kinase 1 (Plk1) (Salimian et al, 2011; Suijkerbuijk et al, 2012b) and several SAC proteins, such as Mps1 (Hewitt et al, 2010;

Maciejowski et al, 2010), Bub1/Bub3 (Warren et al, 2002) and BubR1/Bub3 (Lampson & Kapoor, 2005; Suijkerbuijk et al, 2012b) showing that the spindle assembly checkpoint and the error correction machinery are working closely together (Santaguida et al, 2011). This interconnection creates feedback mechanisms thereby facilitating a rapid response to microtubule binding. Aurora B recruitment to centromeres mostly depends on Haspin-dependent phosphorylation of histone H3 (Kelly et al, 2010; Yamagishi et al, 2010), but also in part on the phosphorylation of Histone H2A by Bub1 (Kawashima et al, 2010). On the contrary, $PP2A^{B56}$ kinetochore recruitment depends on Plk1-mediated phosphorylation of the kinetochore associated regulatory domain of BubR1. Interfering with $PP2A^{B56}$ recruitment leads to increased levels of Aurora B-mediated phosphorylation and prevents the formation of stable kinetochore-microtubule attachments (Kruse et al, 2013; Suijkerbuijk et al, 2012b; Xu et al, 2013). $PP2A^{B56}$ itself regulates phosphorylation of BubR1 and Plk1 recruitment (Foley et al, 2011). The fact that Aurora B is required for the recruitment of SAC proteins to the KMN network in the presence of microtubule depolymerizing drugs (Ditchfield et al, 2003) and that intra-kinetochore stretching determines the state of kinetochore phosphorylation as well as the state of the SAC (Maresca & Salmon, 2009; Uchida et al, 2009) further underscores the close relationship between these two pathways.

1.4 Molecular basis of the spindle assembly checkpoint (SAC)

The spindle assembly checkpoint (SAC) is an ubiquitous molecular safety mechanism that ensures genomic stability. To do so, the SAC coordinates cell cycle progression with the attachment status of chromosomes to microtubules of the mitotic spindle, restricting mitotic exit to cells that have bi-oriented all of their chromosomes. In contrast to what its name suggests, the SAC does not monitor spindle assembly *per se*, but rather the status of kinetochore-microtubule attachments. The overall aim of the SAC is to prevent premature chromosome segregation in the presence of unattached or incorrectly attached chromosomes, which could lead to missegregation resulting in aneuploidy and a high risk for tumorigenesis (Kolodner et al, 2011; Musacchio & Salmon, 2007). In comparison to the above described error correction pathway, which as a "local" mechanism selectively (de-)stabilizes kinetochore-microtubule interactions, the SAC can extend

into a "global" signaling pathway that can operate away from kinetochores and that is able to prevent exit from mitosis in the presence of even a single unattached kinetochore (Dick & Gerlich, 2013; Krenn & Musacchio, 2015).

1.4.1 Generation of the SAC signal

SAC proteins were first identified by genetic screens in *S. cerevisiae* for mutants that bypassed the ability of wild type cells to arrest in mitosis in the presence of spindle poisons (Hoyt et al, 1991; Li & Murray, 1991). Identified SAC components included the mitotic arrest deficient (Mad) genes Mad1, Mad2 and Mad3 (BubR1 in humans) (Li & Murray, 1991), the budding uninhibited by benzimidazole genes Bub1 and Bub3 (Hoyt et al, 1991; Roberts et al, 1994), monopolar spindle protein 1 (Mps1) (Weiss & Winey, 1996) and Aurora B/Ipl1 kinase (Biggins et al, 1999). All of these genes are highly conserved in eukaryotes. Micromanipulation (Li & Nicklas, 1995) and laser ablation experiments (Rieder et al, 1995) indicated that the anaphase-inhibitory signal originates from unattached kinetochores. Indeed, almost all SAC components localize to unattached kinetochores underscoring the theory that the SAC signal is started at kinetochores (Lara-Gonzalez et al, 2012). Despite our knowledge of many of the main players of the SAC, the molecular details of how erroneous attachments are translated into a signal that prevents anaphase onset are still incompletely understood.

The downstream target of the SAC is the anaphase promoting complex or cyclosome (APC/C). The APC/C (a 1.2 MDa protein complex) is a crucial E3 ubiquitin ligase that targets several proteins for degradation via the proteasome. APC/C needs to be activated by one of two co-activators, Cdc20 (responsible for activation of mitotic APC/C) or Cdh1 (responsible for APC/C activation after mitotic exit and therefore not further discussed here) in order to promote ubiquitination of substrates containing specific degron motifs, called destruction (D)-boxes and KEN-boxes (Kramer et al, 1998; Kramer et al, 2000; Peters, 1998). Together with the APC/C subunit Apc10, the co-activator forms a binding site for destruction-box motifs. The KEN-box binding site is on the co-activator (Carroll et al, 2005; Chao et al, 2012; He et al, 2013). Two crucial substrates of APC/C^{Cdc20} are Cyclin B and Securin (Glotzer et al, 1991; Yamamoto et al, 1996). APC/C^{Cdc20}-mediated destruction of Cyclin B results in inactivation of the mitotic driver kinase Cdk1, leading to dephosphorylation of Cdk1

substrates and allowing subsequent exit from mitosis. Degradation of Securin liberates the protease Separase, which in turn cleaves Cohesin thereby eliminating the linkage between sister chromatids, allowing sister chromatid separation and anaphase onset (Funabiki et al, 1996; Holloway et al, 1993; Sudakin et al, 1995) (Figure 1-8).

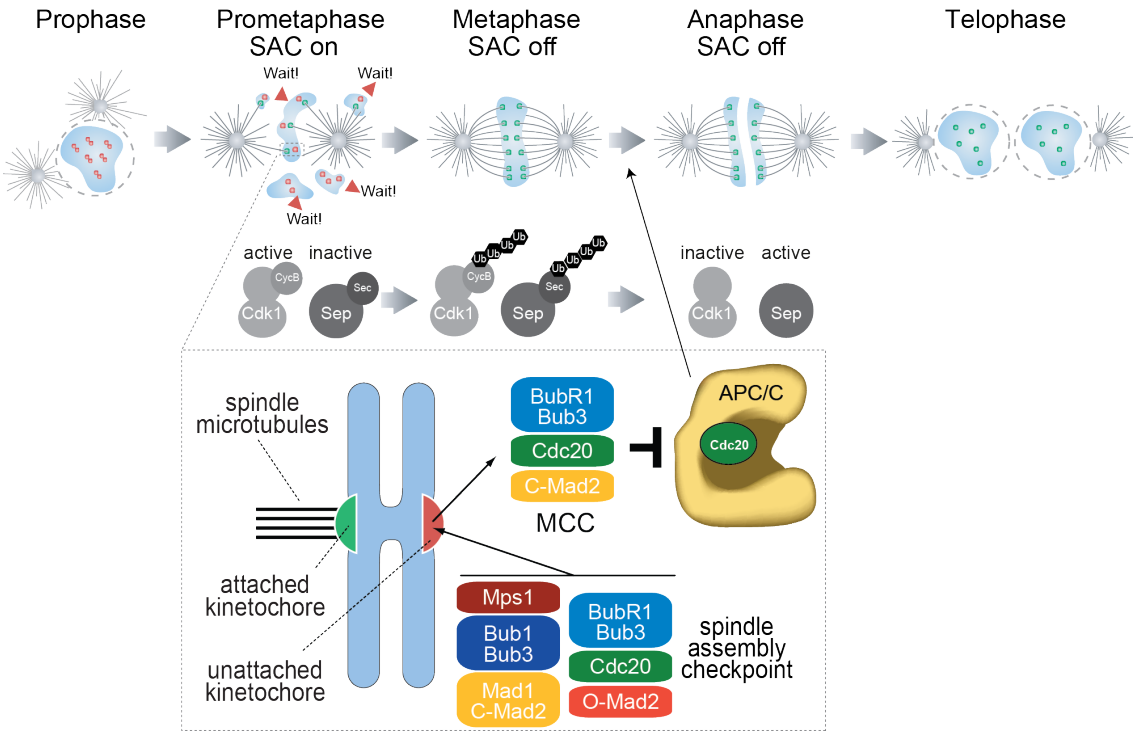

Figure 1-8 Principles of spindle assembly checkpoint signaling

On top a schematic overview of the sequential phases of mitosis is shown. After nuclear envelope breakdown, at the start of prometaphase, unattached kinetochores generate a wait signal to arrest cells in mitosis (box shows schematically what happens at unattached kintochores). This wait signal is generated by the SAC. SAC proteins are recruited to unattached kinetochores, resulting in the formation of the MCC which inhibits APC/C^{Cdc20} thereby stabilizing its substrates Cyclin B (CycB) and Securin (Sec) and preventing progression into anaphase. Once also the last kinetochore has reached bi-orientation the SAC is switched off. This involves among other events the disassembly of the MCC, thereby allowing activation of APC/C^{Cdc20}. This leads to ubiquitination (Ub) and degradation of Cyclin B and Securin, allowing sister chromatid separation through the action of Separase (Sep, liberated from Securin inhibition) and mitotic exit through inactivation of Cdk1. For further details see text. Figure modified from (Overlack et al, 2014).

The SAC inhibits APC/C^{Cdc20} by catalyzing the formation of an inhibitory effector complex, known as the mitotic checkpoint complex (MCC). Thereby APC/C

substrates are stabilized and mitotic exit is prevented to provide time for the cell to establish correct kinetochore-microtubule attachments. MCC is a hetero-tetrameric complex composed of Cdc20/Mad2 and BubR1/Bub3, in which BubR1 and Mad2 bind to distinct sites on Cdc20 (Fraschini et al, 2001; Hardwick et al, 2000; Kulukian et al, 2009; Sudakin et al, 2001) (Figure 1-8). In how far the individual components of the MCC contribute to APC/C^{Cdc20} inhibition remains controversially discussed. Most studies agree that BubR1 and Mad2 synergistically inhibit APC/C via several binding mechanisms (Fang, 2002; Izawa & Pines, 2012; Lau & Murray, 2012; Tang et al, 2001). By binding to the Mad2-interaction motif (MIM) of Cdc20, Mad2 competes directly with the co-activator role of Cdc20 (Izawa & Pines, 2012). BubR1 promotes docking of the MCC onto APC/C, stabilizes the MCC and directly prevents APC/C substrate ubiquitination as a pseudo-substrate through its KEN- and D-boxes (Alfieri et al, 2016; Burton & Solomon, 2007; Lara-Gonzalez et al, 2011; Yamaguchi et al, 2016). Additionally, a displacement of Cdc20 from Apc10 has been observed in cryo-EM studies upon MCC binding to the APC/C, impairing the ability of these proteins to form the D-box receptor (Alfieri et al, 2016; Buschhorn et al, 2011; Herzog et al, 2009; Yamaguchi et al, 2016). Furthermore, incorporation of Cdc20 into MCC has been shown to enhance APC/C-mediated autoubiquitination of Cdc20, which might be required to keep Cdc20 levels below a certain threshold to allow full Cdc20 inhibition by the SAC, but seems at the same time to be required for SAC inactivation (discussed in 1.4.3) (Foe et al, 2011; Foster & Morgan, 2012; Uzunova et al, 2012). Still questionable is the role of Bub3 in the MCC, although recently a role of Bub3 in promoting binding of BubR1 to Cdc20 has been proposed (Han et al, 2014).

A key step in SAC signaling is the catalytic assembly of Mad2 and Cdc20 into a subcomplex that finally forms the MCC with the constitutive BubR1/Bub3 subcomplex (De Antoni et al, 2005; Kulukian et al, 2009; Simonetta et al, 2009; Sironi et al, 2001). Mad2 exists in two distinct conformations in cells. It can adopt an "open" conformation (O-Mad2), that does not bind to Cdc20, and a "closed" conformation (C-Mad2) upon binding to Mad1 or Cdc20, both of which contain a similar Mad2-interaction motif (Luo et al, 2000; Luo et al, 2002; Luo et al, 2004; Sironi et al, 2002; Sironi et al, 2001). Upon mitotic entry a Mad1/C-Mad2 complex is recruited to kinetochores. O-Mad2, which can dimerize with C-Mad2, is recruited to this Mad1/C-Mad2 complex, thereby being converted into C-Mad2 that captures Cdc20 at

kinetochores and forms the Cdc20/C-Mad2 complex (see Figure 1-9). This so called "Mad2-template model" thus proposes a mechanism for the catalytic formation of the Mad2/Cdc20 subcomplex at unattached kinetochores (De Antoni et al, 2005; Mapelli et al, 2007). Elegant *in vitro* FRAP studies (Vink et al, 2006) confirming that two pools of Mad2 exist at kinetochores, one pool being relatively stable (corresponding to Mad1/C-Mad2) and the other pool turning over rather quickly (corresponding to O-Mad2), support this model. In this way, the Mad1/C-Mad2 complex acts as a template for the conversion of O-Mad2 and the generation of a copy, the Cdc20/C-Mad2 complex (De Antoni et al, 2005). This complex is able to engage with BubR1/Bub3 in MCC, although it is still not fully clear how this subsequent step in MCC assembly happens.

The determination of the crystal structure of *S. pombe* MCC (although including only the very N-terminal region of Mad3/BubR1) provided crucial insights into the organization of this complex. The structure reveals that MCC is a cooperative assembly in which each subunit reinforces the binding of the other two subunits (Chao et al, 2012). Mad2 binds to the MIM of Cdc20, exposing Cdc20 for efficient BubR1 binding and BubR1 establishes contacts with both Mad2 and Cdc20 via its N-terminal KEN-box and its TPR repeats (see Figure 1-11 for BubR1 domain organization). This is in agreement with studies showing that Mad2 needs to bind to Cdc20 in order to allow an interaction with BubR1 (Burton & Solomon, 2007; Davenport et al, 2006; Kulukian et al, 2009). Furthermore, as already mentioned, Mad2 and BubR1 have been shown to synergistically inhibit APC/C^{Cdc20} (Fang, 2002; Tang et al, 2001). Interestingly, C-Mad2 bound to Cdc20 interacts with BubR1 via the same interface that is required for O-Mad2 binding (Chao et al, 2012), indicating that C-Mad2 in the MCC is not equivalent to C-Mad2 in the Mad1/C-Mad2 complex and that it might not be able to catalyze the formation of new Cdc20/C-Mad2 subcomplexes. The actual composition of the MCC, also with regard to Bub3 is still not fully understood. In *S. pombe* Bub3, for example, is not part of the MCC and might instead contribute to SAC silencing (Vanoosthuyse et al, 2009). Furthermore, MCC composition has been questioned recently by the observation that a second Cdc20 molecule could be bound by the MCC, presumably via the second KEN-box of BubR1 (Izawa & Pines, 2015; Primorac & Musacchio, 2013). An appealing model proposed that the core MCC, containing one Cdc20, binds to the second Cdc20

molecule when this is already bound to the APC/C (i.e. active APC/C^{Cdc20}), providing an explanation for how kinetochores, through the generation of MCC, can gain control over already active APC/C^{Cdc20} (Izawa & Pines, 2015; Musacchio, 2015; Primorac & Musacchio, 2013). Recent structural work from the laboratories of David Barford, Jan-Michael Peters and Brenda Schulman confirmed this hypothesis (Alfieri et al, 2016; Yamaguchi et al, 2016) Further analyses of APC/C showed that Mad2 may be present in sub-stoichiometric amounts on the APC/C in comparison to Cdc20 and BubR1/Bub3 (Kulukian et al, 2009; Nilsson et al, 2008) and suggested that this remaining "BBC" (BubR1/Bub3-Cdc20) complex might be less stable than MCC but still a good APC/C^{Cdc20} inhibitor. BBC is thought to originate from APC/C^{MCC} after extraction of Mad2 and Cdc20, a necessary reaction for silencing of the SAC (see 1.4.3). Extracted Mad2, after being converted back to its open conformation (Eytan et al, 2014; Ye et al, 2015), can be recycled to form additional MCC complexes. This contributes to maintaining a steady state condition of continuous MCC assembly and disassembly (Musacchio, 2015; Varetti et al, 2011).

1.4.2 Kinetochore recruitment of SAC components

Kinteochores are of crucial importance for the generation of the SAC signal and can be regarded as "catalytic platforms" that determine the rate of MCC formation in response to the kinetochore-microtubule attachment status (Howell et al, 2000; Howell et al, 2004; Shah et al, 2004). Nonetheless, the network of molecular events that initiates the recruitment of SAC proteins to unattached kinetochores is not yet fully understood. Many studies of localization dependencies of SAC proteins have identified the KMN network (see 1.2.3) as the crucial hub in the outer kinetochore that recruits almost all SAC proteins (with the possible exception of Aurora B) in prometaphase (Fava et al, 2011; Kiyomitsu et al, 2011; Kiyomitsu et al, 2007; Liu et al, 2006; London et al, 2012; Martin-Lluesma et al, 2002; McAinsh et al, 2006; Miller et al, 2008; Nijenhuis et al, 2013; Pagliuca et al, 2009; Schittenhelm et al, 2009; Shepperd et al, 2012; Yamagishi et al, 2012). In particular, the Knl1- and the Ndc80-complex have emerged as the crucial receptors for checkpoint proteins.

The recruitment process of checkpoint proteins to the KMN network seems to occur in a partially hierarchical but highly interdependent manner (Figure 1-9).

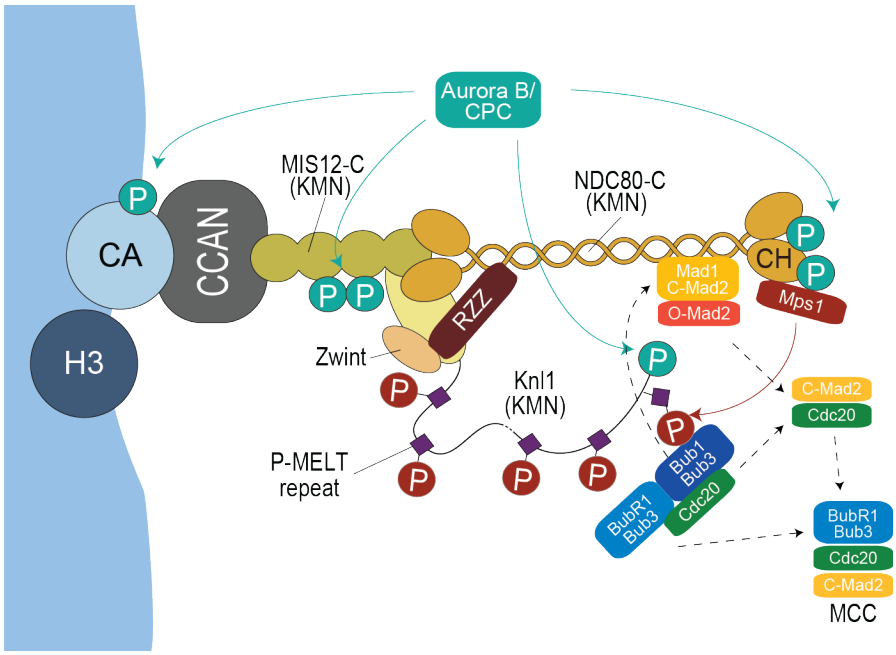

Figure 1-9 Model for the kinetochore recruitment pathways of SAC proteins

Kinetochore recruitment of SAC proteins relies on the Ndc80-branch and the Knl1-branch of the KMN network. Aurora B kinase (enriched at the centromeric region) and Mps1 kinase (recruited to Ndc80 upon Aurora B phosphorylation) phosphorylate several sites on these complexes (P). This leads to recruitment of Bub1/Bub3, BubR1/Bub3, Mad1/Mad2, Cdc20 and RZZ and in ways that are not fully understood results in formation of the MCC. For more details see text. Figure modified from (Musacchio, 2015). CCAN, constitutive centromere associated network; CA, CENP-A; H3, Histone H3.

Chemical inhibition of Aurora B and Mps1 revealed that these kinases significantly contribute to the recruitment of the SAC proteins Bub1, Bub3, BubR1, Mad1 and Mad2 and additional SAC regulatory proteins, such as the RZZ-complex and Dynein. Additionally, their inhibition impaired checkpoint signaling (Ditchfield et al, 2003; Emanuele et al, 2008; Hauf et al, 2003; Kasuboski et al, 2011; Santaguida et al, 2010; Saurin et al, 2011; Vigneron et al, 2004), suggesting that both kinases must act upstream in the hierarchy of the SAC signaling pathway. How these kinases are initially recruited to kinetochores is incompletely understood. Aurora B is a member of the chromosomal passenger complex (CPC) together with INCENP, Survivin and Borealin (Carmena et al, 2012). The CPC localizes to centromeres during early mitosis via the recognition of two histone marks, phospho-Thr3 on Histone H3 and phospho-Thr120 on Histone H2A, created by the kinases Haspin and Bub1, respectively (Kawashima et al, 2010; Kelly et al, 2010; Wang et al, 2010; Yamagishi et al, 2010). Recent studies have proposed that Mps1 is recruited to kinetochores via

a direct interaction with the Ndc80-complex (Aravamudhan et al, 2015; Dou et al, 2015; Hiruma et al, 2015; Ji et al, 2015; Kemmler et al, 2009; Nijenhuis et al, 2013) and this interaction requires Aurora B activity (Santaguida et al, 2010; Vigneron et al, 2004). The identification of a Mps1 binding site near the microtubule binding site of Hec1/Ndc80 raises the question whether Mps1- and microtubule binding is compatible or competitive, which remains controversial due to contradictory evidence (Aravamudhan et al, 2015; Hiruma et al, 2015; Ji et al, 2015; Vazquez-Novelle & Petronczki, 2010). How Aurora B and Mps1 contribute to the recruitment of downstream SAC proteins is slowly emerging. Recent studies have shown that Mps1 phosphorylates so-called MELT ([M/I/L/V]-[D/E]-[I/L/V/M]-[S/T]) repeats in the N-terminal region of Knl1 in yeast and human to recruit Bub1/Bub3 complexes to kinetochores (London et al, 2012; Shepperd et al, 2012; Yamagishi et al, 2012). In turn, the Bub1/Bub3 complex is necessary to recruit BubR1/Bub3, Cdc20 and Mad1/Mad2 (Brady & Hardwick, 2000; Johnson et al, 2004; Vanoosthuyse et al, 2004). However, Bub1/Bub3 is not sufficient to recruit Mad1/Mad2 in the absence of Mps1 activity (Ito et al, 2012; Yamagishi et al, 2012), suggesting that Mps1 in addition to Knl1 phosphorylation contributes another factor to Mad1/Mad2 kinetochore recruitment. Mad1/Mad2 kinetochore recruitment indeed seems to rely on several low-affinity interactions with proteins such as Bub1, RZZ and possibly the Ndc80-complex (Bharadwaj et al, 2004; Brady & Hardwick, 2000; Kim et al, 2012; Klebig et al, 2009; Kops et al, 2005; Martin-Lluesma et al, 2002).

In summary, the localization of SAC components to kinetochores relies on two branches of the KMN network, the Knl1-complex (Bub1/Bub3, BubR1/Bub3) and the Ndc80-complex (Mps1, Mad1/Mad2, RZZ), through various and only partly understood contributions from the kinases Aurora B and Mps1. RZZ and Mad1/Mad2 might be further stabilized by additional interactions with Knl1-bound Zwint-1 and Bub1/Bub3, respectively. This arrangement of SAC proteins provides the molecular basis for MCC formation at unattached kinetochores, but it is still not fully established how exactly subcomplexes are combined in the final MCC complex.

1.4.3 Silencing of the SAC signal

Whereas it is crucial to inhibit APC/C in the presence of unattached kinetochores, it is equally important to relieve APC/C inhibition once all kinetochores have reached bi-

orientation to ensure progression through the cell cycle. SAC silencing is achieved in different ways, through the active removal of checkpoint proteins from attached kinetochores, through phosphatases that counteract the activity of mitotic kinases and through mechanisms that result in disassembly of the MCC to allow APC/C activation (Lara-Gonzalez et al, 2012).

The active removal of SAC components occurs through the minus-end directed motor protein Dynein upon stable kinetochore-microtubule attachment and is called "stripping" (Howell et al, 2001). The Mad1/Mad2 complex is an important SAC component that is removed from attached kinetochores by stripping. This seems to be crucial for efficient SAC inactivation, since tethering of Mad1 to bi-oriented kinetochores by fusing it to Mis12 delays anaphase onset (Maldonado & Kapoor, 2011). The RZZ complex has been implicated in this process of SAC silencing by recruiting Spindly to kinetochores. Spindly in turn is thought to contribute to Dynein recruitment, as Spindly depletion impairs Dynein kinetochore localization. Consequently, RZZ, Mad1/Mad2 and Spindly are removed from kinetochores via Dynein (Chan et al, 2009; Gassmann et al, 2008; Gassmann et al, 2010; Griffis et al, 2007; Karess, 2005; Starr et al, 1998). However, as this Dynein-dependent pathway does not seem to be conserved in yeast and as Mad1/Mad2 is still removed from attached kinetochores in mammalian cells depleted of Spindly, it is likely that other Dynein-independent pathways exist, possibly also in organisms where Dynein is present (Funabiki & Wynne, 2013).

Phosphorylation plays a crucial role in activation of the SAC, consequently phosphatases are expected to play an important role in SAC inactivation. Indeed, SAC silencing has been shown to depend on the recruitment of the phosphatase PP1 to the N-terminal region of Knl1 (Liu et al, 2010; Meadows et al, 2011; Rosenberg et al, 2011) suggesting that especially Knl1 contributes both to SAC activation and inactivation. Disruption of the PP1-binding motif in Spc105 (Knl1 homolog in *S. cerevisiae*) is lethal in *S. cerevisiae* due to a failure in SAC silencing. This phenotype can be rescued by fusing a catalytically active PP1 to Spc105, suggesting that dephosphorylation of PP1 substrates is crucial for its role in SAC silencing (Rosenberg et al, 2011). In human cells, the recruitment of PP1 to the N-terminal region of Knl1 in addition to its role in stabilizing kinetochore-microtubule attachments has recently been implicated in SAC silencing through

dephosphorylation of MELT repeats in Knl1. This dephosphorylation is potentially necessary to remove Bub1/BubR1/Bub3 SAC protein complexes from kinetochores (Espert et al, 2014; Nijenhuis et al, 2014). In agreement with this, the deletion of the PP1 binding domain from the N-terminal region of Knl1 (for domain organization of Knl1 see Figure 1-11) results in elevated Bub1 and BubR1 levels at kinetochores (Zhang et al, 2014). Additionally, the phosphatase $PP2A^{B56}$ has been reported (in addition to its role in monitoring kinetochore-microtubule attachments through counteracting Aurora B activity, thereby promoting PP1 recruitment) to contribute to switching off the SAC. This has been proposed to occur as well through counteracting Mps1 activity by dephosphorylation of MELT repeats in Knl1 (Espert et al, 2014). This illustrates how SAC silencing is regulated by a negative feedback loop in which checkpoint activation results in recruitment of its own inactivators. Since PP1 and $PP2A^{B56}$ do not show substrate selectivity *in vitro* (Boens et al, 2013), little is known about their substrates. Identification of specific phosphatase substrates would therefore help our understanding of how these phosphatases can perform specific regulatory functions at kinetochores. Alternatively, differential spatial targeting of phosphatases could also contribute to establishing substrate specificity (Foley & Kapoor, 2013).

Finally, SAC silencing requires the release of Cdc20 from its inhibitors BubR1/Bub3 and Mad2 in order to allow activation of APC/C. MCC disassembly seems to occur at least via two mechanisms. In one mechanism, the APC/C subunit Apc15 and a protein called $p31^{comet}$ promote APC/C-dependent ubiquitination and subsequent degradation of Cdc20 and the release of C-Mad2 from APC/C^{MCC} (Mansfeld et al, 2011; Uzunova et al, 2012; Varetti et al, 2011; Westhorpe et al, 2011). $p31^{comet}$ has emerged as a bona fide SAC antagonist, as overexpression results in a SAC override and RNAi-mediated depletion delays anaphase onset (Hagan et al, 2011; Jia et al, 2011; Varetti et al, 2011; Westhorpe et al, 2011). Structural data show that $p31^{comet}$ binds to the C-Mad2/O-Mad2 dimerization interface on C-Mad2 (Chao et al, 2012), which, as clarified above, is the same interface that also BubR1 binds to. Thus, $p31^{comet}$ may act at two different levels: 1) by preventing the O-Mad2 interaction with Mad1/C-Mad2, and 2) by interfering with the stability of MCC. Since MCC is a thermodynamically stable complex, the active dissociation of MCC from APC/C requires ATP (Teichner et al, 2011). Therefore, in another, most likely related,

mechanism the recently identified AAA ATPase Trip13 works together with p31^{comet} to disassemble MCC (Eytan et al, 2014; Wang et al, 2014; Ye et al, 2015). Trip13 has been shown to promote the conversion of C-Mad2 back to O-Mad2 *in vitro*, providing a mechanism for its contribution to MCC disassembly (Ye et al, 2015). Whether Trip13 acts on MCC itself, bound to APC/C or rather free MCC, or on Cdc20/C-Mad2 subcomplexes is currently unclear (Figure 1-10). A resulting product of these reactions presumably is the above mentioned APC/C^{BBC}, which as described before is a less stable complex than MCC itself, suggesting that transformation of MCC into BBC may facilitate SAC silencing. How BBC further dissociates from APC/C is currently unclear (Westhorpe et al, 2011). It also remains to be tested, how these mechanisms are controlled by microtubule attachment.

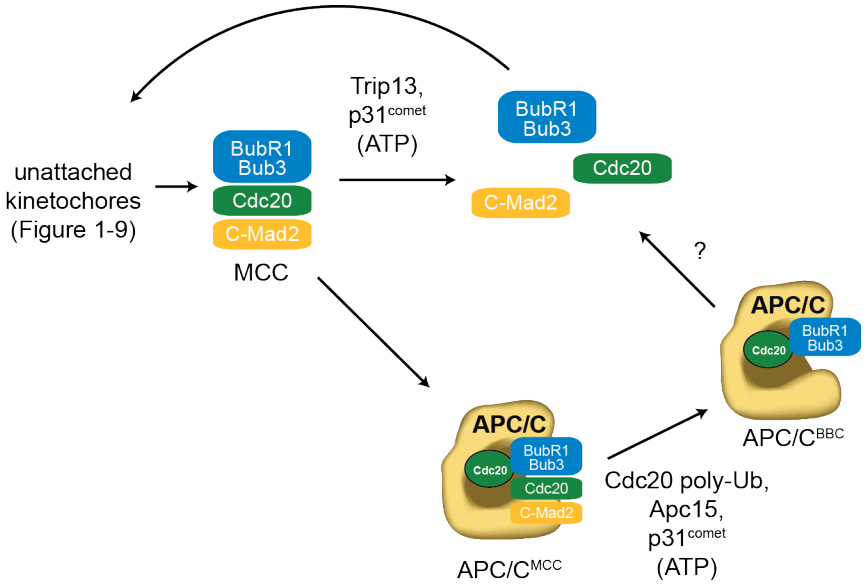

Figure 1-10 Mechanisms of MCC disassembly

Schematic depiction of the different ways contributing to MCC disassembly and reactivation of the APC/C. For details see text. Figure adapted from (Musacchio, 2015).

In conclusion, although many aspects of the dynamic regulation of the SAC are still not fully understood, a few general concepts exist (Musacchio, 2015). First, the SAC can react with different strengths depending on the severity of the condition that activates it (Collin et al, 2013; Dick & Gerlich, 2013). Second, the MCC is a dynamic complex, which is continuously assembled and disassembled, a feature that might be crucial for maintaining the responsiveness of the SAC (Musacchio & Ciliberto, 2012;

Varetti et al, 2011). And third, kinetochore localization of SAC proteins does not only promote SAC activation (1.4.2), but also the active process of SAC inactivation as described above.

1.5 The checkpoint components Bub1 and BubR1

Bub1 and BubR1 are paralogous proteins, that both fulfill crucial functions for the SAC. Bub1 and BubR1 originated from an ancestral gene, that was already present in the hypothetical last eukaryotic common ancestor (LECA), through nine independent gene-duplication events. This invariably led to sub-functionalization of the resulting gene products (Suijkerbuijk et al, 2012a). Therefore, the sequence and domain organization of Bub1 and BubR1 are remarkably conserved (Figure 1-11), however, their mitotic functions are quite distinct.

1.5.1 Functions of Bub1 and BubR1 in mitosis

Bub1 and BubR1 were originally described as essential SAC components (Hoyt et al, 1991; Li & Murray, 1991; Taylor et al, 1998; Taylor & McKeon, 1997). More recently, both were also shown to play an important role in chromosome alignment (Elowe et al, 2010; Harris et al, 2005; Johnson et al, 2004; Lampson & Kapoor, 2005; Meraldi & Sorger, 2005; Taylor et al, 1998). How exactly Bub1 and BubR1 fulfill these functions at the molecular level is not completely understood yet (Bolanos-Garcia & Blundell, 2011; Elowe, 2011).

Bub1 contains a tetratricopeptide repeat (TPR) domain, followed by a Bub3-binding domain in its N-terminal region and a kinase domain in its C-terminal part (Figure 1-11). More recently, a conserved domain I (CDI) and II (CDII) have been identified, the function of which however is so far unclear (Klebig et al, 2009). Very recently, a so-called "ABBA"-motif (due to its presence in the proteins cyclinA, Bub1, BubR1 and Acm1) was identified in Bub1 and in combination with at least one KEN (Lys-Glu-Asp)-box shown to bind to Cdc20 and contribute to kinetochore recruitment of Cdc20 (Di Fiore et al, 2015; Kang et al, 2008; Vleugel et al, 2015a). Bub1 forms a stoichiometric constitutive complex with the checkpoint protein Bub3, a seven-bladed WD40 ß-propeller, a structural domain often used to mediate protein-protein interactions (Hardwick et al, 2000; Larsen et al, 2007; Neer et al, 1994; Roberts et al, 1994; Taylor et al, 1998). The Bub1/Bub3 interaction is mediated by the Bub3-

binding domain (B3BD) of Bub1, which is defined as the segment that *in vitro* is necessary and sufficient for the interaction (Larsen et al, 2007). The B3BD of Bub1 binds to the top surface of the ß-propeller of Bub3 and undergoes a disorder to order transition upon binding (Larsen et al, 2007).

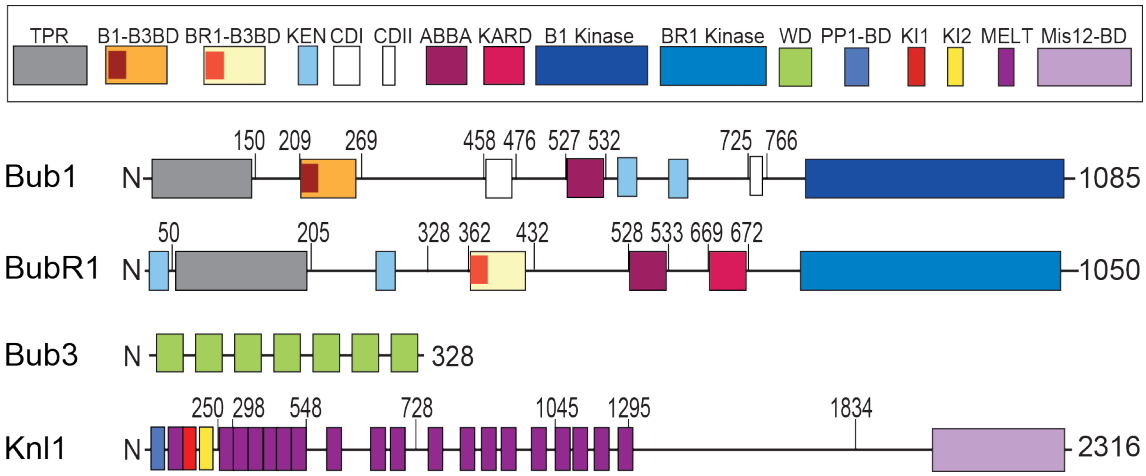

Figure 1-11 Domain organization of checkpoint components

Schematic of the domain organization of human Bub1, BubR1, Bub3 and Knl1. Indicated numbers refer to protein residues. TPR, tetratricopeptide repeats; B1, Bub1; BR1, BubR1; B3BD, Bub3-binding domain; KEN, lysine (K)- glutamic acid (E)- asparagine (N) box; CDI/II, conserved domain I/II; ABBA, cyclinA, Bub1, BubR1, Acm1-motif; KARD, kinetochore associated regulatory domain; WD, tryptophane (W)- aspartic acid (D) repeats; PP1-BD, protein phosphatase 1-binding domain; KI, lysine (K)- isoleucine (I) motif; MELT, methionine (M)- glutamic acid (E)- leucine (L)- threonine (T) repeats; Mis12-BD, Mis12-binding domain.

The interaction with Bub3 is crucial for Bub1 kinetochore localization (see 1.5.2) and Bub1 kinetochore localization might be important or even essential for its functions (Gillett et al, 2004; Taylor et al, 1998; Vanoosthuyse et al, 2004). Bub1 localizes to kinetochores in early prometaphase and is thought to perform its main role in the SAC by acting as a scaffold for the recruitment of other downstream SAC components, such as Mad1, Mad2, BubR1, Bub3 and Cdc20 (Boyarchuk et al, 2007; Brady & Hardwick, 2000; Chen, 2002; Johnson et al, 2004; Klebig et al, 2009; Meraldi & Sorger, 2005; Rischitor et al, 2007; Sharp-Baker & Chen, 2001; Vigneron et al, 2004). Bub1 promotes the incorporation of a subset of these proteins, BubR1/Bub3, Cdc20 and Mad2, into the MCC. Catalysis of MCC formation is likely to occur through positioning these components in close proximity to form a favorable

interaction [discussed in (Overlack et al, 2014)]. Consistently, in yeast and worms, Mad1 is recruited to kinetochores via a direct interaction with Bub1, but it has been challenging to identify such a direct interaction in human cells so far (Kim et al, 2012; London & Biggins, 2014a; Moyle et al, 2014). A physical but weak interaction between Bub1 and BubR1 has been suggested by yeast-two-hybrid assays (D'Arcy et al, 2010; Kiyomitsu et al, 2007). However, direct biochemical evidence and molecular details of such an interaction have been missing so far. Bub1 is a Ser/Thr kinase (Kang et al, 2008) and has been shown to phosphorylate the APC/C co-activator Cdc20 resulting in inhibition of the catalytic activity of APC/C (Kang et al, 2008; Tang et al, 2004). To what extent the phosphorylation of Cdc20 by Bub1 contributes to SAC signaling is unclear, since Bub1 kinase activity does not seem to be required for SAC activation in yeast (Fernius & Hardwick, 2007; Kawashima et al, 2010), in Xenopus egg extracts (Sharp-Baker & Chen, 2001) and in mammalian cells (Klebig et al, 2009; Perera et al, 2007; Ricke et al, 2012). A recent study shows that Plk1, which is recruited to Bub1, also phosphorylates Cdc20 and that this contributes to APC/C inhibition *in vitro*. This might provide an explanation for why Bub1 kinase activity is not strictly required for the SAC, but still little amounts of Bub1 are sufficient to amplify the SAC signal (Jia et al, 2016). However, Bub1 kinase activity is certainly important for its role in establishing stable kinetochore-microtubule attachments. The major established substrate of Bub1 kinase is histone H2A at Ser121 in fission yeast or at Thr120 in human (Kawashima et al, 2010). Histone H2A phosphorylation leads to centromere recruitment of shugoshin (Sgo) proteins (Fernius & Hardwick, 2007; Kawashima et al, 2010; Kitajima et al, 2005) and PP2A, which binds to the N-terminal region of shugoshin (Kitajima et al, 2006; Liu et al, 2013b; Tang et al, 2006; Tanno et al, 2010). PP2A and shugoshin are both important for maintaining sister chromatid cohesion. Furthermore, shugoshin at centromeres has been suggested to facilitate the accumulation of the CPC at centromeres (Kawashima et al, 2010; Yamagishi et al, 2010). Bub1 activity thus contributes to the shugoshin-dependent recruitment of Aurora B to centromeres and to the protection of centromeric cohesion, both required for proper chromosome alignment (Liu et al, 2013a; Liu et al, 2015; Liu et al, 2013b).

BubR1 (Mad3 in yeast) shows an overall very similar domain organization to Bub1 (Figure 1-11). Like Bub1, BubR1 forms a 1:1 complex with Bub3 via its B3BD, with

the binding mechanism being similar and therefore mutually exclusive to Bub1 (Larsen et al, 2007). Unlike Bub1, BubR1 contributes directly to the SAC, as it is a crucial component of the MCC, together with Bub3, Cdc20 and Mad2 (Hardwick et al, 2000; Sudakin et al, 2001). Two KEN-boxes in the N-terminal region of BubR1 have been implicated in Cdc20-binding and APC/C inhibition. The first KEN-box is essential for binding to Cdc20/Mad2 and thus to become incorporated into MCC (Burton & Solomon, 2007; Elowe et al, 2010; King et al, 2007; Lara-Gonzalez et al, 2011), which has been validated by structural data of the *S. pombe* MCC (Chao et al, 2012). The MCC structure furthermore shows that also the TPR domain of BubR1 establishes contacts with Cdc20, consistent with observations that mutations in the TPR domain or the first KEN-box of BubR1 disrupt Cdc20 binding and impair SAC signaling (Burton & Solomon, 2007; Davenport et al, 2006; Kiyomitsu et al, 2007; Lara-Gonzalez et al, 2011). The second KEN-box has been shown to promote BubR1 SAC function by blocking the recruitment of substrates to the APC/C as a pseudo-substrate (Burton & Solomon, 2007; Lara-Gonzalez et al, 2011). Recently, this second KEN-box of BubR1 has been implicated in binding to a second Cdc20 molecule (Alfieri et al, 2016; Izawa & Pines, 2015; Primorac & Musacchio, 2013; Yamaguchi et al, 2016) (see also 1.4.1). Similar to Bub1, BubR1 contains also a binding site for Cdc20 in its C-terminal region, variably called internal Cdc20-binding domain, A-motif, ABBA-motif or Phe-box (due to the presence of two conserved phenylalanines). The functional relevance of this motif has however remained unclear, since mutations of it did not significantly impair BubR1 SAC function in human cells (Davenport et al, 2006; Di Fiore et al, 2015; Diaz-Martinez et al, 2015; Han et al, 2014; Lischetti et al, 2014; Lu et al, 2014).

In addition to its functions in the SAC, BubR1 performs also crucial functions for chromosome alignment. Cells depleted of BubR1 by RNAi do not form stable kinetochore-microtubule attachments (Lampson & Kapoor, 2005). The underlying mechanism for this observation has been subsequently identified. BubR1 contains a highly conserved kinetochore associated regulatory domain (KARD) in its C-terminal region. Phosphorylation of this domain by the kinases Cdk1 and Plk1 promotes a direct interaction with $PP2A^{B56}$, the phosphatase that counteracts Aurora B activity to allow the establishment of stable kinetochore-microtubule interactions (Foley et al,

2011; Kruse et al, 2013; Suijkerbuijk et al, 2012b; Xu et al, 2013). Recently, $PP2A^{B56}$ recruited to kinetochores via the KARD domain of BubR1 has also been implicated in SAC silencing by opposing Mps1 activity [as described in section 1.4.3, (Espert et al, 2014)]. BubR1 comprises, like Bub1, a kinase domain at its C-terminal end. However, whether BubR1 is an active kinase has been a matter of debate. In some studies BubR1 kinase activity was proposed to be required for SAC function as well as SAC silencing, involving inactivation of BubR1 kinase activity upon microtubule capture by the kinesin CENP-E (Malureanu et al, 2009; Mao et al, 2003; Mao et al, 2005). Additionally, it was suggested to contribute to chromosome alignment (Guo et al, 2012; Zhang et al, 2007). However, other studies indicated both SAC function and chromosome alignment to be independent of BubR1 kinase activity (Chen, 2002; Elowe et al, 2007; Huang et al, 2008). More recently, a study by the Kops' laboratory suggested that BubR1 evolved into an inactive pseudokinase, in which the inactive kinase domain is still required to maintain protein conformational stability (Suijkerbuijk et al, 2012a). This may explain previous discrepancies, as point mutations commonly introduced to interfere with kinase activity were shown to impair the structural integrity of BubR1 (Suijkerbuijk et al, 2012a). Furthermore, this is in line with the fact that in other organisms, e.g. in budding and fission yeast, BubR1/Mad3 completely lacks the kinase domain (Suijkerbuijk et al, 2012a; Vleugel et al, 2012) and that human BubR1 *in vitro* can bind to but not hydrolyze nucleotides (Breit et al, 2015). Therefore, the loss of the kinase activity in BubR1 but not in Bub1 can be regarded as one manifestation of the divergence of these proteins after duplication.

Overall, despite a high degree of sequence and structural similarity, Bub1 and BubR1, both assisted by Bub3, perform distinct and non-redundant roles in the SAC and in chromosome bi-orientation.

1.5.2 Kinetochore recruitment mechanism of Bub1 and BubR1

Like all SAC components, Bub1 and BubR1 are recruited to unattached kinetochores in early mitosis (Musacchio & Salmon, 2007). Understanding exactly how these recruitment mechanisms work is therefore highly important, as kinetochore localization might be closely related to the activation and the mitotic functions of Bub1 and BubR1. Pioneering biochemical studies showed that 300 residues in the N-terminal region of murine Bub1, that included the TPR and the B3BD (Figure 1-11),

are sufficient for kinetochore localization (Taylor et al, 1998; Taylor & McKeon, 1997). Further studies demonstrated that the TPR domain of Bub1 is dispensable for kinetochore localization and that the B3BD might be sufficient for Bub1 kinetochore recruitment (Klebig et al, 2009; Krenn et al, 2012; Taylor et al, 1998). This is consistent with studies showing that mutations in the B3BD that prevent binding to Bub3 also prevent kinetochore localization of Bub1 (Klebig et al, 2009) and BubR1 (Elowe et al, 2010; Lara-Gonzalez et al, 2011). These studies argue that the interaction with Bub3 might be necessary and sufficient for kinetochore localization of Bub1 and BubR1. In agreement with this, in yeast Bub3 is required for kinetochore localization of Bub1 and BubR1 (Gillett et al, 2004; Vanoosthuyse et al, 2004; Windecker et al, 2009). In human cells the recruitment dependencies are more controversial, as depletion of Bub3 does not seem to affect Bub1 kinetochore localization although it might affect BubR1 localization (Logarinho et al, 2008).

In agreement with the already presented idea that the KMN network is the crucial recruitment platform for SAC components, dependency studies in different organisms have identified the KMN component Knl1 as the kinetochore receptor for Bub1 and BubR1 (Kiyomitsu et al, 2007; Pagliuca et al, 2009). Two short motifs in the N-terminal region of Knl1, according to the first two residues of their consensus sequence called KI (lysine-isoleucine)-motifs, have been identified to interact with the TPR domains of Bub1 and BubR1, respectively (Bolanos-Garcia et al, 2011; Kiyomitsu et al, 2011; Kiyomitsu et al, 2007; Krenn et al, 2012) (Figure 1-11). KI1 and KI2 have been proposed to be responsible for the kinetochore recruitment of Bub1/Bub3 and BubR1/Bub3, respectively (Kiyomitsu et al, 2011; Kiyomitsu et al, 2007). However, deletions or mutations of the TPR domains of Bub1 and BubR1 that abolish their interaction with KI-motifs do not significantly affect kinetochore localization (Krenn et al, 2012; Lara-Gonzalez et al, 2011). Moreover, also KI1 and KI2 are not necessary for robust kinetochore localization of Bub1 and BubR1 (Yamagishi et al, 2012), arguing that the TPR-KI interaction is not critical for the association of Bub1 and BubR1 with their kinetochore receptor Knl1. This is also somehow in agreement with the described requirement for Bub3 and the fact that KI-motifs so far have only been identified in vertebrate Knl1 orthologs (Bolanos-Garcia et al, 2011; Kiyomitsu et al, 2011; Vleugel et al, 2012). More recently, another motif

has been identified in Knl1, which in contrast to the KI-motifs is conserved in most organisms. This motif conforms to the consensus sequence [M/I/L/V]-[D/E]-[I/L/V/M]-[S/T] and is now generally referred to as MELT repeat [for methionine (M)- glutamic acid (E)- leucine (L)- threonine (T)]. The exact number of MELT repeats in Knl1 largely varies across species. Human Knl1, for example, contains 19 MELT repeats (Figure 1-11), with the repeats being however larger than "MELT" and sequence varying significantly (Vleugel et al, 2015b; Vleugel et al, 2013). The Thr in position four of these MELT repeats has been shown to be a target for the SAC kinase Mps1 (London et al, 2012; Shepperd et al, 2012; Yamagishi et al, 2012) and this phosphorylation is a crucial prerequisite for kinetochore recruitment of Bub1/Bub3. Preventing the phosphorylation of MELT repeats by mutation of the Thr in position four results in chromosome congression defects and a failure to establish a SAC arrest in *S. pombe* and *S. cerevisiae* (London et al, 2012; Shepperd et al, 2012; Yamagishi et al, 2012). A detailed mechanistic insight into how phosphorylation of MELT repeats recruits the Bub1/Bub3 complex has been gained by a recent structural and biochemical study using the *S. cerevisiae* proteins. It demonstrated that phosphorylated MELT repeats bind directly and with high affinity to a well-conserved region on the side of the ß-propeller of Bub3 (Primorac et al, 2013). The ability of Bub3 to bind to phosphorylated MELT repeats is required for kinetochore recruitment of Bub1/Bub3 and for checkpoint function in *S. cerevisiae* (Primorac et al, 2013). Interestingly, it has emerged that not all MELT repeats are equally efficient in Bub1/Bub3 recruitment, and that repeat activity at least in human Knl1 correlates with the presence of additional flanking sequences to the core MELT repeats (Vleugel et al, 2015b; Vleugel et al, 2013). Furthermore, another recent study showed that Plk1 kinase, which has a similar substrate preference as Mps1, cooperates with Mps1 in phosphorylation of MELT repeats (von Schubert et al, 2015). This is in agreement with a study showing that in *C. elegans*, which lacks a gene coding for Mps1, Knl1 MELT repeats are phosphorylated by Plk1 to direct Bub1/Bub3 kinetochore localization (Espeut et al, 2015). Although, all these studies indicate the importance of phosphorylated MELT repeats for the kinetochore recruitment of Bub1/Bub3, it remains unclear how Bub1/Bub3 recruitment can promote downstream SAC signaling events, especially BubR1/Bub3 recruitment. Furthermore, an extremely puzzling fact is that BubR1, which like Bub1 is constitutively bound to Bub3, still

depends on Bub1 for its kinetochore localization whereas Bub1 kinetochore localization is independent of BubR1 (Chen, 2002; Johnson et al, 2004; Klebig et al, 2009; Krenn et al, 2014; Millband et al, 2002; Millband & Hardwick, 2002; Vleugel et al, 2013). This led to the speculation that the ability of Bub3 to bind to phosphorylated MELT repeats might be at least partly suppressed when bound to BubR1 (Krenn et al, 2014; Primorac et al, 2013) and suggests, that there might be yet another interaction that targets BubR1 to kinetochores, distinct from those provided by phosporylated MELT repeats and KI2. Determining precisely how BubR1 is recruited to kinetochores and whether this relies on a direct interaction with Bub1 will be important to complete our understanding of the kinetochore recruitment mechanism of these essential SAC components.

1.6 Objectives

The Spindle Assembly Checkpoint (SAC) is a surveillance mechanism that ensures accuracy of chromosome segregation during mitosis. Bub1 and BubR1, structurally related but functionally distinct checkpoint kinases, are essential SAC components. Unraveling the mechanisms through which protein-protein interactions among checkpoint components are established at kinetochores is essential for understanding how the SAC signal is generated at the molecular level. Specifically, the regulation of kinetochore localization of the essential checkpoint components Bub1 and BubR1 during SAC activation is still not fully understood. Although both proteins are very conserved at the sequence and domain level, they are not only functionally distinct, but also behave differently at kinetochores. Whereas kinetochore recruitment of BubR1 seems strictly dependent on Bub1, Bub1 localizes to kinetochores independently of BubR1. The molecular basis for these differences is still unclear, as Bub1 and BubR1 bind to the same kinetochore-targeting adaptor Bub3 via their conserved Bub3-binding domains. Bub3 has been shown to mediate the binding to phosphorylated MELT repeats of the outer kinetochore protein Knl1. Therefore, subordination of BubR1 to Bub1 recruitment, despite both proteins being bound to Bub3, suggests that Bub3 may operate differently when bound to Bub1 or BubR1.

Consequently, the main aim of my PhD project is to understand the differences in the kinetochore recruitment mechanisms of Bub1 and BubR1 by addressing the following

questions: 1) what is the molecular basis for these differences, 2) how does the recruitment mechanism of BubR1 work and ultimately 3) what are the functional implications of these differences for SAC signaling and kinetochore-microtubule attachments. In particular, the described dependencies shall first be recapitulated in a suitable cellular environment. Subsequently, based on the available structural information mutants will be created to investigate *in vivo* how the Bub3-binding domains of Bub1 and BubR1 account for the different behavior of the proteins. Furthermore, preliminary data hint at a direct interaction between Bub1 and BubR1 as being responsible for BubR1 kinetochore localization. Thus, deletion mapping will be used to identify the exact regions in both proteins mediating the interaction and accounting for BubR1 kinetochore localization. These *in vivo* studies will be complemented by biochemical *in vitro* assays with recombinant material. Thereby, this study will help to further clarify the roles of Bub1 and BubR1 at the kinetochore and shed light on an ubiquitous molecular device that is essential for genome stability of human cells.

2 Materials and Methods

2.1 Materials

2.1.1 Consumables and chemicals

Chemicals that were used in this study were obtained from Fluka, Invitrogen, Merck, Roth and Sigma. Protein- and DNA-ladders were purchased from MBI Fermentas, BioRad and Thermo Scientific.

2.1.2 Kits

Kits used in this study are listed in Table 2-1.

Table 2-1 Kits

Kit	Purpose	Supplier
Nucleo Spin Plasmid (NoLid)	Isolation of plasmid DNA from small bacterial cultures	Macherey-Nagel
QIAGEN Plasmid Maxi Kit	Isolation of plasmid-DNA from large bacterial cultures	Qiagen
QIAquick Gel extraction and PCR purification kit	Purification of DNA	Qiagen

2.1.3 Buffers and solutions

All buffers and solutions that were used are listed with the corresponding method.

2.1.4 Antibiotics

Antibiotics were added to the culture media in the following concentrations (Table 2-2 and Table 2-3).

Table 2-2 Antibiotics for bacteria

Antibiotic	Concentration
Ampicillin	100 µg/ml
Kanamycin	50 µg/ml
Gentamycin	10 ug/ml
Tetracyclin	7 ug/ml

Table 2-3 Antibiotics for mammalian cells

Antibiotics	Concentration
Blasticidin	5 µg/ml
Hygromycin	250 µg/ml
Penicillin	100 U/ml
Streptomycin	0.1 mg/ml
Zeocin	50 µg/ml

2.1.5 Antibodies

All primary and secondary antibodies that were used are listed in the following tables.

Table 2-4 Primary antibodies

Antigen	Origin	Dilution	Supplier/Reference
Apc4	goat	1:100 (WB)	Santa Cruz
Apc7	rabbit, SI0651	1:500 (WB)	in-house made
Bub1	rabbit	1:5000 (WB)	Abcam
Bub1	mouse	1:400 (IF)	Abcam
Bub1	sheep, SB1.3	1:750 (IF)	Taylor et al., 2001
Bub3	mouse	1:1000 (WB)	BD
BubR1	mouse	1:1000 (WB)	BD
BubR1	rabbit	1:1000 (IF)	Bethyl
Cdc20	mouse, H7	1:500 (WB)	Santa Cruz
Cdc27	mouse	1:3000 (WB) 1.5 µg/mg (IP)	BD
c-myc	mouse	1.5 µg/mg (IP)	Calbiochem
CREST	human	1:100 (IF)	Antibodies Inc.
GFP	rabbit	1:1000-1:3000 (WB)	in-house made
Knl1-N	rabbit, SI0787	1:1000 (WB)	in-house made
Knl1-C	mouse, clone 909-1-6	1:500 (WB)	in-house made
Mad2	mouse, clone AS55-A12	1:500 (WB)	in-house made

Mis12	mouse, clone QA21-74-4-3	1:1000 (WB)	in-house made
Tubulin	mouse	1:10000 (WB)	Sigma
Vinculin	mouse	1:20000 (WB)	Sigma

Table 2-5 Secondary antibodies

Antigen	Origin	Dilution	Enzymatic activity/Fluorophor	Supplier
IgG α-mouse	sheep	1:10000	HRP	Amersham
IgG α-goat	donkey	1:10000	HRP	Santa Cruz
IgG α-rabbit	donkey	1:10000	HRP	Amersham
F_c portion of IgG	recombinant ProteinG	1:8000	HRP	Life technologies
IgG α-mouse	goat	1:200	Alexa 488	Jackson Immuno Research
IgG α-mouse	goat	1:200	Rhodamine Red	Jackson Immuno Research
IgG α-mouse	donkey	1:200	Alexa 647	Jackson Immuno Research
IgG α-rabbit	goat	1:200	Rhodamine Red	Jackson Immuno Research
IgG α-rabbit	chicken	1:200	Alexa 647	Invitrogen
IgG α-sheep	donkey	1:200	Rhodamine Red	Jackson Immuno Research
IgG α-sheep	donkey	1:200	Alexa 647	Jackson Immuno Research
IgG α-human	goat	1:200	Rhodamine Red	Jackson Immuno Research
IgG α-human	goat	1:200	Alexa 647	Jackson Immuno Research
IgG α-human	donkey	1:400	DyLight405	Jackson Immuno Research

2.1.6 Oligonucleotides

Oligonucleotides that were used for the polymerase chain reaction (PCR), cloning and site-specific mutagenesis were synthesized by Eurofins MWG Synthesis GmbH or Sigma and are listed in Table 2-6.

Table 2-6 Oligonucleotides

Name	Sequence (5'→3')
Bub1_209_Bf	CGCGGATCCGGAACCATGCGAAGAGTGATCACGATTTC
Bub1_270_Sr	GCGTCGGTCGACTCAATTTACCCATTGCTCATGCTTTC
Bub1_409_Sr	GCGTCGGTCGACTCAattcacacatccagcatctttgc
Bub1_BR1-L 209_Bf	CGCGGATCCGGAACCATGcgaagagtgatcacgaccagaaag
Bub1_Δ271-409_f	gcaatgggtaaataagagtactcatgaattcaagccacagagtggagcagagatc aaag
Bub1_Δ271-409_r	catgagtactcttatttacccattgctcatgctttctccgttgattgtatttctgggc
Bub1_BR1 -LL_f	TATCTTCAGCTTGTGATAAAGAGTCAAATATGGAAAACCA CATCCTAAGCACCAG
Bub1_BR1-LL_r	CCCACGAATAAGCTTCTCCTTGCAATACATCATCTTCTCT TTCTTCTCCTCAGA
Bub1_209-270 ΔL_f	gtgatcacgtccaaagttgatGTTGAGCAGGTTGTTATGTATTGCA AGGAGAAG
Bub1_209-270 ΔL_r	atcaactttggacgtgatcacTCTTCGGGATCCCTTGTACAGCTCG TC
Bub1_Bf	cgcgggatccatggacaccccggaa
Bub1_Xhr	ccgCTCGAGTTATTTTCGTGAACGCTTACATTC
BubR1_Bf	cgcGGATCCatggcggcggtgaagaag
BubR1_432_Bf	cgcGGATCCACCATGctattgaccagtgcagagaag
BubR1_571_Sr	gcgtcgGTCGACtcattcatttgaggtgatgctttctg
BubR1_E409K+E4 13K_f	gaagatttatgcaggagtagggAaattctcctttAaagaaattcgggctgaagttttc c
BubR1_E409K+E4 13K_r	ggaaaacttcagcccgaatttcttTaaaggagaattTccctactcctgcataaatctt c

BubR1_ΔH_f	gaagccgaggagtctcagaaaataccaggaatgactctatccagttctg
BubR1_ΔH_r	ctgagactcctcggcttccctttgctcttttaatttcttccggaaaacttcag
BubR1_B1-LL_f	CAGTTATGACACCATGTAAAATTGAACCTAGTATACGAAG AGTGATCACGATTTCTAAAT
BubR1_B1-LL_r	CCTACTCCTGCATAAATCTTCTCCTTACAATACATAACAA CCTGCTCAACATCAAC
BubR1_vector_f	CTCGGCATGGACGAGCTGTACAAGGGATCCgcggcggtgaa gaaggaaggggtgc
BubR1_vector_r	CGTTAGGGGGGGGGGAGGGAGAGGGGCCTCGACtcactg aaagagcaaagccccaggac
BubR1_ΔL_f	AACCACATCCTAAGCCAAAGGGTTCAGAGCCATCAGCAA GCGTCTGAGGAGAAGAAAGAG
BubR1_ΔL_r	GCTCTGAACCCTTTGGCTTAGGATGTGGTTtatactaggttcaat tttacatggtgtcataac
BubR1_ΔLL_f	attgaacctagtatAAtgtattgtaaggagaagatttatgcaggagtaggggaattct c
BubR1_ΔLL_r	ctccttacaatacaTTatactaggttcaattttacatggtgtcataactggctgttgtg
BubR1-B1 Frag1_r	GATTTAGAAATCGTGATCACTCTTCGtatactaggttcaattttacat ggtgtcataactg
BubR1_B1-B3BD/ B1-H Frag2_f	cagttatgacaccatgtaaaattgaacctagtataCGAAGAGTGATCACG ATTTCTAAAT
BubR1_B1-B3BD/ B1-H Frag2_r	gatagagtcattcctggtattttctgagactcctcggacctttcctgggaag
Bub1-BR1 Frag3_f	cttcccaggaaaggtccgaggagtctcagaaaataccaggaatgactctatc
BubR1_ΔL(Liu)_f	CATCCTAAGCCAAAGGGTTCAGagccatcagcaagcgtctgagga gaag
BubR1_ΔL(Liu)_r	CTGAACCCTTTGGCTTAGGATGtggtttatGGATCCcttgtacagc tcgtccatg
BubR1_ΔL in ΔH_r	CTGAACCCTTTGGCTTAGGATGtggtttatactaggttcaattttacatg gtgtcataactggc

2.1.7 Plasmids for mammalian expression

Plasmids for mammalian expression were derived from the pCDNA5/FRT/TO-EGFP-IRES, a previously modified version (Krenn et al, 2012) of the pCDNA5/FRT/TO vector (Invitrogen). To create N-terminally-tagged EGFP Bub1 and BubR1 truncation constructs, Bub1 and BubR1 sequences were obtained by PCR amplification (2.2.1.1) from the previously generated pCDNA5/FRT/TO-EGFP-Bub1-IRES and pCDNA5/FRT/TO-EGFP-BubR1-IRES vector, respectively (Krenn et al, 2012) and subcloned in frame with the EGFP-tag. All Bub1 constructs were RNAi resistant (Kiyomitsu et al, 2007). BubR1-expressing constructs were made siRNA-resistant by changing the sequence targeted by the RNAi oligos to 'AACGTGCCTTCGAGTACGAGA'. pCDNA5/FRT/TO-based plasmids were used for generation of stable cell lines as well as for transient transfection. All plasmids were verified by sequencing.

2.1.8 Bacterial strains and Media

Plasmids were amplified in OmniMax *E.coli* cells (kindly provided by the Dortmund Protein Facility), bacmids for insect cell expression were recombined in *E.coli* DH10EmBacY cells. Bacteria were cultured in LB (Luria Bertani)-medium or on LB-agar plates supplemented with the appropriate antibiotics and grown at 37 °C.

LB-medium:	10 g Bacto-tryptone, 5 g Yeast extract, 10 g NaCl filled up to 1 l with H_2O and autoclaved pH 7.4
LB-agar:	LB-medium + 1.5 % Bacto Agar

Table 2-7 Bacterial strains

Bacterial strain	Genotype	Supplier
E. coli OmniMax	F- mcrA Δ(mrr-hsdRMS-mcrBC) φ80lacZΔM15 ΔlacZYA-argF U169 endA1 recA1 supE44 thi-1 gyrA96 relA1 tonA panD	Invitrogen
E.coli DH10EmBacY	F$^-$*mcr*A Δ(*mrr*-hsdRMS-*mcr*BC) Φ80*lac*ZΔM15 Δ*lac*X74 *rec*A1 *end*A1	ATG:biosynthetics

	*ara*D139 Δ(*ara*, *leu*)7697 *gal*U *gal*K λ⁻*rps*L *nup*G/pMON14272/pMON7124	

2.1.9 Cell lines

All Flp-In T-REx cell lines (Table 2-8) inducibly express indicated Bub1, Bub3 or BubR1 constructs that were made resistant to the according siRNAs and were generated as described in 2.2.3.4.

Table 2-8 Cell lines

Cell line	Origin	Inducible protein
HeLa	Cervix Adenocarcinoma, human	-
Flp-In T-REx HeLa	human	-
Flp-In T-REx HeLa	human	EGFP
Flp-In T-REx HeLa	human	EGFP-Bub1
Flp-In T-REx HeLa	human	EGFP-Bub1 1-284
Flp-In T-REx HeLa	human	EGFP-Bub1 1-788
Flp-In T-REx HeLa	human	EGFP-Bub1 1-409
Flp-In T-REx HeLa	human	EGFP-Bub1 209-409
Flp-In T-REx HeLa	human	EGFP-Bub1 209-270
Flp-In T-REx HeLa	human	EGFP-Bub1 Δ271-409
Flp-In T-REx HeLa	human	EGFP-Bub1 BR1-L
Flp-In T-REx HeLa	human	EGFP-Bub1 BR1-LL
Flp-In T-REx HeLa	human	EGFP-Bub1 209-270 ΔL
Flp-In T-REx HeLa	human	EGFP-Bub3
Flp-In T-REx HeLa	human	EGFP-BubR1
Flp-In T-REx HeLa	human	EGFP-BubR1 E409K+E413K
Flp-In T-REx HeLa	human	EGFP-BubR1 1-571
Flp-In T-REx HeLa	human	EGFP-BubR1 362-571
Flp-In T-REx HeLa	human	EGFP-BubR1 362-571 E409K+E413K
Flp-In T-REx HeLa	human	EGFP-BubR1 362-431

Flp-In T-REx HeLa	human	EGFP-BubR1 432-571
Flp-In T-REx HeLa	human	EGFP-BubR1 ΔH
Flp-In T-REx HeLa	human	EGFP-BubR1 1-431
Flp-In T-REx HeLa	human	EGFP-BubR1 B1-L
Flp-In T-REx HeLa	human	EGFP-BubR1 B1-L/ΔH
Flp-In T-REx HeLa	human	EGFP-BubR1 B1-LL
Flp-In T-REx HeLa	human	EGFP-BubR1 1-431 B1-LL
Flp-In T-REx HeLa	human	EGFP-BubR1 ΔL
Flp-In T-REx HeLa	human	EGFP-BubR1 ΔLL
Flp-In T-REx HeLa	human	EGFP-BubR1 362-431 ΔL
Flp-In T-REx HeLa	human	EGFP-BubR1 B1-B3BD/B1-H
Flp-In T-REx HeLa	human	EGFP-BubR1 B1-LL/ΔH
Flp-In T-REx HeLa	human	EGFP-BubR1 ΔL/ΔH

2.1.10 Software

For data analysis and figure preparation the following software was used (Table 2-9).

Table 2-9 Software

Software	Version	Supplier
Illustrator CS5.1	15.1.0	Adobe
Photoshop CS5.1	12.1	Adobe
ApE – A plasmid Editor	2.0.45	M. Wayne Davis
Image J	1.46r	National Institutes of Health
Excel	14.5.2	Microsoft
Word	14.5.2	Microsoft
GraphPad Prism	6.0	GraphPad Software
Imaris	7.3.4	Bitplane

2.2 Methods

2.2.1 Microbiological methods

2.2.1.1 Polymerase chain reaction (PCR)

The polymerase chain reaction (PCR) technique allows amplification of a specific DNA sequence. A standard protocol for a PCR is shown in Table 2-10.

Table 2-10 standard PCR procedure

Reaction Mix	PCR programme	
30-60 ng DNA template	1. 98 °C	30 s
10 µM forward primer	2. 98 °C	15 s
10 µM reverse primer	3. 58 °C	30 s
1x Flash Phusion	4. 72 °C	30 s goto 2x29
Polymerase Mix	5. 72 °C	10 min
H_2O ad 20 µl	6. 4 °C	hold

In this study, two different DNA-polymerases were used, depending on the purpose of the PCR. To generate DNA fragments of the SAC proteins, which should be used for further cloning, Phusion Flash Polymerase (Finnzymes) was used. This enzyme has a high fidelity (error rate of $4.4x10^{-7}$) and processivity, which allows rapid and accurate amplification of DNA fragments. The temperature optimum of Phusion Flash Polymerase is at 72 °C and the polymerase needs an extension time of 15 s/1 kb.
Analytical PCRs were carried out to check whether cloning was successful. Since the DNA fragments generated in this PCR were not used in any downstream procedures Crimson Taq Polymerase (NEB) was chosen. This enzyme is less active than Phusion Flash Polymerase and shows a higher error rate ($2x10^{-5}$-$2x10^{-4}$) during DNA amplification. The temperature optimum of Crimson Taq Polymerase is at 68 °C and the polymerase needs an extension time of 1 min/1 kb.

2.2.1.2 Agarose gelelectrophoresis

Agarose gelelectrophoresis was used to separate dsDNA molecules according to their molecular weight for example after PCR or restriction digestions. The agarose concentration in the gel depends on the size of the DNA fragments to be separated.

Here, an agarose concentration of 0.9 % (w/v) was used most of the times. The agarose was dissolved in 1x TAE buffer. Midori green advanced DNA stain (Nippon Genetics) was added in a 1:25000 dilution. DNA loading buffer was added to the samples before loading them onto the gel. Electrophoresis was performed at 100 V. After electrophoresis, the DNA was visualized using blue or UV light.

TAE (10x)	48.4 g Tris, 11.4 ml glacial acetic acid, 3.7 g EDTA fill up to 1 l with H_2O
DNA loading buffer (6x)	30 % (w/v) sucrose, 20 % (v/v) glycerol, 0.2 % (w/v) orange G

2.2.1.3 DNA extraction from agarose gels

DNA extraction from agarose gels was performed with the Gel extraction and PCR purification kit (Qiagen) according to manufacturer's instructions.

2.2.1.4 Determination of DNA concentration

Concentration of nucleic acids was determined by measuring the absorbance at 260 nm with a NanoDrop2000 spectrophotometer (Thermo Scientific). An absorbance of 1 corresponds to a dsDNA concentration of 50 µg/ml. Contamination with proteins is determined by measuring the absorbance at 280 nm. Contamination with salt or organic compounds is measured at 230 nm. For pure DNA the ratios of $A_{260nm/280nm}$ and $A_{260nm/230nm}$ should be greater than 1.8.

2.2.1.5 Restriction enzyme digestion, dephosphorylation, ligation

Restriction enzyme digestions of vectors and inserts were performed in the recommended buffers for the corresponding enzymes supplied by the company New England Biolabs (NEB) either for 3-4 h or over-night at 37 °C. Typically, 1-2 µg of DNA were digested in one reaction using approximately 1 µl of each restriction enzyme per µg of DNA. To avoid self-ligation of digested vectors 0.5 µl of fast alkaline phosphatase was added to these reactions. After successful restriction digestions of inserts and vectors, both were purified by gel extraction with the Gel Extraction and PCR Purification Kit (Qiagen). For ligation of insert and vector with the Rapid DNA Ligation Kit (Thermo Scientific) a 3-6 fold molar excess of insert and 10-100 ng of linearized vector were used in a 20 µl reaction. The reaction mix was

incubated according to manufacturer's instructions. Ligation of the vector without insert was used as negative control. Reactions were subsequently transformed into competent *E.coli* OmniMax cells by heat-shock and the mix was plated on LB-agar plates containing the appropriate antibiotics. Positive clones were verified by DNA sequencing (Beckman Coulter Genomics).

2.2.1.6 Restriction free cloning

This method, which is independent of restriction enzyme sites, uses two rounds of PCR to first generate a "megaprimer" containing complementary sequences to both the insert and the target vector. This megaprimer is subsequently used in the second PCR with the target vector as template to create the desired construct (Bond & Naus, 2012).

2.2.1.7 Site-directed mutagenesis

Site-directed mutagenesis was used to introduce single or multiple base substitutions into the DNA of the corresponding constructs to obtain mutations in the amino acid sequence according to the QuickChange site-directed mutagenesis protocol (Stratagene). Deletion constructs of Bub1 and BubR1 were created according to a mutagenesis protocol by Liu and Naismith, 2008.

2.2.1.8 Transformation of chemically competent bacterial cells

Chemically competent *E. coli* OmniMax cells were thawed on ice. 0.2-1 µg of plasmid-DNA was added to 50 µl of competent cells. The mixture was incubated on ice for 10 min, followed by a heat-shock for 45 s at 42 °C in a heating block (Eppendorf). Afterwards, LB-medium was added and cells were incubated at 37 °C for 1 h shaking at 300 rpm. After incubation, 150 µl of the bacterial suspension was plated on a LB-agar plate containing the appropriate antibiotic and incubated over-night at 37 °C.

2.2.1.9 Plasmid isolation from bacterial cells

For isolation of plasmid-DNA the principle of alkaline lysis followed by a chromatographic purification was applied. For small-scale plasmid preparations, 4 ml of LB-medium containing the appropriate antibiotic was inoculated with one bacterial clone and grown at 37 °C over-night. For large-scale plasmid preparations, 250 ml of

LB-medium were inoculated 1:10 with an over-day grown starter culture. Isolation of plasmid-DNA was performed using the Mini- or Maxiprep Kits (Macherey-Nagel, Qiagen) according to manufacturer's instructions.

2.2.2 Biochemical methods

2.2.2.1 SDS polyacrylamide gel electrophoresis (SDS-PAGE)

Sodiumdodecylsulfate (SDS) polyacrylamide gel electrophoresis is an analytical method, which allows separation of proteins according to their molecular weight. The negatively charged detergent SDS denatures protein structure and evenly covers the polypeptide chain with portions of negative charge. As a consequence, proteins move through the network of polyacrylamide towards the anode with a speed corresponding to their molecular weight. Smaller proteins pass faster through the polyacrylamide network, whereas larger proteins move more slowly. The concentration of polyacrylamide determines the size of pores in the resulting gel matrix and is therefore chosen according to the size of the protein of interest.
SDS-gels (12.5 %) were prepared according to the scheme in Table 2-11.

Table 2-11 Composition of SDS polyacrylamide gels

	Separating gel (12.5 %)	Stacking gel (4%)
Acrylamide (30 %)	3.3 ml	0.8 ml
Separating/Stacking gel buffer (4x)	2.5 ml	1.25 ml
H_2O	4.2 ml	3 ml
APS (10 %)	100 µl	50 µl
Temed	10 µl	5 µl

To analyze shifts in the migration behavior of SAC proteins caused by phosphorylation special 7.5 % SDS-gels (with a 80:1 acrylamide/bis-acrylamide ratio) were used. Before loading the protein samples on the gel, they were mixed with SDS-loading buffer and denatured for 5 min at 95 °C. Electrophoretic separation of proteins was performed at 150 V in 1x SDS running buffer.

Acrylamide/Bisacrylamide 30 % (w/v)/ 0.8 % (w/v)

APS 10 % (w/v) in H_2O

Separating gel buffer (4x)	1.5 M Tris-HCl, 0.4 % SDS, pH 8.8
Stacking gel buffer (4x)	0.5 M Tris-HCl, 0.4 % SDS, pH 6.76
SDS running buffer	25 mM Tris-HCl, 192 mM Glycine, 0.1 % SDS (w/v)
SDS loading buffer (5x)	5 mM EDTA, 60 mM Tris-HCl pH 6.8, 7.5 % (v/v) 250 mM DTT, 15 % (w/v) SDS, 30 % (v/v) Glycerol, 0.1 % (w/v) Bromphenolblue

2.2.2.2 Coomassie blue staining

Proteins separated by SDS-PAGE were visualized by Coomassie brilliant blue staining. This method allows identification of proteins by protein size. Gels were stained in buffer A and subsequently destained in buffer B for several hours on a shaker.

Buffer A	25 % (v/v) isopropanol, 10 % (v/v) acetic acid, 0.05 % (w/v) Coomassie R250
Buffer B	10 % (v/v) acetic acid

2.2.2.3 Western Blot

Immunodetection of proteins by Western blotting was performed as follows. After electrophoresis, proteins were transferred onto a nitrocellulose membrane (GE Healthcare) in the blotting apparatus (BioRad) at 100 V for 1.5 h at 4 °C. The transfer was controlled by staining the membrane with PonceauS solution (BioRad), which rapidly and reversibly detects proteins. After washing the PonceauS stain away, the membrane was blocked in 5 % milk powder/TBST either over-night at 4 °C or for 30 min at RT. All incubation steps were performed on a shaker. Sufficient primary antibody was diluted in 5 % milk powder/TBST (Table 2-4) and incubated with the membrane for 2 h at room temperature or over-night at 4 °C. After washing with TBST (3x5 min), the membrane was incubated with the appropriate secondary antibody diluted in 5 % milk powder/TBST (see Table 2-5) for 45 min at room temperature. This step was followed by three washes with TBST for 5 min. Bound antibodies were visualized via chemiluminescence with the ECL Prime Western Blotting Detection Reagent™ (GE Healthcare) according to manufacturer's instructions. After incubation with the ECL Western blotting reagent, images were acquired with ChemiBIS 3.2 (DNR Bio-Imaging Systems) or the ChemiDoc™ MP

Imaging System (BioRad) in 16-bit TIFF format. Images were cropped and converted to 8-bit using ImageJ software, brightness and contrast was adjusted using Photoshop CS5.1 (Adobe). Unmodified 16-bit TIFF images were used for quantification with ImageJ software. Measurements were graphed with Excel (Microsoft) and GraphPad Prism version 6.0 for Mac OS X (GraphPad Software).

Transfer buffer (1x)	25 mM Tris, 200 mM Glycine, 20 % (v/v) Methanol
TBST	50 mM Tris-HCl, 150 mM NaCl, 0.1 % Tween 20

2.2.2.4 Immunoprecipitation

To generate mitotic populations for immunoprecipitation experiments, cells were treated with 330 nM nocodazole for 16 h. Mitotic cells were then harvested by shake off and lysed in lysis buffer. Extracts were precleared using a mixture of protein A–Sepharose (CL-4B; GE Healthcare) and protein G-Sepharose (rec-Protein G-Sepharose 4B; Invitrogen) for 1 h at 4 °C. Subsequently, extracts were incubated with GFP-Traps (ChromoTek; 3 µl/mg of extract) for 3 h at 4 °C. Immunoprecipitates were washed with wash buffer and resuspended in SDS loading buffer, boiled and analyzed by SDS-PAGE and Western blotting using 4-12 % gradient gels (NuPAGE® Bis-Tris Gels, Life technologies).

For Cdc27 IPs harvested mitotic cells were lysed in lysis buffer and extracts were precleared with protein G-Sepharose for 1 h at 4 °C. Afterwards, extracts were incubated with 1.5 ug/mg of the Cdc27 primary antibody for 2 h at 4 °C. Subsequently, protein G-Sepharose was added for 4 h at 4 °C. Immunoprecipitates were washed and analyzed as described above.

Lysis buffer	150 mM KCl, 75 mM Hepes, pH 7.5, 1.5 mM EGTA, 1.5 mM $MgCl_2$, 10 % glycerol, 0.075 % NP-40 supplemented with protease inhibitor cocktail (Serva) and PhosSTOP phosphatase inhibitors (Roche)
Wash buffer	Lysis Buffer without protease and phosphatase inhibitors
Mild wash buffer (used for SILAC IPs)	75 mM Hepes, pH 7.5, 1.5 mM EGTA, 1.5 mM $MgCl_2$, 10 % glycerol, 0.075 % NP-40 supplemented with PhosSTOP phosphatase inhibitors

2.2.2.5 Virus production and protein expression in insect cells

The genes for the BubR1 constructs to be expressed in the baculovirus/insect cell system were subcloned into the pFLMultiBac vector (Trowitzsch et al, 2010) and verified by sequencing. Those plasmids were transformed into DH10EMBacY cells following the standard transfection protocol, with the exception of extending the recovery time to 5 h at 37 °C. EMBacY cells contain the baculovirus genome as a bacterial artificial chromosome into which the gene of interest is integrated by homologous recombination. Transformed cells were plated in different dilutions onto LB-agar plates containing 50 µg/ml Kanamycin, 10 µg/ml Gentamycin, 7 µg/ml Tetracyclin, 40 µg/ml IPTG and 100 µg/ml X-Gal. Positive integrants were selected by blue (negative)-white (positive) screening. Single white colonies were grown over night at 37 °C in LB medium supplemented with 50 µg/ml Kanamycin, 10 µg/ml Gentamycin and 7 µg/ml Tetracyclin. From these cultures the Bacmid-DNA was isolated using the QIAprep Miniprep Kit (Qiagen), but instead of purifying the Bacmid-DNA via the provided column, it was precipitated with 100 % isopropanol at -20 °C over night. The Bacmid-DNA was washed in 70 % Ethanol and afterwards resuspended in sterile TE-buffer. For virus production, the Bacmid-DNA was transfected using Fugene (Promega) into Sf9 (*Spodoptera frugiperda*) cells in a 6-well plate at a density of $1*10^6$ cells/ml. Cells were incubated at 27 °C for 72 h. Then, the supernatant was transferred to fresh Sf9 cells at a density of $1*10^6$ cells/ml in a 10 cm dish. Cells were incubated at 27 °C for 96 h to allow virus amplification. The supernatant was collected and stored as $Virus_0$ at 4 °C. Subsequently, 50 ml of Sf9 cells at $1*10^6$ cells/ml growing in suspension were infected with 1:100 V_0 to produce V_1 or with 1:100 V_1 to produce V_2, respectively and incubated for 96 h at 27 °C in a shaker. V_2 was used to infect 1 l of a Tnao38 (*Trichoplusia ni*) insect cell culture 1:20 at a density of $1*10^6$ cells/ml. For co-expression of the BubR1 mutants with Bub3, insect cells were co-infected with the V_2s for Bub3 and the corresponding BubR1 mutant. Cells were grown for 72 h at 27 °C and afterwards harvested at 750 g for 12 min in a Sorvall centrifuge RC3BP+ with a H6000A rotor (Thermo Fisher Scientific). The pellet was resuspended in PBS, centrifuged at 500 g for 5 min, the supernatant was discarded and the pellet was stored at -20 °C.

2.2.2.6 Protein purification from insect cells

The pellet was thawed on ice and resuspended in 250 ml of lysis buffer. Directly before sonication, 1mM PMSF protease inhibitor was added. Lysates were sonicated (Sonifier® Cell Disruptor, Branson Ultrasonics Corp.), centrifuged at 30000 rpm for 30 min at 4 °C (Rotor JA30.50, Avanti-J30I, Beckman Coulter) and filtered using 0.8 µm Rotilabo® syringe filters (Carl Roth GmbH). The cleared lysate was passed onto a 5 ml HisTrap FF affinity column (GE Healthcare) using the ÄKTA Prime Plus system (GE Healthcare). The bound complex was washed with lysis buffer to get rid of unspecifically bound proteins and subsequently eluted with 300 mM imidazole. The eluted protein was concentrated using Amicon Ultra-15 Centrifugal Filters 30K MWCO (Merck Millipore) at 5000 rpm at 4 °C until a volume of approximately 2 ml was reached. The concentrated protein was further purified by size exclusion chromatography on a S200 16/60 gelfiltration column (GE Healthcare) using an ÄKTA Purifier (GE Healthcare). The fractions containing the protein sample were monitored by the absorption at 280 nm, analyzed by SDS-PAGE, pooled and concentrated as described above. All purification steps were performed at 4 °C. Afterwards, protein was aliquoted, snap frozen in liquid nitrogen and stored at -80 °C.

Lysis buffer	25 mM Hepes pH 7.5, 300 mM NaCl, 5 % glycerol, 10 mM imidazole, 1 mM TCEP
Elution buffer	25 mM Hepes pH 7.5, 300 mM NaCl, 5 % glycerol, 300 mM imidazole, 1 mM TCEP
Gelfiltration buffer	10 mM Hepes pH 7.5, 150 mM NaCl, 5 % glycerol, 1 mM TCEP

2.2.2.7 Analytical size exclusion chromatography (SEC) migration shift assay

This chromatographic method separates protein complexes based on their size and shape. It is based on the principle that larger proteins do not enter the pores of the column matrix as well as smaller proteins do and therefore elute earlier. Proteins tested for interactions were diluted to a final concentration of 5 µM in 50 ul reactions in binding buffer and incubated at 4 °C over night. Complex formation was analyzed by size exclusion chromatography on a Superdex 200 5/150 increase column (GE Healthcare). Eluates were analysed by SDS-PAGE and Coomassie staining.

Binding buffer	10 mM Hepes pH 7.5, 150 mM NaCl, 5 % glycerol, 1 mM TCEP, 1 mM $MgCl_2$

2.2.2.8 APC/C-mediated ubiquitination assay

To measure the activity of APC/C its ability to form poly-ubiquitin chains on its substrate Cyclin B was analyzed. HeLa cells were treated with 330 nM nocodazole for 16 h to generate mitotic populations and harvested by shake-off. Cell were lysed in extract buffer and APC/C was precipitated with anti-Cdc27 or anti-Apc7 beads for 1.5 h at 4 °C. Co-purifying endogenous MCC was subsequently disassembled from this APC/C through incubation with 12.5 µM UbcH10 for 1.5 h at 23 °C. Resulting apo-APC/C was pre-activated with 1 µM Cdc20 for 1 h at 23 °C using 5 µl APC/C-bound beads per reaction. Afterwards, over-night pre-formed MCCs were added in different concentrations together with the ubiquitination mix (4 µM Uba1, 12.5 µM UbcH10, 200 µM Ubiquitin, 20 mM ATP, 20 mM $MgCl_2$, 0.25 mg/ml BSA, 1 mM DTE in UBA-buffer). Reactions were started by the addition of 1 µM fluorescein-labelled Cyclin B (residues 1-87) substrate. After an incubation of 1 h at 37 °C, samples were centrifuged, the supernatant was transferred into a new tube and mixed with SDS loading buffer to stop the reaction. Samples were analyzed by SDS-PAGE and fluorescence scanning.

extract buffer	30 mM Tris pH 7.5, 150 mM NaCl, 5 % glycerol, 0.05 % Tween, 2 mM EDTA, 2 mM DTE
1x UBA-buffer	35 mM Tris pH 7.5, 150 mM NaCl

2.2.3 Cell biological methods

2.2.3.1 Cell culture and transfections

HeLa cells were grown in 10 cm dishes (Sarstedt) in DMEM (PAN Biotech) supplemented with 10 % FBS (Clontech), penicillin and streptomycin (GIBCO) and 2 mM L-glutamine (PAN Biotech). Cells were grown in a humidified atmosphere of 37 °C and 5 % CO_2. To prevent contamination, all working steps were performed under a laminar flow. For all transient plasmid transfections of HeLa cells X-tremeGENE transfection agent (Roche) was used according to manufacturer's instructions at a 3:1 ratio with plasmid DNA.

2.2.3.2 Freezing cells

For long-term storage cells were frozen in FBS containing 10 % DMSO as cryoprotective agent. Cells are placed in a special isopropanol containing container and stored over night at -80 °C in order to allow a slow and continous lowering of the temperature to -80 °C. Afterwards, cells were transferred to -150 °C.

2.2.3.3 Thawing cells

In contrast to freezing, thawing needs to occur rapidly. Therefore, frozen aliquots were thawed at 37 °C. Then, cells were resuspended in the corresponding medium and centrifuged for 3 min at 1200 rpm to remove remaining DMSO. Afterwards, the pellet was resuspended in fresh medium and cells were plated on the culture dish.

2.2.3.4 Generation of stable cell lines

To generate stable cell lines, the Flp-In T-REx system (Invitrogen) was used. This system allows the generation of stable mammalian cell lines showing Tetracycline-inducible expression of a gene of interest (GOI) from a defined genomic locus. Briefly, this system is based on a Flp-In T-REx host cell line carrying a unique Flp Recombination Target (FRT) site together with a Zeocin resistance gene. This host cell line has been engineered to contain a Tet repressor cassette (combined with a Blasticidin resistance) that drives constitutive expression of the Tet repressor protein. Therefore, the Flp-In T-REx host cell line is Zeocin and Blasticidin resistant. The GOI is cloned into the pCDNA5FRT-TO plasmid containing a FRT site and a Hygromycin resistance gene. To generate the corresponding stable Flp-In T-REx cell line, the pCDNA5FRT-TO plasmid with the GOI is cotransfected with the pOG44 vector, that codes for the Flp recombinase, into the host cell line. The Flp recombinase mediates the homologous recombination between the two FRT sites, resulting in integration of the GOI into the genome at the unique FRT site. Upon successful integration, Zeocin resistance is lost and Hygromycin resistance is gained. Cells that integrated the GOI therefore become sensitive to Zeocin, but resistant to Hygromycin and Blasticidin and can be selected with medium containing these two antibiotics. The constitutively expressed Tet repressor binds to the Tet operator in the promotor region of the GOI, resulting in repression of transcription. Expression of the GOI can be induced by the addition of Tetracycline or its analog Doxycycline to the culture medium. Tetracycline

binds the Tet repressor and thereby prevents it from binding to the Tet operator, hence allowing transcription of the GOI.

Flp-In T-REx HeLa host cells used to generate stable Doxycycline-inducible cell lines were a gift from S. S. Taylor (University of Manchester, Manchester, England, UK). Flp-In T-REx host cell lines were maintained in DMEM with 10 % tetracycline-free FBS (Clontech) supplemented with 50 µg/ml Zeocin (Invitrogen). Flp-In T-REx HeLa expression cell lines were generated by co-transfections of the pCDNA5FRT-TO plasmid containing the GOI and the pOG44 vector using X-tremeGENE 9 DNA transfection reagent (Roche) according to manufacturer's instructions. 48 h after transfection, the selection was started in DMEM supplemented with 10 % Tet-free FBS, 2 mM L-glutamine, 250 µg/ml Hygromycin (Roche) and 5 µg/ml Blasticidin (ICN chemicals). After two weeks, single cell clones were transferred to separate dishes and expanded to be frozen and characterized for expression of the GOI. Gene expression was induced by addition of 0.05-0.5 µg/ml Doxycycline (Sigma) for 24 h.

2.2.3.5 RNA interference and synchronization

To downregulate the expression of specific endogenous genes of interest, the technique of RNA interference was used. siBUB1 (GE Healthcare Dharmacon; 5'-GGUUGCCAACACAAGUUCU-3') or siBUBR1 (GE Healthcare Dharmacon; 5'-CGGGCAUUUGAAUAUGAAA-3') duplexes were transfected with Lipofectamine 2000 (Invitrogen) at 50 nM for 24 h according to manufacturer's instructions. Doxycycline was added together with the siRNA for 24 h to induce expression of the siRNA resistant transgenes.

For experiments in HeLa cells, cells were synchronized with a double thymidine arrest 5 h after transfection with siRNA duplexes. In brief, after washing the cells with PBS they were treated with thymidine for 16 h and then released into fresh medium. 3 h after the release, 50 nM siRNA duplexes were transfected for a second time. 5 h after transfection, cells were treated again with thymidine for 16 h and afterwards released in fresh medium. For synchronization of cells, nocodazole (Sigma-Aldrich) was used at 3.3 µM. MG132 (Calbiochem) was used at 5-10 µM, thymidine (Sigma-Aldrich) at 2 mM, unless differently specified. Reversine (Calbiochem) was used at 0.5 µM.

2.2.3.6 Microtubule stability assay

When cells are subjected to cold-treament for short time periods, less stable microtubules are depolymerized first, whereas preferentially stabilized microtubules, such as kinetochore fibres, remain intact (Mitchison et al, 1986; Rieder, 1981). In case the stability of kinetochore fibres is impaired, they also depolymerize in this assay (Sillje et al, 2006).

For analysis of cold-stable microtubules, cells that were synchronized with a single thymidine arrest, released for 6.5 h and kept for 4 h in 5 µM MG132, were incubated for 5 min on ice in medium with 10 mM HEPES pH 7.5 and then directly fixed in 4 % PFA. Cells were stained for Tubulin and CREST, DNA was labeled with DAPI. CREST staining was used to identify kinetochores in image z-stacks to count kinetochores attached to cold-stable microtubules. Each kinetochore was classified as “attached” or “not attached” depending on whether a microtubule fibre ended at the kinetochore. On average 120 kinetochores were counted per cell and seven cells were analyzed for each condition.

2.2.3.7 Stable Isotope labeling by Amino acids in Cell culture (SILAC)

The stable isotope labeling by amino acids in cell culture (SILAC) is a method for quantitative proteomics, which is based on the labeling of different populations of cells with non-radioactive isotopes (Ong et al, 2002; Ong & Mann, 2005). In this study $^{15}N_2{}^{13}C_6$-lysine and $^{15}N_4{}^{13}C_6$-arginine (referred to as Lys8 and Arg10; SILANTES) were used as heavy labels and their natural counterparts as light labels (referred to as Arg0/Lys0; Sigma). By incorporating heavy amino acids into proteins the masses of the corresponding peptides are shifted by 8 and 10 Da respectively. Thus, if heavy and light samples are mixed, they can still be distinguished by the mass shift in the mass spectrometer. The ratio of the peak intensities of heavy to light peptides reflects the ratio of the corresponding protein abundances.

For SILAC, light cells were grown under normal conditions in DMEM without lysine and arginine, supplemented with 10 % FCS and 1 % penicillin/streptomycin. In order to remove all kinds of small molecules, especially amino acids, which could be used as an external amino acids source, FCS was dialyzed against a 10 kDa cut-off filter before ensuring efficient labeling. Heavy labeled cells were grown in DMEM, which contained in contrast to the light cells $^{15}N_2{}^{13}C_6$-lysine and $^{15}N_4{}^{13}C_6$-arginine. To

ensure the complete incorporation of the labeled amino acids into all cellular proteins, cells were passaged at least 5 times in the corresponding medium. Afterwards, cells were treated according to the experimental protocol and harvested by mitotic shake off. During the following anti-GFP IP the washing steps were performed in a mild wash buffer without salt (see 2.2.2.4) to preserve potentially weak interactions. Afterwards, samples were processed for mass spectrometry. IPs were usually performed in duplicates swapping the labels (called FOR and REV) and repeated three times to be able to perform statistical analyses of the results.

2.2.3.8 Mass spectrometry (LC MS/MS)

A nanoflow high performance liquid chromatography instrument (Easy nLC 1000) especially designed for high pressures up to 1000 bars (UPLC) was coupled on-line to a Q Exactive mass spectrometer (both from Thermo Fisher Scientific) with a column oven (Sonation) mounted on a nanoelectrospray ion source (Proxeon). Chromatography columns were packed in-house with ReproSil-Pur C_{18}-AQ 3 µm resin (Dr. Maisch GmbH) in buffer A (0.5 % acetic acid). The peptide mixture was loaded onto a C_{18}-reversed phase column (20 cm long, 75 µm inner diameter) and separated with a linear gradient of 5–60 % buffer B (100 % acetonitrile and 0.1 % formic acid) at a flow rate of 250 nl/min controlled by IntelliFlow technology over 120 min. The Q Exactive was operated in a data-dependent manner: One MS spectrum was acquired, and then the 10 most abundant precursor ions from this survey scan (300–1650 *m/z*) were dynamically chosen for higher-energy C-trap dissociation (HCD) fragmentation. The maximum filling time for MS spectra was set to 20 ms and for MS/MS spectra to 120 ms. Dynamic exclusion duration was 20 s. Isolation of precursors was performed with a 4-Thompson window and MS/MS scans were acquired with a starting mass of 100 *m/z*. Survey scans were acquired at a resolution of 70000 at 200 *m/z* on the Q Exactive. Resolution for HCD spectra was set to 17500 at 200 *m/z*. Normalized collision energy was 25 eV. The instrument was run with peptide recognition mode enabled and peaks with charge one or unassigned charge states were excluded.

2.2.3.9 Mass spectrometry data analysis

The raw data files were analyzed with the quantitative proteomics software MaxQuant, version 1.5.2.18 (Cox & Mann, 2008), which was used for peak list generation, identification and quantitation of SILAC pairs and filtering. The software has an integrated search engine [Andromeda, (Cox et al, 2011)], which is used for peptide and protein identification. MS/MS spectra were searched against the human Uniprot database. For the search deamidation (NQ), oxidatation (M) and acetylation at the N-terminus were given as variable modification, carbamidomethylation (C) as fixed modification. A false discovery rate cut-off of 1 % was applied at the peptide and protein levels. Only peptides of at least six amino acids were considered. For quantification, proteins were filtered for at least two SILAC ratio counts per protein and experiment. Obtained data were further processed in perseus (version 1.5.1.5). Contaminants and reverse hits were removed from the protein lists. For t-tests and volcano plots, proteins were further filtered to be quantified in at least 2 out of 3 replicates.

2.2.3.10 Live cell imaging

Cells were plated on a 24-well µ-Plate (Ibidi®). Drugs were diluted in CO_2 Independent Medium (Gibco®) and added to the cells 1 h before filming. Cells were imaged every 20 to 30 min in a heated chamber (37 °C) on a 3i Marianas™ system (Intelligent Imaging Innovations Inc.) equipped with Axio Observer Z1 microscope (Zeiss), Plan-Apochromat 40x/1.4NA Oil Objective, M27 with DIC III Prism (Zeiss), Orca Flash 4.0 sCMOS Camera (Hamamatsu) and controlled by Slidebook Software 6.0 (Intelligent Imaging Innovations Inc). Only cells that were GFP-positive (and – in the case of the GFP-BubR1 constructs that are supposed to localize to kinetochores – in which kinetochores were visible) were considered for the analysis.

2.2.3.11 Fluorescence recovery after photobleaching (FRAP)

The technique of Fluorescence Recovery After Photobleaching (FRAP) is used to measure rates of molecular movement through observations of changes in fluorescence in small regions of a cell. In FRAP the “system” is displaced from equilibrium by the use of a focused high-power laser beam, that irreversibly photobleaches a fraction of the fluorescent molecules in the observed region. The

measured recovery of the fluorescence back to its prebleaching level characterizes the rates at which unbleached molecules move into the observed region (Carrero et al, 2003; Elson, 1985).

For FRAP experiments, cells were cultured in 35 mm glass bottom µ-dishes (Ibidi®). Experiments were performed in the presence of 3.3 µM nocodazole, the presence of the GFP-tagged wild type or mutant fusionprotein and in the absence of the endogenous protein. Cells were imaged on a 3i Marianas™ system (Intelligent Imaging Innovations Inc., described above) using a 100x/1.4NA Oil Objective (Zeiss). Photobleaching was performed as described previously (Maddox et al, 2000). Images were binned 2x2 to increase signal-over-camera noise. At each time point a z-stack consisting of 3 sections at 0.27 µm intervals was acquired. The GFP-signal was imaged for 5 timeframes before photobleaching. After opening the laser shutter for 5 ms, cells were imaged by time-lapse microscopy, taking a z-series every 0.8 s for a total duration of 2 min with an exposure time of 125 ms. Images were converted into maximal intensity projections and exported as 16-bit TIFF files. Measurements of fluorescence intensity were made on the 16-bit maximal intensity projections using Image J. Apart from the bleached kinetochore, a non-bleached kinetochore from the same nucleus and a region of the same size outside of the cell were also measured. Afterwards, measurements were exported into excel. The relative fluorescence intensity was calculated as RFI= $(F_{ROI}(t)/F_{BG}(t)) / (F_{ROI}(t_0)/F_{BG}(t_0))$ as described in (Chen & Huang, 2001) to correct for background intensity and for photobleaching that occurred during image acquisition. $F_{ROI}(t)$ is the intensity of the bleached kinetochore at different timepoints after bleaching, $F_{BG}(t)$ is the intensity of the control non-bleached kinetochore at the corresponding timepoints. $F_{ROI}(t_0)$ is the average intensity of the bleached kinetochore before bleaching, $F_{BG}(t_0)$ is the average intensity of the control non-bleached kinetochore before bleaching. A baseline value, calculated from the region outside of the cell, was subtracted from all values before entering the values into the formula shown above. The final data were analyzed using Graph Pad Prism 6.0. Between 5 and 20 cells from at least two independent experiments were analyzed for each investigated construct.

2.2.3.12 Immunofluorescence

HeLa cells and Flp-In T-REx HeLa cells were grown on coverslips precoated with poly-D-Lysine (Millipore, 15 µg/ml) and poly-L-Lysine (Sigma), respectively. For the experiments with HeLa cells, cells were synchronized with a double thymidine block and after release from that arrested in prometaphase by the addition of 330 nM nocodazole for 3 h. For all other experiments, asynchronously growing cells were arrested in prometaphase by the addition of nocodazole for 3-4 h and fixed using 4 % PFA. Cells were incubated with the corresponding primary antibodies diluted in 2 % BSA-PBS for 1.5 h at room temperature. Goat anti–human and chicken anti–rabbit Alexa Fluor 647 (Invitrogen), goat anti–rabbit and anti–mouse RRX and donkey anti-human Alexa Fluor 405 (Jackson ImmunoResearch Laboratories, Inc.) were used as secondary antibodies diluted in 2 % BSA-PBS and incubated for 45 min at room temperature. DNA was stained with 0.5 µg/ml DAPI (Serva) for 1 min. Afterwards, coverslips were washed with PBS and H_2O and mounted with Mowiol mounting media (Calbiochem). Cells were imaged at room temperature using a spinning disk confocal device on the 3i Marianas™ system, equipped with an Axio Observer Z1 microscope (Zeiss), a CSU-X1 confocal scanner unit (Yokogawa Electric Corporation), Plan-Apochromat 63x or 100x/1.4NA Oil Objectives (Zeiss) and Orca Flash 4.0 sCMOS Camera (Hamamatsu). Images were acquired as z-sections at 0.27 µm. Images were converted into maximal intensity projections, exported and converted into 8-bit. Quantification of kinetochore signals was performed on unmodified 16-bit z-series images using Imaris 7.3.4 32-bit software (Bitplane). After background subtraction, all signals were normalized to CREST. At least 138 kinetochores were analyzed per condition. Measurements were exported in Excel (Microsoft) and graphed with GraphPad Prism 6.0 (GraphPad Software).

3 Results

Kinetochore recruitment of Bub1 and BubR1 in human cells requires Bub3 (Larsen et al, 2007; Taylor et al, 1998). Consequently, the Bub3-binding domains (B3BD) of Bub1 and BubR1 are necessary, and in the case of Bub1 also sufficient, for kinetochore localization (Elowe et al, 2010; Krenn et al, 2012; Logarinho et al, 2008; Taylor et al, 1998). The described subordination of BubR1 to Bub1 kinetochore recruitment, despite both proteins being bound to Bub3, suggests that Bub3 may work differently when bound to Bub1 or BubR1. In this study we aim to investigate the molecular basis of this observed difference and its implications for kinetochore-microtubule attachment and especially spindle assembly checkpoint signaling.

3.1 The B3BDs of Bub1 and BubR1 behave differently

First, we wanted to confirm the described dependency of BubR1 kinetochore recruitment on Bub1 and the independence of Bub1 kinetochore recruitment from BubR1. To activate the SAC, we treated HeLa cells with the microtubule depolymerizing drug nocodazole and found that Bub1 localized to kinetochores at essentially normal levels after depletion of BubR1 (Figure 3-1 A-B). Conversely, BubR1 decorated kinetochores only weakly after Bub1 depletion (Figure 3-1 C-D). Quantifications of RNAi-based depletion efficiencies are shown in Figure 3-1 E-F. In agreement with previous studies, these results confirm that BubR1 requires Bub1 for kinetochore recruitment, but that Bub1 is independent of BubR1 (Gillett et al, 2004; Johnson et al, 2004; Klebig et al, 2009; Logarinho et al, 2008; Millband & Hardwick, 2002; Perera et al, 2007). To further validate these results, we also assessed the behavior of the constitutive binding partner of Bub1 and BubR1, Bub3, by monitoring kinetochore localization of a GFP-Bub3 fusionprotein in absence of either endogenous Bub1 or BubR1. GFP-Bub3 did not decorate kinetochores after Bub1 depletion, but could be observed at kinetochores after BubR1 depletion (Figure 3-1 G-J). This is in agreement with our data from above showing that upon Bub1 depletion BubR1 localization is lost and consequently also Bub3 localization, since none of its binding partners remains at kinetochores. However, upon BubR1 depletion Bub1 kinetochore localization is not affected, and therefore Bub3, constitutively bound to Bub1, can still be detected at kinetochores.

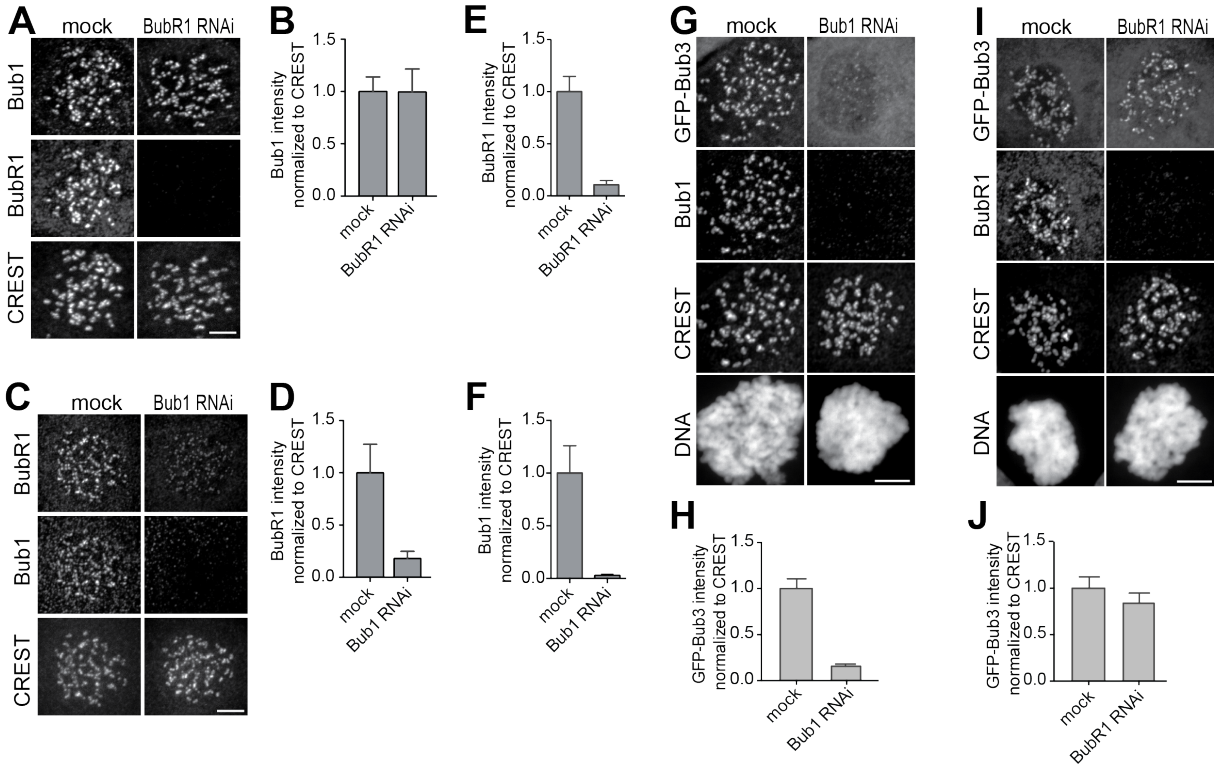

Figure 3-1 Bub1 is required for kinetochore localization of BubR1

A, C) Representative images of Flp-In T-REx cell lines in BubR1 (A) and Bub1 (C) RNAi, respectively, after treatment with nocodazole, showing that Bub1 is required for BubR1 kinetochore localization. Scale bar: 10 µm. B, D) Quantification of Bub1 and BubR1 kinetochore levels, respectively, in cells treated as in A and C. The graph shows mean intensity, error bars indicate SD. The mean value for non-depleted cells is set to 1. E, F) Quantification of BubR1 and Bub1 kinetochore levels, respectively, in cells treated as in panel A and C to show RNAi depletion efficiency. The graph shows mean intensity, error bars indicate SD. The mean value for non-depleted cells is set to 1. G, I) Representative images of Flp-In T-REx cells expressing GFP-Bub3 in Bub1 (G) and BubR1 (I) RNAi, respectively, after treatment with nocodazole, showing that Bub3 localization is lost only upon Bub1 depletion. Scale bar: 10 µm. H, J) Quantification of Bub3 kinetochore levels, in cells treated as in G and I. The graph shows mean intensity, error bars indicate SD. The mean value for non-depleted cells is set to 1.

By monitoring the localization of a GFP-Bub1 reporter construct, it has been previously demonstrated that Bub1$^{209\text{-}270}$, consisting of the B3BD, is the minimal Bub1 construct localizing to kinetochores (Elowe et al, 2010; Krenn et al, 2012; Taylor et al, 1998). Bub1$^{209\text{-}270}$ targeted kinetochores very efficiently even after depletion of endogenous Bub1 (Figure 3-2 A-B). We asked if an equivalent GFP-reporter construct containing the B3BD of BubR1, BubR1$^{362\text{-}431}$, was also recruited to

kinetochores. BubR1$^{362-431}$ did not localize to kinetochores even in the presence of Bub1 (Figure 3-2 A, C).

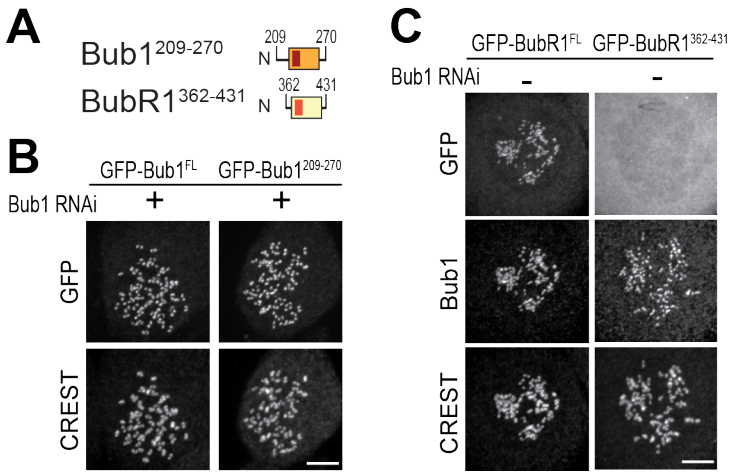

Figure 3-2 The B3BDs of Bub1 and BubR1 behave differently *in vivo*

A) Schematic of the B3BD constructs. B-C) Representative images of stable Flp-In T-REx cell lines expressing the indicated GFP-Bub1 constructs (panel B) or HeLa cells transfected with the indicated GFP-BubR1 constructs (C) after treatment with nocodazole. For the BubR1 constructs the same images are also shown in Figures 3-9 B and D, and quantified in Figure 3-9 C. Scale bar: 10 µm.

Thus, even if Bub1 and BubR1 share a related B3BD to interact with the same kinetochore-targeting subunit (Bub3) and interact in a phosphorylation-dependent manner with Knl1, the mechanisms of their kinetochore recruitment are different. These initial results further refine our first two main questions stated in the objectives to: Why is the B3BD region of Bub1 sufficient for kinetochore recruitment, while the equivalent region of BubR1 is not? And if binding to Bub3 is not sufficient for robust kinetochore recruitment of BubR1, how is BubR1 then recruited to kinetochores? These questions will be addressed sequentially.

3.2 The loop regions of Bub1 and BubR1 modulate the interaction of Bub3 with phosphorylated MELT repeats

To investigate if and how Bub1$^{209-270}$ and BubR1$^{362-431}$ modulate the binding affinity of Bub3 for the phosphorylated MELT (MELT^{P}) repeats of Knl1, we tested *in vitro* the ability of Bub3, Bub1$^{209-270}$/Bub3 and BubR1$^{362-431}$/Bub3 to bind to immobilized MBP-Knl1$^{138-168}$, a region containing a single and functional MELT repeat [the most N-terminal, called MELT1 (Krenn et al, 2014)], in the presence or absence of the kinase

Mps1, which is responsible for MELT phosphorylation (London et al, 2012; Shepperd et al, 2012; Yamagishi et al, 2012). Bound proteins were visualized by western blotting. Bub3 on its own did not bind MBP-Knl1^{MELT1}, in agreement with our previous data (Krenn et al, 2014). The B3BD of Bub1 strongly enhanced binding of Bub3 to phosphorylated MBP-Knl1^{MELT1} but not to unphosphorylated MBP-Knl1^{MELT1}, while the B3BD of BubR1 showed a negligible effect (Figure 3-4 A). These results *in vitro* correlate with the ability of the equivalent B3BD to support (or not) kinetochore recruitment in cells (Figure 3-2 B-C). Our previous structural and biochemical characterization of the Bub1^{B3BD}/Bub3/MELT^{P} ternary complex of *S. cerevisiae* demonstrated that while Bub3 carries most of the crucial (and evolutionarily conserved) residues involved in high-affinity binding to MELT^{P}, a short segment of Bub1, named the “loop (L)”, also contributes to the binding affinity (Primorac et al, 2013). The loop region of Bub1 or BubR1 is located between strands β1 and β2 and precedes the highly conserved core of the B3BD. The loop abuts the binding site for the MELT^{P} peptide and is therefore ideally positioned to modulate the binding affinity of Bub3 for MELT^{P} (Figure 3-4 B-D).

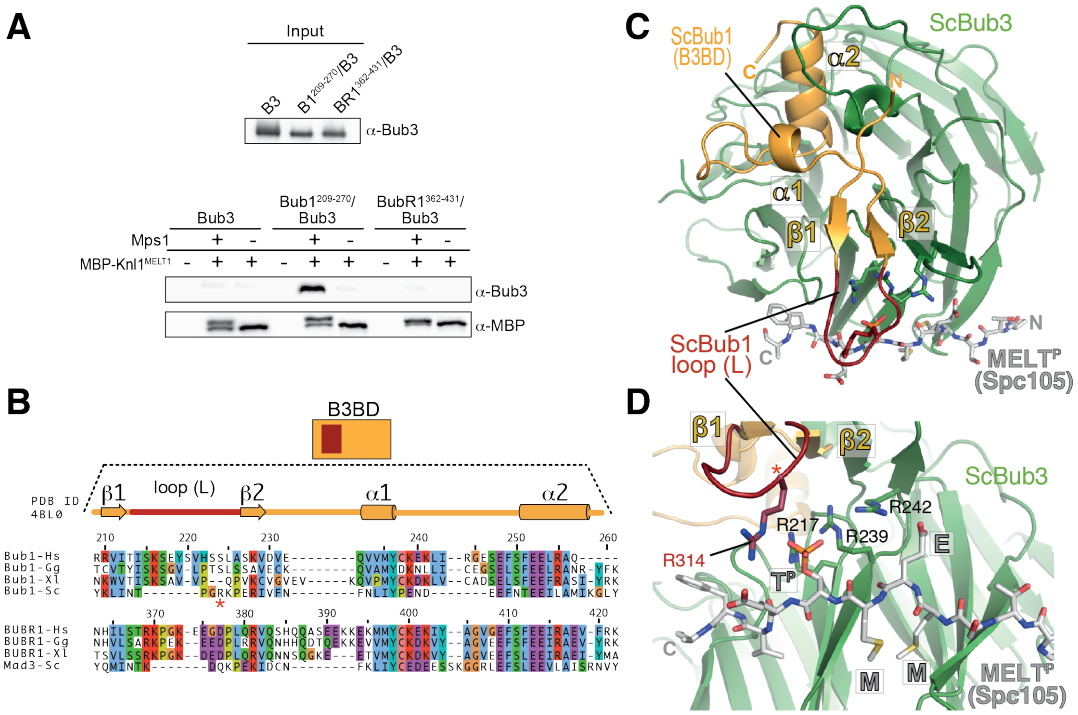

Figure 3-3 The B3BDs of Bub1 and BubR1 behave differently *in vitro*

A) Recombinant Bub3, Bub1$^{209-270}$/Bub3 and BubR1$^{362-431}$/Bub3 were incubated with immobilized MBP-Knl1^{MELT1} (residues 138-168 of human Knl1) prephosphorylated with Mps1 (+) or

unphosphorylated (-). Empty lanes (-) demonstrate lack of background binding to empty beads. wt, wild type; B3, Bub3; B1, Bub1; BR1, BubR1. B) Multiple sequence alignments of the B3BDs of human (*Homo sapiens*, Hs), chicken (*Gallus gallus*, gg), frog (*Xenopus laevis*, Xl) and budding yeast (*Saccharomyces cerevisiae*, Sc) Bub1s and BubR1s. Mad3 is the budding yeast BubR1 homolog. ScBub1^{R314} (red asterisk) directly contributes to the interaction with the MELT^{P} peptide. The different Bub1 and BubR1 sequences were aligned manually on the basis of the crystal structures of the B3BDs of Mad3 and Bub1 in complex with Bub3 (Larsen et al, 2007; Primorac et al, 2013). C) Crystal structure of the ScBub1$^{289-359}$-Bub3-MELT^{P} ternary complex (Primorac et al, 2013). N and C indicate the N- and C-terminus, respectively. D) Close-up of the MELT^{P} binding site indicating the role of ScBub1^{R314} in MELT^{P} binding.

Because the loops of Bub1 and BubR1 have quite divergent sequences (Figure 3-4 B), we tested their role in modulating the binding affinity of Bub1$^{209-270}$/Bub3 or BubR1$^{362-431}$/Bub3 for immobilized MBP-Knl1^{MELT1}. Thus, we swapped the loop regions of Bub1 and BubR1 as schematized in Figure 3-4 A. Recombinant versions of the chimeric mutants Bub1$^{209-270\ BR1-L}$ and BubR1$^{362-431\ B1-L}$ were co-expressed with Bub3. Both the wild type and chimeric constructs interacted with apparently similar affinity with Bub3, excluding major structural perturbations (data not shown). We then tested the ability of these recombinant constructs to interact with immobilized MBP-Knl1^{MELT1}. Bub1$^{209-270}$/Bub3 bound tightly and in an Mps1-phosphorylation-dependent manner to MBP-Knl1^{MELT1}, while Bub1$^{209-270\ BR1-L}$/Bub3 bound weakly. Conversely, BubR1$^{362-431\ B1-L}$/Bub3 bound more strongly to phosphorylated MBP-Knl1^{MELT1} than BubR1$^{362-431}$/Bub3 (Figure 3-4 B). These results demonstrate a crucial role of the loop region of Bub1 in the recognition of a phosphorylated MELT repeat. (This experiment was carried out by Ivana Primorac, a former post-doctoral fellow in the laboratory.) Immunoprecipitation (IP) experiments on protein extracts from stable cell lines expressing GFP-fusions of the wild type or loop-swap mutants in the context of full length Bub1 or BubR1 recapitulated the *in vitro* results (Figure 3-4 C-D). Loop-swap mutants interacted with Bub3 as efficiently as wild type proteins, but the interaction with the Knl1 receptor, mediated by Bub3, was strongly enhanced when the Bub1-loop region was grafted onto BubR1.

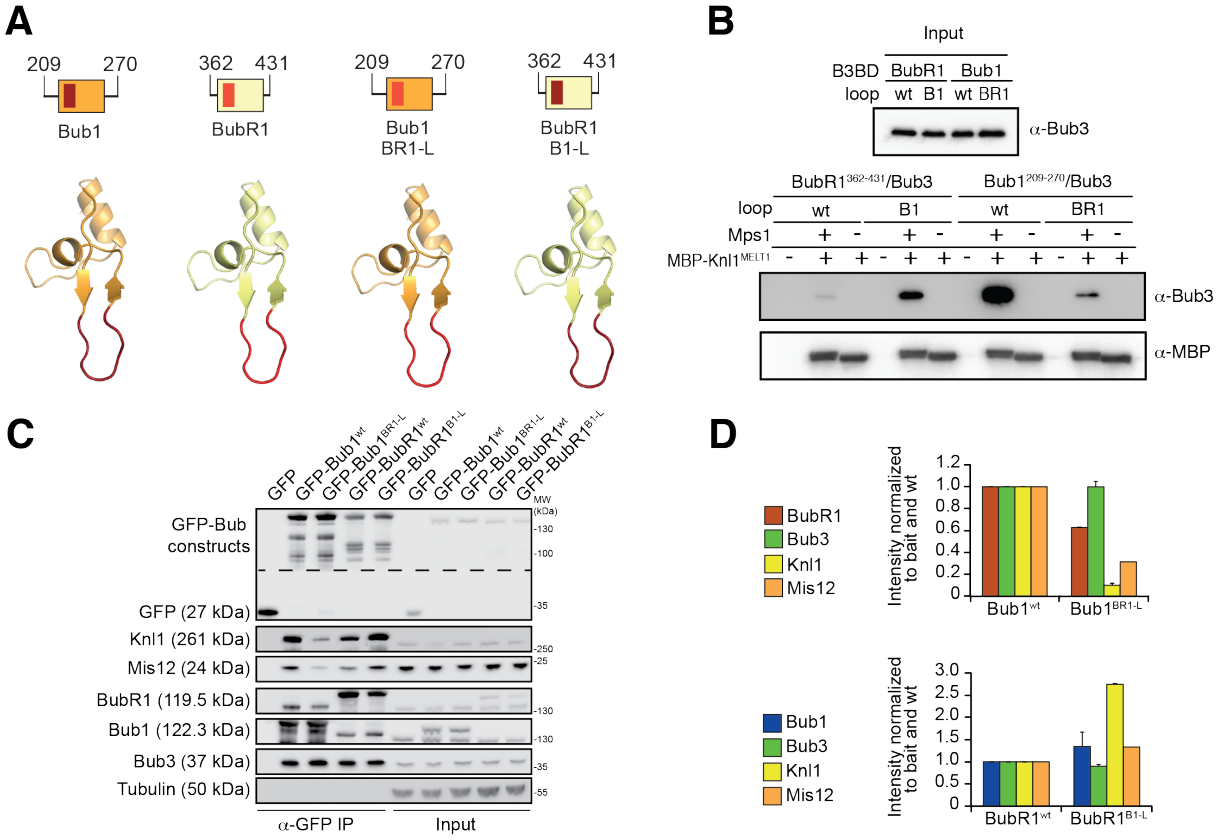

Figure 3-4 The loop regions of Bub1 and BubR1 modulate the interaction of Bub3 with MELT^{P} repeats

A) Schematic depiction of short Bub1 and BubR1 loop-swap constructs, containing the loop (different shades of red) followed by the B3BD (different shades of yellow). L, loop. B) Recombinant BubR1$^{362-431}$/Bub3 with its own loop (wt) or with the Bub1 loop (B1) and recombinant Bub1$^{209-270}$/Bub3 with its own loop (wt) or with the BubR1 loop (BR1) were incubated with immobilized MBP-Knl1^{MELT1} prephosphorylated with Mps1 (+) or unphosphorylated (-) as in Figure 3-3 A. Empty lanes (-) demonstrate lack of background binding to empty beads. C) Western Blot of immunoprecipitates (IP) from mitotic Flp-In T-REx cell lines expressing the indicated GFP-Bub1 and -BubR1 constructs showing the influence of the loop on the ability to pull down the kinetochore components Knl1 and Mis12. Tubulin was used as loading control. D) Quantification of the Western Blot in C. In the upper graph the amounts of co-precipitating proteins were normalized to the amount of GFP-Bub1 bait present in the IP. In the lower graph the amounts of co-precipitating proteins were normalized to the amount of GFP-BubR1 bait. Values for GFP-Bub1^{wt} and GFP-BubR1^{wt}, respectively were set to 1. The graphs show mean intensity of two independent experiments (for Mis12 only one). Error bars represent SD.

3.3 Behavior of the loop-swap mutants in HeLa cells

We next tested the kinetochore localization behavior of these loop-swap mutants. Kinetochore localization of GFP-Bub1^{BR1-L} was weaker than that of wild type Bub1

(Figure 3-5 A-B), whereas kinetochore localization of GFP-BubR1$^{B1\text{-}L}$ was stronger than that of BubR1^{wt} (Figure 3-5 C-D). Indeed, GFP-BubR1$^{B1\text{-}L}$ localized to kinetochores even after depletion of endogenous Bub1. Thus, when grafted onto BubR1, the Bub1-loop region is sufficient to make BubR1 gain the ability to target kinetochores independently of Bub1 (Figure 3-5 E-F). Kinetochore localization of GFP-BubR1$^{B1\text{-}L}$ in cells depleted of Bub1 was inhibited by the Mps1 inhibitor Reversine (Santaguida et al, 2010), suggesting a dependency of this localization on MELT^{P} sequences (Figure 3-5 G-H, images for BubR1^{wt} are not shown). Expression of BubR1$^{B1\text{-}L}$ did not significantly influence kinetochore levels of endogenous Bub1 (Figure 3-5 I), suggesting that the multiple MELT repeats of Knl1 are probably not saturated with Bub1 even in the presence of high nocodazole concentrations (3.3 µM) to obtain strong SAC activating conditions in our assay.

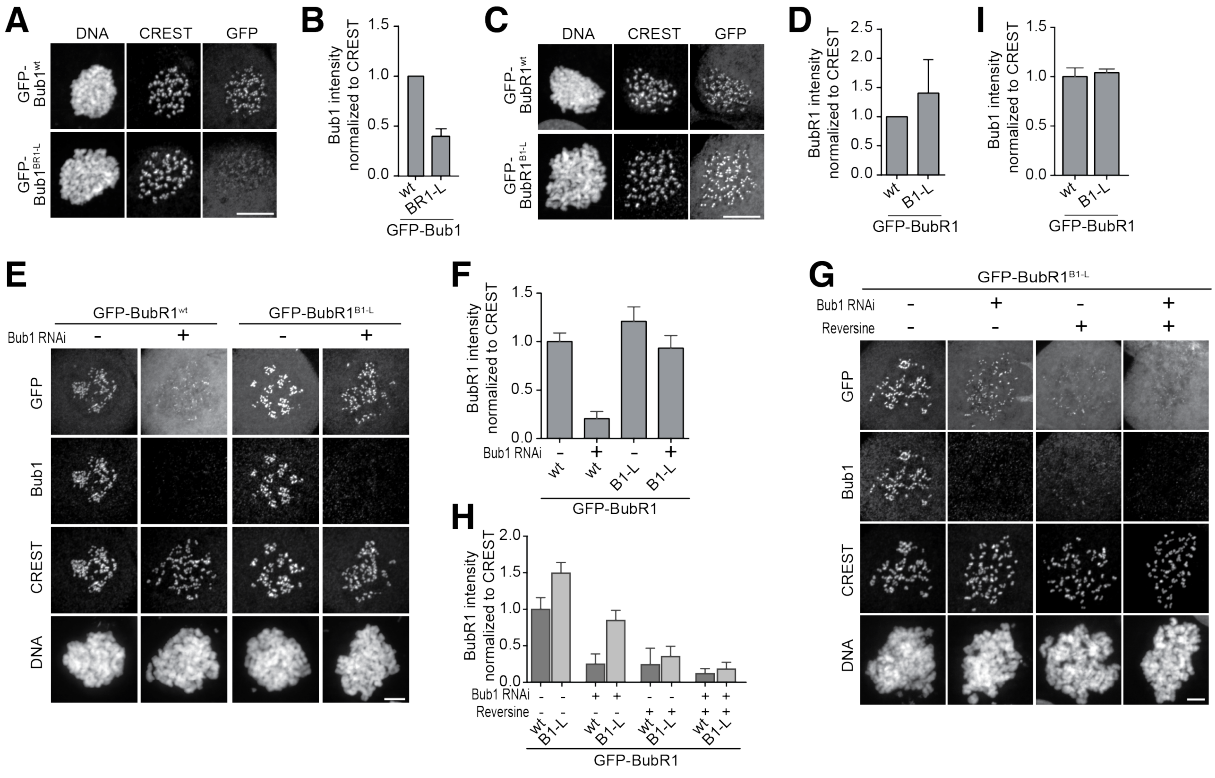

Figure 3-5 Kinetochore localization of loop-swap mutants in HeLa cells

A, C) Representative images of stable Flp-In T-REx cells expressing either the wild type (wt) or the loop mutant of GFP-Bub1 (A) or GFP-BubR1 (C) showing that the BR1-loop (L) impairs (A) whereas the Bub1-loop (L) enhances (C) kinetochore localization. Scale bar: 10 µm. B, D) Quantification of Bub1 and BubR1 kinetochore levels in cells treated as in A and C, respectively. The graphs show mean intensity from three independent experiments. Error bars represent SEM. Values for Bub1^{wt} and

BubR1^{wt} respectively are set to 1. E) Representative images of HeLa cells transfected with the indicated GFP-BubR1 constructs, showing that BubR1$^{B1\text{-}L}$ does not depend on Bub1 for its kinetochore localization. In brief, after transfection, cells were depleted of endogenous Bub1 by RNAi, synchronized with a double thymidine block and arrested in mitosis with nocodazole. Scale bar: 10 µm. F) Quantification of BubR1 kinetochore levels in cells treated as in E. The graph shows mean intensity from three independent experiments. Error bars represent SEM. Values for BubR1^{wt} in non-depleted cells are set to 1. G) Representative images of HeLa cells transfected with GFP-BubR1$^{B1\text{-}L}$ treated as in E in the presence (+) or absence (-) of the Mps1 inhibitor Reversine, showing that BubR1$^{B1\text{-}L}$ kinetochore localization is dependent on Mps1. Scale bar: 10 µm. H) Quantification of BubR1 kinetochore levels in cells treated as in G. The graph shows mean intensity from two independent experiments. Error bars represent SEM. Values for BubR1^{wt} in non-depleted cells without Reversine treatment are set to 1.

In a quantitative SILAC (Stable Isotope Labeling with Amino acids in Cell culture) immune-precipitation experiment, followed by mass-spectrometry (Ong et al, 2002; Ong & Mann, 2006) we identified Casc5/Knl1 as specific interaction partner of the B3BD of Bub1 in comparison to the B3BD of BubR1 (Figure 3-6). This is a further confirmation for the specific role of the Bub1-loop in Knl1 binding.

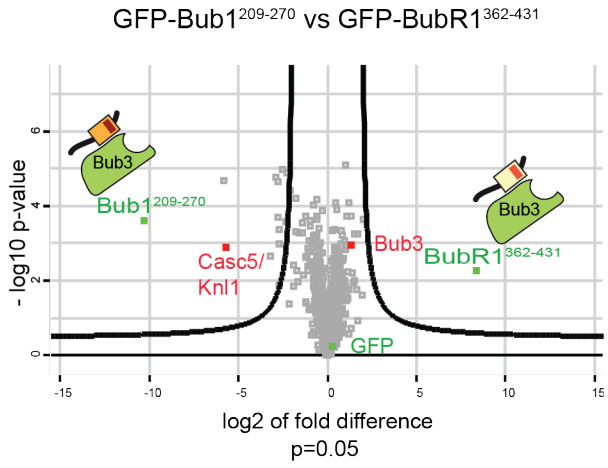

Figure 3-6 The B3BD of Bub1 interacts specifically with Knl1

Volcano plot showing the results from two independent SILAC experiments using GFP-Bub1$^{209\text{-}270}$ or GFP-BubR1$^{362\text{-}431}$ as affinity resins to identify specific interaction partners in mitotic lysates. A p-value of 0.05 was used as cut-off for significance.

Next, we asked if GFP-BubR1^{B1-L} could complement the SAC function of BubR1. In cells depleted of endogenous BubR1, GFP-BubR1^{wt} rescued SAC function very efficiently but GFP-BubR1^{B1-L} failed to do so (Figure 3-7 A). Comparison of IPs of GFP-BubR1^{wt} and of GFP-BubR1^{B1-L} from extracts obtained from nocodazole-treated mitotic cells showed a reduced association of the latter with MCC and APC/C subunits (Figure 3-7 B-C). Similarly, IPs of the APC/C subunit Cdc27 demonstrated binding of GFP-BubR1^{wt}, but not GFP-BubR1^{B1-L}, to the APC/C (Figure 3-7 D-E). Comparison of IPs of GFP-Bub1^{wt} and GFP-Bub1^{BR1-L} showed only a minor increase in binding of the latter to MCC and APC/C (Figure 3-7 B-C). Interestingly, APC/C subunits could be detected in the IPs of Bub1, albeit at a much lower level than in the BubR1 IPs.

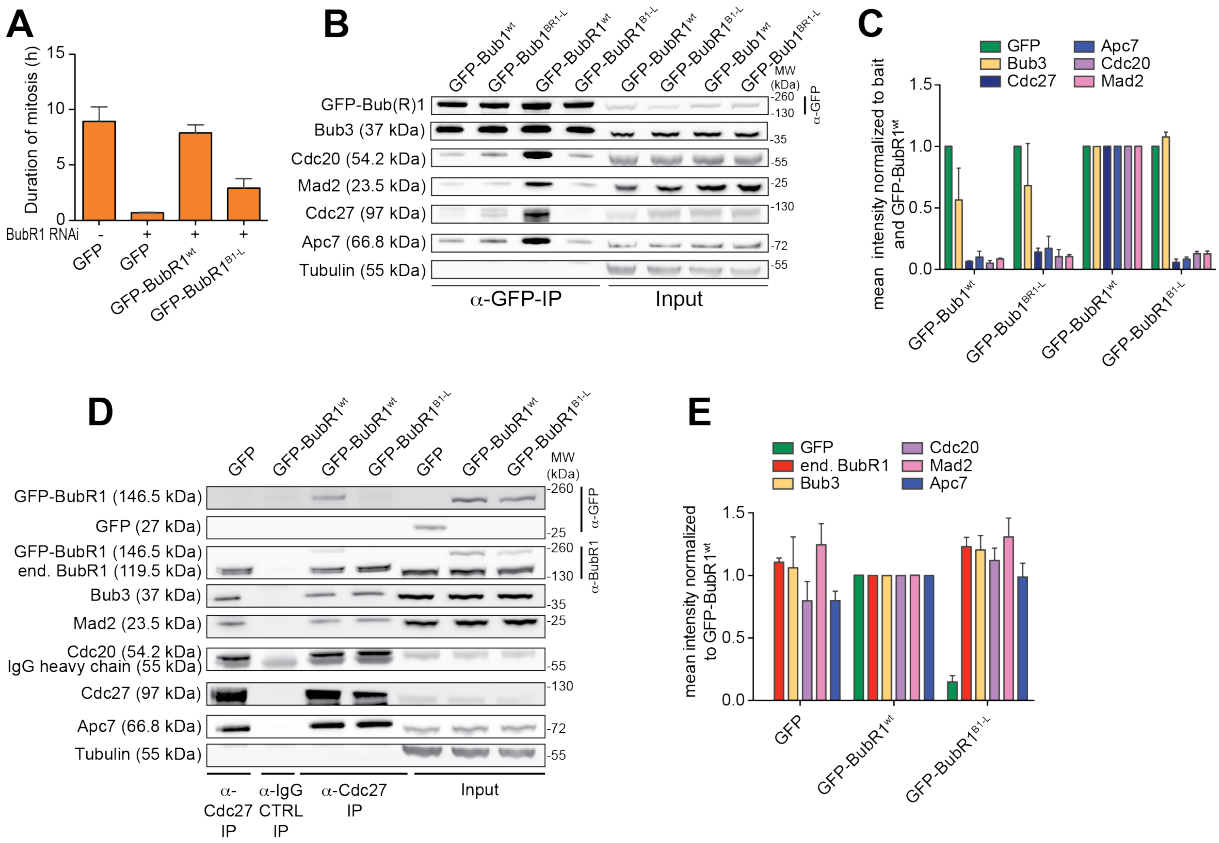

Figure 3-7 Functional analysis of BubR1^{B1-L} in HeLa cells

A) Mean duration of mitosis of Flp-In T-REx stable cell lines expressing GFP-BubR1^{wt} or the loop mutant in the absence of endogenous BubR1 and in the presence of 50 nM nocodazole. Cell morphology was used to measure entry into and exit from mitosis by time-lapse-microscopy (n>58 per cell line per experiment) from three independent experiments. Error bars depict SEM. B) Western Blot of immunoprecipitates (IP) from mitotic Flp-In T-REx cell lines expressing the indicated GFP-Bub(R)1

constructs showing the influence of the loop on the ability to pull down MCC and APC/C components. Tubulin was used as loading control. C) Quantification of the Western Blot in B. The amounts of co-precipitating MCC and APC/C components were normalized to the amount of GFP-Bub(R)1 bait present in the IP. Values for GFP-BubR1^{wt} were set to 1. The graph shows mean intensity of two independent experiments. Error bars represent SEM. D) Western Blot of IPs of the APC/C subunit Cdc27 from mitotic Flp-In T-REx cell lines expressing the indicated GFP-BubR1 constructs showing the influence of the loop on binding to the APC/C. Tubulin was used as loading control. E) Quantification of the Western Blot in D. The amounts of proteins co-precipitating with the APC/C were normalized to the amounts present in GFP-BubR1^{wt} expressing cells. The graph shows mean intensity of two independent experiments. Error bars indicate SEM.

These results demonstrate that sequence divergence in the short loop region of Bub1 and BubR1 has strong functional consequences. In Bub1, the loop enhances the ability of Bub3 to recognize MELT^{P} repeats of Knl1. In BubR1, the precise role of the loop is so far unknown, but the results in Figure 3-7 suggest it plays a role in MCC assembly or in the interaction with the APC/C. Both hypotheses will be investigated in more detail in the further progress of this work.

3.4 Characterization of the Bub1-BubR1 interaction

The second question we wanted to address, how BubR1 is recruited to kinetochores, contains three distinct aspects. First, the region of Bub1 required for BubR1 kinetochore recruitment should be identified. Second, the region within BubR1 required for its own kinetochore localization should be determined. Third, it should be examined if Bub1 and BubR1 interact directly and if kinetochore proteins other than Bub1 contribute to BubR1 recruitment.

3.4.1 A minimal BubR1-binding region of Bub1

To map the region of Bub1 that is required for BubR1 kinetochore recruitment, we created GFP-fusions of several deletion mutants of Bub1 and tested their kinetochore localization together with their ability to recruit BubR1 (Figure 3-8 A). Bub1$^{209-270}$, which contains the B3BD, localized to kinetochores as reported previously (Krenn et al, 2012) but was not able to recruit BubR1 in cells depleted of endogenous Bub1. Another construct, consisting of the N-terminal tetratricopeptide repeats (TPRs) and the B3BD, Bub1$^{1-284}$, also targeted kinetochores but did not recruit BubR1. On the contrary, a segment (Bub1$^{209-409}$) consisting of the B3BD and a ~140-residue C-

terminal extension (CTE), localized to kinetochores and mediated robust kinetochore localization of BubR1. Thus, Bub1 does not require the CTE (residues 271-409) for its own kinetochore localization (the B3BD, residues 209-270, is sufficient), but requires it to recruit BubR1. Consistently, a mutant of the full-length protein in which we deleted the CTE ($Bub1^{\Delta 271-409}$) targeted kinetochores efficiently but failed to recruit BubR1 (Figure 3-8 B-E).

In IP experiments, both in the presence and absence of endogenous Bub1, GFP-$Bub1^{209-409}$ interacted with similar amounts of BubR1 as GFP-$Bub1^{FL}$. Conversely, GFP-$Bub1^{209-270}$ did not pull down BubR1, consistent with the inability of this construct to mediate BubR1 kinetochore localization (Figure 3-8 F-G).

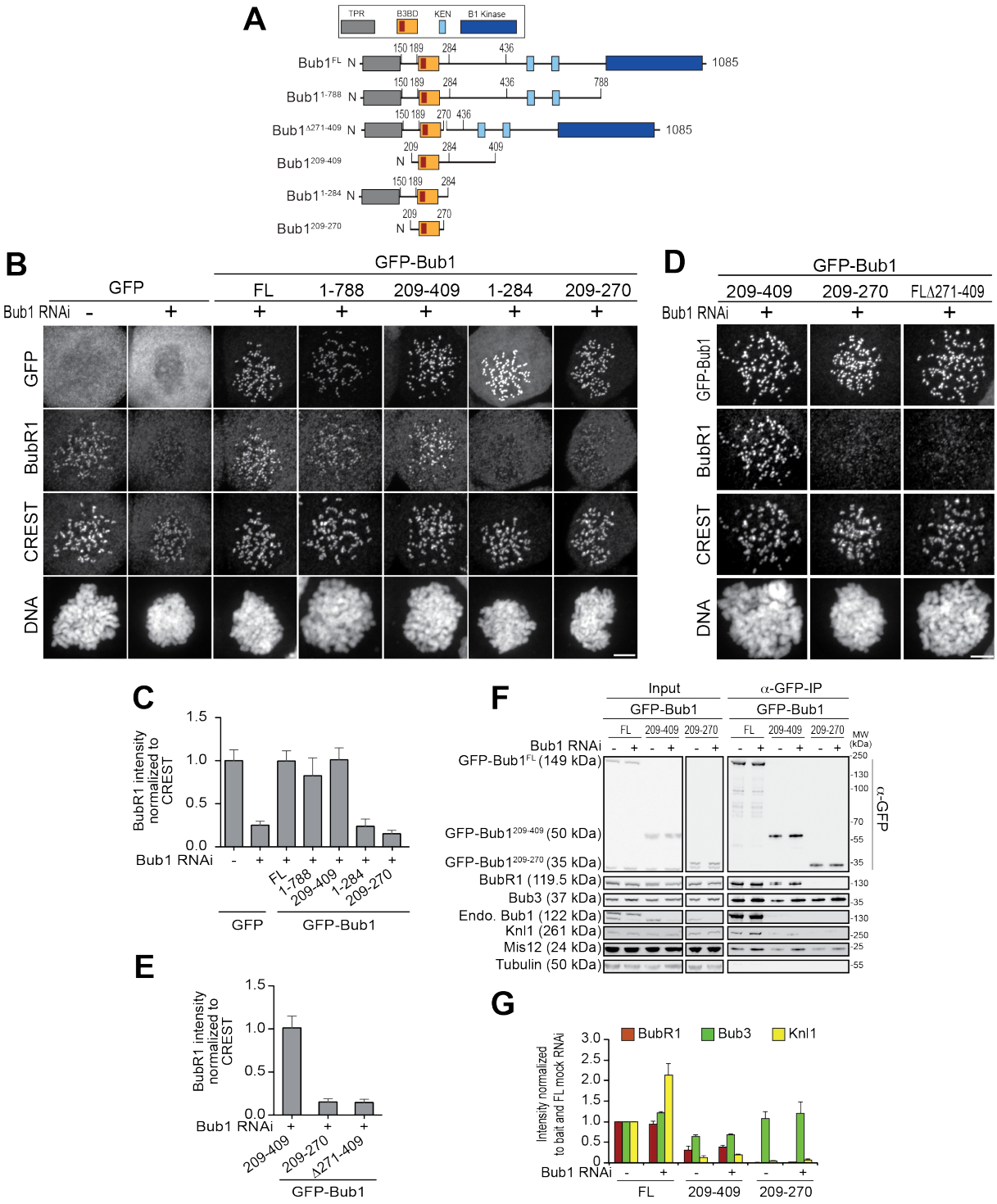

Figure 3-8 Bub1$^{209-409}$ is sufficient to recruit BubR1 to kinetochores

A) Schematic depiction of the Bub1 deletion constructs used in this study. TPR, tetratricopeptide repeats; B3BD, Bub3-binding domain; FL, full-length; N, N-terminus. B, D) Representative images of stable Flp-In T-REx cell lines expressing the indicated GFP-Bub1 constructs after treatment with nocodazole, showing that Bub1$^{209-409}$ is sufficient to recruit BubR1 (B) and that residues 271-409 are essential for this function (D). Scale bar: 10 µm. C, E) Quantification of BubR1 kinetochore levels in cells treated as in panels B and D. The graphs show mean intensity of two independent experiments,

the error bars indicate SEM. The mean value for non-depleted cells expressing GFP (B) or GFP-Bub1$^{209-409}$ (D) is set to 1. F) Western blot of immunoprecipitates (IP) from mitotic Flp-In T-REx cell lysates expressing the indicated GFP-Bub1 constructs in the presence or absence of endogenous Bub1, showing that Bub1$^{209-409}$ is sufficient to pull down BubR1. Tubulin was used as loading control. G) Quantification of the Western Blot in F. The amounts of co-precipitating proteins were normalized to the amount of GFP-Bub1 bait present in the IP. Values for GFP-Bub1^{FL} in non-depleted cells were set to 1. The graph shows mean intensity of two independent experiments. Error bars represent SD.

These *in vivo* data were fully supported by *in vitro* size exclusion chromatography (SEC) experiments with purified recombinant proteins (carried out by Ivana Primorac), indicating that Bub1 binds directly to BubR1 and that both Bub1 regions (B3BD and CTE) contribute to the interaction with BubR1 [data shown in (Overlack et al, 2015) Figure 4 G-J].

3.4.2 A minimal Bub1-binding region of BubR1

To identify the minimal region of BubR1 that targets kinetochores, we created GFP-fusions of several deletion mutants of BubR1 (Figure 3-9 A) and tested their ability to localize to kinetochores in presence and absence of endogenous Bub1. BubR1$^{362-571}$, which contains the B3BD and a ~140-residue CTE, localized to kinetochores in a Bub1-dependent manner (Figure 3-9 B-C). Shorter fragments of BubR1, containing the isolated B3BD (BubR1$^{362-431}$, see also Figure 3-2 C) or the isolated CTE (BubR1$^{432-571}$), did not localize to kinetochores, no matter whether endogenous Bub1 was RNAi depleted or not (for RNAi condition only the quantification is shown) (Figure 3-9 C-D).

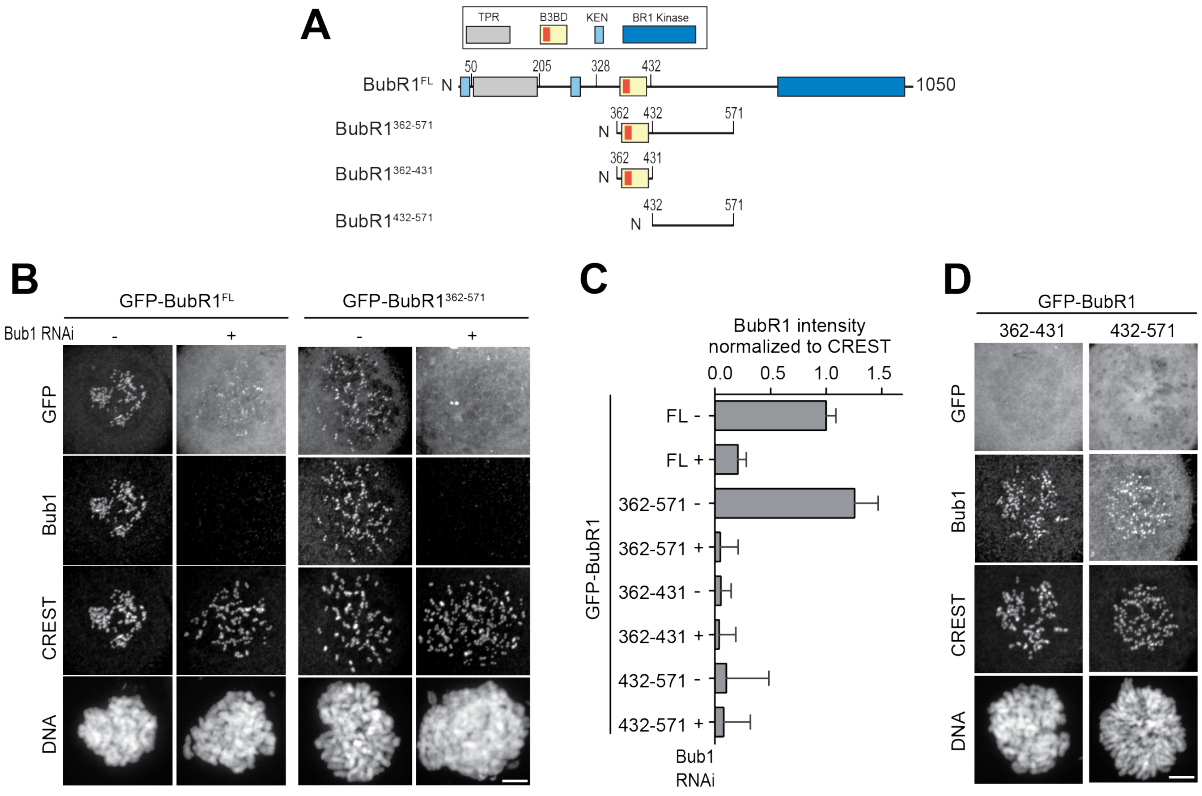

Figure 3-9 BubR1$^{362-571}$ is sufficient to localize to kinetochores

A) Schematic depiction of the BubR1 deletion constructs used in this study. TPR, tetratricopeptide repeats; B3BD, Bub3-binding domain; FL, full-length; N, N-terminus. B, D) Representative images of HeLa cells transfected with the indicated GFP-BubR1 constructs. Cells were treated as described in Figure 3-5 E. BubR1$^{362-571}$ is the minimal construct that is able to localize to kinetochores in presence of Bub1. Scale bar: 10 µm. C) Quantification of BubR1 kinetochore levels in cells treated as in B and D. The graph shows mean intensity of at least two independent experiments, error bars depict SEM. Values for GFP-BubR1^{FL} in non-depleted cells are set to 1.

These *in vivo* data were also confirmed by *in vitro* SEC experiments with purified recombinant proteins [carried out by Ivana Primorac, data shown in (Overlack et al, 2015) Figure 5 D-F].

3.4.3 Bub1 and BubR1 form a pseudo-symmetric heterodimer

Our results suggest that BubR1$^{362-571}$ and Bub1$^{209-409}$ should be sufficient for the Bub1/BubR1 interaction *in vitro*. Indeed, BubR1$^{362-571}$ and Bub1$^{209-409}$/Bub3 formed a stoichiometric complex in SEC runs (Figure 3-10 A). An alignment of these domains of Bub1 and BubR1 [residues 209-409 and 362-571, respectively; the alignment was obtained with programs Muscle (Edgar, 2004) and JPRED (Cole et al, 2008); an excerpt is shown in Figure 3-10 B; full alignment is shown in the supplementary

Figure 7-1] shows that their sequences are structurally equivalent. Both start with the B3BD, continue with a segment predicted to form a helix and end with a region predicted to lack defined secondary structure (this part is not contained in the excerpt of the alignment). An updated scheme of the domain organization of Bub1 and BubR1 is shown in Figure 3-10 C. We assume that the ability to hetero-dimerize of modern-day Bub1 and BubR1 using the described structurally equivalent ("pseudo-symmetric") segments may reflect the ability of their common ancestor to form homodimers.

Deletion of residues 432-484 of BubR1 in the predicted helical region (this mutant will from now on be abbreviated as GFP-BubR1$^{\Delta H}$ to indicate that it lacks the predicted helix) impaired kinetochore localization of BubR1 (Figure 3-10 D-E). Additionally, two point-mutations in the B3BD of BubR1 (E409K+E413K) known to interfere with Bub3 binding (Larsen et al, 2007; Taylor et al, 1998) prevented kinetochore localization of BubR1^{FL} (Figure 3-10 F-G) and of BubR1$^{362-571}$ (data not shown). Thus, also Bub3 binding is necessary for efficient kinetochore localization of BubR1 *in vivo*.

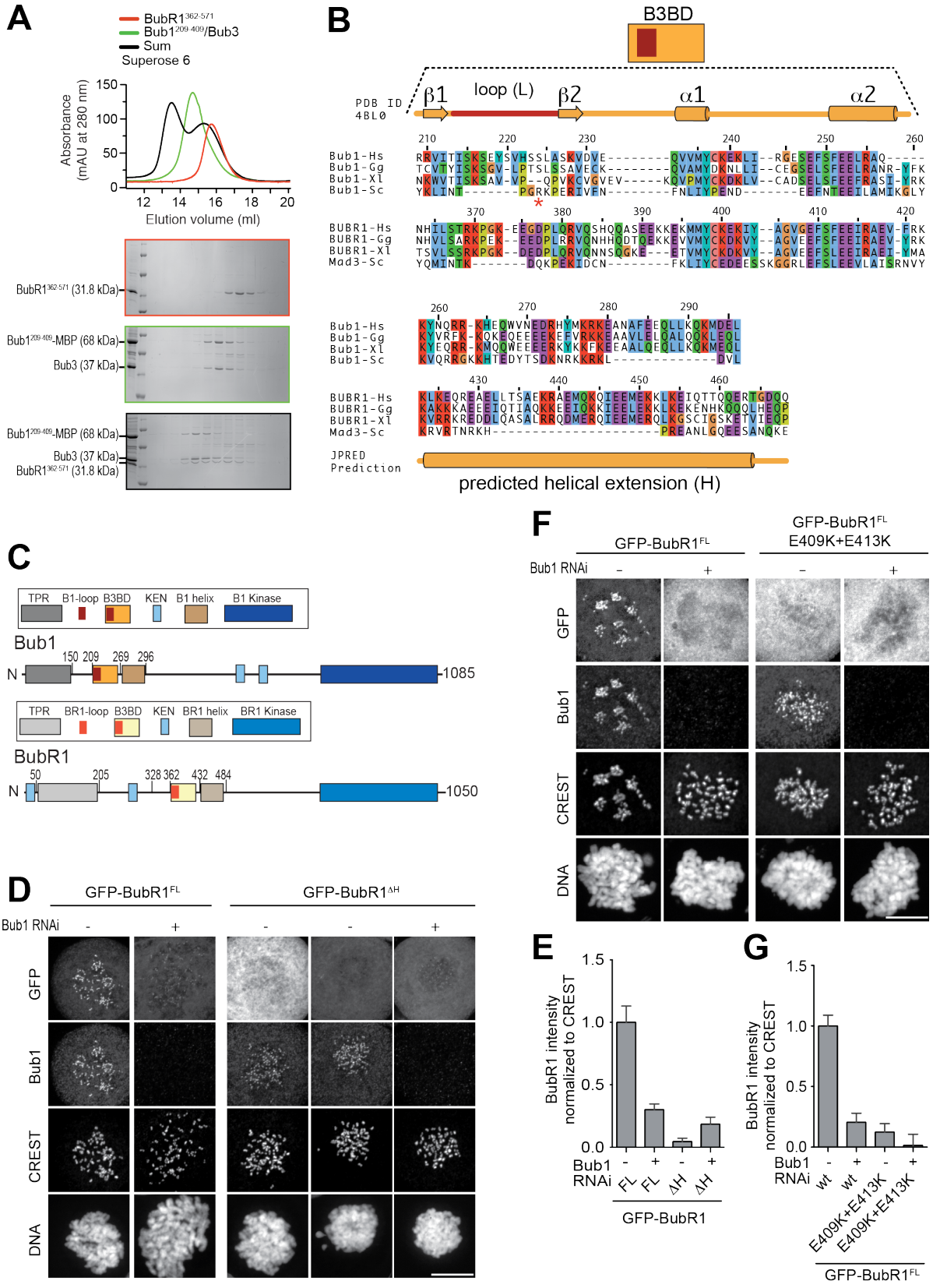

Figure 3-10 A pseudo-symmetric Bub1-BubR1 interaction

A) The identified minimal constructs BubR1$^{362-571}$ and Bub1$^{209-409}$/Bub3 interact in size exclusion chromatography. B) Multiple sequence alignments of the interacting domains of Bub1 and BubR1 from

four different species: *Homo sapiens* (Hs), *Gallus gallus* (Gg), *Xenopus laevis* (Xl) and *Saccharomyces cerevisiae* (Sc). Mad3 is the budding yeast BubR1 homolog. C) Updated schematic overview of Bub1 and BubR1 domain organization. TPR, tetratricopeptide repeats; B1, Bub1; BR1, BubR1; B3BD, Bub3-binding domain; KEN, lysine-glutamate-asparagine motif. D, F) Representative images of HeLa cells transfected with the indicated GFP-BubR1 constructs showing that neither BubR1$^{\Delta H}$ (D), which lacks the predicted helical segment of the CTE, nor BubR1$^{E409K+E413K}$ (F), which cannot bind Bub3, are able to localize to kinetochores. Cells were treated as in Figure 3-5 E. For BubR1$^{\Delta H}$ two different expression levels are depicted in the non-depleted condition. Scale bar: 10 µm. E, G) Quantification of BubR1 kinetochore levels in cells treated as in D and F, respectively. The graphs show mean intensity from at least two independent experiments. Error bars represent SEM. Values for BubR1^{FL} or the corresponding wt in non-depleted cells are set to 1.

This requirement for Bub3 binding may reflect a direct contribution to the interaction with Bub1 or alternatively a residual ability of BubR1/Bub3 to bind phosphorylated motifs on Knl1 or other kinetochore proteins. To try distinguishing between these possibilities, our collaborators in Prof. Geert Kops' laboratory (Hubrecht Institute and University Medical Centre Utrecht, Utrecht, The Netherlands) showed that Bub1 can recruit BubR1 to an ectopic site on chromosomes distinct from kinetochores (Janicki et al, 2004) and that this also requires Bub3 binding of Bub1 [data shown in (Overlack et al, 2015) Figure 6 G-H]. This result suggests that 1) Bub1/Bub3 is sufficient for recruitment of BubR1/Bub3 and kinetochores are not required for this interaction, and 2) that the role of Bub3 in recruitment of BubR1 might be direct and not through Knl1. Moreover, Bub3 seems to be required for a robust interaction between Bub1 and BubR1 on both sides of the complex.

In summary, we show that the mechanism of BubR1 kinetochore localization depends on a direct, pseudo-symmetric hetero-dimerization interaction with Bub1 (Figure 3-11). This interaction involves structurally equivalent segments of Bub1 and BubR1 comprising their B3BD and a CTE the first part of which is predicted to form a helix. Moreover, the interaction of Bub1 and BubR1 requires that each protein is bound to Bub3.

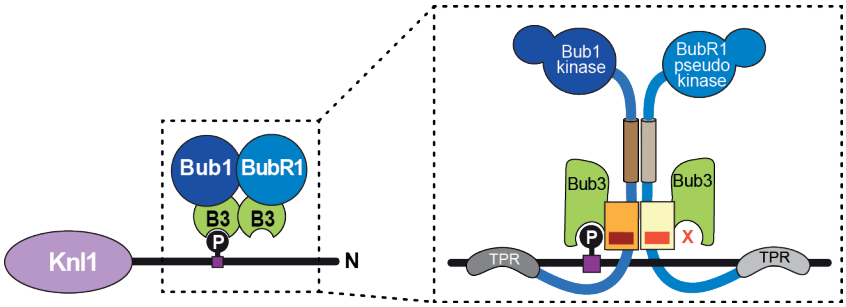

Figure 3-11 Model of the identified Bub1-BubR1 interaction

The left part shows the described kinetochore recruitment mechanism of BubR1/Bub3 to a Bub1/Bub3 complex on Knl1. The right part depicts a close-up of the identified pseudo-symmetric Bub1-BubR1 interaction, which involves equivalent segments of Bub1 and BubR1 comprising the B3BD and the CTE, the first part of which is predicted to form a helix in both proteins. The presence of Bub3 on both proteins seems to be essential for this interaction. The TPR regions of human Bub1 and BubR1 bind to non-conserved short motifs of Knl1 named KI1 and KI2, respectively, which for simplicity are not shown here (Kiyomitsu et al, 2007; Krenn et al, 2012; 2014). Figure adapted from (Overlack et al, 2015).

3.5 Functional dissection of BubR1 kinetochore recruitment

BubR1 plays an important role in both SAC signalling and chromosome bi-orientation and congression. We therefore asked if abrogating BubR1 kinetochore localization impaired these processes. HeLa cells depleted of endogenous BubR1 failed to arrest in mitosis in the presence of nocodazole. Under these experimental conditions, SAC function was rescued upon expression of GFP-BubR1^{wt} but not GFP-BubR1$^{E409K+E413K}$. GFP-BubR1$^{\Delta H}$, on the contrary, restored a robust SAC response (Figure 3-12 A). IP experiments showed that, unlike GFP-BubR1^{wt}, both GFP-BubR1$^{E409K+E413K}$ and GFP-BubR1$^{\Delta H}$ did not interact with Bub1 or Knl1, as expected based on their lack of kinetochore localization. Interestingly, GFP-BubR1$^{E409K+E413K}$ was slightly impaired in its ability to interact with Mad2 and Cdc20, two additional MCC subunits and was even more strongly impaired in its interaction with the APC/C. Conversely, GFP-BubR1$^{\Delta H}$ interacted with the MCC subunits (including Bub3, as expected) and with the APC/C at levels comparable to those of the GFP-BubR1^{wt} control (Figure 3-12 B-C). Thus, two distinct mutations in BubR1 that both impair its kinetochore localization, show opposite behaviors with regard to SAC proficiency. Furthermore, because GFP-BubR1$^{E409K+E413K}$ does not bind Bub3, whereas GFP-BubR1$^{\Delta H}$ does (Figure 3-12 B-C), it seems that at least in human cells BubR1 needs

to bind Bub3 to become incorporated into the MCC or bind to the APC/C. Given the phenotype observed in the IP (Figure 3-12 B), the latter possibility seems more likely and will be investigated in more detail in the progress of this work. Involvement of BubR1-bound Bub3 in an unknown SAC mechanism downstream of kinetochores has also recently been proposed (Han et al, 2014).

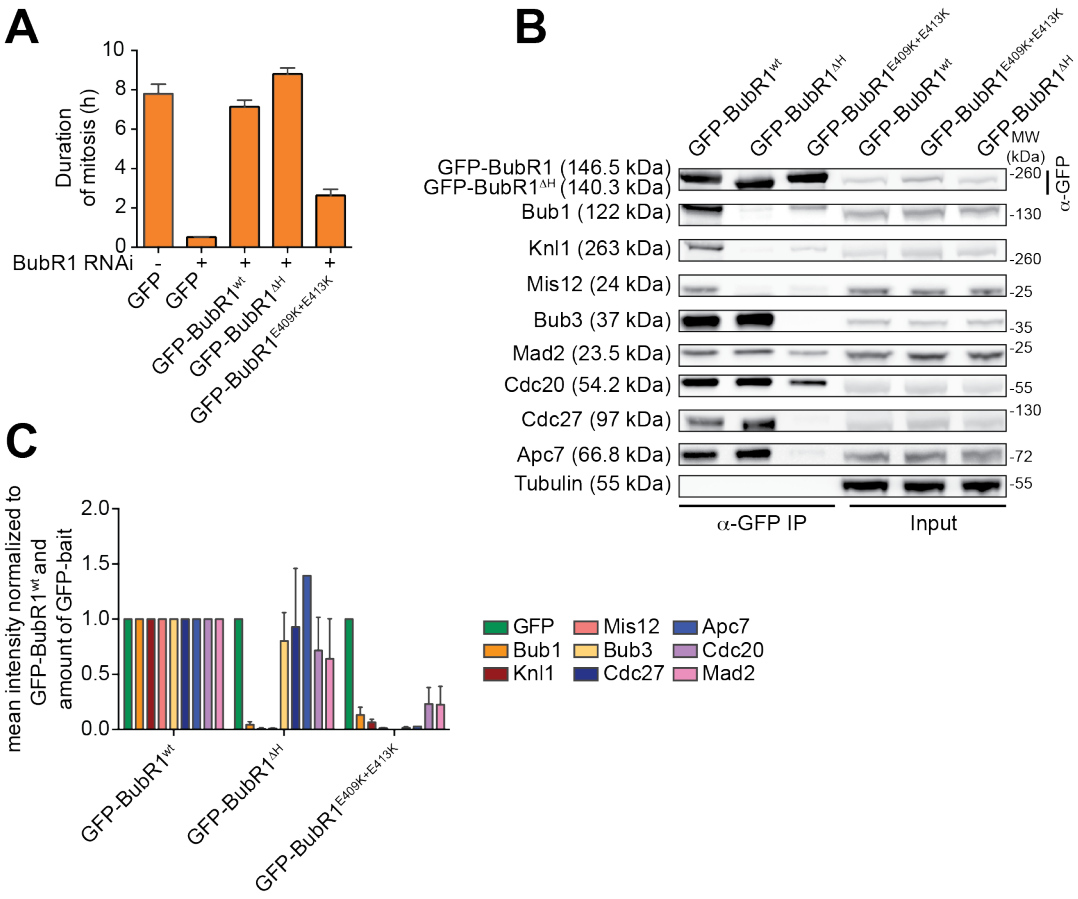

Figure 3-12 SAC function of kinetochore-localization defective BubR1 mutants

A) Mean duration of mitosis of Flp-In T-REx stable cell lines expressing GFP-BubR1^{wt} or the indicated mutants in the absence of endogenous BubR1 and in the presence of 50 nM nocodazole. Cell morphology was used to measure entry into and exit from mitosis by time-lapse-microscopy (n>44 per cell line per experiment) from at least three independent experiments. Error bars depict SEM. B) Western Blot of immunoprecipitates (IP) from mitotic Flp-In T-REx cell lines expressing the indicated GFP-BubR1 constructs. Tubulin was used as loading control. C) Quantification of the Western Blot in B. The amounts of co-precipitating proteins were normalized to the amount of GFP-BubR1 bait present in the IP. Values for GFP-BubR1^{wt} were set to 1. The graph shows mean intensity of two independent experiments. Error bars represent SEM.

In addition to its role in the SAC, BubR1 is important for establishing chromosome bi-orientation in HeLa cells, and this role requires its kinetochore localization (Johnson et al, 2004; Kruse et al, 2013; Lampson & Kapoor, 2005; Meraldi & Sorger, 2005; Suijkerbuijk et al, 2012b; Xu et al, 2013). Both GFP-BubR1$^{E409K+E413K}$ and GFP-BubR1$^{\Delta H}$, neither of which localizes to kinetochores, failed to promote the formation of stable kinetochore-microtubule attachments in cells depleted of endogenous BubR1 (Figure 3-13 A). This role of BubR1 in kinetochore-microtubule attachment has been attributed to its interaction with the B56 regulatory subunit of protein phosphatase 2A (PP2A^{B56}) (Espert et al, 2014; Kruse et al, 2013; Nijenhuis et al, 2014; Suijkerbuijk et al, 2012b; Xu et al, 2013). Recently, this function of BubR1 has been further implicated in SAC silencing (Espert et al, 2014; Nijenhuis et al, 2014). We asked if the defect of the BubR1$^{\Delta H}$ mutant in supporting kinetochore-microtubule attachment correlated with an impaired interaction with PP2A^{B56}. Indeed, in IPs, the B56 regulatory subunit associated with the GFP-BubR1$^{\Delta H}$ mutant less strongly than with the wild type protein (Figure 3-13 B). Furthermore, BubR1 is known to be hyperphosphorylated by Cdk1 and Plk1 kinases in mitosis. This phosphorylation has been shown to be important for the chromosome alignment function of BubR1, because it occurs at residues within and around the KARD domain in the C-terminal part of BubR1, and has been shown to be crucial for PP2A^{B56} binding (Elowe et al, 2010; Elowe et al, 2007; Huang et al, 2008; Suijkerbuijk et al, 2012b). In agreement with the impaired ability of the GFP-BubR1$^{\Delta H}$ mutant to bind to PP2A^{B56}, we found that this kinetochore-localization defective mutant did not show the typical mitotic mobility upshift of BubR1^{wt}. Interestingly, in absence of endogenous Bub1, also a condition in which BubR1^{wt} does not localize to kinetochores, the mobility upshift was also lost (Figure 3-13 C). Taken together, these results argue that lack of BubR1 phosphorylation away from kinetochores might prevent PP2A^{B56} binding and therefore interfere with chromosome alignment.

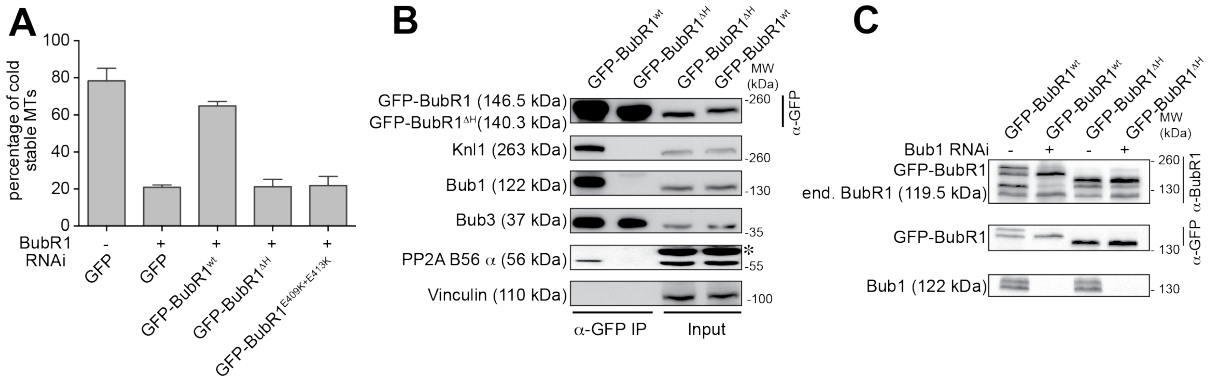

Figure 3-13 Chromosome alignment function of kinetochore-localization defective BubR1 mutants

A) Analysis of cold-stable kinetochore-microtubule attachments in cells expressing the indicated GFP-BubR1 constructs. B) Western Blot of immunoprecipitates (IP) from mitotic Flp-In T-REx cell lines expressing the indicated GFP-BubR1 constructs. The asterisk represents an unspecific band recognized by the PP2A antibody. C) Western Blot of extracts from mitotic Flp-In T-REx cell lines expressing the indicated GFP-BubR1 constructs in presence or absence of endogenous Bub1. Samples were run on a 7.5 % SDS-PAGE gel with an 80:1 acrylamide/bis-acrylamide ratio in order to assess the mobility upshift of BubR1 caused by phosphorylation.

3.6 Analysis of the role of the BubR1-loop

Our studies so far allowed us to gain a quite good understanding of the BubR1 kinetochore recruitment mechanism. Furthermore, we have established that the loop of Bub1 and BubR1 seems to be the main discriminating factor with regard to their kinetochore localization behavior. In this chapter, we therefore wanted to use this knowledge to study in more detail what the exact function of the BubR1-loop might be.

3.6.1 Refining the loop region of Bub1 and BubR1

BubR1$^{\Delta H}$ does not localize to kinetochores due to the impaired interaction with Bub1. Thus, we asked whether grafting the Bub1-loop into this BubR1 rescued kinetochore localization of BubR1$^{\Delta H}$. Surprisingly, neither in mock-depleted cells nor in cells depleted of endogenous Bub1 the Bub1-loop was able to restore kinetochore localization of BubR1$^{\Delta H}$ (Figure 3-14 A-C). The Bub1-loop was also unable to rescue kinetochore localization of a different truncation construct of BubR1 also impaired in the interaction with Bub1, BubR1$^{1-431}$ (Figure 3-14 A and first four panels D-E). This rules out a potential artificial auto-inhibition of BubR1$^{\Delta H}$, created by the lack of the

helix. Thus, we tried to understand this discrepancy to the results obtained with the full length proteins. We reasoned that the segment of the loop that we had initially swapped might have been too short to mediate kinetochore localization of these dimerization deficient constructs, and that the rescue we obtained with the full length BubR1$^{B1\text{-}L}$ could have, at least in parts, still profited from the ability of the BubR1 helix to dimerize with (also after RNAi depletion remaining) Bub1. Therefore, we decided to swap a longer region of the loop ranging from the first ß-sheet (ß1) until the start of the highly conserved core of the B3BD (Figure 3-14 F), since there is also considerable sequence divergence in the regions neighboring the actual loop. For simplicity, we called this newly swapped sequence “long loop“ (LL). Strikingly, Bub1$^{BR1\text{-}LL}$ was more severely impaired in kinetochore localization than the short swap mutant (Bub1$^{BR1\text{-}L}$) (Figure 3-14 G-H). Moreover, BubR1$^{B1\text{-}LL}$ showed even better kinetochore localization than the short swap mutant (BubR1$^{B1\text{-}L}$), especially in the absence of endogenous Bub1 (Figure 3-14 I-J). Importantly, BubR1$^{1\text{-}431\ B1\text{-}LL}$ localized to kinetochores in presence and absence of endogenous Bub1 (panels 5 and 6 Figure 3-14 D-E), confirming that, if the swapped sequence is sufficiently long, the loop can mediate kinetochore localization even of a dimerization deficient BubR1 mutant.

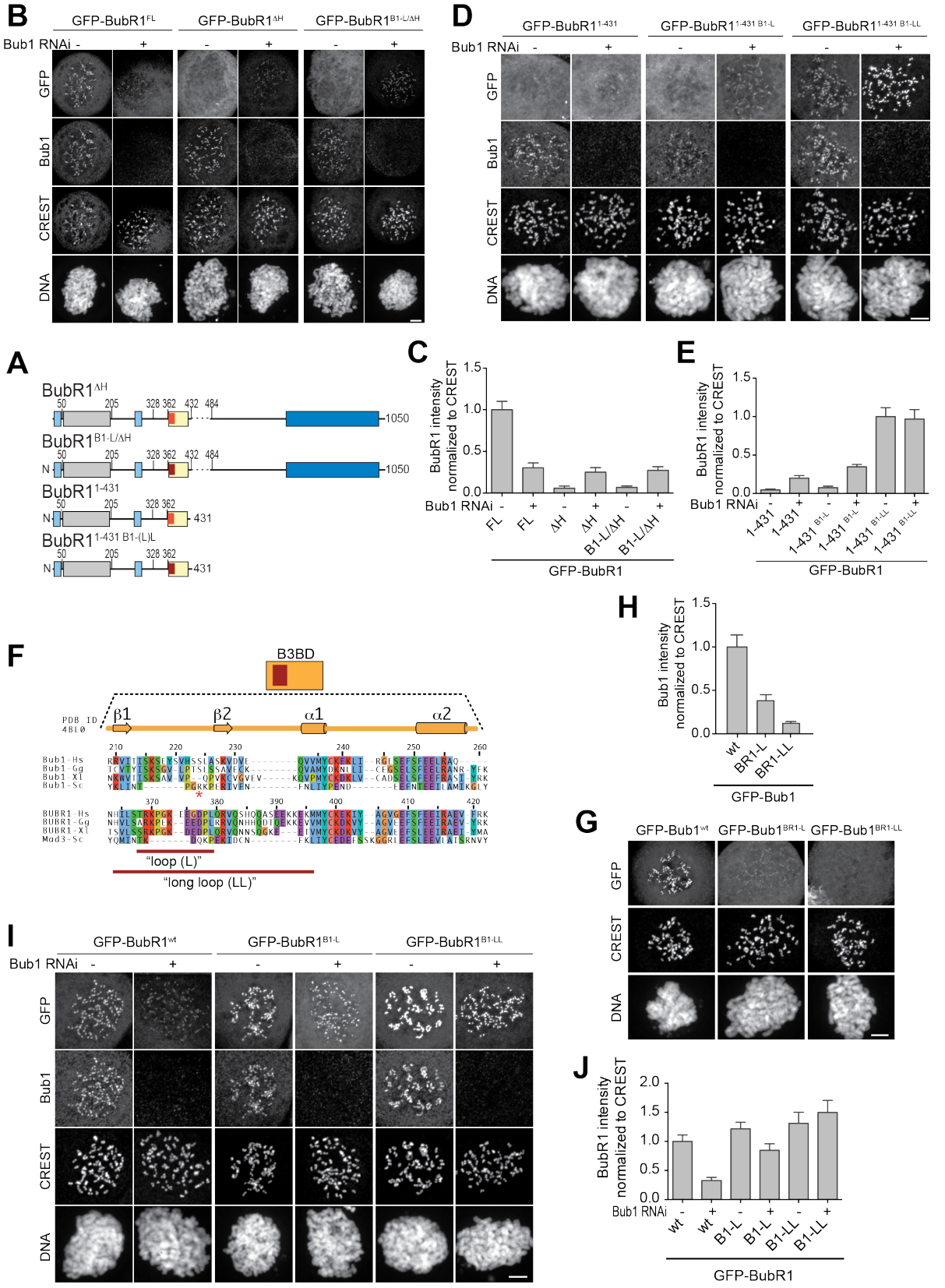

Figure 3-14 Refining the loop region of Bub1 and BubR1

A) Schematic of domain organization of BubR1 truncation/deletion constructs. B, D) Representative images of HeLa cells transfected with the indicated GFP-BubR1 constructs showing that the short

Bub1-loop (B1-L) is not sufficient to rescue kinetochore localization of $BubR1^{\Delta H}$ (B) or $BubR1^{1-431}$ (first four panels D) but that the long loop (B1-LL) can rescue kinetochore localization of $BubR1^{1-431}$ (last two panels D). Cells were treated as in Figure 3-5 E. Scale bar: 10 µm. C, E) Quantification of BubR1 kinetochore levels in cells treated as in B and D, respectively. The graphs show mean intensity from three independent experiments. Error bars represent SEM. Values for $BubR1^{FL}$ or $BubR1^{1-431\ B1\text{-}LL}$ in non-depleted cells are set to 1, respectively. F) Multiple sequence alignments of the B3BDs of Bub1 and BubR1 from four different species (as in Figure 3-3 B). The initally swapped short loop (L) and the newly swapped long loop (LL) sequence are indicated by the red lines. G) Representative images of HeLa cells transfected with the indicated GFP-Bub1 constructs showing that GFP-$Bub1^{BR1\text{-}LL}$ is stronger impaired in kinetochore localization than the short loop mutant (BR1-L). Scale bar: 10 µm. H) Quantification of Bub1 kinetochore levels in cells treated as in G. The graph shows mean intensity from three independent experiments. Error bars represent SEM. Values for $Bub1^{wt}$ are set to 1. I) Representative images of HeLa cells transfected with the indicated GFP-BubR1 constructs showing that GFP-$BubR1^{B1\text{-}LL}$ localizes better to kinetochores than the short loop mutant (B1-L) in presence and absence of endogenous Bub1. Cells were treated as in Figure 3-5 E. Scale bar: 10 µm. J) Quantification of BubR1 kinetochore levels in cells treated as in I. The graph shows mean intensity from three independent experiments. Error bars represent SEM. Values for $BubR1^{wt}$ in non-depleted cells are set to 1.

Since we have shown that the long swap mutants behave closely to a „perfect“ swap-phenotype, we will concentrate on them from now on.

3.6.2 BubR1 kinetochore turnover is determined by its kinetochore binding sites

To test the mechanism of kinetochore localization of BubR1 (and Bub1), we performed Fluorescence Recovery after Photobleaching (FRAP) experiments to measure the turnover times of BubR1 and its mutants at kinetochores. The half-life of BubR1 at kinetochores is relatively fast ($t_{1/2}$ = 3-20 s) (Howell et al, 2004). It was proposed that this rapid turnover of BubR1 might reflect its cycle of incorporation into the MCC and might therefore be important for its SAC function. Having shown that the loop determines the different kinetochore localization behavior of Bub1 and BubR1, we next wanted to investigate how the loop-swap influences kinetochore turnover of BubR1.

FRAP experiments in cells expressing different GFP-tagged BubR1 constructs (the cartoon besides each graph depicts the way in which each construct localizes to kinetochores), in the absence of the endogenous protein, revealed a different

turnover of BubR1$^{B1\text{-}LL}$ in comparison to BubR1^{wt}. In agreement with published data (Howell et al, 2004), GFP-BubR1^{wt} showed a half life of 7.7 s (fit with a single-exponential curve). By contrast, BubR1$^{B1\text{-}LL}$ data were best fit with a double exponential curve with a fast half-life of 5.2 s (accounting however only for 15.5 % of the curve) and a slow half-life of 56.4 s (Figure 3-15 A-B). The two-phase exponential recovery suggests a dual binding modality for BubR1$^{B1\text{-}LL}$, probably caused by the fact that not all MELT^{P} repeats are occupied with Bub1 (Vleugel et al, 2015b). Interestingly, in the absence of endogenous Bub1, BubR1$^{B1\text{-}LL}$ restored its fast turnover ($t_{1/2}$=10.8 s, Figure 3-15 C) and behaved like Bub1^{wt}. Bub1^{wt} displayed a fast turnover ($t_{1/2}$=11.6 s, Figure 3-15 D). This observation is in contrast to previous experiments that reported Bub1 to be a rather stable kinetochore component (Howell et al, 2004; Shah et al, 2004), but is in agreement with a recent paper (Asghar et al, 2015) reporting Bub1 turnover to occur with a half-life of 15 s. In summary, these experiments suggest that the additional MELT^{P} binding site in BubR1$^{B1\text{-}LL}$ created by the Bub1-loop slows down the turnover by allowing binding to Bub1 and Knl1 MELT^{P} at the same time. However, if Bub1 is removed, BubR1$^{B1\text{-}LL}$ cannot hetero-dimerize any longer and its turnover is fast, being only determined by binding to Knl1 MELT^{P}.

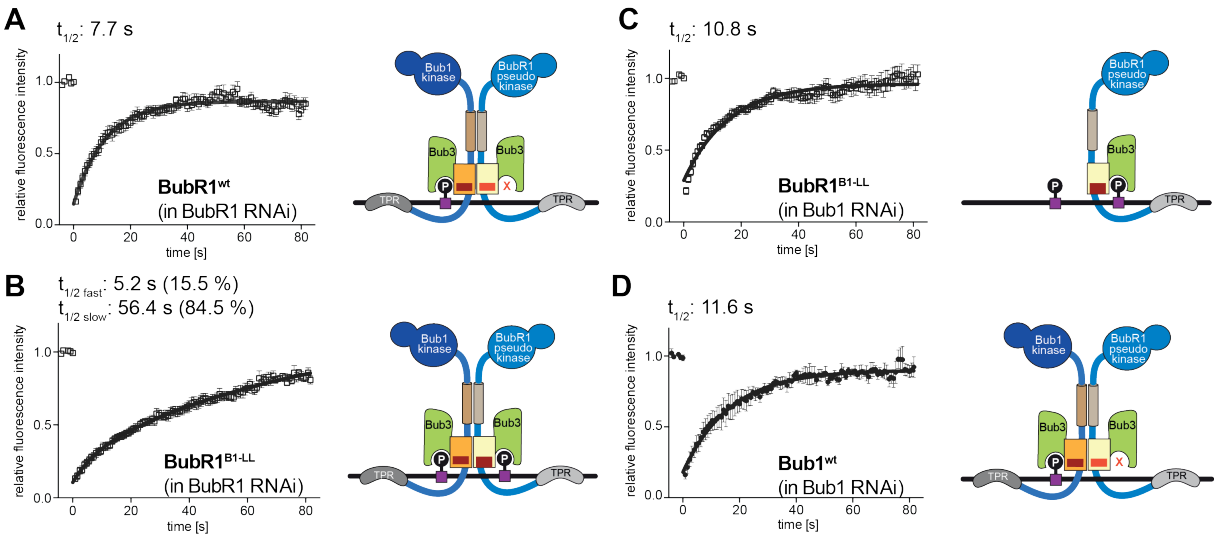

Figure 3-15 Kinetochore turnover of BubR1 with the Bub1-loop

A-D) FRAP analyses of BubR1^{wt} (A), BubR1$^{B1\text{-}LL}$ (B-C) and Bub1^{wt} (D) in different conditions. Relevant recovery parameters are shown above the graph. The cartoons show by which interaction the corresponding construct localizes to kinetochores.

To test the hypothesis that the number of interaction sites at kinetochores determines BubR1 turnover, we created two additional mutants of BubR1 with the rationale to prevent heterodimer formation in different ways. In the first construct, we swapped the whole region of the Bub1 B3BD and the Bub1 helix onto BubR1 (BubR1$^{B1\text{-}B3BD/B1\text{-}H}$). According to our model, this mutant ought to localize to kinetochores via the interaction with MELT^{P} mediated by the Bub1-loop, but cannot interact with Bub1, since the Bub1 helix does not form homotypic interactions. In the second construct, we deleted from BubR1$^{B1\text{-}LL}$ the helix, which is crucial for the interaction with Bub1 (BubR1$^{B1\text{-}LL/\Delta H}$), as shown in Figure 3-10 D-E. Therefore, this construct ought to be unable to dimerize with Bub1, but should still localize to kinetochores via the MELT^{P} Bub1-loop interaction. Both dimerization-deficient BubR1 mutants suppressed the slow turnover observed with BubR1$^{B1\text{-}LL}$, cycling with half-times of 11.2 s in the case of BubR1$^{B1\text{-}B3BD/B1\text{-}H}$ and 6.6 s in the case of BubR1$^{B1\text{-}LL/\Delta H}$ (Figure 3-16 A-B).

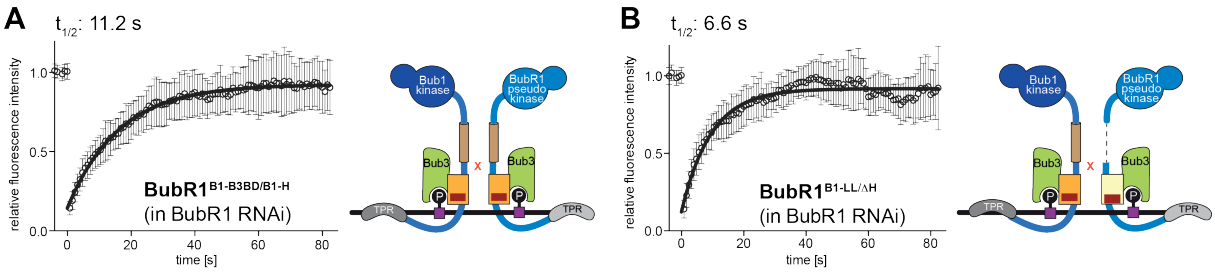

Figure 3-16 Kinetochore turnover of dimerization deficient BubR1 mutants

A-B) FRAP analyses of BubR1$^{B1\text{-}B3BD/B1\text{-}H}$ (A) and BubR1$^{B1\text{-}LL/\Delta H}$ (B) in the absence of endogenous BubR1. Relevant recovery parameters are shown above the graph. The cartoons show by which interaction the corresponding construct localizes to kinetochores.

The results obtained with the dimerization deficient mutants agree with our model for the mechanism of BubR1 turnover at kinetochores, and indicate that the latter is regulated by the number of interaction sites that target BubR1 to kinetochores.

3.6.3 BubR1 with the Bub1-loop cannot maintain a SAC arrest

Next, we asked whether the swapping of domains (an overview of the constructs is presented in Figure 3-17 A) is compatible with the SAC function of BubR1. This question is of particular interest, because of the SAC defect we observed already with the short loop-swap mutant. We reasoned that the slower kinetochore turnover

of the long loop mutant of BubR1 might cause a SAC defect by immobilising BubR1 at kinetochores. Indeed, HeLa cells depleted of endogenous BubR1 failed to arrest in mitosis in the presence of nocodazole. SAC function was re-established upon expression of GFP-BubR1^{wt} but GFP-BubR1$^{B1\text{-}LL}$ was not able to restore a robust SAC response. As a positive control for the SAC defect we employed an alanine mutant of the first KEN-box of BubR1 (GFP-BubR1$^{KEN1/AAA}$), which has been published to be defective in Cdc20-binding, MCC-formation and consequently SAC signaling (Lara-Gonzalez et al, 2011) (Figure 3-17 B). To test our hypothesis that reduced turnover at kinetochores causes impaired SAC function of BubR1$^{B1\text{-}LL}$, we asked if GFP-BubR1$^{B1\text{-}B3BD/B1\text{-}H}$ or GFP-BubR1$^{B1\text{-}LL/_{\Delta}H}$, both of which cycled quickly, were able to restore a robust SAC response. Neither construct, however, restored the SAC in cells depleted of endogenous BubR1 (Figure 3-17 C-D), thus excluding the slow turnover as direct cause of the observed SAC defect of GFP-BubR1$^{B1\text{-}LL}$. Interestingly, BubR1$^{\Delta H}$ was SAC proficient (Figure 3-12 A), as was a BubR1 mutant containing the Bub1 helix instead of its own (data not shown), arguing that the helix does not contribute to the SAC function of BubR1. Instead, these data point to the presence of the Bub1-loop on BubR1, the common element amongst these mutants, as the likely source of the SAC defect.

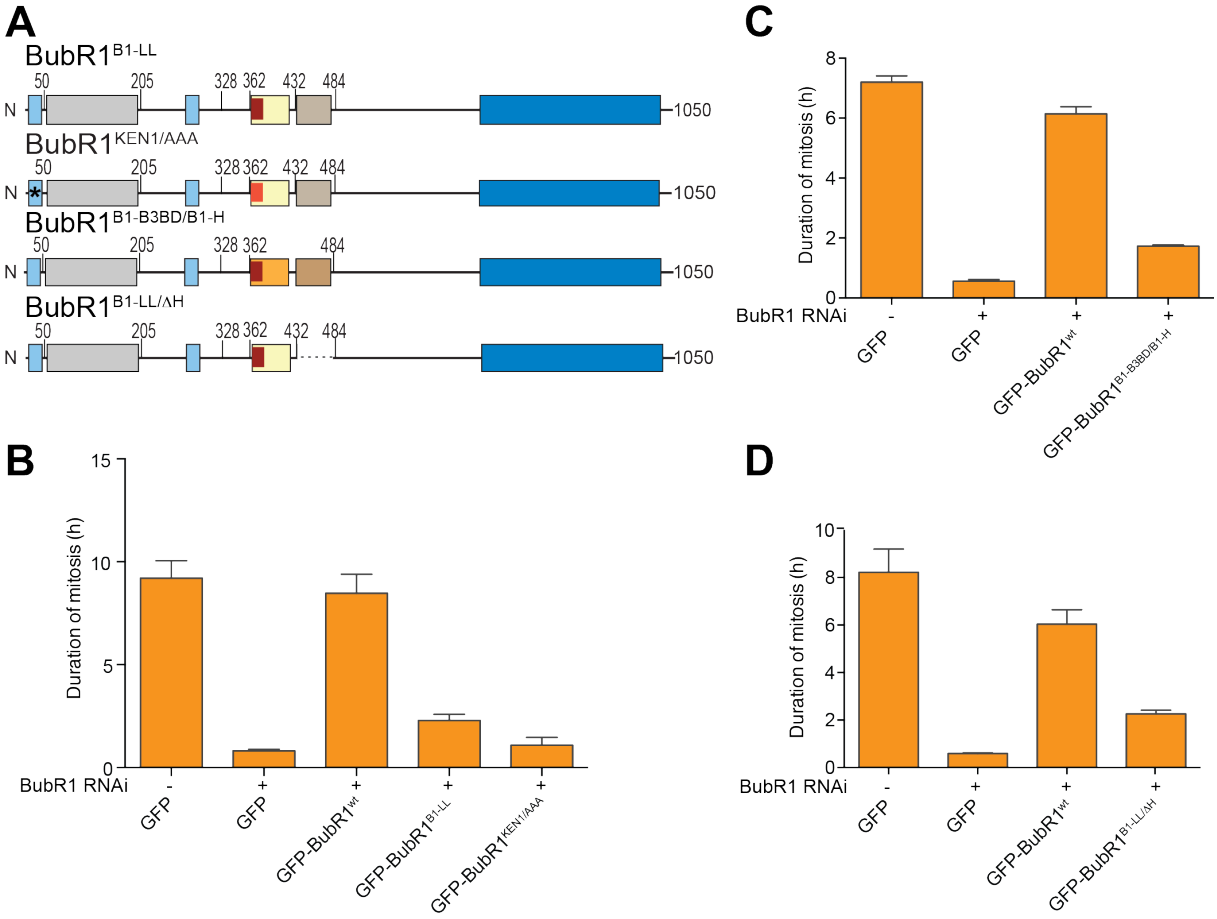

Figure 3-17 BubR1 mutants containing the Bub1-loop are SAC defective

A) Schematic domain organization of the BubR1 constructs used. B-D) Mean duration of mitosis of Flp-In T-REx stable cell lines expressing the indicated GFP-BubR1 constructs in the absence of endogenous BubR1 and in the presence of 50 nM nocodazole. Cell morphology was used to measure entry into and exit from mitosis by time-lapse-microscopy (n>23 for BubR1$^{B1\text{-}LL}$ and BubR1$^{KEN1/AAA}$, n>20 for BubR1$^{B1\text{-}B3BD/B1\text{-}H}$ and n>37 for BubR1$^{B1\text{-}LL/\Delta H}$ per cell line per experiment) from three independent experiments. Error bars depict SEM.

IP experiments showed that all mutants were impaired in their interaction with the MCC components Mad2 and Cdc20 and were even more stongly impaired in their ability to bind APC/C components (Figure 3-18 A-F), in agreement with the observed SAC defect. Interestingly, the BubR1$^{B1\text{-}B3BD/B1\text{-}H}$ mutant showed higher levels of APC/C binding than the other two mutants despite showing similar levels of SAC deficiency, suggesting a possible interaction of the B1-B3BD with the APC/C, which however does not seem to be inhibitory. This observation will be investigated in more detail later in this thesis (see section 3.6.5). All constructs interacted at similar levels with Bub3, excluding major structural perturbations. As expected, GFP-BubR1$^{B1\text{-}}$

$^{B3BD/B1\text{-}H}$ and GFP-BubR1$^{B1\text{-}LL/_{\Delta}H}$ were impaired in the interaction with Bub1. Interestingly, GFP-BubR1$^{B1\text{-}LL}$ seemed to interact considerably more strongly with Knl1, probably because it can also engage in a direct interaction with Knl1 via the Bub1-loop in addition to pulling down Knl1 indirectly via the interaction with Bub1 (Figure 3-18 A-B). Furthermore, it is interesting to note the (although modest) difference in Cdc20-binding of the KEN1/AAA and the loop-swap mutant. This could suggest that BubR1$^{B1\text{-}LL}$ might be able to form MCC but that the interaction with the APC/C is not possible. This would argue that the observed SAC defects might be due to different reasons. Whereas BubR1$^{KEN1/AAA}$ cannot form MCC and therefore never inhibits the APC/C, the loop-swap mutants presumably can be incorporated into MCC but the latter for unknown reason cannot inhibit APC/C. Nevertheless, since Cdc20 is sequestered in this MCC, there may also be reduced levels of free Cdc20 required to activate the APC/C, resulting in the "intermediate“ arrest phenotype observed in the SAC assays with the loop mutants (Figure 3-17).

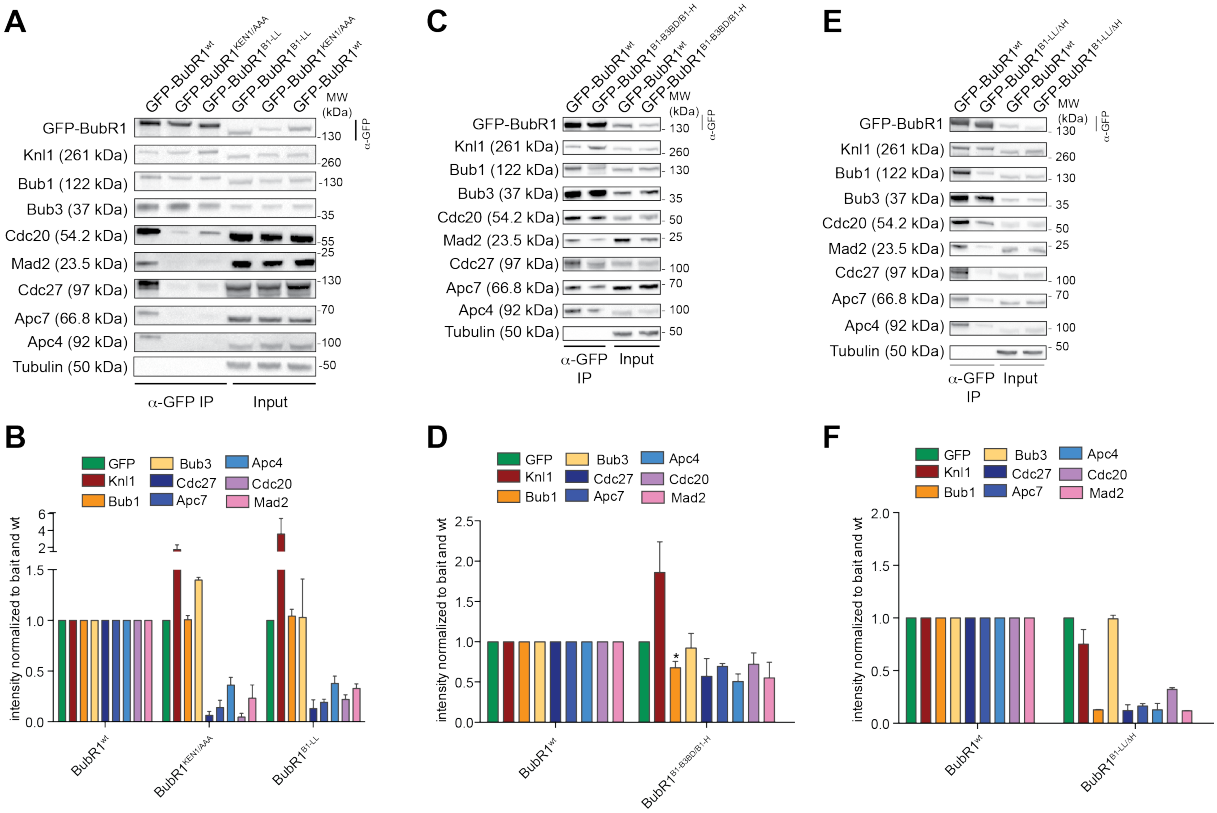

Figure 3-18 IPs confirming the SAC defect of the BubR1 mutants containing the Bub1-loop

A, C, E) Western Blot of immunoprecipitates (IP) from mitotic Flp-In T-REx cell lines expressing the indicated GFP-BubR1 constructs. Tubulin was used as loading control. B, D, F) Quantification of the

Western Blots in A, C and E, respectively. The amounts of co-precipitating proteins were normalized to the amount of GFP-BubR1 bait present in the IP. Values for GFP-BubR1^{wt} were set to 1. The graphs show mean intensity of at least two independent experiments. Error bars represent SEM. The asterisk in D denotes that this apparently high level of Bub1 binding is due to the fact that the epitope of the used Bub1-antibody partly overlaps with the swapped region and therefore the antibody also recognizes the GFP-BubR1$^{B1\text{-}B3BD/B1\text{-}H}$ mutant.

Summarizing these results, whenever BubR1 contains the Bub1-loop it is unable to rescue the SAC defect caused by depletion of endogenous BubR1, arguing that the BubR1-loop cannot be replaced by a related sequence without disturbing BubR1 SAC function. The comparison of BubR1$^{\Delta H}$, which is SAC proficient despite the lack of kinetochore localization (Figure 3-12 A), with BubR1$^{B1\text{-}LL/\Delta H}$, which only differs for the presence of the Bub1-loop, but which is SAC defective, illustrates this very clearly (Figure 3-17 D) and argues that grafting the Bub1-loop on BubR1 suppresses BubR1 SAC function. Levels of endogenous Bub1 at kinetochores in cells expressing the BubR1 mutants with the Bub1-loop were not significantly changed (data not shown) ruling out a potential competition of BubR1 loop-swap mutants with Bub1 for Knl1 MELT^{P} binding as the reason for the observed SAC defect.

3.6.4 The BubR1-loop is needed for BubR1 SAC function

To address the question why the Bub1-loop on BubR1 disrupts its SAC function, we asked whether the BubR1-loop itself is required for the SAC. Thus, we tested GFP-BubR1$^{\Delta L}$ and GFP-BubR1$^{\Delta LL}$, in which either the short or the long loop was deleted and GFP-BubR1$^{GS\text{-}loop}$, in which the loop was replaced by a neutral Gly-Ser linker sequence. Since the deletion and the replacement showed the same phenotype, only the results obtained with the deletion mutants are shown here.

First, we assessed the influence of deleting the loop on kinetochore localization of BubR1. As expected, both deletion mutants (GFP-BubR1$^{\Delta L}$ and $^{\Delta LL}$) still localized to kinetochores in a Bub1-dependent manner, behaving in this respect as GFP-BubR1^{wt} (Figure 3-19 A-C). In agreement with our proposed model for regulation of kinetochore turnover of BubR1, BubR1$^{\Delta LL}$ cycled quickly with a half-life of 9.9 s, reflecting its single mode of kinetochore localization via the interaction with Bub1 (Figure 3-19 D).

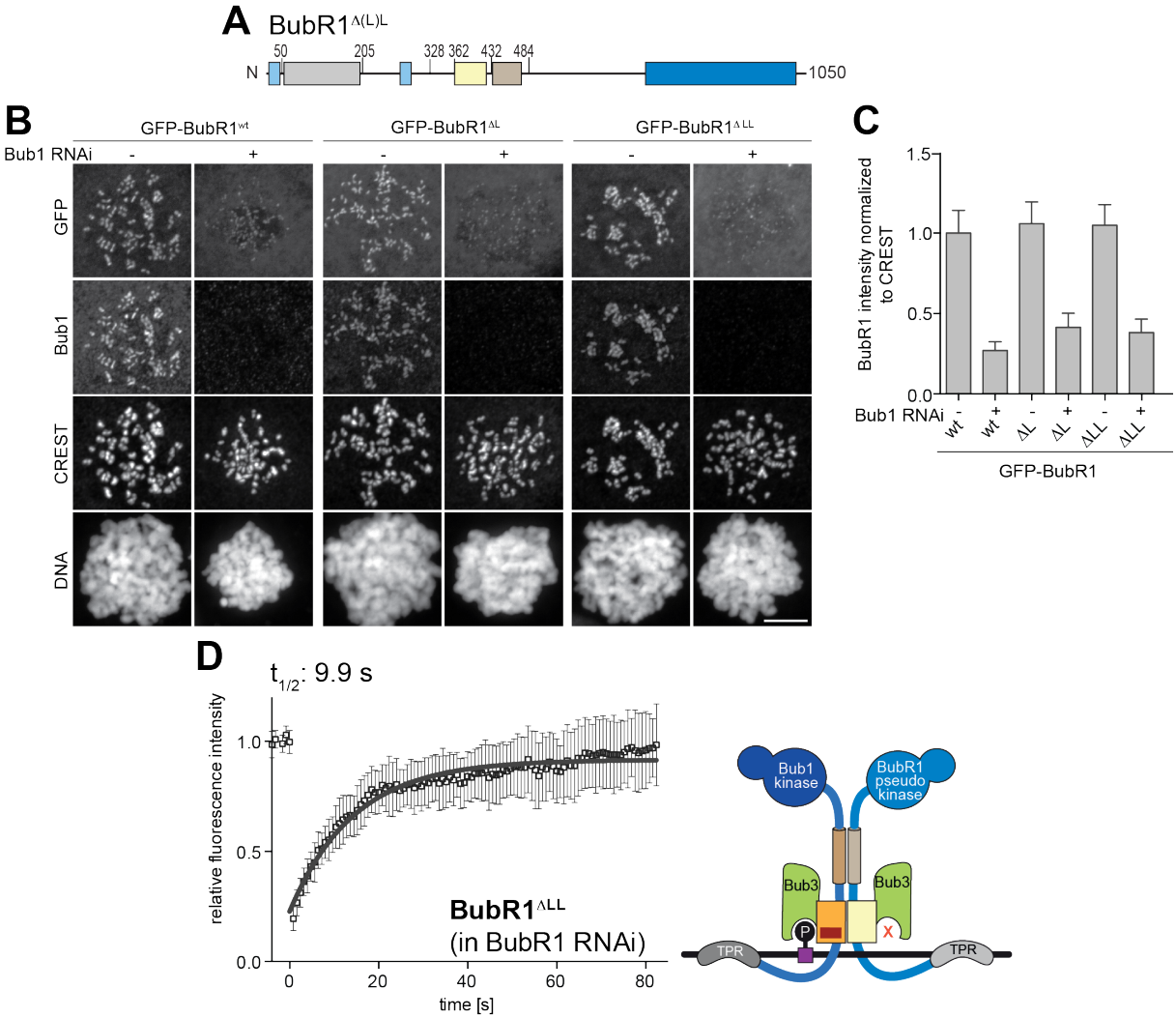

Figure 3-19 The BubR1-loop is not required for kinetochore localization or turnover

A) Schematic domain organization of the BubR1$^{\Delta(L)L}$ construct. Constructs lacking the short (L) and long loop (LL) versions were created by deleting residues 368-379 or 363-396 of BubR1, respectively. B) Representative images of HeLa cells transfected with the indicated GFP-BubR1 constructs in presence or absence of endogenous Bub1 showing that the lack of the loop does not influence kinetochore localization, as expected. Scale bar: 10 µm. C) Quantification of BubR1 kinetochore levels in cells treated as in B. The graph shows mean intensity from three independent experiments. Error bars represent SEM. Values for BubR1^{wt} in non-depleted cells are set to 1. D) FRAP analysis of BubR1$^{\Delta LL}$ in the absence of endogenous BubR1. Relevant recovery parameters are shown above the graph. The cartoon depicts by which interaction this construct localizes to kinetochores.

Next, we asked, whether the BubR1-loop is required for the SAC function of BubR1. As shown before, HeLa cells depleted of endogenous BubR1 failed to arrest in mitosis in the presence of nocodazole. SAC function was re-gained upon expression of GFP-BubR1^{wt}, but BubR1 lacking the loop (GFP-BubR1$^{\Delta L}$ and GFP-BubR1$^{\Delta LL}$) was

not able to restore a robust SAC response (Figure 3-20 A). This SAC defect was confirmed in IP experiments showing that the loop deletion mutants were strongly impaired in their ability to interact with the APC/C, and, to a lower extent, also impaired in their interaction with the MCC components Mad2 and Cdc20 (Figure 3-20 B-C). This suggests that the loop of BubR1 might be required to establish a robust interaction of MCC with the APC/C.

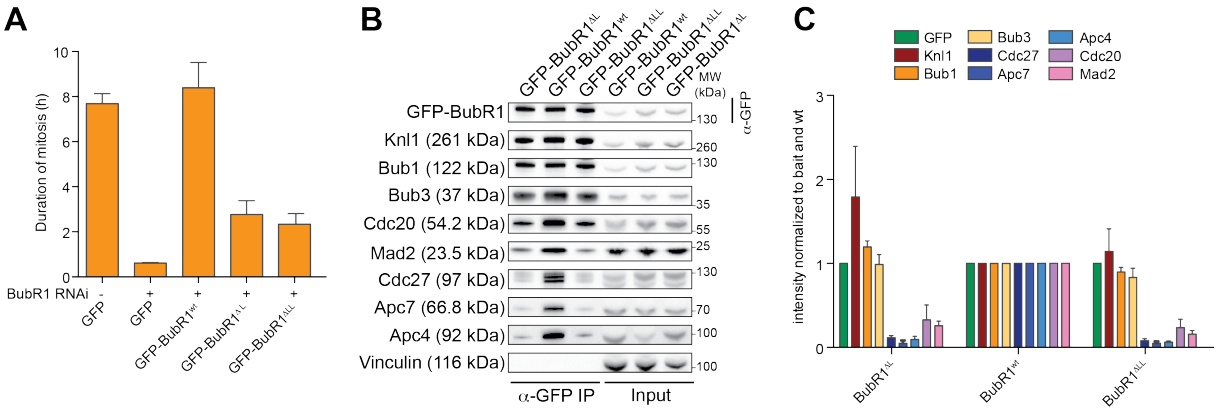

Figure 3-20 The BubR1-loop is required for BubR1 SAC function

A) Mean duration of mitosis of Flp-In T-REx stable cell lines expressing the indicated GFP-BubR1 constructs in the absence of endogenous BubR1 and in the presence of 50 nM nocodazole. Cell morphology was used to measure entry into and exit from mitosis by time-lapse-microscopy (n>32 per cell line per experiment) from two independent experiments. Error bars depict SEM. B) Western Blot of immunoprecipitates (IP) from mitotic Flp-In T-REx cell lines expressing the indicated GFP-BubR1 constructs showing that the lack of the loop results in strongly impaired APC/C binding. Vinculin was used as loading control. C) Quantification of the Western Blot in B. The amounts of co-precipitating proteins were normalized to the amount of GFP-BubR1 bait present in the IP. Values for GFP-BubR1^{wt} were set to 1. The graph shows mean intensity of at least three independent experiments. Error bars represent SEM.

Importantly, the deletion of the loop in the BubR1$^{\Delta H}$ mutant (which on its own was SAC proficient despite the lack of kinetochore localization) also resulted in a SAC defect and in an impaired interaction with APC/C subunits and the MCC components Cdc20 and Mad2 (Figure 3-21 A-C). As previously observed, the reduction in binding to the APC/C was more striking than the reduction in binding to the MCC in these IPs.

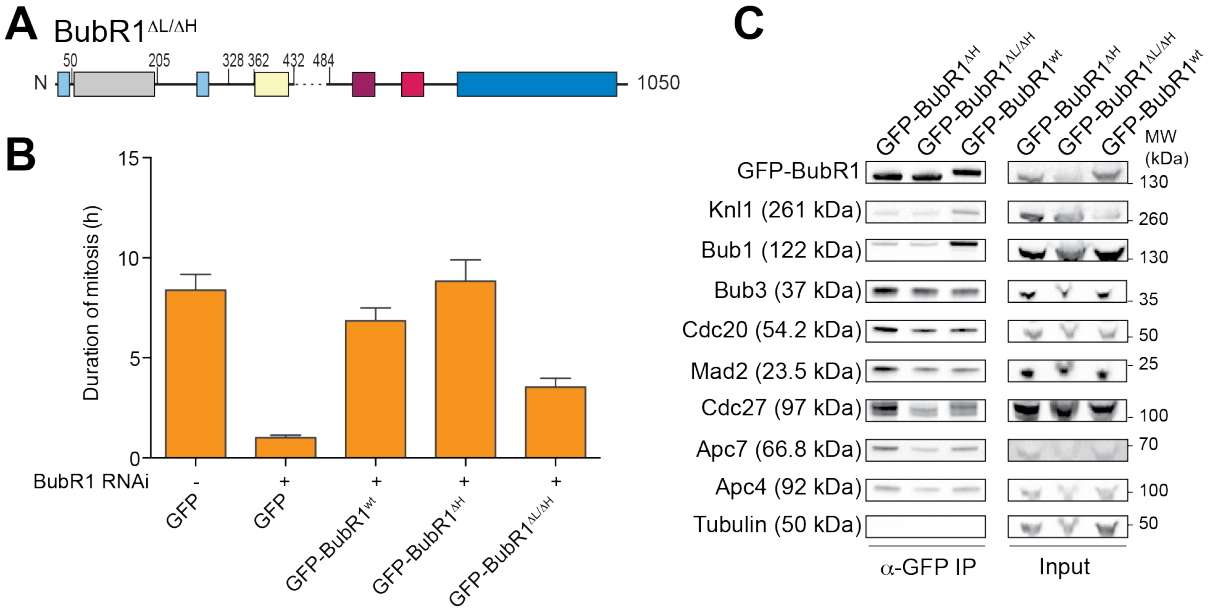

Figure 3-21 Deletion of the loop causes a SAC defect of BubR1$^{\Delta H}$

A) Domain organization of the BubR1 construct that lacks the loop and the helix. B) Mean duration of mitosis of Flp-In T-REx stable cell lines expressing the indicated GFP-BubR1 constructs in the absence of endogenous BubR1 and in the presence of 50 nM nocodazole. Cell morphology was used to measure entry into and exit from mitosis by time-lapse-microscopy (n>25 per cell line per experiment) from at least two independent experiments. Error bars depict SEM. C) Western Blot of immunoprecipitates (IP) from mitotic Flp-In T-REx cell lines expressing the indicated GFP-BubR1 constructs showing that the deletion of the loop results in impaired APC/C binding. Tubulin was used as loading control.

Collectively, these results suggest a role of the BubR1-loop in the SAC and point to the possibility that the loop might be involved in binding of BubR1 (as part of the MCC) to the APC/C. This seems to be a specific feature of the BubR1-loop sequence, as it was neither possible to replace it with another sequence, nor to delete it without significantly impairing BubR1 SAC function.

3.6.5 The BubR1-loop directs binding to the APC/C

To investigate whether the role of the BubR1-loop in the SAC is to mediate specific interactions with the APC/C, as suggested by the IPs, we performed a series of quantitative SILAC immune-precipitation experiments followed by mass-spectrometry. In these IPs we used the short reporter construct of BubR1 (and Bub1), consisting of the B3BD, as a bait to identify potential interaction partners in mitotic lysates.

First, we aimed to identify interaction partners of the B3BD of BubR1 (residues 362-431) by comparing it to GFP. With these settings, we identified several of the APC/C subunits (always represented as blue rectangles) as specific interaction partners of the BubR1 B3BD (Figure 3-22 A). These interactions could be further validated in a GFP-IP, in which the B3BD of BubR1 pulled down the APC/C subunits Cdc27/Apc3, Apc7 and Apc4. In the reciprocal IP of the APC/C subunit Cdc27 small amounts of the BubR1 B3BD could be identified as bound to the APC/C (Figure 3-22 B-C).

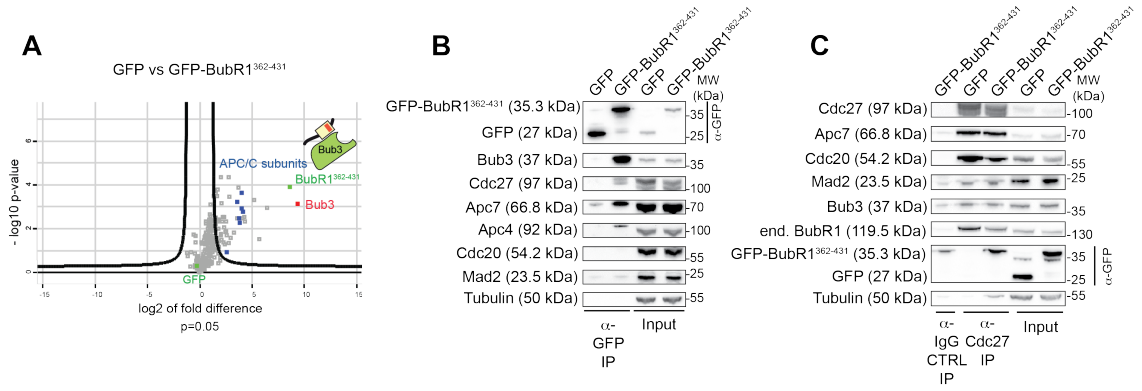

Figure 3-22 The B3BD of BubR1 binds to the APC/C

A) Volcano plot showing the results from three independent SILAC experiments using GFP and GFP-BubR1$^{362-431}$ as affinity resins to identify specific interaction partners in mitotic lysates. A p-value of 0.05 was used as cut-off for significance. B, C) Western Blot of α-GFP (B) or α-Cdc27 (C) immunoprecipitates (IP) from mitotic Flp-In T-REx cell lines expressing either GFP or GFP-BubR1$^{362-431}$ showing that the B3BD of BubR1 is able to pull down APC/C subunits (B) and vice-versa (C). Tubulin was used as loading control. Background binding of GFP-BubR1$^{362-431}$ in the IgG control IP can most likely be explained by low stringency washes performed in this experiment.

We then performed another SILAC experiment to compare the interactions of the B3BD of BubR1 without (GFP-BubR1$^{362-431\ \Delta L}$) and with the loop (GFP-BubR1$^{362-341}$). This comparison showed that APC/C was preferentially bound to the B3BD of BubR1 containing the loop (Figure 3-23 A). Besides, the dependency of APC/C binding on the BubR1-loop could be recapitulated in IPs (Figure 3-23 B-C). These results provide further evidence that the loop of BubR1 is involved in APC/C binding and might explain the observed checkpoint defect of the BubR1$^{\Delta(L)L}$ mutants (Figure 3-20).

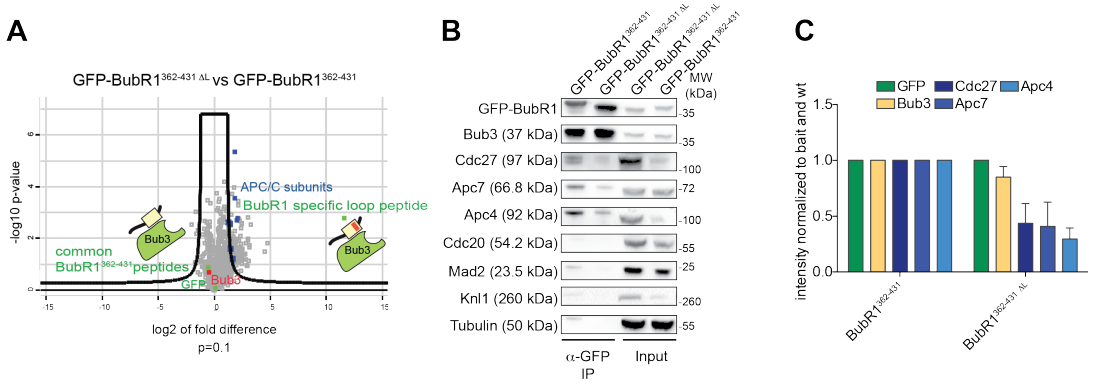

Figure 3-23 The BubR1 B3BD-APC/C interaction depends on the BubR1-loop

A) Volcano plot showing the results from three independent SILAC experiments using GFP-BubR1$^{362\text{-}431\ \Delta L}$ and GFP-BubR1$^{362\text{-}431}$ as affinity resins to identify specific interaction partners in mitotic lysates. A p-value of 0.1 was used as cut-off for significance. B) Western Blot of immunoprecipitates (IP) from mitotic Flp-In T-REx cell lines expressing either GFP-BubR1$^{362\text{-}431}$ or GFP-BubR1$^{362\text{-}431\ \Delta L}$ showing that the interaction with the APC/C is impaired if the loop is deleted. Tubulin was used as loading control. C) Quantification of the Western Blot in B. The amounts of co-precipitating proteins were normalized to the amount of GFP-BubR1 bait present in the IP. Values for GFP-BubR1$^{362\text{-}431}$ were set to 1. The graph shows mean intensity of two independent experiments. Error bars represent SEM.

As all results shown so far predict the B3BD of BubR1 to be an APC/C binder and the B3BD of Bub1 to be a Knl1 binder, we wanted to validate these results in another SILAC experiment, by making a direct comparison between these two B3BD constructs. (This experiment has already been shown in Figure 3-6 to emphasize that Knl1 binding is a specific feature mediated by the loop of Bub1.) Slightly surprisingly, we did not find an enrichment of APC/C subunits with the B3BD of BubR1 in this comparison to Bub1, but instead identified APC/C subunits to be equally well associated with both B3BDs of BubR1 and Bub1, as indicated by their localization in the middle of the volcano plot (Figure 3-24 A). This suggests that also the B3BD of Bub1 somehow confers the ability to interact with the APC/C. Longer constructs of Bub1 (GFP-Bub1$^{1\text{-}284}$) and BubR1 (GFP-BubR1$^{1\text{-}431}$), including the entire N-terminal region, contain the TPR repeats and in the case of BubR1 also its two KEN boxes, the first of which is essential for binding to Cdc20 and therefore incorporation into the MCC (Lara-Gonzalez et al, 2011). We carried out SILAC experiments with these constructs and the specificity of APC/C binding to BubR1 was clearly regained. Furthermore, because of the presence of the KEN boxes in the BubR1 construct, we

identified Cdc20 and Mad2 specifically with BubR1. Knl1, on the other hand, was clearly preferentially associated with Bub1 (Figure 3-24 B).

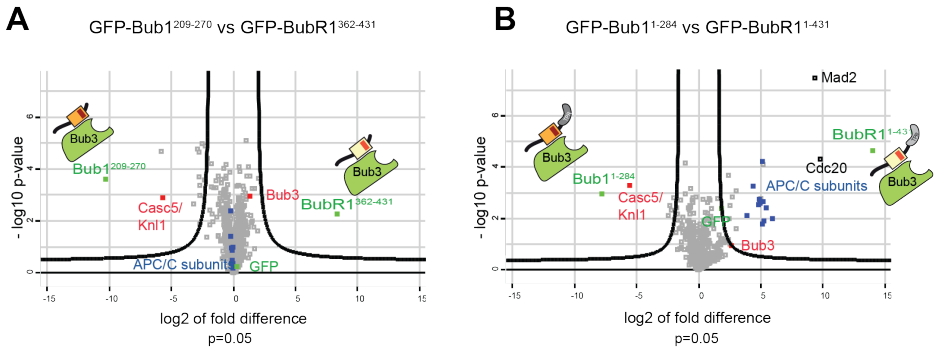

Figure 3-24 The N-terminal region of BubR1 increases the specificity of the BubR1-APC/C interaction

A, B) Volcano plot showing the results from two (A) or three (B) independent SILAC experiments using GFP-Bub1$^{209-270}$ and GFP-BubR1$^{362-431}$ (A) or GFP-Bub1$^{1-284}$ and GFP-BubR1$^{1-431}$ (B) as affinity resins to identify specific interaction partners in mitotic lysates. A p-value of 0.05 was used as cut-off for significance.

These results suggest that the selectivity of BubR1 for APC/C binding can be attributed to a combination of factors, which include the role of the loop in mediating the interaction with the APC/C but also the neighboring domains, which greatly increase the affinity of this interaction.

We had shown before that the Bub1-loop mediates the interaction with Knl1 and if grafted onto BubR1 suppresses the interaction with the APC/C (e.g. Figure 3-17, Figure 3-18). Thus, we suspected that APC/C binding of Bub1 might be mediated by the non-loop region of its B3BD. To test this hypothesis, we performed a SILAC experiment to compare the interaction partners of the B3BD of Bub1 with and without its loop. Strikingly, the results show an enrichment of APC/C subunits with the version of the B3BD of Bub1 lacking the loop, whereas Knl1 once more is specifically associated with the loop-containing Bub1 B3BD (Figure 3-25). Stronger APC/C binding by the Bub1 B3BD lacking the loop suggests that Knl1 competes with the APC/C for the interaction with Bub1. This hypothesis might also explain why only little APC/C is associated with Bub1^{FL} and the N-terminal region of Bub1 in comparison to equivalent BubR1 constructs (as shown in Figure 3-7 B and Figure 3-24 B).

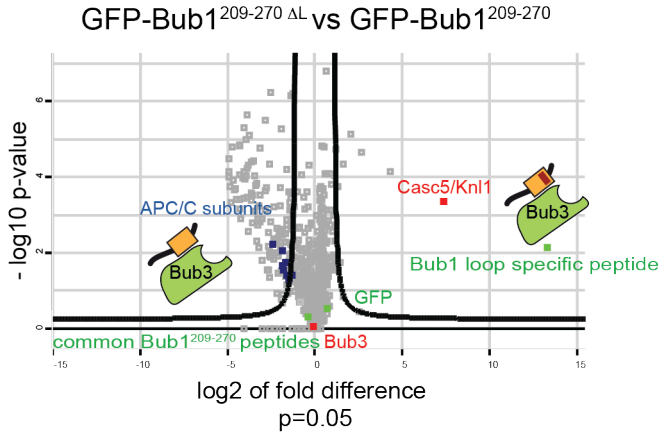

Figure 3-25 The non-loop region of the Bub1 B3BD can bind APC/C

Volcano plot showing the results from three independent SILAC experiments using GFP-Bub1$^{209\text{-}270\ \Delta L}$ and GFP-Bub1$^{209\text{-}270}$ as affinity resins to identify specific interaction partners in mitotic lysates. A p-value of 0.05 was used as cut-off for significance.

The fact that the non-loop region of the Bub1 B3BD confers binding to APC/C likely explains why the full swap mutant BubR1$^{B1\text{-}B3BD/B1\text{-}H}$ was able to bind to APC/C (Figure 3-18 C-D; a phenotype which is clearly not attributed to the presence of the Bub1 helix, since such a mutant showed normal APC/C binding - data not shown). The SAC defect observed with this mutant, however, strongly suggests that the Bub1 B3BD APC/C binding activity cannot rescue the function of the BubR1-loop and suggests that binding might occur at different sites on the APC/C and that it does not contribute to SAC function.

3.6.6 APC/C inhibition by BubR1 loop mutants *in vitro*

Recombinant versions of the chimeric mutants BubR1$^{1\text{-}571\ B1\text{-}LL}$ and BubR1$^{1\text{-}571\ \Delta LL}$ as well as BubR1$^{1\text{-}571\ wt}$ were co-expressed with Bub3 in insect cells. The wild type and chimeric constructs were purified to homogeneity. All constructs interacted with apparently similar affinity with Bub3, excluding major structural perturbations (data not shown) and in agreement with the IPs from mammalian cells performed with these mutants in context of the full length protein.

To assess the functionality of these BubR1 mutants *in vitro*, we first performed size exclusion chromatography to test whether the mutants are able to form MCC. Both BubR1$^{1\text{-}571\ B1\text{-}LL}$/Bub3 and BubR1$^{1\text{-}571\ \Delta LL}$/Bub3 formed a stoichiometric complex with Cdc20 and Mad2, as BubR1^{wt}/Bub3 did (Figure 3-26). This result agrees with our *in vivo* data arguing that the BubR1-loop *per se* is not needed for MCC formation but rather for the interaction with the APC/C. Furthermore, the mutants showed wt-like kinetics in an *in vitro* assay measuring the rate of MCC assembly in presence of catalytic proteins (data not shown, assay described in Faesen et al, 2016, manuscript under review).

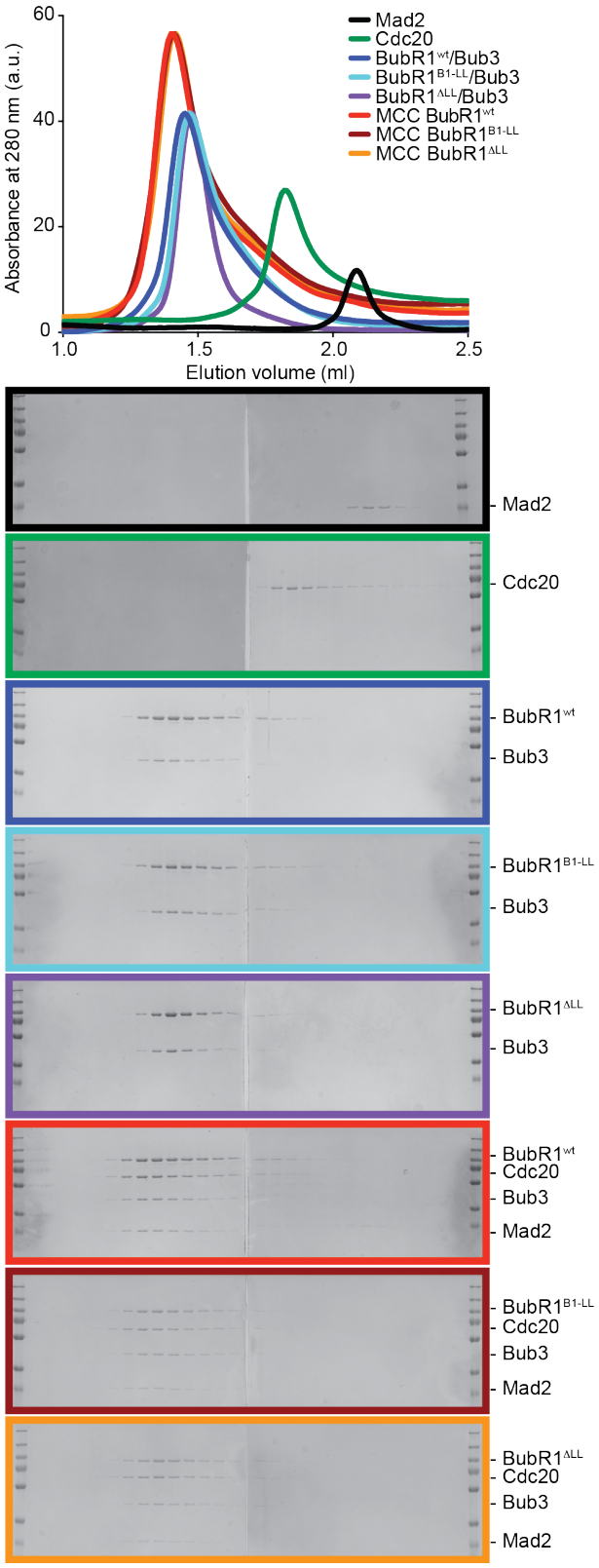

Figure 3-26 BubR1 loop mutants can form MCC *in vitro*

BubR1$^{1\text{-}571\ wt}$/Bub3 as well as the two loop mutants BubR1$^{1\text{-}571\ B1\text{-}LL}$/Bub3 and BubR1$^{1\text{-}571\ \Delta LL}$/Bub3 interact in size exclusion chromatography with the other two MCC components Cdc20 and Mad2. In the chromatogram, the curves for the three different MCC complexes have been normalized in height

against MCC containing BubR1$^{1\text{-}571\ \Delta LL}$, the curves for the three different BubR1/Bub3 complexes have been normalized against BubR1$^{1\text{-}571\ wt}$/Bub3. All BubR1s are N-terminally tagged with CFP. a.u. - arbitrary units.

Therefore, we next tested the ability of MCC containing either BubR1^{wt} or the BubR1 loop mutants to inhibit APC/C activity *in vitro* by evaluating ubiquitination of the APC/C substrate Cyclin B. In this assay, we found that MCCs containing the loop mutants of BubR1 were less efficient in preventing Cyclin B ubiquitination than MCC with BubR1^{wt} (Figure 3-27).

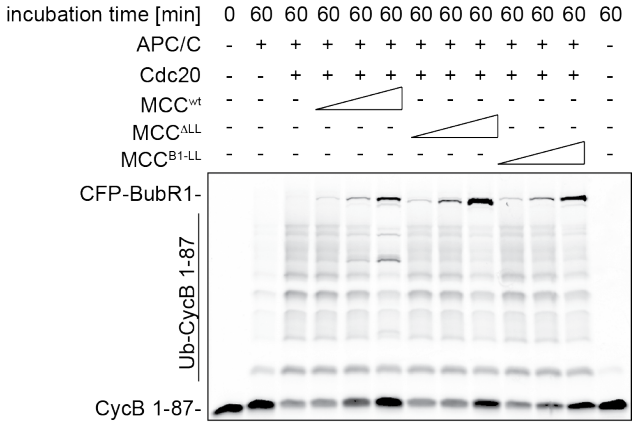

Figure 3-27 *In vitro* APC/C inhibition by BubR1 loop mutants

Ubiquitination reactions in the presence of APC/C immunoprecipitated from mitotic HeLa cells and the fluorescently labelled 87 N-terminal residues of Cyclin B were analyzed by SDS-PAGE and fluorescence scanning. The MCCs containing the BubR1 loop mutants were less efficient in inhibiting APC/C Cyclin B-ubiquitination activity in comparison to MCC containing BubR1^{wt}. Triangles indicate the use of increasing MCC concentrations.

However, the difference was minor and difficult to reproduce in our assay. Therefore, these assays will be repeated using recombinant APC/C in collaboration with Dr. Jan-Michael Peter's laboratory at the Research Institute of Molecular Pathology (IMP) in Vienna and can only be taken as a first indication for the role of the BubR1-loop in APC/C inhibition.

4 Discussion

The Spindle Assembly Checkpoint (SAC) is a surveillance mechanism that ensures accuracy of chromosome segregation during mitosis. Bub1 and BubR1, essential SAC components, are paralogous proteins that evolved through nine gene-duplication events from one common ancestor gene (Suijkerbuijk et al, 2012a; Vleugel et al, 2012). Subsequent sub-functionalization during evolution led to the creation of two gene products with very similar domain organization but highly diversified functions and distinct kinetochore localization behavior. This observation raised the question why these proteins behave so differently. My PhD work identified the region in Bub1 and BubR1 that accounts for the different localization behavior and unravelled how BubR1 localizes to kinetochores. This study has significantly contributed to understanding the molecular basis of the evolutionary divergence of Bub1 and BubR1 and of its functional relevance in SAC signaling.

4.1 BubR1 kinetochore recruitment mechanism

The phosphorylation of so-called "MELT" repeats in the outer kinetochore protein Knl1 by the SAC kinase Mps1 has been shown to be a crucial prerequisite for Bub1 kinetochore localization (London et al, 2012; Primorac et al, 2013; Shepperd et al, 2012; Yamagishi et al, 2012). However, BubR1 kinetochore recruitment is subordinate to Bub1 localization (Gillett et al, 2004; Johnson et al, 2004; Klebig et al, 2009; Logarinho et al, 2008; Millband & Hardwick, 2002), despite the similar domain organization and despite both proteins being bound to the same kinetochore targeting adaptor Bub3. The reason for this dependency on Bub1 and the exact recruitment mechanism of BubR1 were largely unknown. In this work, we identified the molecular basis for the different kinetochore localization behavior of Bub1 and BubR1 and subsequently the molecular mechanism of BubR1 kinetochore recruitment. We showed that the loop region of the Bub3-binding domains (B3BDs) of Bub1 and BubR1 modulates the interaction of Bub3 with $MELT^{P}$ motifs. The loop of Bub1 enhances this interaction, while the loop of BubR1 is suboptimal for this. This makes BubR1 depend on an alternative mechanism of kinetochore localization. We found this alternative mechanism to be a direct pseudo-symmetric interaction with Bub1. By swapping loops, we created a gain-of-function BubR1 mutant that localized to kinetochores independently of Bub1, and a loss-of-function Bub1 mutant severely

impaired in autonomous kinetochore binding, clearly underscoring the role of the Bub1-loop for kinetochore localization.

The identified hetero-dimerization interaction, which in agreement with a previous study in *S. pombe* (Rischitor et al, 2007) does not require kinetochores, involves structurally equivalent domains of Bub1 and BubR1, including the B3BD and a short segment in the C-terminal extension directly following the B3BD predicted to form a helix in both proteins. Furthermore, the interaction requires that both Bub1 and BubR1 are bound to Bub3 (Figure 4-1).

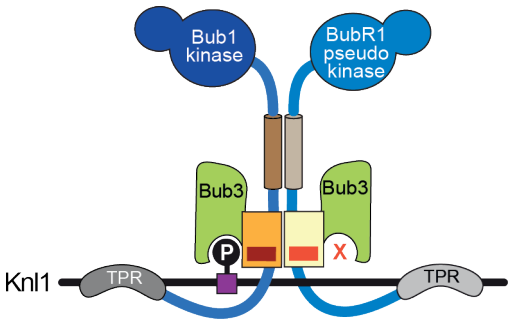

Figure 4-1 BubR1 kinetochore recruitment mechanism

Scheme of the identified pseudo-symmetric Bub1-BubR1 interaction accounting for BubR1 kinetochore localization (already shown as part of Figure 3-11).

Therefore, Bub3 might have several distinct functions. It recruits Bub1 to MELT^{P} repeats of Knl1 and it contributes to the dimerization of Bub1 and BubR1, which is required for BubR1 kinetochore localization. Moreover, it seems to have a further role in downstream SAC signaling, if in complex with BubR1, as also recently proposed (Han et al, 2014). This conclusion was reached with a BubR1 mutant incapable of Bub3 binding and kinetochore localization (BubR1$^{E409K+E413K}$). However, the observed SAC defect is unlikely to be caused by the lack of kinetochore localization, as another kinetochore localization deficient mutant (BubR1$^{\Delta H}$) was clearly SAC proficient. Thus, our data suggest a role of BubR1-bound Bub3 in the SAC that will be discussed in more detail below (see section 4.4).

4.2 Kinetochore turnover of BubR1 and Bub1

BubR1 kinetochore turnover is fast, and most likely reflects its cycle of incorporation into the MCC and release into the cytoplasm as soluble inhibitor of the APC/C

(Howell et al, 2004). As we have shown that the loop determines the different kinetochore localization behavior of Bub1 and BubR1, we investigated how the loop-swap influences BubR1 kinetochore turnover. We found that the half-life of BubR1 kinetochore turnover depends on the number of binding sites for BubR1 on kinetochores. The BubR1 loop-swap mutant (BubR1$^{B1\text{-}LL}$) showed significantly delayed turnover times, as it hetero-dimerizes with Bub1 while binding directly to the Knl1 MELT^{P} motifs. If hetero-dimerization of this mutant was prevented (BubR1$^{B1\text{-}B3BD/B1\text{-}H}$ and BubR1$^{B1\text{-}LL/_{\Delta}H}$), fast turnover could be restored, completing our understanding of the behavior of the system. Furthermore, this analysis excluded the slow turnover of the loop-swap mutant as a possible direct reason for its inability to rescue SAC function, as also the mutants that cycled quickly were SAC defective.
Bub1 also cycled quickly (in agreement with a recent paper (Asghar et al, 2015)), revising the view of Bub1 as a stably-associated SAC component (Howell et al, 2004; Shah et al, 2004). This observation needs to be reconciled with the role of Bub1 as a scaffolding platform for additional SAC proteins. Faster turnover of Bub1 might be required for the catalytic function of Bub1 in MCC formation (Faesen et al, 2016, manuscript under review). Whether Bub1 is also slowed down by the expression of the slowly cycling BubR1 loop-swap mutant, and whether the phosphatases PP1 and PP2A^{B56} [which were both implicated in dephosphorylation of MELT repeats and SAC silencing (Espert et al, 2014; Nijenhuis et al, 2014)] play a role for the observed turnover rates remains to be tested.

4.3 The functional implications of BubR1 kinetochore localization

4.3.1 The role of BubR1 kinetochore localization for the SAC

In mitotic cells, BubR1 can be detected at kinetochores after nuclear envelope breakdown and until the onset of anaphase (Howell et al, 2004). However, the need for kinetochore localization of BubR1, especially for its function in the SAC, has been a controversial issue, as some studies have suggested that it is not strictly needed (Essex et al, 2009; Kulukian et al, 2009; Malureanu et al, 2009; Vanoosthuyse et al, 2009), whereas others suggested the opposite (Elowe et al, 2010; Han et al, 2014; Lara-Gonzalez et al, 2011; Zhang et al, 2016a). Whether kinetochore localization is

crucial for all functions of BubR1 or only for a subset of them is an important question that we tried to address in this work.

We found that a BubR1 mutant that cannot bind to Bub1 and therefore does not localize to kinetochores (BubR1$^{\Delta H}$) was still SAC proficient. This may suggest that BubR1 kinetochore localization is not essential for SAC function and implies that substantial amounts of MCC can be generated even when BubR1/Bub3 cannot be recruited to kinetochores. This could also be consistent with the fact that in *C. elegans* and *S. cerevisiae* Mad3/BubR1 may not localize to kinetochores (Essex et al, 2009; Gillett et al, 2004). Moreover, the very recently identified catalytic role of Bub1 in MCC formation does not require an interaction with BubR1 (Faesen et al, 2016, manuscript under review), which argues indirectly that kinetochore localization of BubR1 is not strictly required for SAC function. We note however, that the kinetochore localization defective mutant (BubR1$^{\Delta H}$) interacts only weakly with PP2A^{B56}, the phosphatase that is normally recruited to kinetochores by BubR1 and which has been implicated in SAC silencing through counteracting Mps1 by dephosphorylating Knl1 MELT motifs (Espert et al, 2014; Nijenhuis et al, 2014). Therefore, BubR1 mutants that cannot localize to kinetochores might carry an additional SAC silencing defect that could compensate an underlying SAC defect. Furthermore, it is possible that BubR1 kinetochore localization is required under conditions that challenge the SAC, e.g. in presence of a single unattached kinetochore. Unfortunately, our cellular system is currently not sensitive enough to test such a hypothesis.

4.3.2 The role of BubR1 kinetochore localization for chromosome alignment

In contrast to its role for BubR1 SAC function, the requirement of BubR1 kinetochore localization for kinetochore-microtubule attachment and the establishment of bi-orientation is clearer. Previously, it has been shown that BubR1 promotes chromosome alignment through recruitment of PP2A^{B56} (Kruse et al, 2013; Suijkerbuijk et al, 2012b; Xu et al, 2013), which counteracts Aurora B activity at kinetochores and thereby stabilizes kinetochore-microtubule attachments (Foley et al, 2011; Lampson & Kapoor, 2005). Our results confirm this, as they demonstrate a strong defect in the formation of stable kinetochore-microtubule attachments if BubR1 does not localize to kinetochores. This correlated with a defect in the

interaction of BubR1 with PP2A^{B56}. The potential roles of BubR1 at kinetochores are summarized in Figure 4-2.

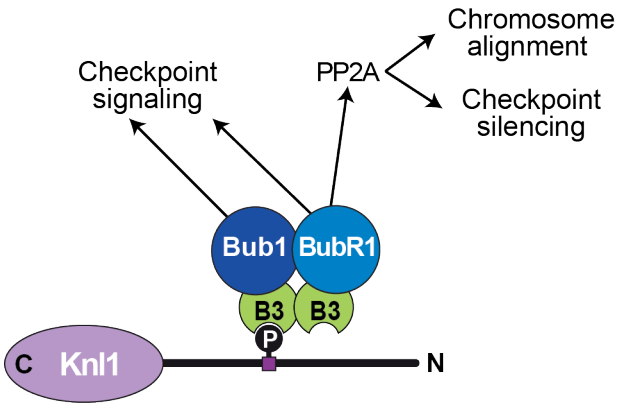

Figure 4-2 Model for functional implications of BubR1 kinetochore recruitment

BubR1 is recruited to kinetochores through a direct interaction with the Bub1/Bub3 complex bound to MELT^{P} motifs on Knl1. BubR1 in turn recruits the phosphatase PP2A^{B56}. For details see text. Figure from (Overlack et al, 2015).

Interestingly, we found that BubR1 does not show the typical mitotic hyperphosphorylation when it does not localize to kinetochores. These results suggest that kinetochore localization of BubR1 is a prerequisite for phosphorylation in its kinetochore associated regulatory domain (KARD) by the mitotic kinases Cdk1 and Plk1, which is known to be important for the interaction with PP2A^{B56} (Kruse et al, 2013; Suijkerbuijk et al, 2012b; Xu et al, 2013). Thus, lack of BubR1 kinetochore localization results in reduced phosphorylation, lack of PP2A^{B56} binding and therefore the described chromosome alignment and potential SAC silencing problems. Interestingly, the introduction of two Plk1-phosphorylation-mimicking mutations in the kinetochore localization defective BubR1 mutant (BubR1$^{\Delta H/S676D,T680D}$) restored its ability to bind to PP2A^{B56} but did not expose a SAC defect of this construct (data not shown). This suggests that the BubR1-PP2A^{B56} interaction has to occur specifically at kinetochores, in order to localize PP2A^{B56} to fulfill its functions for chromosome alignment and SAC silencing. Therefore, it is not clear whether restoring the ability of a kinetochore localization defective BubR1 to bind PP2A^{B56} will overcome a potential SAC silencing defect (as alluded to in section 4.3.1). The use of a kinetochore-tethered PP2A^{B56} might be an option to further test this potential SAC silencing defect

of kinetochore localization defective BubR1 constructs. Furthermore, as Bub1 has been suggested to bind to Plk1 at kinetochores (Qi et al, 2006), these observations also raise the question whether Bub1 contributes to loading of $PP2A^{B56}$ onto BubR1 at kinetochores as part of its role in BubR1 recruitment.

4.3.3 Extension of the template model

Understanding the requirements for recruitment of SAC proteins to kinetochores is essential for distinguishing their roles in the SAC from their roles in chromosome bi-orientation (Brady & Hardwick, 2000; De Antoni et al, 2005; London & Biggins, 2014b; London et al, 2012; Nijenhuis et al, 2013; Overlack et al, 2015; Shepperd et al, 2012; Yamagishi et al, 2012). By unraveling the recruitment mechanism of BubR1 and the role of the loop motifs of Bub1 and BubR1 in modulating kinetochore affinity, this study fills an important gap. Interestingly, the recruitment of the BubR1/Bub3 complex to a kinetochore bound Bub1/Bub3 complex is reminiscent of the Mad2-template model (described in section 1.4.1). According to this model, Mad1 acts as a stable placeholder for C-Mad2 (De Antoni et al, 2005). Once at kinetochores, the Mad1/C-Mad2 complex recruits O-Mad2 and converts it into the active C-Mad2 form thereby promoting its binding to Cdc20 and thus overcoming a rate-limiting step in MCC formation (De Antoni et al, 2005; Mapelli et al, 2007; Simonetta et al, 2009). This scheme is summarized in Figure 4-3. It identifies Mad1/C-Mad2 as a "template" for the establishment of the Cdc20/C-Mad2 complex, with the latter representing a structural "copy" of the former (De Antoni et al, 2005). Therefore, when considering the identified BubR1 recruitment mechanism, the complete MCC, consisting of Cdc20/C-Mad2 and BubR1/Bub3, could be interpreted as a "copy" of the kinetochore bound "templates" Mad1/C-Mad2 and Bub1/Bub3.

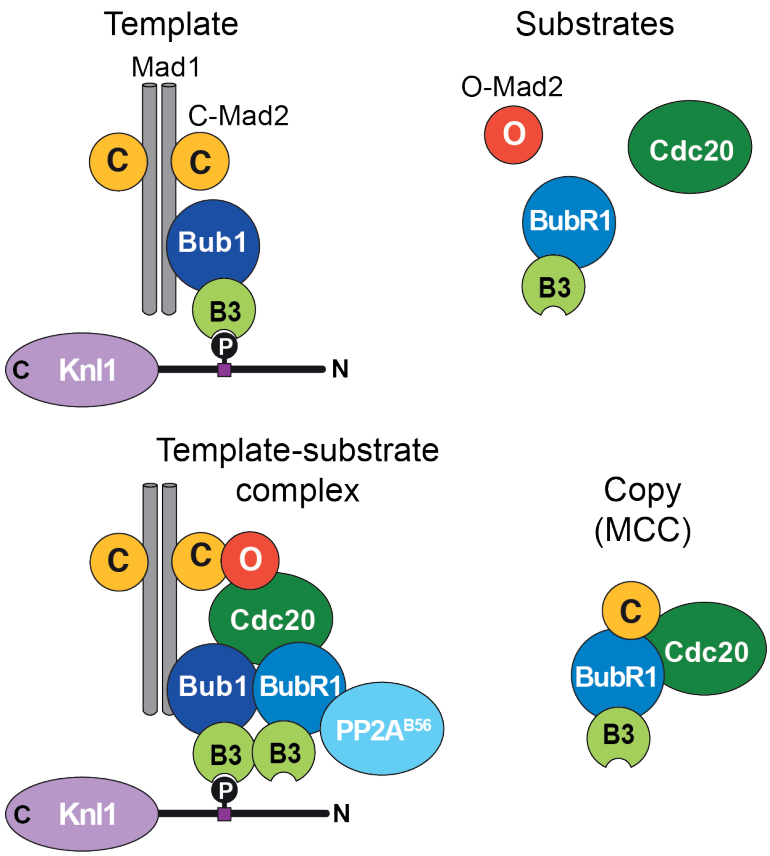

Figure 4-3 Extension of the template model

Mad1/C-Mad2 at kinetochores has been shown to act as a template for the formation of the Cdc20/C-Mad2 interaction. This seems similar to the identified BubR1 recruitment mechanism through a pseudo-symmetric interaction with Bub1/Bub3. Ultimately, the entire MCC could represent a copy of kinetochore-localized templates. Figure from (Overlack et al, 2015).

This idea is consistent with the recent model proposed for catalysis of MCC formation. This model reports a transient interaction between Mad1/C-Mad2 and Bub1/Bub3 required to recruit O-Mad2 and Cdc20 to catalyze their interaction for MCC formation. Interestingly, BubR1 was not an essential component of the catalytic mechanism. This suggests that BubR1 might also be incorporated into MCC only after a Mad2/Cdc20 seed has formed (Faesen et al, 2016, manuscript under review), in agreement with the fact that MCC can form also if BubR1 is not at kinetochores, at least under certain conditions, as discussed in 4.3.1. How MCC dissociates from kinetochores, if Bub1 leaves with the MCC, or if Bub1 dissociates from, and rebinds, kinetochores independently of MCC are interesting questions to be addressed in the future.

4.4 The differential functions of the loop regions of Bub1 and BubR1

Previously, the evolution of BubR1 into an inactive pseudokinase has been interpreted as a manifestation of the divergence of BubR1 and Bub1 after duplication (Suijkerbuijk et al, 2012a). In this study, we wanted to identify the molecular basis for the observed differences in the behavior of Bub1 and BubR1 to further our understanding of the evolutionary divergence of these two important SAC proteins.

We established the loop regions of Bub1 and BubR1 as the main discriminating factor determining kinetochore localization behavior and distinct functions in the SAC. The crucial function of the human Bub1-loop is to enhance the interaction of Bub3 with phosphorylated MELT repeats of Knl1 [similarly to *S. cerevisiae* (Primorac et al, 2013)]. In contrast, the human BubR1-loop does not enhance the interaction with $MELT^{P}$ repeats. The dependence on Bub1 for kinetochore localization (extensively characterized in the first and second part of this study and discussed in section 4.1) reflects this property of the BubR1-loop. In the third part, we therefore concentrated on understanding in more detail the role of the BubR1-loop. In our cell biological assays it was not possible to delete the loop from BubR1, nor to replace it with a neutral Gly-Ser linker sequence or with the Bub1-loop sequence, without creating a SAC defect and loosing considerable binding affinity for the APC/C. Furthermore, SILAC experiments identified an interaction of the B3BD of BubR1 with the APC/C, which was reduced if the BubR1-loop was deleted from the construct. Collectively, these results suggest that the specific sequence of the BubR1-loop is required to mediate an interaction with the APC/C, which in turn seems to be crucial for SAC signaling (Figure 4-4).

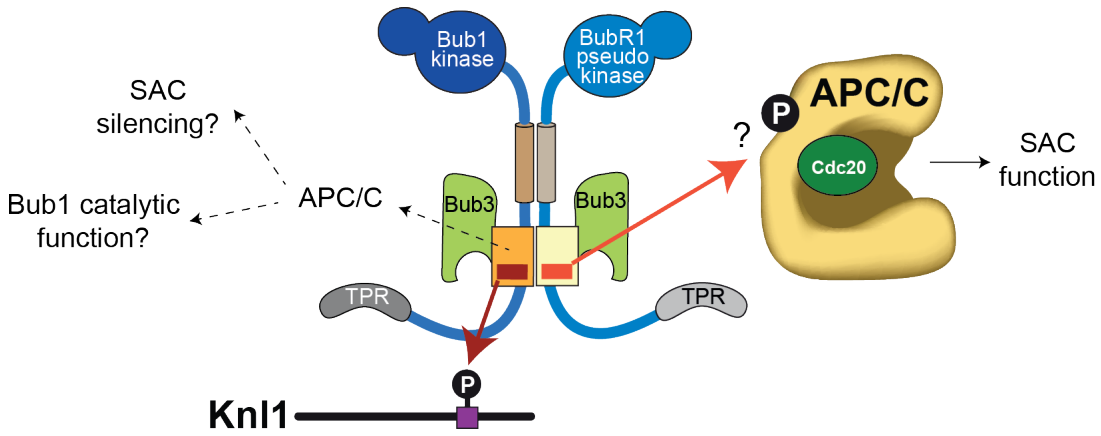

Figure 4-4 Model for the differential functions of the Bub1- and BubR1-loop

Model showing the differential functions of the loops in BubR1 and Bub1. Bub1 and BubR1 form a pseudo-symmetric heterodimer requiring the B3BDs and the helix as well as the presence of Bub3. The loops are not involved in this interaction but serve different functions. The Bub1-loop enhances binding of the Bub1/Bub3 complex to Knl1 $MELT^{P}$ motifs, which in turn recruits BubR1/Bub3 to kinetochores. The BubR1-loop however is not able to enhance the interaction of Bub3 with $MELT^{P}$, but instead seems to promote binding of BubR1 to the APC/C. This is required for the SAC function of BubR1. We hypothesize that this interaction could work via modulation of Bub3 and be regulated in a phosphorylation-dependent manner, arguing that the BubR1-loop functions in analogy to the Bub1-loop. In the case of Bub1 the non-loop region might also be able to establish an interaction with the APC/C, which we speculate to be at a distinct place from the binding site of BubR1. This Bub1-APC/C interaction could be important for SAC silencing or for the catalytic function of Bub1 in MCC assembly.

Interestingly, BubR1 loop mutants seemed to bind slightly more Cdc20 and Mad2 in co-IPs and showed a slightly longer arrest in nocodazole than a BubR1 mutant ($BubR1^{KEN1/AAA}$) defective in Cdc20-binding. This argues that the loop mutants are able to form MCC, which however cannot inhibit APC/C. Nevertheless, capturing of Cdc20 in a (non-functional) MCC prevents it from directly activating the APC/C, contrarily to the Cdc20-binding defective mutant ($BubR1^{KEN1/AAA}$). This likely accounts for the observed different penetrance of these SAC mutants. Size exclusion chromatography runs with the recombinant loop mutants ($BubR1^{B1\text{-}LL}$ and $BubR1^{\Delta LL}$) confirmed that both were able to engage in a stable MCC complex with Mad2 and Cdc20 *in vitro*, as well as the wild type protein. Recent structural studies confirmed previous hypotheses, revealing that a core MCC complex (containing one copy of each BubR1, Bub3, Cdc20 and Mad2 protein) binds a second Cdc20 molecule via the first D-box, an ABBA-motif and the second KEN-box of BubR1 when this second

Cdc20 is already bound to the APC/C (Alfieri et al, 2016; Izawa & Pines, 2015; Musacchio, 2015; Primorac & Musacchio, 2013; Yamaguchi et al, 2016). The BubR1 B3BD, however, was disordered and not visible in these structures (Alfieri et al, 2016; Yamaguchi et al, 2016). Since the recombinant loop mutants seemed to form the core MCC as well as BubR1^{wt}, it could be speculated that the SAC defect observed with the loop mutants could also be related to an inability to inhibit the second Cdc20 molecule, especially as the loop region is located only 60 residues downstream of the second BubR1 KEN-box.

In agreement with our proposed role for the BubR1-loop in APC/C binding, two studies from the early 2000s reported that BubR1 inhibits APC/C activation by Cdc20 also in isolation. This inhibitory activity is synergistically enhanced by the addition of Mad2. However, if APC/C is pre-activated by Cdc20, inhibition by BubR1 seemed less potent (Fang, 2002; Tang et al, 2001). Our attempts to confirm a role of the BubR1-loop in APC/C inhibition until now only showed a minor defect in the ability of the loop mutant containing MCCs to inhibit APC/C *in vitro*. These results will now be reproduced with recombinant APC/C in collaboration with Dr. Jan-Michael Peters' laboratory at the Research Institute of Molecular Pathology in Vienna using BubR1 alone and within the context of the MCC.

Disassembly of the MCC occurs continously during mitosis to keep its steady-state levels constant (Liang et al, 2012; Musacchio & Ciliberto, 2012). At least two mechanisms contribute to MCC disassembly (Musacchio, 2015). In one mechanism, a protein called p31^{comet} and the APC/C subunit Apc15 promote ubiquitination and subsequent degradation of Cdc20, thereby stimulating the release of C-Mad2 from APC/C-bound MCC (Uzunova et al, 2012; Varetti et al, 2011; Westhorpe et al, 2011). In another mechanism, p31^{comet} works together with the AAA ATPase Trip13 to disassemble MCC, probably by promoting the energy-consuming re-conversion of C-Mad2 to O-Mad2 (see section 1.4.3) (Eytan et al, 2014; Wang et al, 2014; Ye et al, 2015). Thus, after extraction of C-Mad2 from the MCC by one of these mechanisms, the remaining complexes containing the BubR1 loop mutants might dissociate faster from APC/C than remaining complexes containing BubR1^{wt}. Faster dissociation might result in the SAC defect observed in cells, providing yet another explanation for the observed SAC defect of the BubR1 loop mutants. Which of these hypotheses accounts for the SAC defect of the loop mutants remains to be tested.

Another open question is whether the BubR1-loop functions via the regulation of Bub3 (in analogy to the Bub1-loop). A Bub3-binding defective BubR1 mutant (BubR1$^{E409K+E413K}$) showed the same SAC defect phenotype as described for the loop mutants and was also not able to bind APC/C subunits in co-IPs. This suggested that Bub3, if in complex with BubR1, plays a role in the SAC (as already briefly discussed in section 4.1) and argues in favor of the theory that the BubR1-loop works through regulation of Bub3. A function for Bub3 in the SAC has also been proposed by the Cleveland laboratory (Han et al, 2014). These authors suggested that the function of Bub3 is the catalytic promotion of BubR1/Cdc20 interactions at kinetochores and in the cytosol and interpreted the moderate stimulation by Bub3 of MCC-dependent APC/C inhibition as an effect of this catalytic function. This is at odds with our hypothesis that the BubR1-loop and Bub3 increase the affinity of MCC for APC/C.

Promoting the docking of the MCC to the APC/C might be one of the crucial inhibitory functions of BubR1 (Musacchio, 2015). Two very recent studies reporting an EM structure of APC/C^{Cdc20} bound to MCC reinforced this idea. Unfortunately, in both structures, Bub3 and large parts of BubR1 (including the loop and the B3BD) are disordered and not visible (Alfieri et al, 2016; Yamaguchi et al, 2016). Bub3 is an adaptor protein for phosphorylated motifs, and in complex with Bub1 it binds to phosphorylated MELT repeats of Knl1. Thus, Bub3 may further enhance binding of BubR1 to the APC/C by binding to a phosphate on the APC/C (Musacchio, 2015). If this were the case, it would be of high interest to identify the kinase that creates this phospho-epitope and to map the Bub3 binding site on APC/C. APC/C is highly phosphorylated in mitosis by the kinases Plk1 and Cdk1 (Herzog et al, 2005; Kraft et al, 2003). APC/C phosphorylation in the loop of the APC/C subunit Apc1 specifically allows binding of Cdc20 (Fujimitsu et al, 2016; Qiao et al, 2016; Zhang et al, 2016), promoting APC/C activation (Golan et al, 2002; Kraft et al, 2003; Kramer et al, 2000; Shteinberg et al, 1999). This raises the possibility that also inhibition of APC/C could be regulated by phosphorylation. If Bub3 is involved in this inhibitory process it might be expected to bind sequences related to the MELT^{P} motifs of Knl1. Two such motifs exist on APC/C, on the subunits Apc4 and Apc5. Along similar lines, it has been proposed that phosphorylation of Cdc20 inhibits APC/C activation and vice-versa de-phosphorylation of Cdc20 helps in activating the APC/C (Craney et al, 2016; Hein & Nilsson, 2016; Labit et al, 2012; Yudkovsky et al, 2000). This raises the possibility

that phosphorylation on Cdc20 regulates MCC binding to it and that the BubR1-loop plays a role in this process as well.

4.5 A Bub1-APC/C interaction

Bub1/Bub3 is recruited in a Mps1-phosphorylation-dependent manner to MELT repeats on Knl1 (London et al, 2012; Shepperd et al, 2012; Yamagishi et al, 2012). This has been shown to be important for the SAC function, requiring only rather low levels of Bub1, and the chromosome alignment function of Bub1, requiring higher Bub1 kinetochore levels (Krenn et al, 2014; Vleugel et al, 2015b; Vleugel et al, 2013). As part of our attempts to understand the molecular basis for the difference in the kinetochore localization behavior of Bub1 and BubR1, we identified the loop region of Bub1 and BubR1 as the main discriminating factor determining localization behavior and SAC function (discussed in 4.4). Concerning Bub1, we established the Bub1-loop to be crucially important to enhance the Bub1/Bub3-Knl1 $MELT^{P}$ interaction, for which otherwise Bub3 carries most of the important and conserved residues (Overlack et al, 2015; Primorac et al, 2013). In addition to the identification of the Bub1-loop as regulator of Knl1 binding, we discovered another interesting feature of Bub1. A chimeric mutant, containing the B3BD and the helix of Bub1 in BubR1 ($BubR1^{B1\text{-}B3BD/B1\text{-}H}$), was on the one hand SAC defective, but on the other hand bound to a surprisingly large amount of APC/C subunits in co-IPs. After dissecting this observation, we excluded a role of the Bub1 helix in APC/C binding, as a different chimeric mutant containing the Bub1 helix ($BubR1^{B1\text{-}H}$) was SAC proficient and bound normal amounts of APC/C. Furthermore, we ruled out a function of the Bub1-loop in APC/C binding since when grafted onto BubR1 the Bub1-loop suppressed the interaction with the APC/C. Therefore, our data suggest that the B3BD of Bub1 is somehow able to mediate an interaction with the APC/C, which however does not seem to be inhibitory. Furthermore, also our SILAC data argue that this interaction of Bub1 with the APC/C is not mediated by the loop, but by the remaining part of the Bub1 B3BD. However, the same region of the Bub1 B3BD mediates weaker binding to the APC/C in presence of the Bub1-loop, raising the possibility that the ability to bind to Knl1 reduces APC/C binding (see Figure 4-4). This raises the evolutionary question whether the expansion of MELT repeats on Knl1 has the functional significance to subtract Bub1 from APC/C. Our ability to detect APC/C subunits

associated with Bub1 in co-IPs, but always in substoichiometric amounts, seems to agree with this hypothesis. To further validate the non-loop region of the B3BD of Bub1 as mediator of the interaction with the APC/C, it will be instrumental to test different mutants of BubR1 and Bub1 in which the B3BDs are swapped and in which it will be possible to exclude the potential competitive Knl1-binding function of the Bub1-loop. Thus, our data suggest that the B3BD of Bub1 might bind to a different site on APC/C in comparison to BubR1. Possibly binding occurs in a non-phosphorylation dependent manner, as in contrast to the BubR1-loop, which we have shown to be required for APC/C binding, the Bub1-loop does not seem to be involved in the Bub1-APC/C interaction (Figure 4-4). However, this remains to be tested.

Certainly, this observation raises the question about the functional relevance of the detected Bub1-APC/C interaction. We have not been able to look at SAC defect phenotypes with mutants of Bub1, because in our assay conditions we always observed only modest effects on the SAC, likely due to incomplete depletion of Bub1. As mentioned above, the Bub1 B3BD-APC/C interaction does not seem to be inhibitory, as the chimeric mutant that still bound considerable amounts of APC/C ($BubR1^{B1\text{-}B3BD/B1\text{-}H}$) is SAC defective. Moreover, APC/C inhibition that has been observed by Bub1 has been advocated to happen in a kinase-dependent manner through phosphorylation of Cdc20 by Bub1 (Tang et al, 2004). Therefore, one could imagine a role of the Bub1-APC/C interaction for the catalytic function of Bub1 in MCC assembly recently identified in our laboratory (Faesen et al, 2016, manuscript under review), maybe consisting in bringing all components in close proximity. Recent studies showed that deletions of Bub1/Bub3 in *C. elegans* or *S. cerevisiae* delayed the onset of anaphase. This was claimed to depend on kinetochores but not on the SAC, because simultaneous deletion of other SAC proteins could not bypass the effect of the deletion of Bub1 or Bub3 (Kim et al, 2015; Yang et al, 2015). A role of the Bub1/Bub3 complex in SAC silencing was also proposed in fission yeast (Vanoosthuyse et al, 2009). These observations point towards a role of Bub1/Bub3 in re-activation of the APC/C after a SAC arrest and might therefore also provide a possible explanation for the need of a Bub1-APC/C interaction.

Collectively, our results, summarized in Figure 4-4, identify the mechanism of BubR1 kinetochore localization and establish the role of the Bub1-loop in promoting Knl1-

binding and the role of the BubR1-loop in APC/C binding, which is crucial for BubR1 SAC function. Thereby, my doctoral work has considerably extended the understanding of the divergence of Bub1 and BubR1 by identifying the loop region of the two proteins as crucial determinant for their diversification after duplication. Furthermore, we find a previously unknown interaction of Bub1 with the APC/C, the functional relevance of which will remain a matter of investigation. Finally, our analysis once more illustrates how gene duplication of an ancestor gene and subsequent sub-functionalization leads to the creation of two gene products with highly diversified functions and provides another step forward in our understanding of how the SAC functions at the molecular level to prevent genetic instability.

5 Summary

Cell division or loss of sister chromatid cohesion prior to achievement of bi-orientation leads to missegregation of chromosomes and causes aneuploidy, which is closely associated with tumorigenesis. To prevent this, the Spindle Assembly Checkpoint (SAC) monitors correct attachment of spindle microtubules to kinetochores (large protein assemblies on centromeric DNA) and coordinates this with cell cycle progression. Bub1 and BubR1, essential SAC components, evolved through several duplication events from an ancestor gene creating two structurally related gene products with highly diversified functions. Previously, BubR1 has been shown to depend on Bub1 for its kinetochore localization, whereas Bub1 localizes to kinetochores independently of BubR1. However, the molecular basis for such differences in recruitment has been unclear, as Bub1 and BubR1 both bind to Bub3, a targeting adaptor for phosphorylated kinetochores. In my PhD project, the basis of the different localization behavior has been identified. I demonstrated that Bub1, but not BubR1, enhances binding of Bub3 to phosphorylated kinetochores via a short motif in its Bub3-binding domain (B3BD) called the "loop". This provided an explanation for why BubR1 relies on an alternative mechanism for kinetochore localization. Consequently, swapping loops created a loss-of-function Bub1, impaired in kinetochore localization, and a gain-of-function BubR1, localizing to kinetochores independently of Bub1. However, the inability of the loop-swap mutant of BubR1 to retain BubR1 SAC function led to the subsequent identification of the specific role of the BubR1-loop. *In vivo* and *in vitro* experiments established that the unique sequence of the BubR1-loop promotes binding of BubR1 to the APC/C. Additionally, this study showed for the first time that kinetochore localization of BubR1 relies on a direct interaction with Bub1. Hetero-dimerization requires structurally equivalent domains in both proteins, the B3BD and a subsequent helical segment. Furthermore, both proteins need to be bound to Bub3 for this interaction to take place. Interestingly, hetero-dimerization of Bub1 and BubR1 did not require kinetochores. Collectively, my PhD work illustrates how gene duplication and subsequent sub-functionalization determine the differences in the behavior of two closely related proteins as part of an essential molecular network providing a further step in our understanding of how the checkpoint signal is generated at the molecular level.

6 Zusammenfassung

Für die Zellteilung ist es wichtig, dass die Chromosomen über große Proteinkomplexe (sogenannte Kinetochore) richtig an die mitotische Spindel angeheftet sind. Fehler bei der Verteilung der Chromosomen auf die Tochterzellen können zu einer veränderten Chromosomenanzahl führen. Solche sogenannten "Aneuploidien" sind eng mit der Entstehung von Tumoren verknüpft. Der "Spindle Assembly Checkpoint (SAC)" hat sich als essentieller Kontrollmechanismus entwickelt, um Fehler bei der Chromosomenverteilung zu verhindern. Der SAC überwacht die korrekte Anheftung der Mikrotubuli der mitotischen Spindel an die Kinetochore und synchronisiert dies mit dem Voranschreiten der Zelle im Zellzyklus.

Bub1 und BubR1 sind wichtige Bestandteile des SAC, die sich durch mehrere Genduplikationen aus einem gemeinsamen Vorläufergen entwickelt haben. So sind zwei Genprodukte mit sehr ähnlichem Aufbau, aber unterschiedlichen Funktionen entstanden. Bisher ist bekannt, dass die Kinetochor-Lokalisation von BubR1 von der vorherigen Anwesenheit Bub1s abhängt, die Kinetochor-Lokalisation von Bub1 jedoch unabhängig von BubR1 ist. Die molekulare Grundlage für diese Unterschiede im Rekrutierungsmechanismus von Bub1 und BubR1 war jedoch bisher unbekannt, da beide Proteine an Bub3, ein Adapterprotein für phosphorylierte Kinetochore, binden. In dieser Doktorarbeit wurde die Grundlage für das unterschiedliche Verhalten identifiziert. Bub1, jedoch nicht BubR1, verstärkt die Bindung von Bub3 an phosphorylierte Kinetochore durch eine kurze Region in der Bub3-Bindedomäne von Bub1, die "Loop" genannt wird. Dies erklärt warum BubR1 über einen alternativen Weg ans Kinetochor gelangen muss. Der Austausch der Loops zwischen Bub1 und BubR1 bewirkte einen Funktionsverlust von Bub1, welches nicht mehr in der Lage war am Kinetochor zu lokalisieren und einen Funktionsgewinn von BubR1, das so unabhängig von Bub1 ans Kinetochor gelangen konnte. Die Beobachtung, dass diese Loop-Austausch-Mutante von BubR1 jedoch nicht in der Lage war die SAC Funktion von BubR1 zu erfüllen, führte zur Identifikation der genauen Funktion des Loops in BubR1. *In vivo* und *in vitro* Experimente haben gezeigt, dass die besondere Sequenz des BubR1 Loops eine entscheidende Rolle in der Vermittlung der Bindung von BubR1 an den APC/C spielt. Ferner wurde in dieser Arbeit gezeigt, dass eine direkte Interaktion zwischen Bub1 und BubR1 Voraussetzung für die Kinetochor-

Lokalisation von BubR1 ist. Diese Heterodimerisierung erfordert strukturell equivalente Domänen in beiden Proteinen, zum einen die Bub3-Bindedomäne und zum anderen eine Region, die sich direkt an die Bub3-Bindedomäne anschließt und eine Helix bilden soll. Des Weiteren müssen Bub1 und BubR1 für ihre Interaktion an Bub3 gebunden sein. Interessanterweise kann die Heterodimerisierung auch ohne Kinetochore stattfinden. Zusammenfassend zeigt diese Doktorarbeit wie Genduplikation und die anschließende Subfunktionalisierung die Unterschiede im Verhalten von zwei eng verwandten Proteinen, die beide Teil eines essentiellen molekularen Netzwerkes sind, entscheidend beeinflussen können. Dies liefert ein tiefergehendes Verständnis darüber, wie das SAC Signal auf molekularer Ebene erzeugt wird.

7 Appendices

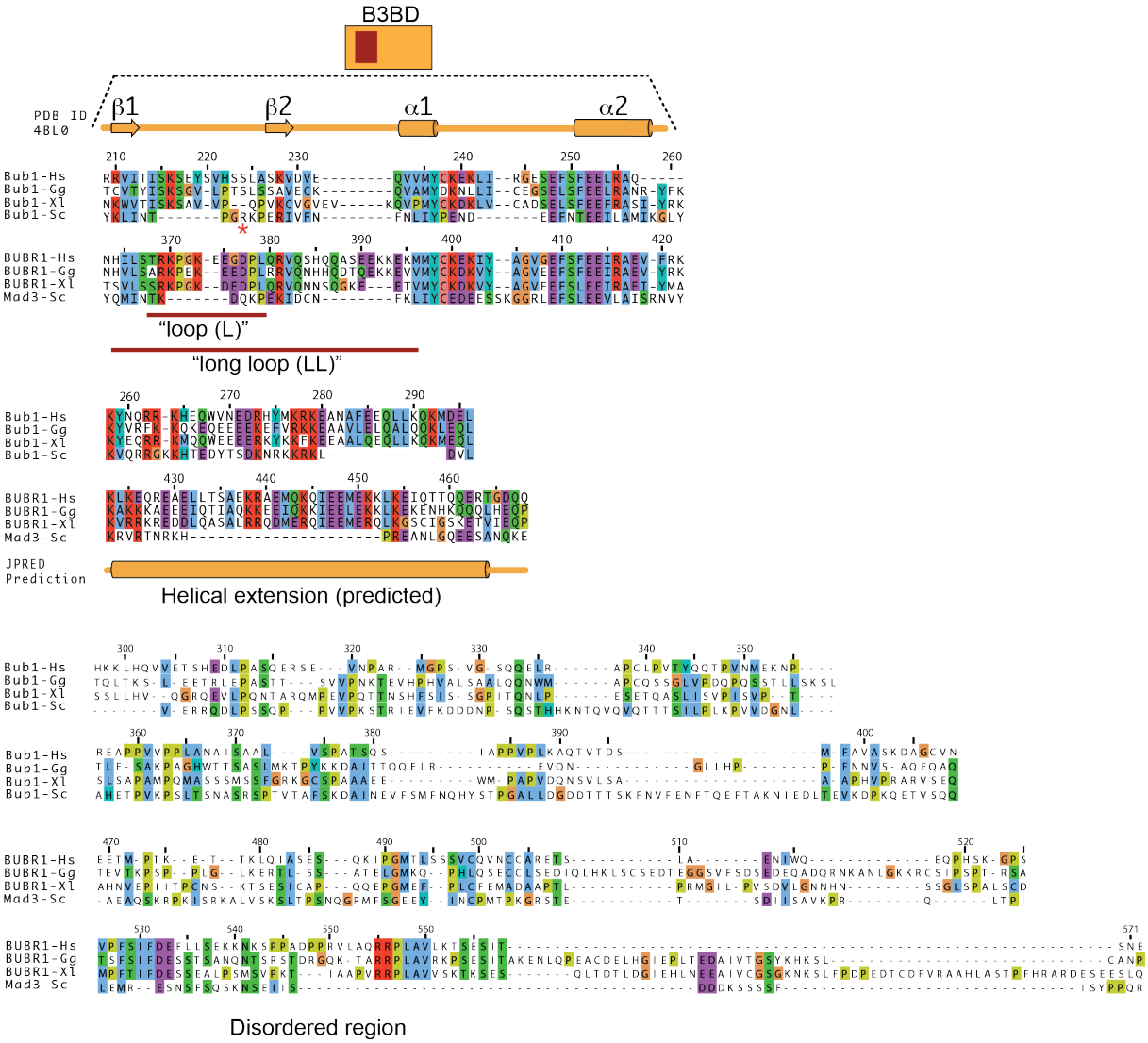

Figure 7-1 Complete alignment of the interacting regions of Bub1 and BubR1

Multiple sequence alignments of the interacting domains of Bub1 and BubR1 from four different species *Homo sapiens* (Hs), *Gallus gallus* (Gg), *Xenopus laevis* (Xl) and *Saccharomyces cerevisiae* (Sc). Mad3 is the budding yeast BubR1 homolog. The region following the helix is predicted to be disordered.

For completeness, in the following tables all the specific interactors identified in the SILAC experiments in this study are listed.

Table 7-1 Interactors identified in the SILAC experiment comparing GFP-Bub1$^{209-270}$ with GFP-BubR1$^{362-431}$

Listed are the specific interactors identified for GFP-Bub1$^{209-270}$ and for GFP-BubR1$^{362-431}$. As common interactors only the APC/C subunits are listed, due to space limitations. A p-value of 0.05 was chosen as cut-off for significance. The bait is always highlighted in grey. The experiment is shown in Figure 3-6 and Figure 3-24A.

Binders specific to Bub1$^{209-270}$ (p-value 0.05; S0=2)	
Protein name	**Gene name**
Mitotic checkpoint serine/threonine-protein kinase BUB1	BUB1
Protein CASC5	CASC5
T-complex protein 1 subunit eta	CCT7
mRNA export factor	RAE1
Scaffold attachment factor B1	SAFB
Scaffold attachment factor B2	SAFB2
Serine/arginine-rich splicing factor 9	SRSF9
Sjoegren syndrome/scleroderma autoantigen 1	SSSCA1
Zinc finger protein 638	ZNF638
Binders specific to BubR1$^{362-431}$ (p-value 0.05; S0=2)	
Protein name	**Gene name**
Mitotic checkpoint serine/threonine-protein kinase BUB1 beta	BUB1B
Common or background binders	
Protein name	**Gene name**
GFP	GFP
Anaphase-promoting complex subunit 1	ANAPC1
Anaphase-promoting complex subunit 15	ANAPC15
Anaphase-promoting complex subunit 16	ANAPC16
Anaphase-promoting complex subunit 2	ANAPC2
Anaphase-promoting complex subunit 4	ANAPC4
Anaphase-promoting complex subunit 5	ANAPC5
Anaphase-promoting complex	ANAPC7

subunit 7	
Cell division cycle protein 16 homolog	CDC16
Cell division cycle protein 23 homolog	CDC23
Anaphase-promoting complex subunit CDC26	CDC26
Cell division cycle protein 27 homolog	CDC27

Table 7-2 Interactors identified in the SILAC experiment comparing GFP and GFP-BubR1$^{362-431}$

Listed are the specific interactors identified for GFP-BubR1$^{362-431}$. Common interactors and background binders are not listed, due to space limitations. A p-value of 0.05 was chosen as cut-off for significance. The bait is highlighted in grey. The experiment is shown in Figure 3-22A.

Binders specific to the BubR1$^{362-431}$ (p-value 0.05; S0=2)	
Protein name	**Gene name**
Mitotic checkpoint serine/threonine-protein kinase BUB1 beta	BUB1B
Alpha-actinin-1	ACTN1
Alpha-actinin-4	ACTN4
Alpha-centractin	ACTR1A
Actin filament-associated protein 1	AFAP1
Anaphase-promoting complex subunit 1	ANAPC1
Anaphase-promoting complex subunit 4	ANAPC4
Anaphase-promoting complex subunit 7	ANAPC7
Annexin A2;Annexin	ANXA2
Intron-binding protein aquarius	AQR
Coatomer subunit delta	ARCN1
Aurora kinase B	AURKB
Brain acid soluble protein 1	BASP1
Pre-mRNA-splicing factor SPF27	BCAS2
Bone marrow stromal antigen 2	BST2
Mitotic checkpoint protein BUB3	BUB3
Calnexin	CANX
F-actin-capping protein subunit alpha-1	CAPZA1
F-actin-capping protein subunit beta	CAPZB
CD44 antigen	CD44
Cell division cycle protein 16 homolog	CDC16
Cell division cycle protein 23 homolog	CDC23

Cell division cycle protein 27 homolog	CDC27
Cell division cycle 5-like protein	CDC5L
Coronin-1C	CORO1C
Drebrin	DBN1
Probable ATP-dependent RNA helicase DDX46	DDX46
7-dehydrocholesterol reductase	DHCR7
EF-hand domain-containing protein D2	EFHD2
116 kDa U5 small nuclear ribonucleoprotein component	EFTUD2
Epiplakin	EPPK1
Filamin-A	FLNA
Filamin-B	FLNB
Guanine nucleotide-binding protein G(i) subunit alpha-2	GNAI2
Guanine nucleotide-binding protein G(I)/G(S)/G(T) subunit beta-1	GNB1
Non-histone chromosomal protein HMG-17	HMGN2
Endoplasmin	HSP90B1
Heat shock protein beta-1	HSPB1
Heat shock protein 105 kDa	HSPH1
Inner centromere protein	INCENP
Ras GTPase-activating-like protein IQGAP1	IQGAP1
Lamin-B receptor	LBR
Galectin-1	LGALS1
LIM domain and actin-binding protein 1	LIMA1;TRMT1
LIM domain only protein 7	LMO7
Leucine zipper protein 1	LUZP1
Mitotic interactor and substrate of PLK1	MISP
Neuronal growth regulator 1	NEGR1
Nexilin	NEXN
NK-tumor recognition protein;Putative peptidyl-prolyl cis-trans isomerase	NKTR
PDZ and LIM domain protein 7	PDLIM7
PHD finger-like domain-containing protein 5A	PHF5A
Plectin	PLEC
Plastin-3	PLS3
Podocalyxin	PODXL
Serine/threonine-protein	PPP1CB

phosphatase PP1-beta catalytic subunit	
Protein phosphatase 1 regulatory subunit 12A	PPP1R12A
Phostensin	PPP1R18
Pre-mRNA-processing factor 19	PRPF19
Pre-mRNA-processing-splicing factor 8	PRPF8
26S protease regulatory subunit 6A	PSMC3
26S protease regulatory subunit 6B	PSMC4
26S protease regulatory subunit 8	PSMC5
Poly(U)-binding-splicing factor PUF60	PUF60
mRNA export factor	RAE1
Ras-related protein Rap-1b	RAP1B
RNA-binding motif protein, X chromosome	RBMX
Protein S100-A10	S100A10
Scaffold attachment factor B1	SAFB
Scaffold attachment factor B2	SAFB2
U4/U6.U5 tri-snRNP-associated protein 1	SART1
Protein SCAF11	SCAF11
Splicing factor 1	SF1
Splicing factor 3A subunit 1	SF3A1
Splicing factor 3A subunit 2	SF3A2
Splicing factor 3A subunit 3	SF3A3
Splicing factor 3B subunit 1	SF3B1
Splicing factor 3B subunit 2	SF3B2
Splicing factor 3B subunit 3	SF3B3
Splicing factor 3B subunit 4	SF3B4
Superkiller viralicidic activity 2-like 2	SKIV2L2
Neutral amino acid transporter B(0)	SLC1A5
Sodium-coupled neutral amino acid transporter 2	SLC38A2
U2 small nuclear ribonucleoprotein B	SNRPB2
Small nuclear ribonucleoprotein Sm D2	SNRPD2
SNW domain-containing protein 1	SNW1
Cytospin-B	SPECC1
Cytospin-A	SPECC1L;SPECC1L-ADORA2A
Spectrin alpha chain, non-erythrocytic 1	SPTAN1
Spectrin beta chain, non-erythrocytic 1	SPTBN1
Sjoegren syndrome/scleroderma	SSSCA1

autoantigen 1	
Transgelin-2	TAGLN2
Transformer-2 protein homolog beta	TRA2B
Splicing factor U2AF 35 kDa subunit	U2AF1
E3 ubiquitin-protein ligase UBR5	UBR5
Vimentin	VIM
Zinc finger C3H1 domain-containing protein	ZFC3H1

Table 7-3 Interactors identified in the SILAC experiment comparing GFP-BubR1$^{362\text{-}431}{}_{\Delta}{}^{L}$ and GFP-BubR1$^{362\text{-}431}$

Listed are the specific interactors identified for GFP-BubR1$^{362\text{-}431}$ with and without the loop. Common interactors and background binders are not listed, due to space limitations. A p-value of 0.1 was chosen as cut-off for significance. The bait is highlighted in grey. The experiment is shown in Figure 3-23A.

Binders specific to the BubR1 loop (p-value 0.1; S0=2)	
Protein name	**Gene name**
BubR1loop	BubR1loop
Alpha-actinin-1	ACTN1
Actin filament-associated protein 1	AFAP1
Anaphase-promoting complex subunit 1	ANAPC1
Anaphase-promoting complex subunit 15	ANAPC15
Anaphase-promoting complex subunit 5	ANAPC5
Anaphase-promoting complex subunit 7	ANAPC7
Actin-binding protein anillin	ANLN
Annexin A2; Annexin; Putative annexin A2-like protein	ANXA2;ANXA2P2
Rho GTPase-activating protein 11A	ARHGAP11A
Sodium/potassium-transporting ATPase subunit alpha-1	ATP1A1
Brain acid soluble protein 1	BASP1
Bone marrow stromal antigen 2	BST2
Caldesmon	CALD1
Calmodulin	CALM1;GTPBP2;SWAP70;CALM3;ARHGAP5
CD44 antigen	CD44
Cell division cycle protein 16 homolog;Lymphocyte activation gene 3 protein	CDC16;LAG3

Cell division cycle protein 23 homolog	CDC23
Anaphase-promoting complex subunit CDC26	CDC26
Cofilin-1	CFL1
Coronin-1C;Carcinoembryonic antigen-related cell adhesion molecule 16	CORO1C;CEACAM16
Cysteine and glycine-rich protein 1	CSRP1
Src substrate cortactin	CTTN
Drebrin	DBN1
Epiplakin	EPPK1
Filamin-A	FLNA
Filamin-B	FLNB;DDR1
Flotillin-1	FLOT1
Flotillin-2	FLOT2
Fascin	FSCN1
Guanine nucleotide-binding protein subunit alpha-11;Guanine nucleotide-binding protein G(q) subunit alpha	GNA11;GNAQ
Guanine nucleotide-binding protein G(i) subunit alpha-2	GNAI2;CCDC86
Guanine nucleotide-binding protein G(k) subunit alpha	GNAI3
Guanine nucleotide-binding protein G(s) subunit alpha isoforms short	GNAS
Guanine nucleotide-binding protein G(I)/G(S)/G(T) subunit beta-1	GNB1
Guanine nucleotide-binding protein G(I)/G(S)/G(T) subunit beta-2;T-complex protein 11 homolog	GNB2;TCP11;EPHA3;CRHR2
Heat shock protein beta-1	HSPB1
Integrin alpha-9	ITGA9;PRDX4
Inward rectifier potassium channel 2;Profilin-3	KCNJ2;PFN3;LPCAT3;MFAP5
	KRT17
Galectin-1	LGALS1
LIM domain and actin-binding protein 1	LIMA1
LIM domain only protein 7	LMO7
Leucine zipper protein 1	LUZP1
MARCKS-related protein	MARCKSL1
Cell surface glycoprotein MUC18	MCAM
Mitotic interactor and substrate of PLK1	MISP
Metallothionein-1G	MT1G

Matrix-remodeling-associated protein 7	MXRA7
Myosin light chain 3;Calbindin	MYL3;CALB1
Unconventional myosin-Ib	MYO1B
Unconventional myosin-Ic	MYO1C
NADH dehydrogenase [ubiquinone] 1 alpha subcomplex subunit 5	NDUFA5;ITIH1;ACTR3C
Nexilin	NEXN
NK-tumor recognition protein;Putative peptidyl-prolyl cis-trans isomerase	NKTR
Neuronal pentraxin-2;Putative cytochrome b-c1 complex subunit Rieske-like protein 1	NPTX2;UQCRFS1P1
PDZ and LIM domain protein 7	PDLIM7
Plastin-1	PLS1
Plastin-3	PLS3
Peptidyl-prolyl cis-trans isomerase-like 3	PPIL3
Serine/threonine-protein phosphatase PP1-alpha catalytic subunit	PPP1CA
Serine/threonine-protein phosphatase PP1-beta catalytic subunit	PPP1CB
Protein phosphatase 1 regulatory subunit 12A	PPP1R12A;EPS8;ARFGAP1;ELMO3
cAMP-dependent protein kinase type II-alpha regulatory subunit	PRKAR2A
Very-long-chain (3R)-3-hydroxyacyl-CoA dehydratase 2	PTPLB
Rho-related GTP-binding protein RhoG	RHOG
E3 ubiquitin-protein ligase RNF135	RNF135
Protein S100-A10	S100A10
Scaffold attachment factor B1	SAFB
Neutral amino acid transporter B(0)	SLC1A5;NUDT6
Sodium-coupled neutral amino acid transporter 2	SLC38A2
Synaptosomal-associated protein 23	SNAP23
Cytospin-B	SPECC1
Cytospin-A	SPECC1L;SPECC1L-ADORA2A
	SPTBN2
Transgelin-2	TAGLN2
Transmembrane protein 43	TMEM43
Tropomodulin-3	TMOD3

Tropomyosin alpha-1 chain;Serine/threonine-protein phosphatase 2A 56 kDa regulatory subunit gamma isoform	TPM1;PPP2R5C
Tropomyosin alpha-3 chain	TPM3
Tropomyosin alpha-4 chain	TPM4
Tropomyosin alpha-4 chain	TPM4
Splicing factor U2AF 35 kDa subunit	U2AF1
E3 ubiquitin-protein ligase UBR5	UBR5
Vesicle-associated membrane protein-associated protein B/C	VAPB
WD repeat-containing protein 1	WDR1
CAAX prenyl protease 1 homolog	ZMPSTE24
G3V1M8	G3V1M8
B4E2U7	B4E2U7
E7EQV2	E7EQV2
Binders specific to BubR1$^{362-431}$ without the loop (p-value 0.1; S0=2)	
Protein name	**Gene name**
Alpha-centractin	ACTR1A
Beta-centractin;tRNA-splicing endonuclease subunit Sen2	ACTR1B;TSEN2
Protein-L-isoaspartate(D-aspartate) O-methyltransferase	PCMT1
Paraspeckle component 1	PSPC1
	PCBP2

Table 7-4 Interactors identified in the SILAC experiment comparing GFP-Bub1$^{1-284}$ and GFP-BubR1$^{1-431}$

Listed are the specific interactors identified for GFP-Bub1$^{1-284}$ and GFP-BubR1$^{1-431}$. Common interactors and background binders are not listed, due to space limitations. A p-value of 0.005 was chosen as cut-off for significance. The bait is highlighted in grey. The experiment is shown in Figure 3-24B.

Binders specific to the Bub1$^{1-284}$ (p-value 0.005; S0=2)	
Protein name	**Gene name**
Mitotic checkpoint serine/ threonine-protein kinase BUB1	BUB1
Protein CASC5	CASC5
Binders specific to the BubR1$^{1-431}$ (p-value 0.005; S0=2)	
Protein name	**Gene name**
Mitotic checkpoint serine/ threonine-protein kinase BUB1	BUB1B

beta	
Alpha-centractin	ACTR1A
Anaphase-promoting complex subunit 1	ANAPC1
Anaphase-promoting complex subunit 10	ANAPC10
Anaphase-promoting complex subunit 15	ANAPC15
Anaphase-promoting complex subunit 16	ANAPC16
Anaphase-promoting complex subunit 2	ANAPC2
Anaphase-promoting complex subunit 4	ANAPC4
Anaphase-promoting complex subunit 5	ANAPC5
Anaphase-promoting complex subunit 7	ANAPC7
Cell division cycle protein 16 homolog	CDC16
Cell division cycle protein 20 homolog	CDC20
Cell division cycle protein 23 homolog	CDC23
Anaphase-promoting complex subunit CDC26	CDC26
Cell division cycle protein 27 homolog	CDC27
Dynactin subunit 2	DCTN2
Mitotic spindle assembly checkpoint protein MAD2A	MAD2L1
Ubiquitin-conjugating enzyme E2 S	UBE2S

Table 7-5 Interactors identified in the SILAC experiment comparing GFP-Bub1$^{209-270}$ with and without the loop

Listed are the specific interactors identified for GFP-Bub1$^{209-270}$ with and without the loop. Common interactors and background binders are not listed, due to space limitations. A p-value of 0.05 was chosen as cut-off for significance. The bait is highlighted in grey. The experiment is shown in Figure 3-25.

Binders specific to the Bub1-loop (p-value 0.05; S0=2)	
Protein name	**Gene name**
Bub1loop	Bub1loop
A-kinase anchor protein 8-like	AKAP8L
Barrier-to-autointegration factor	BANF1

Calumenin	CALU
Protein CASC5	CASC5
Ribosomal RNA small subunit methyltransferase NEP1	EMG1
	FAM135B
Probable 28S rRNA (cytosine(4447)-C(5))-methyltransferase	NOP2
Protein-L-isoaspartate(D-aspartate) O-methyltransferase	PCMT1
Polymerase delta-interacting protein 3	POLDIP3
Putative trypsin-6	PRSS3P2
Double-strand-break repair protein rad21 homolog	RAD21
Reticulocalbin-1	RCN1
Septin-7	SEPT7
Y-box-binding protein 3	YBX3
Binders specific to Bub1$^{209-270}$ without the loop (p-value 0.05; S0=2)	
Protein name	**Gene name**
Actin-related protein 2	ACTR2;ZNF836
Actin filament-associated protein 1	AFAP1
Fructose-bisphosphate aldolase A	ALDOA
Intestinal-type alkaline phosphatase	ALPI
Anaphase-promoting complex subunit 1	ANAPC1
Anaphase-promoting complex subunit 2	ANAPC2
Anaphase-promoting complex subunit 4	ANAPC4
Anaphase-promoting complex subunit 5	ANAPC5
Anaphase-promoting complex subunit 7	ANAPC7
Actin-binding protein anillin	ANLN
Annexin A2; Annexin; Putative annexin A2-like protein	ANXA2;ANXA2P2
Actin-related protein 2/3 complex subunit 1B	ARPC1B
Sodium/potassium-transporting ATPase subunit alpha-1	ATP1A1
Sodium/potassium-transporting ATPase subunit beta-3	ATP1B3

Sarcoplasmic/endoplasmic reticulum calcium ATPase 2	ATP2A2
Potassium-transporting ATPase subunit beta	ATP4B
Aurora kinase B	AURKB
Basigin	BSG
Bone marrow stromal antigen 2	BST2
Basic leucine zipper and W2 domain-containing protein 1	BZW1
Calnexin	CANX
F-actin-capping protein subunit alpha-1	CAPZA1
F-actin-capping protein subunit alpha-2	CAPZA2
F-actin-capping protein subunit beta	CAPZB;MPZL1
CD44 antigen	CD44
CD59 glycoprotein	CD59
Cell division cycle protein 23 homolog	CDC23
Anaphase-promoting complex subunit CDC26	CDC26
Cell division cycle protein 27 homolog	CDC27;ZNF652
Cell division control protein 42 homolog	CDC42
Cadherin-2	CDH2
Cofilin-1	CFL1;RELB
MICOS complex subunit MIC19	CHCHD3
CDGSH iron-sulfur domain-containing protein 1	CISD1
CDGSH iron-sulfur domain-containing protein 2	CISD2
Cytoskeleton-associated protein 4	CKAP4
Clathrin heavy chain 1	CLTC
Coronin-1B;Coronin	CORO1B
Coronin-1C;Coronin	CORO1C
Cleavage and polyadenylation specificity factor subunit 7	CPSF7
Exportin-2	CSE1L
Cysteine and glycine-rich protein 1	CSRP1
Cysteine and glycine-rich protein 2	CSRP2
Catenin delta-1	CTNND1
Src substrate cortactin	CTTN

NADH-cytochrome b5 reductase 3	CYB5R3
DDRGK domain-containing protein 1	DDRGK1
7-dehydrocholesterol reductase	DHCR7
Desmoglein-2	DSG2
Elongation factor 1-alpha 2	EEF1A2
EF-hand domain-containing protein D2	EFHD2
Band 4.1-like protein 2	EPB41L2
Eukaryotic peptide chain release factor subunit 1	ETF1
Ezrin	EZR
FAS-associated factor 2	FAF2
Protein FAM111B	FAM111B
Filamin-A	FLNA
Filamin-B	FLNB
Flotillin-2	FLOT2
Polypeptide N-acetylgalactosaminyltransferase 2	GALNT2
Translational activator GCN1	GCN1L1
Guanine nucleotide-binding protein G(I)/G(S)/G(T) subunit beta-1	GNB1
Guanine nucleotide-binding protein G(I)/G(S)/G(T) subunit beta-2	GNB2
Guanine nucleotide-binding protein G(I)/G(S)/G(O) subunit gamma-12	GNG12
	GYPE;RHOBTB3
Endoplasmin	HSP90B1
Heat shock protein beta-1	HSPB1
MICOS complex subunit MIC60	IMMT
Ras GTPase-activating-like protein IQGAP1	IQGAP1
Junction plakoglobin	JUP
Kinesin-like protein KIF20A	KIF20A
Lamin-B receptor	LBR
Protein ERGIC-53	LMAN1
LIM domain only protein 7	LMO7
Leucine zipper protein 1	LUZP1
Ensconsin	MAP7
Mitochondrial pyruvate carrier 2	MPC2;OAS2
Myosin-9	MYH9
Myosin regulatory light chain	MYL12B;MYL12A;MYL9

12B;Myosin regulatory light chain 12A;Myosin regulatory light polypeptide 9	
Myosin light polypeptide 6	MYL6;PDE6H
Unconventional myosin-Ib	MYO1B
Unconventional myosin-Ic	MYO1C
Unconventional myosin-Ie	MYO1E
Nuclear migration protein nudC	NUDC
Outer dense fiber protein 4	ODF4
Protein disulfide-isomerase	P4HB
Protein disulfide-isomerase A3	PDIA3
PDZ and LIM domain protein 7	PDLIM7
Membrane-associated progesterone receptor component 1	PGRMC1
Urokinase plasminogen activator surface receptor	PLAUR
Plectin	PLEC
Plastin-1	PLS1
NADPH--cytochrome P450 reductase	POR
Peptidyl-prolyl cis-trans isomerase B	PPIB
Serine/threonine-protein phosphatase PP1-alpha catalytic subunit	PPP1CA;PPP1CC
Protein phosphatase 1 regulatory subunit 12A	PPP1R12A
Polymerase I and transcript release factor	PTRF
Ras-related protein Rab-10	RAB10
Ras-related protein Rab-11B;Ras-related protein Rab-11A	RAB11B;RAB11A
Ras-related protein Rab-1B	RAB1B
Ras-related protein Rab-6A;Ras-related protein Rab-6B	RAB6A;RAB6B
Ras-related protein Rab-7a	RAB7A
Ras-related protein Rap-1b;Ras-related protein Rap-1b-like protein	RAP1B
RNA-binding protein 8A	RBM8A;SLC38A7;FBXL19;ZSCAN29
Transforming protein RhoA; Rho-related GTP-binding protein RhoC	RHOA;RHOC
	RPL23A
Protein S100-A10	S100A10

Scaffold attachment factor B1	SAFB
Scaffold attachment factor B2	SAFB2
SAP domain-containing ribonucleoprotein	SARNP
Protein transport protein Sec61 subunit alpha isoform 1	SEC61A1
Protein transport protein Sec61 subunit beta	SEC61B
Translocation protein SEC63 homolog	SEC63
Sideroflexin-1	SFXN1
Sphingosine-1-phosphate lyase 1	SGPL1
Monocarboxylate transporter 1	SLC16A1
Monocarboxylate transporter 4	SLC16A3
Neutral amino acid transporter B(0)	SLC1A5
ADP/ATP translocase 1	SLC25A4
ADP/ATP translocase 2	SLC25A5
ADP/ATP translocase 3	SLC25A6
4F2 cell-surface antigen heavy chain	SLC3A2
SAFB-like transcription modulator	SLTM
Cytospin-B	SPECC1
Cytospin-A	SPECC1L;SPECC1L-ADORA2A
Sequestosome-1	SQSTM1
Serine/arginine-rich splicing factor 1	SRSF1
Serine/arginine-rich splicing factor 10	SRSF10
Serine/arginine-rich splicing factor 2	SRSF2
Serine/arginine-rich splicing factor 7	SRSF7
Serine/arginine-rich splicing factor 9	SRSF9
Transmembrane emp24 domain-containing protein 10	TMED10
Transmembrane emp24 domain-containing protein 2	TMED2
Tropomodulin-3	TMOD3
Thioredoxin-related transmembrane protein 1	TMX1
Mitochondrial import receptor subunit TOM70	TOMM70A
Tropomyosin alpha-4 chain	TPM4

Taperin	TPRN
Transformer-2 protein homolog alpha	TRA2A
Transformer-2 protein homolog beta	TRA2B
E3 ubiquitin-protein ligase UBR5	UBR5
Transitional endoplasmic reticulum ATPase	VCP
Voltage-dependent anion-selective channel protein 1	VDAC1
Voltage-dependent anion-selective channel protein 3	VDAC3
Vimentin	VIM
YLP motif-containing protein 1	YLPM1
14-3-3 protein gamma	YWHAG
Zinc finger protein 638	ZNF638

Protein sequences

Bub1 (*homo sapiens*)

```
   1 MDTPENVLQM LEAHMQSYKG NDPLGEWERY IQWVEENFPE NKEYLITLLE 50
  51 HLMKEFLDKK KYHNDPRFIS YCLKFAEYNS DLHQFFEFLY NHGIGTLSSP 100
 101 LYIAWAGHLE AQGELQHASA VLQRGIQNQA EPREFLQQQY RLFQTRLTET 150
 151 HLPAQARTSE PLHNVQVLNQ MITSKSNPGN NMACISKNQG SELSGVISSA 200
 201 CDKESNMERR VITISKSEYS VHSSLASKVD VEQVVMYCKE KLIRGESEFS 250
 251 FEELRAQKYN QRRKHEQWVN EDRHYMKRKE ANAFEEQLLK QKMDELHKKL 300
 301 HQVVETSHED LPASQERSEV NPARMGPSVG SQQELRAPCL PVTYQQTPVN 350
 351 MEKNPREAPP VVPPLANAIS AALVSPATSQ SIAPPVPLKA QTVTDSMFAV 400
 401 ASKDAGCVNK STHEFKPQSG AEIKEGCETH KVANTSSFHT TPNTSLGMVQ 450
 451 ATPSKVQPSP TVHTKEALGF IMNMFQAPTL PDISDDKDEW QSLDQNEDAF 500
 501 EAQFQKNVRS SGAWGVNKII SSLSSAFHVF EDGNKENYGL PQPKNKPTGA 550
 551 RTFGERSVSR LPSKPKEEVP HAEEFLDDST VWGIRCNKTL APSPKSPGDF 600
 601 TSAAQLASTP FHKLPVESVH ILEDKENVVA KQCTQATLDS CEENMVVPSR 650
 651 DGKFSPIQEK SPKQALSSHM YSASLLRLSQ PAAGGVLTCE AELGVEACRL 700
 701 TDTDAAIAED PPDAIAGLQA EWMQMSSLGT VDAPNFIVGN PWDDKLIFKL 750
 751 LSGLSKPVSS YPNTFEWQCK LPAIKPKTEF QLGSKLVYVH HLLGEGAFAQ 800
 801 VYEATQGDLN DAKNKQKFVL KVQKPANPWE FYIGTQLMER LKPSMQHMFM 850
 851 KFYSAHLFQN GSVLVGELYS YGTLLNAINL YKNTPEKVMP QGLVISFAMR 900
 901 MLYMIEQVHD CEIIHGDIKP DNFILGNGFL EQDDEDDLSA GLALIDLGQS 950
 951 IDMKLFPKGT IFTAKCETSG FQCVEMLSNK PWNYQIDYFG VAATVYCMLF 1000
1001 GTYMKVKNEG GECKPEGLFR RLPHLDMWNE FFHVMLNIPD CHHLPSLDLL 1050
1051 RQKLKKVFQQ HYTNKIRALR NRLIVLLLEC KRSRK
```

Bub3 (*homo sapiens*)

```
   1 MTGSNEFKLN QPPEDGISSV KFSPNTSQFL LVSSWDTSVR LYDVPANSMR 50
  51 LKYQHTGAVL DCAFYDPTHA WSGGLDHQLK MHDLNTDQEN LVGTHDAPIR 100
 101 CVEYCPEVNV MVTGSWDQTV KLWDPRTPCN AGTFSQPEKV YTLSVSGDRL 150
 151 IVGTAGRRVL VWDLRNMGYV QQRRESSLKY QTRCIRAFPN KQGYVLSSIE 200
 201 GRVAVEYLDP SPEVQKKKYA FKCHRLKENN IEQIYPVNAI SFHNIHNTFA 250
 251 TGGSDGFVNI WDPFNKKRLC QFHRYPTSIA SLAFSNDGTT LAIASSYMYE 300
 301 MDDTEHPEDG IFIRQVTDAE TKPKSPCT
```

BubR1 (*homo sapiens*)

```
   1 MAAVKKEGGA LSEAMSLEGD EWELSKENVQ PLRQGRIMST LQGALAQESA 50
  51 CNNTLQQQKR AFEYEIRFYT GNDPLDVWDR YISWTEQNYP QGGKESNMST 100
 101 LLERAVEALQ GEKRYYSDPR FLNLWLKLGR LCNEPLDMYS YLHNQGIGVS 150
 151 LAQFYISWAE EYEARENFRK ADAIFQEGIQ QKAEPLERLQ SQHRQFQARV 200
 201 SRQTLLALEK EEEEEVFESS VPQRSTLAEL KSKGKKTARA PIIRVGGALK 250
 251 APSQNRGLQN PFPQQMQNNS RITVFDENAD EASTAELSKP TVQPWIAPPM 300
 301 PRAKENELQA GPWNTGRSLE HRPRGNTASL IAVPAVLPSF TPYVEETARQ 350
 351 PVMTPCKIEP SINHILSTRK PGKEEGDPLQ RVQSHQQASE EKKEKMMYCK 400
 401 EKIYAGVGEF SFEEIRAEVF RKKLKEQREA ELLTSAEKRA EMQKQIEEME 450
 451 KKLKEIQTTQ QERTGDQQEE TMPTKETTKL QIASESQKIP GMTLSSSVCQ 500
 501 VNCCARETSL AENIWQEQPH SKGPSVPFSI FDEFLLSEKK NKSPPADPPR 550
 551 VLAQRRPLAV LKTSESITSN EDVSPDVCDE FTGIEPLSED AIITGFRNVT 600
 601 ICPNPEDTCD FARAARFVST PFHEIMSLKD LPSDPERLLP EEDLDVKTSE 650
 651 DQQTACGTIY SQTLSIKKLS PIIEDSREAT HSSGFSGSSA SVASTSSIKC 700
 701 LQIPEKLELT NETSENPTQS PWCSQYRRQL LKSLPELSAS AELCIEDRPM 750
 751 PKLEIEKEIE LGNEDYCIKR EYLICEDYKL FWVAPRNSAE LTVIKVSSQP 800
 801 VPWDFYINLK LKERLNEDFD HFCSCYQYQD GCIVWHQYIN CFTLQDLLQH 850
 851 SEYITHEITV LIIYNLLTIV EMLHKAEIVH GDLSPRCLIL RNRIHDPYDC 900
 901 NKNNQALKIV DFSYSVDLRV QLDVFTLSGF RTVQILEGQK ILANCSSPYQ 950
 951 VDLFGIADLA HLLLFKEHLQ VFWDGSFWKL SQNISELKDG ELWNKFFVRI 1000
1001 LNANDEATVS VLGELAAEMN GVFDTTFQSH LNKALWKVGK LTSPGALLFQ 1050
```

Bibliography

Akiyoshi B, Nelson CR, Biggins S (2013) The aurora B kinase promotes inner and outer kinetochore interactions in budding yeast. *Genetics* **194:** 785-789

Alberts B, Johnson A, Lewis J, Raff M, Roberts K, Walter P (2008) Molecular Biology of the Cell - 5th edition. *Garland Science, Taylor & Francis Group, LLC*

Alfieri C, Chang L, Zhang Z, Yang J, Maslen S, Skehel M, Barford D (2016) Molecular basis of APC/C regulation by the spindle assembly checkpoint. *Nature* **536:** 431-436

Alushin GM, Ramey VH, Pasqualato S, Ball DA, Grigorieff N, Musacchio A, Nogales E (2010) The Ndc80 kinetochore complex forms oligomeric arrays along microtubules. *Nature* **467:** 805-810

Aravamudhan P, Goldfarb AA, Joglekar AP (2015) The kinetochore encodes a mechanical switch to disrupt spindle assembly checkpoint signalling. *Nature cell biology* **17:** 868-879

Asbury CL, Gestaut DR, Powers AF, Franck AD, Davis TN (2006) The Dam1 kinetochore complex harnesses microtubule dynamics to produce force and movement. *Proceedings of the National Academy of Sciences of the United States of America* **103:** 9873-9878

Asghar A, Lajeunesse A, Dulla K, Combes G, Thebault P, Nigg EA, Elowe S (2015) Bub1 autophosphorylation feeds back to regulate kinetochore docking and promote localized substrate phosphorylation. *Nature communications* **6:** 8364

Basilico F, Maffini S, Weir JR, Prumbaum D, Rojas AM, Zimniak T, De Antoni A, Jeganathan S, Voss B, van Gerwen S, Krenn V, Massimiliano L, Valencia A, Vetter IR, Herzog F, Raunser S, Pasqualato S, Musacchio A (2014) The pseudo GTPase CENP-M drives human kinetochore assembly. *eLife* **3:** e02978

Bharadwaj R, Qi W, Yu H (2004) Identification of two novel components of the human NDC80 kinetochore complex. *The Journal of biological chemistry* **279:** 13076-13085

Biggins S, Severin FF, Bhalla N, Sassoon I, Hyman AA, Murray AW (1999) The conserved protein kinase Ipl1 regulates microtubule binding to kinetochores in budding yeast. *Genes & development* **13:** 532-544

Black BE, Brock MA, Bedard S, Woods VL, Jr., Cleveland DW (2007) An epigenetic mark generated by the incorporation of CENP-A into centromeric nucleosomes. *Proceedings of the National Academy of Sciences of the United States of America* **104:** 5008-5013

Boens S, Szeker K, Van Eynde A, Bollen M (2013) Interactor-guided dephosphorylation by protein phosphatase-1. *Methods Mol Biol* **1053:** 271-281

Bolanos-Garcia VM, Blundell TL (2011) BUB1 and BUBR1: multifaceted kinases of the cell cycle. *Trends in biochemical sciences* **36:** 141-150

Bolanos-Garcia VM, Lischetti T, Matak-Vinkovic D, Cota E, Simpson PJ, Chirgadze DY, Spring DR, Robinson CV, Nilsson J, Blundell TL (2011) Structure of a Blinkin-BUBR1 complex reveals an interaction crucial for kinetochore-mitotic checkpoint regulation via an unanticipated binding Site. *Structure* **19:** 1691-1700

Bond SR, Naus CC (2012) RF-Cloning.org: an online tool for the design of restriction-free cloning projects. *Nucleic acids research* **40:** W209-213

Boyarchuk Y, Salic A, Dasso M, Arnaoutov A (2007) Bub1 is essential for assembly of the functional inner centromere. *The Journal of cell biology* **176:** 919-928

Brady DM, Hardwick KG (2000) Complex formation between Mad1p, Bub1p and Bub3p is crucial for spindle checkpoint function. *Current biology : CB* **10:** 675-678

Breit C, Bange T, Petrovic A, Weir JR, Muller F, Vogt D, Musacchio A (2015) Role of Intrinsic and Extrinsic Factors in the Regulation of the Mitotic Checkpoint Kinase Bub1. *PloS one* **10:** e0144673

Burton JL, Solomon MJ (2007) Mad3p, a pseudosubstrate inhibitor of APCCdc20 in the spindle assembly checkpoint. *Genes & development* **21:** 655-667

Buschhorn BA, Petzold G, Galova M, Dube P, Kraft C, Herzog F, Stark H, Peters JM (2011) Substrate binding on the APC/C occurs between the coactivator Cdh1 and the processivity factor Doc1. *Nature structural & molecular biology* **18:** 6-13

Carmena M, Wheelock M, Funabiki H, Earnshaw WC (2012) The chromosomal passenger complex (CPC): from easy rider to the godfather of mitosis. *Nature reviews Molecular cell biology* **13:** 789-803

Carrero G, McDonald D, Crawford E, de Vries G, Hendzel MJ (2003) Using FRAP and mathematical modeling to determine the in vivo kinetics of nuclear proteins. *Methods* **29:** 14-28

Carroll CW, Enquist-Newman M, Morgan DO (2005) The APC subunit Doc1 promotes recognition of the substrate destruction box. *Current biology : CB* **15:** 11-18

Carroll CW, Milks KJ, Straight AF (2010) Dual recognition of CENP-A nucleosomes is required for centromere assembly. *The Journal of cell biology* **189:** 1143-1155

Carroll CW, Silva MC, Godek KM, Jansen LE, Straight AF (2009) Centromere assembly requires the direct recognition of CENP-A nucleosomes by CENP-N. *Nature cell biology* **11:** 896-902

Chan CS, Botstein D (1993) Isolation and characterization of chromosome-gain and increase-in-ploidy mutants in yeast. *Genetics* **135:** 677-691

Chan YW, Fava LL, Uldschmid A, Schmitz MH, Gerlich DW, Nigg EA, Santamaria A (2009) Mitotic control of kinetochore-associated dynein and spindle orientation by human Spindly. *The Journal of cell biology* **185:** 859-874

Chan YW, Jeyaprakash AA, Nigg EA, Santamaria A (2012) Aurora B controls kinetochore-microtubule attachments by inhibiting Ska complex-KMN network interaction. *The Journal of cell biology* **196:** 563-571

Chao WC, Kulkarni K, Zhang Z, Kong EH, Barford D (2012) Structure of the mitotic checkpoint complex. *Nature* **484:** 208-213

Cheeseman IM (2014) The kinetochore. *Cold Spring Harbor perspectives in biology* **6:** a015826

Cheeseman IM, Chappie JS, Wilson-Kubalek EM, Desai A (2006) The conserved KMN network constitutes the core microtubule-binding site of the kinetochore. *Cell* **127:** 983-997

Cheeseman IM, Desai A (2008) Molecular architecture of the kinetochore-microtubule interface. *Nature reviews Molecular cell biology* **9:** 33-46

Cheeseman IM, Hori T, Fukagawa T, Desai A (2008) KNL1 and the CENP-H/I/K complex coordinately direct kinetochore assembly in vertebrates. *Molecular biology of the cell* **19:** 587-594

Cheeseman IM, Niessen S, Anderson S, Hyndman F, Yates JR, 3rd, Oegema K, Desai A (2004) A conserved protein network controls assembly of the outer kinetochore and its ability to sustain tension. *Genes & development* **18:** 2255-2268

Chen D, Huang S (2001) Nucleolar components involved in ribosome biogenesis cycle between the nucleolus and nucleoplasm in interphase cells. *The Journal of cell biology* **153:** 169-176

Chen RH (2002) BubR1 is essential for kinetochore localization of other spindle checkpoint proteins and its phosphorylation requires Mad1. *The Journal of cell biology* **158:** 487-496

Ciferri C, De Luca J, Monzani S, Ferrari KJ, Ristic D, Wyman C, Stark H, Kilmartin J, Salmon ED, Musacchio A (2005) Architecture of the human ndc80-hec1 complex, a critical constituent of the outer kinetochore. *The Journal of biological chemistry* **280:** 29088-29095

Ciferri C, Pasqualato S, Screpanti E, Varetti G, Santaguida S, Dos Reis G, Maiolica A, Polka J, De Luca JG, De Wulf P, Salek M, Rappsilber J, Moores CA, Salmon ED, Musacchio A (2008) Implications for kinetochore-microtubule attachment from the structure of an engineered Ndc80 complex. *Cell* **133:** 427-439

Cole C, Barber JD, Barton GJ (2008) The Jpred 3 secondary structure prediction server. *Nucleic acids research* **36:** W197-201

Collin P, Nashchekina O, Walker R, Pines J (2013) The spindle assembly checkpoint works like a rheostat rather than a toggle switch. *Nature cell biology* **15:** 1378-1385

Collins KA, Castillo AR, Tatsutani SY, Biggins S (2005) De novo kinetochore assembly requires the centromeric histone H3 variant. *Molecular biology of the cell* **16:** 5649-5660

Coudreuse D, Nurse P (2010) Driving the cell cycle with a minimal CDK control network. *Nature* **468:** 1074-1079

Cox J, Mann M (2008) MaxQuant enables high peptide identification rates, individualized p.p.b.-range mass accuracies and proteome-wide protein quantification. *Nature biotechnology* **26:** 1367-1372

Cox J, Neuhauser N, Michalski A, Scheltema RA, Olsen JV, Mann M (2011) Andromeda: a peptide search engine integrated into the MaxQuant environment. *Journal of proteome research* **10:** 1794-1805

Craney A, Kelly A, Jia L, Fedrigo I, Yu H, Rape M (2016) Control of APC/C-dependent ubiquitin chain elongation by reversible phosphorylation. *Proceedings of the National Academy of Sciences of the United States of America* **113:** 1540-1545

D'Arcy S, Davies OR, Blundell TL, Bolanos-Garcia VM (2010) Defining the molecular basis of BubR1 kinetochore interactions and APC/C-CDC20 inhibition. *The Journal of biological chemistry* **285:** 14764-14776

Davenport J, Harris LD, Goorha R (2006) Spindle checkpoint function requires Mad2-dependent Cdc20 binding to the Mad3 homology domain of BubR1. *Experimental cell research* **312:** 1831-1842

De Antoni A, Pearson CG, Cimini D, Canman JC, Sala V, Nezi L, Mapelli M, Sironi L, Faretta M, Salmon ED, Musacchio A (2005) The Mad1/Mad2 complex as a template for Mad2 activation in the spindle assembly checkpoint. *Current biology : CB* **15:** 214-225

DeLuca JG, Dong Y, Hergert P, Strauss J, Hickey JM, Salmon ED, McEwen BF (2005) Hec1 and nuf2 are core components of the kinetochore outer plate essential for organizing microtubule attachment sites. *Molecular biology of the cell* **16:** 519-531

DeLuca JG, Gall WE, Ciferri C, Cimini D, Musacchio A, Salmon ED (2006) Kinetochore microtubule dynamics and attachment stability are regulated by Hec1. *Cell* **127:** 969-982

DeLuca JG, Moree B, Hickey JM, Kilmartin JV, Salmon ED (2002) hNuf2 inhibition blocks stable kinetochore-microtubule attachment and induces mitotic cell death in HeLa cells. *The Journal of cell biology* **159:** 549-555

DeLuca KF, Lens SM, DeLuca JG (2011) Temporal changes in Hec1 phosphorylation control kinetochore-microtubule attachment stability during mitosis. *Journal of cell science* **124:** 622-634

Di Fiore B, Davey NE, Hagting A, Izawa D, Mansfeld J, Gibson TJ, Pines J (2015) The ABBA Motif Binds APC/C Activators and Is Shared by APC/C Substrates and Regulators. *Developmental cell* **32:** 358-372

Diaz-Martinez LA, Tian W, Li B, Warrington R, Jia L, Brautigam CA, Luo X, Yu H (2015) The Cdc20-binding Phe Box of the Spindle Checkpoint Protein BubR1 Maintains the Mitotic Checkpoint Complex During Mitosis. *The Journal of biological chemistry* **290:** 2431-2443

Dick AE, Gerlich DW (2013) Kinetic framework of spindle assembly checkpoint signalling. *Nature cell biology* **15:** 1370-1377

Ditchfield C, Johnson VL, Tighe A, Ellston R, Haworth C, Johnson T, Mortlock A, Keen N, Taylor SS (2003) Aurora B couples chromosome alignment with anaphase by targeting BubR1, Mad2, and Cenp-E to kinetochores. *The Journal of cell biology* **161:** 267-280

Dou Z, Liu X, Wang W, Zhu T, Wang X, Xu L, Abrieu A, Fu C, Hill DL, Yao X (2015) Dynamic localization of Mps1 kinase to kinetochores is essential for accurate spindle microtubule attachment. *Proceedings of the National Academy of Sciences of the United States of America* **112:** E4546-4555

Earnshaw WC, Migeon BR (1985) Three related centromere proteins are absent from the inactive centromere of a stable isodicentric chromosome. *Chromosoma* **92:** 290-296

Earnshaw WC, Rothfield N (1985) Identification of a family of human centromere proteins using autoimmune sera from patients with scleroderma. *Chromosoma* **91:** 313-321

Edgar RC (2004) MUSCLE: a multiple sequence alignment method with reduced time and space complexity. *BMC bioinformatics* **5:** 113

Elowe S (2011) Bub1 and BubR1: at the interface between chromosome attachment and the spindle checkpoint. *Molecular and cellular biology* **31:** 3085-3093

Elowe S, Dulla K, Uldschmid A, Li X, Dou Z, Nigg EA (2010) Uncoupling of the spindle-checkpoint and chromosome-congression functions of BubR1. *Journal of cell science* **123:** 84-94

Elowe S, Hummer S, Uldschmid A, Li X, Nigg EA (2007) Tension-sensitive Plk1 phosphorylation on BubR1 regulates the stability of kinetochore microtubule interactions. *Genes & development* **21:** 2205-2219

Elson EL (1985) Fluorescence correlation spectroscopy and photobleaching recovery. *Ann Rev Phys Chem* **36:** 379-406

Emanuele MJ, Lan W, Jwa M, Miller SA, Chan CS, Stukenberg PT (2008) Aurora B kinase and protein phosphatase 1 have opposing roles in modulating kinetochore assembly. *The Journal of cell biology* **181:** 241-254

Espert A, Uluocak P, Bastos RN, Mangat D, Graab P, Gruneberg U (2014) PP2A-B56 opposes Mps1 phosphorylation of Knl1 and thereby promotes spindle assembly checkpoint silencing. *The Journal of cell biology* **206:** 833-842

Espeut J, Cheerambathur DK, Krenning L, Oegema K, Desai A (2012) Microtubule binding by KNL-1 contributes to spindle checkpoint silencing at the kinetochore. *The Journal of cell biology* **196:** 469-482

Espeut J, Lara-Gonzalez P, Sassine M, Shiau AK, Desai A, Abrieu A (2015) Natural Loss of Mps1 Kinase in Nematodes Uncovers a Role for Polo-like Kinase 1 in Spindle Checkpoint Initiation. *Cell reports* **12:** 58-65

Essex A, Dammermann A, Lewellyn L, Oegema K, Desai A (2009) Systematic analysis in Caenorhabditis elegans reveals that the spindle checkpoint is composed of two largely independent branches. *Molecular biology of the cell* **20:** 1252-1267

Eytan E, Wang K, Miniowitz-Shemtov S, Sitry-Shevah D, Kaisari S, Yen TJ, Liu ST, Hershko A (2014) Disassembly of mitotic checkpoint complexes by the joint action of the AAA-ATPase TRIP13 and p31(comet). *Proceedings of the National Academy of Sciences of the United States of America* **111:** 12019-12024

Faesen AC, Thanasoula M, Maffini S, Breit C, Müller F, van Gerwen S, Bange T, Musacchio A (2016, manuscript under review) In vitro reconstitution of spindle assembly checkpoint signalling identifies the determinants of catalytic assembly of the mitotic checkpoint complex. *Nature*

Fang G (2002) Checkpoint protein BubR1 acts synergistically with Mad2 to inhibit anaphase-promoting complex. *Molecular biology of the cell* **13:** 755-766

Fava LL, Kaulich M, Nigg EA, Santamaria A (2011) Probing the in vivo function of Mad1:C-Mad2 in the spindle assembly checkpoint. *The EMBO journal* **30:** 3322-3336

Fernius J, Hardwick KG (2007) Bub1 kinase targets Sgo1 to ensure efficient chromosome biorientation in budding yeast mitosis. *PLoS genetics* **3:** e213

Flemming W (1882) *Zellsubstanz, Kern und Zelltheilung*: FCW Vogel, Leipzig.

Foe IT, Foster SA, Cheung SK, DeLuca SZ, Morgan DO, Toczyski DP (2011) Ubiquitination of Cdc20 by the APC occurs through an intramolecular mechanism. *Current biology : CB* **21:** 1870-1877

Foley EA, Kapoor TM (2013) Microtubule attachment and spindle assembly checkpoint signalling at the kinetochore. *Nature reviews Molecular cell biology* **14:** 25-37

Foley EA, Maldonado M, Kapoor TM (2011) Formation of stable attachments between kinetochores and microtubules depends on the B56-PP2A phosphatase. *Nature cell biology* **13:** 1265-1271

Foltz DR, Jansen LE, Black BE, Bailey AO, Yates JR, 3rd, Cleveland DW (2006) The human CENP-A centromeric nucleosome-associated complex. *Nature cell biology* **8:** 458-469

Foster SA, Morgan DO (2012) The APC/C subunit Mnd2/Apc15 promotes Cdc20 autoubiquitination and spindle assembly checkpoint inactivation. *Molecular cell* **47:** 921-932

Fraschini R, Beretta A, Sironi L, Musacchio A, Lucchini G, Piatti S (2001) Bub3 interaction with Mad2, Mad3 and Cdc20 is mediated by WD40 repeats and does not require intact kinetochores. *The EMBO journal* **20:** 6648-6659

Fujimitsu K, Grimaldi M, Yamano H (2016) Cyclin-dependent kinase 1-dependent activation of APC/C ubiquitin ligase. *Science (New York, NY)* **352:** 1121-1124

Funabiki H, Wynne DJ (2013) Making an effective switch at the kinetochore by phosphorylation and dephosphorylation. *Chromosoma*

Funabiki H, Yamano H, Kumada K, Nagao K, Hunt T, Yanagida M (1996) Cut2 proteolysis required for sister-chromatid seperation in fission yeast. *Nature* **381:** 438-441

Gaitanos TN, Santamaria A, Jeyaprakash AA, Wang B, Conti E, Nigg EA (2009) Stable kinetochore-microtubule interactions depend on the Ska complex and its new component Ska3/C13Orf3. *The EMBO journal* **28:** 1442-1452

Gascoigne KE, Takeuchi K, Suzuki A, Hori T, Fukagawa T, Cheeseman IM (2011) Induced ectopic kinetochore assembly bypasses the requirement for CENP-A nucleosomes. *Cell* **145:** 410-422

Gassmann R, Essex A, Hu JS, Maddox PS, Motegi F, Sugimoto A, O'Rourke SM, Bowerman B, McLeod I, Yates JR, 3rd, Oegema K, Cheeseman IM, Desai A (2008) A new mechanism controlling kinetochore-microtubule interactions revealed by comparison of two dynein-targeting components: SPDL-1 and the Rod/Zwilch/Zw10 complex. *Genes & development* **22:** 2385-2399

Gassmann R, Holland AJ, Varma D, Wan X, Civril F, Cleveland DW, Oegema K, Salmon ED, Desai A (2010) Removal of Spindly from microtubule-attached kinetochores controls spindle checkpoint silencing in human cells. *Genes & development* **24:** 957-971

Gillett ES, Espelin CW, Sorger PK (2004) Spindle checkpoint proteins and chromosome-microtubule attachment in budding yeast. *The Journal of cell biology* **164:** 535-546

Glotzer M, Murray AW, Kirschner MW (1991) Cyclin is degraded by the ubiquitin pathway. *Nature* **349:** 132-138

Golan A, Yudkovsky Y, Hershko A (2002) The cyclin-ubiquitin ligase activity of cyclosome/APC is jointly activated by protein kinases Cdk1-cyclin B and Plk. *The Journal of biological chemistry* **277:** 15552-15557

Goshima G, Kiyomitsu T, Yoda K, Yanagida M (2003) Human centromere chromatin protein hMis12, essential for equal segregation, is independent of CENP-A loading pathway. *The Journal of cell biology* **160:** 25-39

Griffis ER, Stuurman N, Vale RD (2007) Spindly, a novel protein essential for silencing the spindle assembly checkpoint, recruits dynein to the kinetochore. *The Journal of cell biology* **177:** 1005-1015

Guo Y, Kim C, Ahmad S, Zhang J, Mao Y (2012) CENP-E--dependent BubR1 autophosphorylation enhances chromosome alignment and the mitotic checkpoint. *The Journal of cell biology* **198:** 205-217

Hagan RS, Manak MS, Buch HK, Meier MG, Meraldi P, Shah JV, Sorger PK (2011) p31(comet) acts to ensure timely spindle checkpoint silencing subsequent to kinetochore attachment. *Molecular biology of the cell* **22:** 4236-4246

Han JS, Vitre B, Fachinetti D, Cleveland DW (2014) Bimodal activation of BubR1 by Bub3 sustains mitotic checkpoint signaling. *Proceedings of the National Academy of Sciences of the United States of America* **111:** E4185-4193

Hanisch A, Sillje HH, Nigg EA (2006) Timely anaphase onset requires a novel spindle and kinetochore complex comprising Ska1 and Ska2. *The EMBO journal* **25:** 5504-5515

Hardwick KG, Johnston RC, Smith DL, Murray AW (2000) MAD3 encodes a novel component of the spindle checkpoint which interacts with Bub3p, Cdc20p, and Mad2p. *The Journal of cell biology* **148:** 871-882

Harris L, Davenport J, Neale G, Goorha R (2005) The mitotic checkpoint gene BubR1 has two distinct functions in mitosis. *Experimental cell research* **308:** 85-100

Hartwell LH (1974) Saccharomyces cerevisiae cell cycle. *Bacteriological reviews* **38:** 164-198

Hauf S, Cole RW, LaTerra S, Zimmer C, Schnapp G, Walter R, Heckel A, van Meel J, Rieder CL, Peters JM (2003) The small molecule Hesperadin reveals a role for Aurora B in correcting kinetochore-microtubule attachment and in maintaining the spindle assembly checkpoint. *The Journal of cell biology* **161:** 281-294

He J, Chao WC, Zhang Z, Yang J, Cronin N, Barford D (2013) Insights into degron recognition by APC/C coactivators from the structure of an Acm1-Cdh1 complex. *Molecular cell* **50:** 649-660

Hein JB, Nilsson J (2016) Interphase APC/C-Cdc20 inhibition by cyclin A2-Cdk2 ensures efficient mitotic entry. *Nature communications* **7:** 10975

Herzog F, Mechtler K, Peters JM (2005) Identification of cell cycle-dependent phosphorylation sites on the anaphase-promoting complex/cyclosome by mass spectrometry. *Methods in enzymology* **398:** 231-245

Herzog F, Primorac I, Dube P, Lenart P, Sander B, Mechtler K, Stark H, Peters JM (2009) Structure of the anaphase-promoting complex/cyclosome interacting with a mitotic checkpoint complex. *Science (New York, NY)* **323:** 1477-1481

Hewitt L, Tighe A, Santaguida S, White AM, Jones CD, Musacchio A, Green S, Taylor SS (2010) Sustained Mps1 activity is required in mitosis to recruit O-Mad2 to the Mad1-C-Mad2 core complex. *The Journal of cell biology* **190:** 25-34

Hiruma Y, Sacristan C, Pachis ST, Adamopoulos A, Kuijt T, Ubbink M, von Castelmur E, Perrakis A, Kops GJ (2015) CELL DIVISION CYCLE. Competition between MPS1 and microtubules at kinetochores regulates spindle checkpoint signaling. *Science (New York, NY)* **348:** 1264-1267

Holloway SL, Glotzer M, King RW, Murray AW (1993) Anaphase is initiated by proteolysis rather than by the inactivation of maturation-promoting factor. *Cell* **73:** 1393-1402

Hori T, Haraguchi T, Hiraoka Y, Kimura H, Fukagawa T (2003) Dynamic behavior of Nuf2-Hec1 complex that localizes to the centrosome and centromere and is essential for mitotic progression in vertebrate cells. *Journal of cell science* **116:** 3347-3362

Hori T, Okada M, Maenaka K, Fukagawa T (2008) CENP-O class proteins form a stable complex and are required for proper kinetochore function. *Molecular biology of the cell* **19:** 843-854

Hornung P, Maier M, Alushin GM, Lander GC, Nogales E, Westermann S (2011) Molecular architecture and connectivity of the budding yeast Mtw1 kinetochore complex. *Journal of molecular biology* **405:** 548-559

Howell BJ, Hoffman DB, Fang G, Murray AW, Salmon ED (2000) Visualization of Mad2 dynamics at kinetochores, along spindle fibers, and at spindle poles in living cells. *The Journal of cell biology* **150:** 1233-1250

Howell BJ, McEwen BF, Canman JC, Hoffman DB, Farrar EM, Rieder CL, Salmon ED (2001) Cytoplasmic dynein/dynactin drives kinetochore protein transport to the spindle poles and has a role in mitotic spindle checkpoint inactivation. *The Journal of cell biology* **155:** 1159-1172

Howell BJ, Moree B, Farrar EM, Stewart S, Fang G, Salmon ED (2004) Spindle checkpoint protein dynamics at kinetochores in living cells. *Current biology : CB* **14:** 953-964

Hoyt MA, Totis L, Roberts BT (1991) S. cerevisiae genes required for cell cycle arrest in response to loss of microtubule function. *Cell* **66:** 507-517

Hua S, Wang Z, Jiang K, Huang Y, Ward T, Zhao L, Dou Z, Yao X (2011) CENP-U cooperates with Hec1 to orchestrate kinetochore-microtubule attachment. *The Journal of biological chemistry* **286:** 1627-1638

Huang H, Hittle J, Zappacosta F, Annan RS, Hershko A, Yen TJ (2008) Phosphorylation sites in BubR1 that regulate kinetochore attachment, tension, and mitotic exit. *The Journal of cell biology* **183:** 667-680

Ito D, Saito Y, Matsumoto T (2012) Centromere-tethered Mps1 pombe homolog (Mph1) kinase is a sufficient marker for recruitment of the spindle checkpoint protein Bub1, but not Mad1. *Proceedings of the National Academy of Sciences of the United States of America* **109:** 209-214

Izawa D, Pines J (2012) Mad2 and the APC/C compete for the same site on Cdc20 to ensure proper chromosome segregation. *The Journal of cell biology* **199:** 27-37

Izawa D, Pines J (2015) The mitotic checkpoint complex binds a second CDC20 to inhibit active APC/C. *Nature* **517:** 631-634

Janicki SM, Tsukamoto T, Salghetti SE, Tansey WP, Sachidanandam R, Prasanth KV, Ried T, Shav-Tal Y, Bertrand E, Singer RH, Spector DL (2004) From silencing to gene expression: real-time analysis in single cells. *Cell* **116:** 683-698

Janke C, Ortiz J, Lechner J, Shevchenko A, Shevchenko A, Magiera MM, Schramm C, Schiebel E (2001) The budding yeast proteins Spc24p and Spc25p interact with Ndc80p and Nuf2p at the kinetochore and are important for kinetochore clustering and checkpoint control. *The EMBO journal* **20:** 777-791

Ji Z, Gao H, Yu H (2015) CELL DIVISION CYCLE. Kinetochore attachment sensed by competitive Mps1 and microtubule binding to Ndc80C. *Science (New York, NY)* **348:** 1260-1264

Jia L, Li B, Warrington RT, Hao X, Wang S, Yu H (2011) Defining pathways of spindle checkpoint silencing: functional redundancy between Cdc20 ubiquitination and p31(comet). *Molecular biology of the cell* **22:** 4227-4235

Jia L, Li B, Yu H (2016) The Bub1-Plk1 kinase complex promotes spindle checkpoint signalling through Cdc20 phosphorylation. *Nature communications* **7:** 10818

Joglekar AP, Bloom K, Salmon ED (2009) In vivo protein architecture of the eukaryotic kinetochore with nanometer scale accuracy. *Current biology : CB* **19:** 694-699

Johnson VL, Scott MI, Holt SV, Hussein D, Taylor SS (2004) Bub1 is required for kinetochore localization of BubR1, Cenp-E, Cenp-F and Mad2, and chromosome congression. *Journal of cell science* **117:** 1577-1589

Kang J, Yang M, Li B, Qi W, Zhang C, Shokat KM, Tomchick DR, Machius M, Yu H (2008) Structure and substrate recruitment of the human spindle checkpoint kinase Bub1. *Molecular cell* **32:** 394-405

Karess R (2005) Rod-Zw10-Zwilch: a key player in the spindle checkpoint. *Trends in cell biology* **15:** 386-392

Kasuboski JM, Bader JR, Vaughan PS, Tauhata SB, Winding M, Morrissey MA, Joyce MV, Boggess W, Vos L, Chan GK, Hinchcliffe EH, Vaughan KT (2011) Zwint-1 is a novel Aurora B substrate required for the assembly of a dynein-binding platform on kinetochores. *Molecular biology of the cell* **22:** 3318-3330

Kato H, Jiang J, Zhou BR, Rozendaal M, Feng H, Ghirlando R, Xiao TS, Straight AF, Bai Y (2013) A conserved mechanism for centromeric nucleosome recognition by centromere protein CENP-C. *Science (New York, NY)* **340:** 1110-1113

Kawashima SA, Yamagishi Y, Honda T, Ishiguro K, Watanabe Y (2010) Phosphorylation of H2A by Bub1 prevents chromosomal instability through localizing shugoshin. *Science (New York, NY)* **327:** 172-177

Kelly AE, Ghenoiu C, Xue JZ, Zierhut C, Kimura H, Funabiki H (2010) Survivin reads phosphorylated histone H3 threonine 3 to activate the mitotic kinase Aurora B. *Science (New York, NY)* **330:** 235-239

Kemmler S, Stach M, Knapp M, Ortiz J, Pfannstiel J, Ruppert T, Lechner J (2009) Mimicking Ndc80 phosphorylation triggers spindle assembly checkpoint signalling. *The EMBO journal* **28:** 1099-1110

Kim S, Sun H, Tomchick DR, Yu H, Luo X (2012) Structure of human Mad1 C-terminal domain reveals its involvement in kinetochore targeting. *Proceedings of the National Academy of Sciences of the United States of America* **109:** 6549-6554

Kim S, Yu H (2015) Multiple assembly mechanisms anchor the KMN spindle checkpoint platform at human mitotic kinetochores. *The Journal of cell biology* **208:** 181-196

Kim T, Moyle MW, Lara-Gonzalez P, De Groot C, Oegema K, Desai A (2015) Kinetochore-localized BUB-1/BUB-3 complex promotes anaphase onset in C. elegans. *The Journal of cell biology* **209:** 507-517

King EM, van der Sar SJ, Hardwick KG (2007) Mad3 KEN boxes mediate both Cdc20 and Mad3 turnover, and are critical for the spindle checkpoint. *PloS one* **2:** e342

Kitagawa K, Hieter P (2001) Evolutionary conservation between budding yeast and human kinetochores. *Nature reviews Molecular cell biology* **2:** 678-687

Kitajima TS, Hauf S, Ohsugi M, Yamamoto T, Watanabe Y (2005) Human Bub1 defines the persistent cohesion site along the mitotic chromosome by affecting Shugoshin localization. *Current biology : CB* **15:** 353-359

Kitajima TS, Sakuno T, Ishiguro K, Iemura S, Natsume T, Kawashima SA, Watanabe Y (2006) Shugoshin collaborates with protein phosphatase 2A to protect cohesin. *Nature* **441:** 46-52

Kiyomitsu T, Murakami H, Yanagida M (2011) Protein interaction domain mapping of human kinetochore protein Blinkin reveals a consensus motif for binding of spindle assembly checkpoint proteins Bub1 and BubR1. *Molecular and cellular biology* **31:** 998-1011

Kiyomitsu T, Obuse C, Yanagida M (2007) Human Blinkin/AF15q14 is required for chromosome alignment and the mitotic checkpoint through direct interaction with Bub1 and BubR1. *Developmental cell* **13:** 663-676

Klare K, Weir JR, Basilico F, Zimniak T, Massimiliano L, Ludwigs N, Herzog F, Musacchio A (2015) CENP-C is a blueprint for constitutive centromere-associated network assembly within human kinetochores. *The Journal of cell biology* **210:** 11-22

Klebig C, Korinth D, Meraldi P (2009) Bub1 regulates chromosome segregation in a kinetochore-independent manner. *The Journal of cell biology* **185:** 841-858

Kline SL, Cheeseman IM, Hori T, Fukagawa T, Desai A (2006) The human Mis12 complex is required for kinetochore assembly and proper chromosome segregation. *The Journal of cell biology* **173:** 9-17

Kolodner RD, Cleveland DW, Putnam CD (2011) Cancer. Aneuploidy drives a mutator phenotype in cancer. *Science (New York, NY)* **333:** 942-943

Kops GJ, Kim Y, Weaver BA, Mao Y, McLeod I, Yates JR, 3rd, Tagaya M, Cleveland DW (2005) ZW10 links mitotic checkpoint signaling to the structural kinetochore. *The Journal of cell biology* **169:** 49-60

Kraft C, Herzog F, Gieffers C, Mechtler K, Hagting A, Pines J, Peters JM (2003) Mitotic regulation of the human anaphase-promoting complex by phosphorylation. *The EMBO journal* **22:** 6598-6609

Kramer ER, Gieffers C, Holzl G, Hengstschlager M, Peters JM (1998) Activation of the human anaphase-promoting complex by proteins of the CDC20/Fizzy family. *Current biology : CB* **8:** 1207-1210

Kramer ER, Scheuringer N, Podtelejnikov AV, Mann M, Peters JM (2000) Mitotic regulation of the APC activator proteins CDC20 and CDH1. *Molecular biology of the cell* **11:** 1555-1569

Krenn V, Musacchio A (2015) The Aurora B Kinase in Chromosome Bi-Orientation and Spindle Checkpoint Signaling. *Frontiers in oncology* **5:** 225

Krenn V, Overlack K, Primorac I, van Gerwen S, Musacchio A (2014) KI motifs of human Knl1 enhance assembly of comprehensive spindle checkpoint complexes around MELT repeats. *Current biology : CB* **24:** 29-39

Krenn V, Wehenkel A, Li X, Santaguida S, Musacchio A (2012) Structural analysis reveals features of the spindle checkpoint kinase Bub1-kinetochore subunit Knl1 interaction. *The Journal of cell biology* **196:** 451-467

Kruse T, Zhang G, Larsen MS, Lischetti T, Streicher W, Kragh Nielsen T, Bjorn SP, Nilsson J (2013) Direct binding between BubR1 and B56-PP2A phosphatase complexes regulate mitotic progression. *Journal of cell science* **126:** 1086-1092

Kulukian A, Han JS, Cleveland DW (2009) Unattached kinetochores catalyze production of an anaphase inhibitor that requires a Mad2 template to prime Cdc20 for BubR1 binding. *Developmental cell* **16:** 105-117

Kwon MS, Hori T, Okada M, Fukagawa T (2007) CENP-C is involved in chromosome segregation, mitotic checkpoint function, and kinetochore assembly. *Molecular biology of the cell* **18:** 2155-2168

Labit H, Fujimitsu K, Bayin NS, Takaki T, Gannon J, Yamano H (2012) Dephosphorylation of Cdc20 is required for its C-box-dependent activation of the APC/C. *The EMBO journal* **31:** 3351-3362

Lampson MA, Kapoor TM (2005) The human mitotic checkpoint protein BubR1 regulates chromosome-spindle attachments. *Nature cell biology* **7:** 93-98

Lampson MA, Renduchitala K, Khodjakov A, Kapoor TM (2004) Correcting improper chromosome-spindle attachments during cell division. *Nature cell biology* **6:** 232-237

Lara-Gonzalez P, Scott MI, Diez M, Sen O, Taylor SS (2011) BubR1 blocks substrate recruitment to the APC/C in a KEN-box-dependent manner. *Journal of cell science* **124:** 4332-4345

Lara-Gonzalez P, Westhorpe FG, Taylor SS (2012) The spindle assembly checkpoint. *Current biology : CB* **22:** R966-980

Larsen NA, Al-Bassam J, Wei RR, Harrison SC (2007) Structural analysis of Bub3 interactions in the mitotic spindle checkpoint. *Proceedings of the National Academy of Sciences of the United States of America* **104:** 1201-1206

Lau DT, Murray AW (2012) Mad2 and Mad3 cooperate to arrest budding yeast in mitosis. *Current biology : CB* **22:** 180-190

Lengauer C, Kinzler KW, Vogelstein B (1998) Genetic instabilities in human cancers. *Nature* **396:** 643-649

Li R, Murray AW (1991) Feedback control of mitosis in budding yeast. *Cell* **66:** 519-531

Li X, Nicklas RB (1995) Mitotic forces control a cell-cycle checkpoint. *Nature* **373:** 630-632

Liang H, Lim HH, Venkitaraman A, Surana U (2012) Cdk1 promotes kinetochore bi-orientation and regulates Cdc20 expression during recovery from spindle checkpoint arrest. *The EMBO journal* **31:** 403-416

Lischetti T, Zhang G, Sedgwick GG, Bolanos-Garcia VM, Nilsson J (2014) The internal Cdc20 binding site in BubR1 facilitates both spindle assembly checkpoint signalling and silencing. *Nature communications* **5:** 5563

Liu D, Vader G, Vromans MJ, Lampson MA, Lens SM (2009) Sensing chromosome bi-orientation by spatial separation of aurora B kinase from kinetochore substrates. *Science (New York, NY)* **323:** 1350-1353

Liu D, Vleugel M, Backer CB, Hori T, Fukagawa T, Cheeseman IM, Lampson MA (2010) Regulated targeting of protein phosphatase 1 to the outer kinetochore by KNL1 opposes Aurora B kinase. *The Journal of cell biology* **188:** 809-820

Liu H, Jia L, Yu H (2013a) Phospho-H2A and cohesin specify distinct tension-regulated Sgo1 pools at kinetochores and inner centromeres. *Current biology : CB* **23:** 1927-1933

Liu H, Naismith JH (2008) An efficient one-step site-directed deletion, insertion, single and multiple-site plasmid mutagenesis protocol. *BMC biotechnology* **8:** 91

Liu H, Qu Q, Warrington R, Rice A, Cheng N, Yu H (2015) Mitotic Transcription Installs Sgo1 at Centromeres to Coordinate Chromosome Segregation. *Molecular cell* **59:** 426-436

Liu H, Rankin S, Yu H (2013b) Phosphorylation-enabled binding of SGO1-PP2A to cohesin protects sororin and centromeric cohesion during mitosis. *Nature cell biology* **15:** 40-49

Liu ST, Rattner JB, Jablonski SA, Yen TJ (2006) Mapping the assembly pathways that specify formation of the trilaminar kinetochore plates in human cells. *The Journal of cell biology* **175:** 41-53

Logarinho E, Resende T, Torres C, Bousbaa H (2008) The human spindle assembly checkpoint protein Bub3 is required for the establishment of efficient kinetochore-microtubule attachments. *Molecular biology of the cell* **19:** 1798-1813

London N, Biggins S (2014a) Mad1 kinetochore recruitment by Mps1-mediated phosphorylation of Bub1 signals the spindle checkpoint. *Genes & development* **28:** 140-152

London N, Biggins S (2014b) Signalling dynamics in the spindle checkpoint response. *Nature reviews Molecular cell biology* **15:** 736-747

London N, Ceto S, Ranish JA, Biggins S (2012) Phosphoregulation of Spc105 by Mps1 and PP1 regulates Bub1 localization to kinetochores. *Current biology : CB* **22:** 900-906

Loog M, Morgan DO (2005) Cyclin specificity in the phosphorylation of cyclin-dependent kinase substrates. *Nature* **434:** 104-108

Lu D, Hsiao JY, Davey NE, Van Voorhis VA, Foster SA, Tang C, Morgan DO (2014) Multiple mechanisms determine the order of APC/C substrate degradation in mitosis. *The Journal of cell biology* **207:** 23-39

Luo X, Fang G, Coldiron M, Lin Y, Yu H, Kirschner MW, Wagner G (2000) Structure of the Mad2 spindle assembly checkpoint protein and its interaction with Cdc20. *Nature structural biology* **7:** 224-229

Luo X, Tang Z, Rizo J, Yu H (2002) The Mad2 spindle checkpoint protein undergoes similar major conformational changes upon binding to either Mad1 or Cdc20. *Molecular cell* **9:** 59-71

Luo X, Tang Z, Xia G, Wassmann K, Matsumoto T, Rizo J, Yu H (2004) The Mad2 spindle checkpoint protein has two distinct natively folded states. *Nature structural & molecular biology* **11:** 338-345

Maciejowski J, George KA, Terret ME, Zhang C, Shokat KM, Jallepalli PV (2010) Mps1 directs the assembly of Cdc20 inhibitory complexes during interphase and mitosis to control M phase timing and spindle checkpoint signaling. *The Journal of cell biology* **190:** 89-100

Maddox PS, Bloom KS, Salmon ED (2000) The polarity and dynamics of microtubule assembly in the budding yeast Saccharomyces cerevisiae. *Nature cell biology* **2:** 36-41

Maddox PS, Oegema K, Desai A, Cheeseman IM (2004) "Holo"er than thou: chromosome segregation and kinetochore function in C. elegans. *Chromosome research : an international journal on the molecular, supramolecular and evolutionary aspects of chromosome biology* **12:** 641-653

Magidson V, O'Connell CB, Loncarek J, Paul R, Mogilner A, Khodjakov A (2011) The spatial arrangement of chromosomes during prometaphase facilitates spindle assembly. *Cell* **146:** 555-567

Maldonado M, Kapoor TM (2011) Constitutive Mad1 targeting to kinetochores uncouples checkpoint signalling from chromosome biorientation. *Nature cell biology* **13:** 475-482

Malik HS, Henikoff S (2009) Major evolutionary transitions in centromere complexity. *Cell* **138:** 1067-1082

Malureanu LA, Jeganathan KB, Hamada M, Wasilewski L, Davenport J, van Deursen JM (2009) BubR1 N terminus acts as a soluble inhibitor of cyclin B degradation by APC/C(Cdc20) in interphase. *Developmental cell* **16:** 118-131

Malvezzi F, Litos G, Schleiffer A, Heuck A, Mechtler K, Clausen T, Westermann S (2013) A structural basis for kinetochore recruitment of the Ndc80 complex via two distinct centromere receptors. *The EMBO journal* **32:** 409-423

Mansfeld J, Collin P, Collins MO, Choudhary JS, Pines J (2011) APC15 drives the turnover of MCC-CDC20 to make the spindle assembly checkpoint responsive to kinetochore attachment. *Nature cell biology* **13:** 1234-U1152

Mao Y, Abrieu A, Cleveland DW (2003) Activating and silencing the mitotic checkpoint through CENP-E-dependent activation/inactivation of BubR1. *Cell* **114:** 87-98

Mao Y, Desai A, Cleveland DW (2005) Microtubule capture by CENP-E silences BubR1-dependent mitotic checkpoint signaling. *The Journal of cell biology* **170:** 873-880

Mapelli M, Massimiliano L, Santaguida S, Musacchio A (2007) The Mad2 conformational dimer: structure and implications for the spindle assembly checkpoint. *Cell* **131:** 730-743

Maresca TJ, Salmon ED (2009) Intrakinetochore stretch is associated with changes in kinetochore phosphorylation and spindle assembly checkpoint activity. *The Journal of cell biology* **184:** 373-381

Marshall OJ, Marshall AT, Choo KH (2008) Three-dimensional localization of CENP-A suggests a complex higher order structure of centromeric chromatin. *The Journal of cell biology* **183:** 1193-1202

Martin-Lluesma S, Stucke VM, Nigg EA (2002) Role of Hec1 in spindle checkpoint signaling and kinetochore recruitment of Mad1/Mad2. *Science (New York, NY)* **297:** 2267-2270

McAinsh AD, Meraldi P, Draviam VM, Toso A, Sorger PK (2006) The human kinetochore proteins Nnf1R and Mcm21R are required for accurate chromosome segregation. *The EMBO journal* **25:** 4033-4049

McCleland ML, Gardner RD, Kallio MJ, Daum JR, Gorbsky GJ, Burke DJ, Stukenberg PT (2003) The highly conserved Ndc80 complex is required for kinetochore assembly, chromosome congression, and spindle checkpoint activity. *Genes & development* **17:** 101-114

McCleland ML, Kallio MJ, Barrett-Wilt GA, Kestner CA, Shabanowitz J, Hunt DF, Gorbsky GJ, Stukenberg PT (2004) The vertebrate Ndc80 complex contains Spc24 and Spc25 homologs, which are required to establish and maintain kinetochore-microtubule attachment. *Current biology : CB* **14:** 131-137

McClelland SE, Borusu S, Amaro AC, Winter JR, Belwal M, McAinsh AD, Meraldi P (2007) The CENP-A NAC/CAD kinetochore complex controls chromosome congression and spindle bipolarity. *The EMBO journal* **26:** 5033-5047

McEwen BF, Chan GK, Zubrowski B, Savoian MS, Sauer MT, Yen TJ (2001) CENP-E is essential for reliable bioriented spindle attachment, but chromosome alignment can be achieved via redundant mechanisms in mammalian cells. *Molecular biology of the cell* **12:** 2776-2789

McEwen BF, Dong Y, VandenBeldt KJ (2007) Using electron microscopy to understand functional mechanisms of chromosome alignment on the mitotic spindle. *Methods in cell biology* **79:** 259-293

McKinley KL, Sekulic N, Guo LY, Tsinman T, Black BE, Cheeseman IM (2015) The CENP-L-N Complex Forms a Critical Node in an Integrated Meshwork of Interactions at the Centromere-Kinetochore Interface. *Molecular cell* **60:** 886-898

Meadows JC, Shepperd LA, Vanoosthuyse V, Lancaster TC, Sochaj AM, Buttrick GJ, Hardwick KG, Millar JB (2011) Spindle checkpoint silencing requires association of PP1 to both Spc7 and kinesin-8 motors. *Developmental cell* **20:** 739-750

Meraldi P, Draviam VM, Sorger PK (2004) Timing and checkpoints in the regulation of mitotic progression. *Developmental cell* **7:** 45-60

Meraldi P, McAinsh AD, Rheinbay E, Sorger PK (2006) Phylogenetic and structural analysis of centromeric DNA and kinetochore proteins. *Genome biology* **7:** R23

Meraldi P, Sorger PK (2005) A dual role for Bub1 in the spindle checkpoint and chromosome congression. *The EMBO journal* **24:** 1621-1633

Metzner R (1894) Beiträge zur Granulalehre. I. Kern und Kerntheilung. *Verlag von Veit, Leipzig*

Milks KJ, Moree B, Straight AF (2009) Dissection of CENP-C-directed centromere and kinetochore assembly. *Molecular biology of the cell* **20:** 4246-4255

Millband DN, Campbell L, Hardwick KG (2002) The awesome power of multiple model systems: interpreting the complex nature of spindle checkpoint signaling. *Trends in cell biology* **12:** 205-209

Millband DN, Hardwick KG (2002) Fission yeast Mad3p is required for Mad2p to inhibit the anaphase-promoting complex and localizes to kinetochores in a Bub1p-, Bub3p-, and Mph1p-dependent manner. *Molecular and cellular biology* **22:** 2728-2742

Miller SA, Johnson ML, Stukenberg PT (2008) Kinetochore attachments require an interaction between unstructured tails on microtubules and Ndc80(Hec1). *Current biology : CB* **18:** 1785-1791

Miranda JJ, De Wulf P, Sorger PK, Harrison SC (2005) The yeast DASH complex forms closed rings on microtubules. *Nature structural & molecular biology* **12:** 138-143

Mitchison T, Evans L, Schulze E, Kirschner M (1986) Sites of microtubule assembly and disassembly in the mitotic spindle. *Cell* **45:** 515-527

Mitchison TJ, Salmon ED (2001) Mitosis: a history of division. *Nature cell biology* **3:** E17-21

Morgan DO (1997) Cyclin-dependent kinases: engines, clocks, and microprocessors. *Annual review of cell and developmental biology* **13:** 261-291

Morgan DO (2007) The Cell Cycle - Principles of Control. *New Science Press*

Moroi Y, Peebles C, Fritzler MJ, Steigerwald J, Tan EM (1980) Autoantibody to centromere (kinetochore) in scleroderma sera. *Proceedings of the National Academy of Sciences of the United States of America* **77:** 1627-1631

Moyle MW, Kim T, Hattersley N, Espeut J, Cheerambathur DK, Oegema K, Desai A (2014) A Bub1-Mad1 interaction targets the Mad1-Mad2 complex to unattached kinetochores to initiate the spindle checkpoint. *The Journal of cell biology* **204:** 647-657

Murray AW, Kirschner MW (1989) Dominoes and clocks: the union of two views of the cell cycle. *Science (New York, NY)* **246:** 614-621

Musacchio A (2015) The Molecular Biology of Spindle Assembly Checkpoint Signaling Dynamics. *Current biology : CB* **25:** R1002-1018

Musacchio A, Ciliberto A (2012) The spindle-assembly checkpoint and the beauty of self-destruction. *Nature structural & molecular biology* **19:** 1059-1061

Musacchio A, Salmon ED (2007) The spindle-assembly checkpoint in space and time. *Nature reviews Molecular cell biology* **8:** 379-393

Neer EJ, Schmidt CJ, Nambudripad R, Smith TF (1994) The ancient regulatory-protein family of WD-repeat proteins. *Nature* **371:** 297-300

Nicklas RB, Koch CA (1969) Chromosome micromanipulation. 3. Spindle fiber tension and the reorientation of mal-oriented chromosomes. *The Journal of cell biology* **43:** 40-50

Nijenhuis W, Vallardi G, Teixeira A, Kops GJ, Saurin AT (2014) Negative feedback at kinetochores underlies a responsive spindle checkpoint signal. *Nature cell biology* **16:** 1257-1264

Nijenhuis W, von Castelmur E, Littler D, De Marco V, Tromer E, Vleugel M, van Osch MH, Snel B, Perrakis A, Kops GJ (2013) A TPR domain-containing N-terminal module of MPS1 is required for its kinetochore localization by Aurora B. *The Journal of cell biology* **201:** 217-231

Nilsson J, Yekezare M, Minshull J, Pines J (2008) The APC/C maintains the spindle assembly checkpoint by targeting Cdc20 for destruction. *Nature cell biology* **10:** 1411-1420

Nishino T, Takeuchi K, Gascoigne KE, Suzuki A, Hori T, Oyama T, Morikawa K, Cheeseman IM, Fukagawa T (2012) CENP-T-W-S-X forms a unique centromeric chromatin structure with a histone-like fold. *Cell* **148:** 487-501

Obuse C, Iwasaki O, Kiyomitsu T, Goshima G, Toyoda Y, Yanagida M (2004) A conserved Mis12 centromere complex is linked to heterochromatic HP1 and outer kinetochore protein Zwint-1. *Nature cell biology* **6:** 1135-1141

Okada M, Cheeseman IM, Hori T, Okawa K, McLeod IX, Yates JR, 3rd, Desai A, Fukagawa T (2006) The CENP-H-I complex is required for the efficient incorporation of newly synthesized CENP-A into centromeres. *Nature cell biology* **8:** 446-457

Ong SE, Blagoev B, Kratchmarova I, Kristensen DB, Steen H, Pandey A, Mann M (2002) Stable isotope labeling by amino acids in cell culture, SILAC, as a simple and accurate approach to expression proteomics. *Molecular & cellular proteomics : MCP* **1:** 376-386

Ong SE, Mann M (2005) Mass spectrometry-based proteomics turns quantitative. *Nature chemical biology* **1:** 252-262

Ong SE, Mann M (2006) A practical recipe for stable isotope labeling by amino acids in cell culture (SILAC). *Nature protocols* **1:** 2650-2660

Overlack K, Krenn V, Musacchio A (2014) When Mad met Bub. *EMBO reports* **15:** 326-328

Overlack K, Primorac I, Vleugel M, Krenn V, Maffini S, Hoffmann I, Kops GJ, Musacchio A (2015) A molecular basis for the differential roles of Bub1 and BubR1 in the spindle assembly checkpoint. *eLife* **4**

Pagliuca C, Draviam VM, Marco E, Sorger PK, De Wulf P (2009) Roles for the conserved spc105p/kre28p complex in kinetochore-microtubule binding and the spindle assembly checkpoint. *PloS one* **4:** e7640

Palmer DK, O'Day K, Trong HL, Charbonneau H, Margolis RL (1991) Purification of the centromere-specific protein CENP-A and demonstration that it is a distinctive histone. *Proceedings of the National Academy of Sciences of the United States of America* **88:** 3734-3738

Perera D, Tilston V, Hopwood JA, Barchi M, Boot-Handford RP, Taylor SS (2007) Bub1 maintains centromeric cohesion by activation of the spindle checkpoint. *Developmental cell* **13:** 566-579

Pesenti ME, Weir JR, Musacchio A (2016) Progress in the structural and functional characterization of kinetochores. *Current opinion in structural biology* **37:** 152-163

Peters JM (1998) SCF and APC: the Yin and Yang of cell cycle regulated proteolysis. *Current opinion in cell biology* **10:** 759-768

Petrovic A, Mosalaganti S, Keller J, Mattiuzzo M, Overlack K, Krenn V, De Antoni A, Wohlgemuth S, Cecatiello V, Pasqualato S, Raunser S, Musacchio A (2014) Modular assembly of RWD domains on the Mis12 complex underlies outer kinetochore organization. *Molecular cell* **53:** 591-605

Petrovic A, Pasqualato S, Dube P, Krenn V, Santaguida S, Cittaro D, Monzani S, Massimiliano L, Keller J, Tarricone A, Maiolica A, Stark H, Musacchio A (2010) The MIS12 complex is a protein interaction hub for outer kinetochore assembly. *The Journal of cell biology* **190:** 835-852

Pinsky BA, Kung C, Shokat KM, Biggins S (2006) The Ipl1-Aurora protein kinase activates the spindle checkpoint by creating unattached kinetochores. *Nature cell biology* **8:** 78-83

Pluta AF, Mackay AM, Ainsztein AM, Goldberg IG, Earnshaw WC (1995) The centromere: hub of chromosomal activities. *Science (New York, NY)* **270:** 1591-1594

Primorac I, Musacchio A (2013) Panta rhei: the APC/C at steady state. *The Journal of cell biology* **201:** 177-189

Primorac I, Weir JR, Chiroli E, Gross F, Hoffmann I, van Gerwen S, Ciliberto A, Musacchio A (2013) Bub3 reads phosphorylated MELT repeats to promote spindle assembly checkpoint signaling. *eLife* **2:** e01030

Przewloka MR, Venkei Z, Bolanos-Garcia VM, Debski J, Dadlez M, Glover DM (2011) CENP-C is a structural platform for kinetochore assembly. *Current biology : CB* **21:** 399-405

Qi W, Tang Z, Yu H (2006) Phosphorylation- and polo-box-dependent binding of Plk1 to Bub1 is required for the kinetochore localization of Plk1. *Molecular biology of the cell* **17:** 3705-3716

Qiao R, Weissmann F, Yamaguchi M, Brown NG, VanderLinden R, Imre R, Jarvis MA, Brunner MR, Davidson IF, Litos G, Haselbach D, Mechtler K, Stark H, Schulman BA, Peters JM (2016) Mechanism of APC/CCDC20 activation by mitotic phosphorylation. *Proceedings of the National Academy of Sciences of the United States of America* **113:** E2570-2578

Rago F, Gascoigne KE, Cheeseman IM (2015) Distinct organization and regulation of the outer kinetochore KMN network downstream of CENP-C and CENP-T. *Current biology : CB* **25:** 671-677

Ribeiro SA, Vagnarelli P, Dong Y, Hori T, McEwen BF, Fukagawa T, Flors C, Earnshaw WC (2010) A super-resolution map of the vertebrate kinetochore. *Proceedings of the National Academy of Sciences of the United States of America* **107:** 10484-10489

Richter MM, Poznanski J, Zdziarska A, Czarnocki-Cieciura M, Lipinszki Z, Dadlez M, Glover DM, Przewloka MR (2016) Network of protein interactions within the Drosophila inner kinetochore. *Open biology* **6:** 150238

Ricke RM, Jeganathan KB, Malureanu L, Harrison AM, van Deursen JM (2012) Bub1 kinase activity drives error correction and mitotic checkpoint control but not tumor suppression. *The Journal of cell biology* **199:** 931-949

Rieder CL (1981) The structure of the cold-stable kinetochore fiber in metaphase PtK1 cells. *Chromosoma* **84:** 145-158

Rieder CL, Cole RW, Khodjakov A, Sluder G (1995) The checkpoint delaying anaphase in response to chromosome monoorientation is mediated by an inhibitory signal produced by unattached kinetochores. *The Journal of cell biology* **130:** 941-948

Rischitor PE, May KM, Hardwick KG (2007) Bub1 is a fission yeast kinetochore scaffold protein, and is sufficient to recruit other spindle checkpoint proteins to ectopic sites on chromosomes. *PloS one* **2:** e1342

Roberts BT, Farr KA, Hoyt MA (1994) The Saccharomyces cerevisiae checkpoint gene BUB1 encodes a novel protein kinase. *Molecular and cellular biology* **14:** 8282-8291

Rosenberg JS, Cross FR, Funabiki H (2011) KNL1/Spc105 recruits PP1 to silence the spindle assembly checkpoint. *Current biology : CB* **21:** 942-947

Saitoh H, Tomkiel J, Cooke CA, Ratrie H, 3rd, Maurer M, Rothfield NF, Earnshaw WC (1992) CENP-C, an autoantigen in scleroderma, is a component of the human inner kinetochore plate. *Cell* **70:** 115-125

Salimian KJ, Ballister ER, Smoak EM, Wood S, Panchenko T, Lampson MA, Black BE (2011) Feedback control in sensing chromosome biorientation by the Aurora B kinase. *Current biology : CB* **21:** 1158-1165

Santaguida S, Musacchio A (2009) The life and miracles of kinetochores. *The EMBO journal* **28:** 2511-2531

Santaguida S, Tighe A, D'Alise AM, Taylor SS, Musacchio A (2010) Dissecting the role of MPS1 in chromosome biorientation and the spindle checkpoint through the small molecule inhibitor reversine. *The Journal of cell biology* **190:** 73-87

Santaguida S, Vernieri C, Villa F, Ciliberto A, Musacchio A (2011) Evidence that Aurora B is implicated in spindle checkpoint signalling independently of error correction. *The EMBO journal* **30:** 1508-1519

Saurin AT, van der Waal MS, Medema RH, Lens SM, Kops GJ (2011) Aurora B potentiates Mps1 activation to ensure rapid checkpoint establishment at the onset of mitosis. *Nature communications* **2:** 316

Schittenhelm RB, Chaleckis R, Lehner CF (2009) Intrakinetochore localization and essential functional domains of Drosophila Spc105. *The EMBO journal* **28:** 2374-2386

Schleiffer A, Maier M, Litos G, Lampert F, Hornung P, Mechtler K, Westermann S (2012) CENP-T proteins are conserved centromere receptors of the Ndc80 complex. *Nature cell biology* **14:** 604-613

Schmidt JC, Arthanari H, Boeszoermenyi A, Dashkevich NM, Wilson-Kubalek EM, Monnier N, Markus M, Oberer M, Milligan RA, Bathe M, Wagner G, Grishchuk EL, Cheeseman IM (2012) The kinetochore-bound Ska1 complex tracks depolymerizing microtubules and binds to curved protofilaments. *Developmental cell* **23:** 968-980

Screpanti E, De Antoni A, Alushin GM, Petrovic A, Melis T, Nogales E, Musacchio A (2011) Direct binding of Cenp-C to the Mis12 complex joins the inner and outer kinetochore. *Current biology : CB* **21:** 391-398

Shah JV, Botvinick E, Bonday Z, Furnari F, Berns M, Cleveland DW (2004) Dynamics of centromere and kinetochore proteins; implications for checkpoint signaling and silencing. *Current biology : CB* **14:** 942-952

Sharp-Baker H, Chen RH (2001) Spindle checkpoint protein Bub1 is required for kinetochore localization of Mad1, Mad2, Bub3, and CENP-E, independently of its kinase activity. *The Journal of cell biology* **153:** 1239-1250

Shepperd LA, Meadows JC, Sochaj AM, Lancaster TC, Zou J, Buttrick GJ, Rappsilber J, Hardwick KG, Millar JB (2012) Phosphodependent recruitment of Bub1 and Bub3 to Spc7/KNL1 by Mph1 kinase maintains the spindle checkpoint. *Current biology : CB* **22:** 891-899

Shteinberg M, Protopopov Y, Listovsky T, Brandeis M, Hershko A (1999) Phosphorylation of the cyclosome is required for its stimulation by Fizzy/cdc20. *Biochemical and biophysical research communications* **260:** 193-198

Sillje HH, Nagel S, Korner R, Nigg EA (2006) HURP is a Ran-importin beta-regulated protein that stabilizes kinetochore microtubules in the vicinity of chromosomes. *Current biology : CB* **16:** 731-742

Simonetta M, Manzoni R, Mosca R, Mapelli M, Massimiliano L, Vink M, Novak B, Musacchio A, Ciliberto A (2009) The influence of catalysis on mad2 activation dynamics. *PLoS biology* **7:** e10

Sironi L, Mapelli M, Knapp S, De Antoni A, Jeang KT, Musacchio A (2002) Crystal structure of the tetrameric Mad1-Mad2 core complex: implications of a 'safety belt' binding mechanism for the spindle checkpoint. *The EMBO journal* **21:** 2496-2506

Sironi L, Melixetian M, Faretta M, Prosperini E, Helin K, Musacchio A (2001) Mad2 binding to Mad1 and Cdc20, rather than oligomerization, is required for the spindle checkpoint. *The EMBO journal* **20:** 6371-6382

Smith CA, McAinsh AD, Burroughs NJ (2016) Human kinetochores are swivel joints that mediate microtubule attachments. *eLife* **5**

Starr DA, Saffery R, Li Z, Simpson AE, Choo KH, Yen TJ, Goldberg ML (2000) HZwint-1, a novel human kinetochore component that interacts with HZW10. *Journal of cell science* **113 (Pt 11):** 1939-1950

Starr DA, Williams BC, Hays TS, Goldberg ML (1998) ZW10 helps recruit dynactin and dynein to the kinetochore. *The Journal of cell biology* **142:** 763-774

Sudakin V, Chan GK, Yen TJ (2001) Checkpoint inhibition of the APC/C in HeLa cells is mediated by a complex of BUBR1, BUB3, CDC20, and MAD2. *The Journal of cell biology* **154:** 925-936

Sudakin V, Ganoth D, Dahan A, Heller H, Hershko J, Luca FC, Ruderman JV, Hershko A (1995) The cyclosome, a large complex containing cyclin-selective ubiquitin ligase activity, targets cyclins for destruction at the end of mitosis. *Molecular biology of the cell* **6:** 185-197

Suijkerbuijk SJ, van Dam TJ, Karagoz GE, von Castelmur E, Hubner NC, Duarte AM, Vleugel M, Perrakis A, Rudiger SG, Snel B, Kops GJ (2012a) The vertebrate mitotic checkpoint protein BUBR1 is an unusual pseudokinase. *Developmental cell* **22:** 1321-1329

Suijkerbuijk SJ, Vleugel M, Teixeira A, Kops GJ (2012b) Integration of kinase and phosphatase activities by BUBR1 ensures formation of stable kinetochore-microtubule attachments. *Developmental cell* **23:** 745-755

Suzuki A, Badger BL, Wan X, DeLuca JG, Salmon ED (2014) The architecture of CCAN proteins creates a structural integrity to resist spindle forces and achieve proper Intrakinetochore stretch. *Developmental cell* **30:** 717-730

Suzuki A, Hori T, Nishino T, Usukura J, Miyagi A, Morikawa K, Fukagawa T (2011) Spindle microtubules generate tension-dependent changes in the distribution of inner kinetochore proteins. *The Journal of cell biology* **193:** 125-140

Tang Z, Bharadwaj R, Li B, Yu H (2001) Mad2-Independent inhibition of APCCdc20 by the mitotic checkpoint protein BubR1. *Developmental cell* **1:** 227-237

Tang Z, Shu H, Oncel D, Chen S, Yu H (2004) Phosphorylation of Cdc20 by Bub1 provides a catalytic mechanism for APC/C inhibition by the spindle checkpoint. *Molecular cell* **16:** 387-397

Tang Z, Shu H, Qi W, Mahmood NA, Mumby MC, Yu H (2006) PP2A is required for centromeric localization of Sgo1 and proper chromosome segregation. *Developmental cell* **10:** 575-585

Tanno Y, Kitajima TS, Honda T, Ando Y, Ishiguro K, Watanabe Y (2010) Phosphorylation of mammalian Sgo2 by Aurora B recruits PP2A and MCAK to centromeres. *Genes & development* **24:** 2169-2179

Taylor SS, Ha E, McKeon F (1998) The human homologue of Bub3 is required for kinetochore localization of Bub1 and a Mad3/Bub1-related protein kinase. *The Journal of cell biology* **142:** 1-11

Taylor SS, McKeon F (1997) Kinetochore localization of murine Bub1 is required for normal mitotic timing and checkpoint response to spindle damage. *Cell* **89:** 727-735

Teichner A, Eytan E, Sitry-Shevah D, Miniowitz-Shemtov S, Dumin E, Gromis J, Hershko A (2011) p31comet Promotes disassembly of the mitotic checkpoint complex in an ATP-dependent process. *Proceedings of the National Academy of Sciences of the United States of America* **108:** 3187-3192

Tien JF, Umbreit NT, Gestaut DR, Franck AD, Cooper J, Wordeman L, Gonen T, Asbury CL, Davis TN (2010) Cooperation of the Dam1 and Ndc80 kinetochore complexes enhances microtubule coupling and is regulated by aurora B. *The Journal of cell biology* **189:** 713-723

Trowitzsch S, Bieniossek C, Nie Y, Garzoni F, Berger I (2010) New baculovirus expression tools for recombinant protein complex production. *Journal of structural biology* **172:** 45-54

Uchida KS, Takagaki K, Kumada K, Hirayama Y, Noda T, Hirota T (2009) Kinetochore stretching inactivates the spindle assembly checkpoint. *The Journal of cell biology* **184:** 383-390

Uzunova K, Dye BT, Schutz H, Ladurner R, Petzold G, Toyoda Y, Jarvis MA, Brown NG, Poser I, Novatchkova M, Mechtler K, Hyman AA, Stark H, Schulman BA, Peters JM (2012) APC15 mediates CDC20 autoubiquitylation by APC/C(MCC) and disassembly of the mitotic checkpoint complex. *Nature structural & molecular biology* **19:** 1116-1123

Vanoosthuyse V, Meadows JC, van der Sar SJ, Millar JB, Hardwick KG (2009) Bub3p facilitates spindle checkpoint silencing in fission yeast. *Molecular biology of the cell* **20:** 5096-5105

Vanoosthuyse V, Valsdottir R, Javerzat JP, Hardwick KG (2004) Kinetochore targeting of fission yeast Mad and Bub proteins is essential for spindle checkpoint function but not for all chromosome segregation roles of Bub1p. *Molecular and cellular biology* **24:** 9786-9801

Varetti G, Guida C, Santaguida S, Chiroli E, Musacchio A (2011) Homeostatic Control of Mitotic Arrest. *Molecular cell* **44:** 710-720

Vazquez-Novelle MD, Petronczki M (2010) Relocation of the chromosomal passenger complex prevents mitotic checkpoint engagement at anaphase. *Current biology : CB* **20:** 1402-1407

Vigneron S, Prieto S, Bernis C, Labbe JC, Castro A, Lorca T (2004) Kinetochore localization of spindle checkpoint proteins: who controls whom? *Molecular biology of the cell* **15:** 4584-4596

Vink M, Simonetta M, Transidico P, Ferrari K, Mapelli M, De Antoni A, Massimiliano L, Ciliberto A, Faretta M, Salmon ED, Musacchio A (2006) In vitro FRAP identifies the minimal requirements for Mad2 kinetochore dynamics. *Current biology : CB* **16:** 755-766

Vleugel M, Hoek TA, Tromer E, Sliedrecht T, Groenewold V, Omerzu M, Kops GJ (2015a) Dissecting the roles of human BUB1 in the spindle assembly checkpoint. *Journal of cell science* **128:** 2975-2982

Vleugel M, Hoogendoorn E, Snel B, Kops GJ (2012) Evolution and function of the mitotic checkpoint. *Developmental cell* **23:** 239-250

Vleugel M, Omerzu M, Groenewold V, Hadders MA, Lens SM, Kops GJ (2015b) Sequential Multisite Phospho-Regulation of KNL1-BUB3 Interfaces at Mitotic Kinetochores. *Molecular cell* **57:** 824-835

Vleugel M, Tromer E, Omerzu M, Groenewold V, Nijenhuis W, Snel B, Kops GJ (2013) Arrayed BUB recruitment modules in the kinetochore scaffold KNL1 promote accurate chromosome segregation. *The Journal of cell biology* **203:** 943-955

von Schubert C, Cubizolles F, Bracher JM, Sliedrecht T, Kops GJ, Nigg EA (2015) Plk1 and Mps1 Cooperatively Regulate the Spindle Assembly Checkpoint in Human Cells. *Cell reports* **12:** 66-78

Walczak CE, Heald R (2008) Mechanisms of mitotic spindle assembly and function. *International review of cytology* **265:** 111-158

Wan X, O'Quinn RP, Pierce HL, Joglekar AP, Gall WE, DeLuca JG, Carroll CW, Liu ST, Yen TJ, McEwen BF, Stukenberg PT, Desai A, Salmon ED (2009) Protein architecture of the human kinetochore microtubule attachment site. *Cell* **137:** 672-684

Wang F, Dai J, Daum JR, Niedzialkowska E, Banerjee B, Stukenberg PT, Gorbsky GJ, Higgins JM (2010) Histone H3 Thr-3 phosphorylation by Haspin positions Aurora B at centromeres in mitosis. *Science (New York, NY)* **330:** 231-235

Wang K, Sturt-Gillespie B, Hittle JC, Macdonald D, Chan GK, Yen TJ, Liu ST (2014) Thyroid hormone receptor interacting protein 13 (TRIP13) AAA-ATPase is a novel mitotic checkpoint-silencing protein. *The Journal of biological chemistry* **289:** 23928-23937

Warren CD, Brady DM, Johnston RC, Hanna JS, Hardwick KG, Spencer FA (2002) Distinct chromosome segregation roles for spindle checkpoint proteins. *Molecular biology of the cell* **13:** 3029-3041

Wei RR, Al-Bassam J, Harrison SC (2007) The Ndc80/HEC1 complex is a contact point for kinetochore-microtubule attachment. *Nature structural & molecular biology* **14:** 54-59

Wei RR, Schnell JR, Larsen NA, Sorger PK, Chou JJ, Harrison SC (2006) Structure of a central component of the yeast kinetochore: the Spc24p/Spc25p globular domain. *Structure* **14:** 1003-1009

Wei RR, Sorger PK, Harrison SC (2005) Molecular organization of the Ndc80 complex, an essential kinetochore component. *Proceedings of the National Academy of Sciences of the United States of America* **102:** 5363-5367

Weir JR, Faesen AC, Klare K, Petrovic A, Basilico F, Fischbock J, Pentakota S, Keller J, Pesenti ME, Pan D, Vogt D, Wohlgemuth S, Herzog F, Musacchio A (2016) Insights from biochemical reconstitution into the architecture of human kinetochores. *Nature*

Weiss E, Winey M (1996) The Saccharomyces cerevisiae spindle pole body duplication gene MPS1 is part of a mitotic checkpoint. *The Journal of cell biology* **132:** 111-123

Welburn JP, Grishchuk EL, Backer CB, Wilson-Kubalek EM, Yates JR, 3rd, Cheeseman IM (2009) The human kinetochore Ska1 complex facilitates microtubule depolymerization-coupled motility. *Developmental cell* **16:** 374-385

Welburn JP, Vleugel M, Liu D, Yates JR, 3rd, Lampson MA, Fukagawa T, Cheeseman IM (2010) Aurora B phosphorylates spatially distinct targets to differentially regulate the kinetochore-microtubule interface. *Molecular cell* **38:** 383-392

Westermann S, Avila-Sakar A, Wang HW, Niederstrasser H, Wong J, Drubin DG, Nogales E, Barnes G (2005) Formation of a dynamic kinetochore- microtubule interface through assembly of the Dam1 ring complex. *Molecular cell* **17:** 277-290

Westermann S, Cheeseman IM, Anderson S, Yates JR, 3rd, Drubin DG, Barnes G (2003) Architecture of the budding yeast kinetochore reveals a conserved molecular core. *The Journal of cell biology* **163:** 215-222

Westermann S, Wang HW, Avila-Sakar A, Drubin DG, Nogales E, Barnes G (2006) The Dam1 kinetochore ring complex moves processively on depolymerizing microtubule ends. *Nature* **440:** 565-569

Westhorpe FG, Tighe A, Lara-Gonzalez P, Taylor SS (2011) p31comet-mediated extraction of Mad2 from the MCC promotes efficient mitotic exit. *Journal of cell science* **124:** 3905-3916

Wigge PA, Kilmartin JV (2001) The Ndc80p complex from Saccharomyces cerevisiae contains conserved centromere components and has a function in chromosome segregation. *The Journal of cell biology* **152:** 349-360

Windecker H, Langegger M, Heinrich S, Hauf S (2009) Bub1 and Bub3 promote the conversion from monopolar to bipolar chromosome attachment independently of shugoshin. *EMBO reports* **10:** 1022-1028

Winey M, Mamay CL, O'Toole ET, Mastronarde DN, Giddings TH, Jr., McDonald KL, McIntosh JR (1995) Three-dimensional ultrastructural analysis of the Saccharomyces cerevisiae mitotic spindle. *The Journal of cell biology* **129:** 1601-1615

Wittmann T, Hyman A, Desai A (2001) The spindle: a dynamic assembly of microtubules and motors. *Nature cell biology* **3:** E28-34

Xu P, Raetz EA, Kitagawa M, Virshup DM, Lee SH (2013) BUBR1 recruits PP2A via the B56 family of targeting subunits to promote chromosome congression. *Biology open* **2:** 479-486

Yamagishi Y, Honda T, Tanno Y, Watanabe Y (2010) Two histone marks establish the inner centromere and chromosome bi-orientation. *Science (New York, NY)* **330:** 239-243

Yamagishi Y, Yang CH, Tanno Y, Watanabe Y (2012) MPS1/Mph1 phosphorylates the kinetochore protein KNL1/Spc7 to recruit SAC components. *Nature cell biology* **14:** 746-752

Yamaguchi M, VanderLinden R, Weissmann F, Qiao R, Dube P, Brown NG, Haselbach D, Zhang W, Sidhu SS, Peters JM, Stark H, Schulman BA (2016) Cryo-EM of Mitotic Checkpoint Complex-Bound APC/C Reveals Reciprocal and Conformational Regulation of Ubiquitin Ligation. *Molecular cell* **63:** 593-607

Yamamoto A, Guacci V, Koshland D (1996) Pds1p, an inhibitor of anaphase in budding yeast, plays a critical role in the APC and checkpoint pathway(s). *The Journal of cell biology* **133:** 99-110

Yang Y, Tsuchiya D, Lacefield S (2015) Bub3 promotes Cdc20-dependent activation of the APC/C in S. cerevisiae. *The Journal of cell biology* **209:** 519-527

Yang Y, Wu F, Ward T, Yan F, Wu Q, Wang Z, McGlothen T, Peng W, You T, Sun M, Cui T, Hu R, Dou Z, Zhu J, Xie W, Rao Z, Ding X, Yao X (2008) Phosphorylation of HsMis13 by Aurora B kinase is essential for assembly of functional kinetochore. *The Journal of biological chemistry* **283:** 26726-26736

Ye Q, Rosenberg SC, Moeller A, Speir JA, Su TY, Corbett KD (2015) TRIP13 is a protein-remodeling AAA+ ATPase that catalyzes MAD2 conformation switching. *eLife* **4**

Yudkovsky Y, Shteinberg M, Listovsky T, Brandeis M, Hershko A (2000) Phosphorylation of Cdc20/fizzy negatively regulates the mammalian cyclosome/APC in the mitotic checkpoint. *Biochemical and biophysical research communications* **271:** 299-304

Zaytsev AV, Mick JE, Maslennikov E, Nikashin B, DeLuca JG, Grishchuk EL (2015) Multisite phosphorylation of the NDC80 complex gradually tunes its microtubule-binding affinity. *Molecular biology of the cell* **26:** 1829-1844

Zhang G, Lischetti T, Nilsson J (2014) A minimal number of MELT repeats supports all the functions of KNL1 in chromosome segregation. *Journal of cell science* **127:** 871-884

Zhang G, Mendez BL, Sedgwick GG, Nilsson J (2016a) Two functionally distinct kinetochore pools of BubR1 ensure accurate chromosome segregation. *Nature communications* **7:** 12256

Zhang J, Ahmad S, Mao Y (2007) BubR1 and APC/EB1 cooperate to maintain metaphase chromosome alignment. *The Journal of cell biology* **178:** 773-784

Zhang S, Chang L, Alfieri C, Zhang Z, Yang J, Maslen S, Skehel M, Barford D (2016b) Molecular mechanism of APC/C activation by mitotic phosphorylation. *Nature* **533:** 260-264

Acknowledgements

First of all, I would like to express my sincere gratitude to my supervisor Prof. Andrea Musacchio for giving me the opportunity to do my PhD in his lab, for great scientific discussions and ideas and his continuous support. I would also like to thank the members of my thesis advisory committee, Dr. Gerben Vader and Dr. Alex Bird, for their scientific guidance and valuable suggestions throughout the progress of my project. Finally, I would like to thank Prof. Stefan Westermann and Prof. Silke Hauf for taking the time to be evaluators of my PhD thesis.

I want to thank present and past members of Department I for fruitful scientific discussion, for sharing knowledge and reagents and for creating a great working atmosphere. In particular, I would like to express my deepest gratefulness to Dr. Veronica Krenn, who introduced me to the complicated world of the Bubs. She was always a great help in the lab, answered all my questions and I have learned a lot from her. A very big thank you goes to Dr. Alex Faesen, who showed me how to purify proteins and provided an immense amount of the MCC proteins. He was always willing to discuss results and I highly appreciated his advice. I would like to thank Dr. Stefano Maffini for being always helpful in discussing tissue culture experiments, for sharing knowledge and reagents. Especially, I would like to acknowledge his help with the microscope and the set up of the FRAP experiments. Furthermore, I would like to express my gratitude to Dr. Tanja Bange and Franziska Müller for performing the MS-analyses of numerous SILAC experiments. I wish to thank Dr. Ivana Primorac for the great collaboration on the first part of the project and initial APC/C assays. Thanks are due to Dr. John Weir, who was always willing to provide help especially on cloning problems and to Dr. Claudia Breit for making the labeled Cyclin B and collaborations on other projects. Furthermore, I would like to thank Suzan van Gerwen who always had a helping hand in the cell culture if needed, as well as Beate Voß and Ingrid Hoffmann for help in the lab and for creating such a nice working atmosphere in the lab. Dr. Georg Holtermann and Dr. Ingrid Vetter I would like to thank for invaluable technical support with microscopy. I would like to thank Dr. Kerstin Klare for giving me a ride home from time to time, when there were problems with the trains. My sincere thanks go to Antje Peukert and

also to Christa Hornemann and Lucia Sironi from the IMPRS for being so supportive in overcoming bureaucratic barriers and for help outside of the lab.
Last but not least, I would like to thank my family and friends. Without their help, constant support and faith in me, it would not have been possible to finish this thesis. I would like to express my special gratitude to my boyfriend, Marvin, who does everything to make me feel good and who supports me in every possible way - again, without him this work would not have been possible.

Curriculum Vitae

Der Lebenslauf ist in der Online-Version aus Gründen des Datenschutzes nicht enthalten.

Affidavit

Hiermit erkläre ich, Katharina Overlack, gem. § 7 Abs. (2) d) + f) der Promotionsordnung der Fakultät für Biologie zur Erlangung des Dr. rer. nat., dass ich die vorliegende Dissertation selbständig verfasst und mich keiner anderen als der angegebenen Hilfsmittel bedient, bei der Abfassung der Dissertation nur die angegebenen Hilfsmittel benutzt und alle wörtlich oder inhaltlich übernommenen Stellen als solche gekennzeichnet habe.

Datum:
Unterschrift:

Hiermit erkläre ich, Katharina Overlack, gem. § 7 Abs. (2) e) + g) der Promotionsordnung der Fakultät für Biologie zur Erlangung des Dr. rer. nat., dass ich keine anderen Promotionen bzw. Promotionsversuche in der Vergangenheit durchgeführt habe und dass diese Arbeit von keiner anderen Fakultät/Fachbereich abgelehnt worden ist.

Datum:
Unterschrift:

Hiermit erkläre ich, Prof. Dr. Andrea Musacchio, gem. § 6 Abs. (2) g) der Promotionsordnung der Fakultät für Biologie zur Erlangung des Dr. rer. nat., dass ich das Arbeitsgebiet, dem das Thema "Functional analysis of the interactions of the spindle assembly checkpoint proteins BubR1 and Bub1 at the kinetochore" zuzuordnen ist, in Forschung und Lehre vertrete und den Antrag von Katharina Overlack befürworte und die Betreuung auch im Falle eines Weggangs, wenn nicht wichtige Gründe dem entgegenstehen, weiterführen werde.

Datum:
Unterschrift: